Vector-pathogen interactions within the vector, *Culicoides sonorensis*

by

Mary Katherine Mills

B.A., Georgia Southern University, 2012

AN ABSTRACT OF A DISSERTATION

submitted in partial fulfillment of the requirements for the degree

DOCTOR OF PHILOSOPHY

Division of Biology

College of Arts and Sciences

KANSAS STATE UNIVERSITY

Manhattan, Kansas

2017

Abstract

The biting midge, *Culicoides sonorensis*, vectors orbiviruses of economic importance, such as epizootic hemorrhagic disease virus (EHDV). Due to the limitations in available molecular tools, critical *Culicoides*-orbivirus interactions underlying vector competence remain unclear. To provide a foundation for the study of midge-EHDV interactions, RNA interference (RNAi) was developed as a reverse genetic tool, and EHDV-2 infection dynamics were determined within *C. sonorensis.* To develop RNAi, exogenous double-stranded RNA (dsRNA) was injected into *C. sonorensis* adults specific to the *C. sonorensis* inhibitor of apoptosis protein 1 (CsIAP1) ortholog (ds*CsIAP1*). A significant decrease in *CsIAP1* transcripts was observed in whole midges, with highest reduction in the midgut. In addition, ds*CsIAP1*-injected midges had increased mortality, a loss of midgut tissue integrity, and increased caspase activity. The longevity and midgut phenotypes were partially reversed by the co-injection of dsRNA specific to the *C. sonorensis* initiator caspase Dronc ortholog and *CsIAP1*. These results demonstrated that RNAi can be achieved in the midge midgut through injection of target dsRNAs into the hemolymph. Furthermore, the time course of EHDV-2 infection within *C. sonorensis* was characterized. EHDV-2 infection was observed in the midgut and secondary tissues, including the salivary glands, by 5 days post-feeding (dpf). These data are consistent with dissemination of EHDV-2 to secondary susceptible tissues throughout the midge via the hemolymph and indicate that virus transmission by *C. sonorensis* may occur as early as 5 dpf. This work provides a foundation for the future study of *Culicoides*-orbivirus interactions, including the antiviral role of RNAi at the midgut barrier.

Vector-pathogen interactions within the vector, *Culicoides sonorensis*

by

Mary Katherine Mills

B.A., Georgia Southern University, 2012

A DISSERTATION

submitted in partial fulfillment of the requirements for the degree

DOCTOR OF PHILOSOPHY

Division of Biology

College of Arts and Sciences

KANSAS STATE UNIVERSITY

Manhattan, Kansas

2017

Approved by:

Major Professor

Kristin Michel

Copyright

Abstract

The biting midge, *Culicoides sonorensis*, vectors orbiviruses of economic importance, such as epizootic hemorrhagic disease virus (EHDV). Due to the limitations in available molecular tools, critical *Culicoides*-orbivirus interactions underlying vector competence remain unclear. To provide a foundation for the study of midge-EHDV interactions, RNA interference (RNAi) was developed as a reverse genetic tool, and EHDV-2 infection dynamics were determined within *C. sonorensis.* To develop RNAi, exogenous double-stranded RNA (dsRNA) was injected into *C. sonorensis* adults specific to the *C. sonorensis* inhibitor of apoptosis protein 1 (CsIAP1) ortholog (ds*CsIAP1*). A significant decrease in *CsIAP1* transcripts was observed in whole midges, with highest reduction in the midgut. In addition, ds*CsIAP1*-injected midges had increased mortality, a loss of midgut tissue integrity, and increased caspase activity. The longevity and midgut phenotypes were partially reversed by the co-injection of dsRNA specific to the *C. sonorensis* initiator caspase Dronc ortholog and *CsIAP1*. These results demonstrated that RNAi can be achieved in the midge midgut through injection of target dsRNAs into the hemolymph. Furthermore, the time course of EHDV-2 infection within *C. sonorensis* was characterized. EHDV-2 infection was observed in the midgut and secondary tissues, including the salivary glands, by 5 days post-feeding (dpf). These data are consistent with dissemination of EHDV-2 to secondary susceptible tissues throughout the midge via the hemolymph and indicate that virus transmission by *C. sonorensis* may occur as early as 5 dpf. This work provides a foundation for the future study of *Culicoides*-orbivirus interactions, including the antiviral role of RNAi at the midgut barrier.

Table of Contents

List of Figures

List of Tables

List of Abbreviations

Ae. aegypti (Aa)

An. gambiae (Ag)

Antimicrobial peptides (AMPs)

Argonaute 2 (AGO2)

Baculovirus inhibitor of apoptosis repeat (BIR)

Bluetongue (BT)

Bluetongue virus (BTV)

C. sonorensis (Cs)

C. sonorensis co-injected with dsRNA specific to *CsIAP1* and *CsDRONC* (ds*IAP1/dsDRONC*)

C. sonorensis co-injected with dsRNA specific to *GFP* and *CsDRONC* (ds*GFP/dsDRONC*)

C. sonorensis co-injected with dsRNA specific to *GFP* and *CsIAP1* (ds*GFP/dsIAP1*)

C. sonorensis inhibitor of apoptosis protein 1 (CsIAP1)

C. sonorensis ortholog to Dronc; GAWM01016707 (CsDRONC)

C. sonorensis ortholog to IAP1; GAWM01009039 (CsIAP1)

Caspase recruitment domain (CARD)

Culex quinquefasciatus (Cq)

Cytopathic effect (CPE)

D. melanogaster (Dm)

Days (d)

Days post-feeding (dpf)

Days post-injection (dpi)

Death caspase-1 (DCP-1)

Death effector domain (DED)

Death-related ced-3/Nedd2-like protein (Dredd)

Dengue virus (DENV)

Double knockdown (dkd)

Double-stranded RNA (dsRNA)

Drosophila Apaf-1-related killer (DARK)

D. melanogaster IAP1 (DIAP1)

Drosophila melanogaster interleukin-1 converting enzyme (DrICE)

Drosophila Nedd-2-like Caspase (Dronc)

dsRNA specific to CsDRONC (ds*CsDRONC* or ds*DRONC*)

dsRNA specific to CsIAP1 (ds*CsIAP1* or ds*IAP1*)

dsRNA specific to GFP (ds*GFP*)

Epizootic hemorrhagic disease (EHD)

Epizootic hemorrhagic disease virus (EHDV)

Extrinsic incubation period (EIP)

Flock House virus (FHV)

Genome equivalents (GE)

Green fluorescent protein (GFP)

Head involution defect (hid)

Hemorrhagic disease (HD)

Hours post-feed (hpf)

IAP binding motifs (IBM)

*IAP1*knockdown within *C. sonorensis* (*IAP1*kd)

Immunodeficiency (IMD)

Immunohistochemistry (IHC)

Inhibitor of apoptosis (IAP)

Inhibitor of apoptosis 1 (IAP1)

Intrathoracically (IT)

Janus Kinase/Signal Transducer and Activator of Transcription (JAK/STAT)

Knockdown (kd)

Large catalytic caspase subunit (p20)

Mesenteron escape barrier (MEB)

Mesenteron infection barrier (MIB)

Nonstructural protein (Ns)

Nucleotides (nt)

Phosphate Buffered Saline (PBS)

Plaque forming units (PFU)

Polymerase chain reaction (PCR)

Quantitative PCR (qPCR)

Really interesting new gene (RING)

Reverse transcription–quantitative PCR (RT-qPCR)

Rift Valley fever virus (RVFV)

RNA interference (RNAi)

RNA-induced silencing complex (RISC)

Sindbis virus (SNV)

Single-stranded RNA (ssRNA)

Small catalytic caspase subunit (p10)

Small interfering RNA (siRNA)

Systemic RNAi deficient (SID)

United States (US)

Untreated (UT)

Vesicular stomatitis virus (VSV)

Viral inclusion bodies (VIBs)

Viral particle (VP)

West Nile virus (WNV)

Acknowledgements

My graduate work was funded by Specific Cooperative Agreements (SCAs 58-5430-4-022 and 58-3430-1-360) between Kristin Michel and the Arthropod-Borne Animal Diseases Research Unit (USDA-ARS) as well as NIH grant R01AI095842 awarded to Kristin Michel. I would like to thank all past and present members of the Michel, Nayduch, Clem, and Drolet labs, as they were my lab family throughout this process, and without their intellectual input, the work in the dissertation would not be achieved. I would also like to thank the insectary, managed by Jim Kempert and William Yarnell, and the countless midges that gave their lives for my experiments. In addition, I would like to thank my friends I've made through this journey for keeping me sane and allowing me to be a part of their wonderful lives. I would also like to thank my committee for their encouragement and input on the work presented in this dissertation. Furthermore, I would like to specifically thank Dana Nayduch, Tori Rhodes, Binny Bhandary, and Bart Bryant for providing me with both emotional support and intellectual input throughout my graduate career. Finally, I would like to extend thanks to Kristin Michel for mentoring me throughout this process and providing me with a helping hand at every crossroads.

The work in this dissertation is published or *submitted for publication* as follows:

Chapter 1: **Mills, M. K., K. Michel, R. S. Pfannenstiel, M. G. Ruder, E. Veronesi, and D. Nayduch**. **2017**. *Culicoides* – virus interactions: infection barriers and possible factors underlying vector competence. Curr. Opin. Insect Sci. 22: 7–15.

Chapter 2: **Mills, M. K., D. Nayduch, and K. Michel. 2015.** Inducing RNA interference in the arbovirus vector, *Culicoides sonorensis*. Insect Mol. Biol. 24: 105–14.

Chapter 3: **Mills, M. K., D. Nayduch, D. S. McVey, and K. Michel. 2017.** Functional validation of apoptosis genes *IAP1* and *Dronc* in the biting midge *Culicoides sonorensis* by RNAi. J. Med. Entomol. 54: 559-567.

Chapter 4: ***Mills, M.K., M. Ruder, D. Nayduch, K. Michel, and B. Drolet. 2017*** *Dynamics of epizootic hemorrhagic disease virus serotype 2 infection within the vector,* Culicoides sonorensis*. PLoS One.*

Dedication

This dissertation is dedicated to my friends and family who supported me throughout my graduate career, and, even when they didn't understand what I was saying, listened intently to my woes and celebrations. Thank you.

Chapter 1 - Introduction

I. *Culicoides* biting midges

Culicoides midges are hematophagous dipterans in the family Ceratopogonidae, which contain over 5,500 species, including the 1270 species within the genus *Culicoides* (Borkent 2005). Within the United States (US) and Canada there are approximately 151 species of *Culicoides* biting midges (Borkent and Grogan 2009, Vigil et al. 2014). Midges are typically viewed as nuisance biters and pests, since they are blood-feeders with a wide host range and are able to transmit a variety of pathogens (Hopken et al. 2017).

IA. Lifecycle and ecology

For most species, females are anautogenous, requiring a blood meal to produce eggs. Immature *Culicoides* develop through four larval stages that live in moist habitats (Borkent 2005). Complete larval development can occur in as fast as 14 days (d) after hatching (Mullens and Rutz 1983), but can be altered by temperature and substrate quality. Adults are sexually mature 28-48 hours post-eclosion, and, after mating and blood feeding, females oviposit approximately 200 eggs 2-4 d later. Adult females are capable of 3-4 gonotrophic cycles within their lifetimes (Mullens and Schmidtmann 1982), but survival for more than one or two cycles is unlikely.

Midge activity peaks during sunrise and sunset within the summer months, with *Culicoides* inactive during the winter months (Gerry et al. 2001, Viennet et al. 2012). Midge fourth-instar larvae were thought to be the overwintering stage (Barnard and Jones 1980). However, recent evidence demonstrated that the *Culicoides* eggs had high survival against desiccation and temperature reduction, implicating the egg stage to be the essential

overwintering stage of *Culicoides* (McDermott and Mullens 2014). In addition, a previous study determined that *Culicoides* life history traits, such as survival and oviposition, were temperature dependent (Lysyk and Danyk 2007). Higher temperatures reduced survival and time for oviposition, but increased egg clutch size per female (Lysyk and Danyk 2007), suggesting these time periods to be relative to climate. These temperature dependent relationships of fecundity are likely a survival mechanism against increasing temperatures.

IB. Geographic Distribution

The geographic distribution of *Culicoides* was limited to 40°N - 35°S, but changes in climate have increased the range of suitable habitats for these insects (Purse et al. 2005, 2015, Elbers et al. 2015). Only *Culicoides sonorensis* and *Culicoides insignis* are confirmed arbovirus vectors within the US (Figure 1.1A and B) (Foster et al. 1963, 1977, Tanya et al. 1992, Tabachnick 1996), but other vectors of importance remain to be identified, since disease transmission occurs outside the range of these two midge species (Figure 1.1E and F) (Pfannenstiel et al. 2015, Ruder et al. 2015a). While *C. sonorensis* is an important vector in the western US, this species is infrequently recovered in studies of *Culicoides* populations east of the Mississippi river (Holbrook et al. 2000, Borkent and Grogan 2009) and is unlikely to be the primary vector in this region (Vigil et al. 2014). *C. insignis*, which primarily resides in the far southeast US (Vigil et al. 2014), is also unlikely to be an important vector outside of Florida. *Culicoides stellifer* and *Culicoides debilipalpis* are also suspected orbivirus vectors within the US (Figure 1.1C and D) (Smith and Stallknecht 1996, Becker et al. 2010).

IC. *Culicoides* as an arbovirus vector

Regardless of the habitat, *Culicoides* midges are opportunistic blood feeders, and different species have been shown to take blood meals from reptiles (Borkent 2005), birds

(VotÝpka et al. 2009), and mammals (Blackwell et al. 1994). While midges take relatively small blood meals of approximately 100 nl (Mellor et al. 2008), these these insects are able to transmit both non-viral (Linley 1985) and viral (Mellor et al. 2000) pathogens to humans (Pinheiro et al. 1982), birds (Santiago-Alarcon et al. 2012, Ferraguti et al. 2013), and ruminants (Mellor et al. 2000). The World Organization of Animal Health (OIE: www.oie.int/en/animal-health-in-the-world/oie-listed-diseases-2016) outlines the *Culicoides*-vectored pathogens of livestock that are of economic concern. The orbiviruses, bluetongue (BT) virus (BTV) and epizootic hemorrhagic disease (EHD) virus (EHDV) are of significant economic importance worldwide, including the US (Figure 1.1E-F).

II. Orbiviruses transmitted by *Culicoides* midges

BTV and EHDV are both orbiviruses in the family *Reoviridae*. These viruses have a double-stranded RNA (dsRNA) genome, which is composed of ten segments that encode seven structural proteins and four non-structural proteins. The structural proteins that form the outer capsid, viral protein 2 and 5, are encoded by genomic segments 2 and 6, respectively, and the inner capsid, subcore, contains viral proteins 1, 3, 4, 6, and 7, which are encoded on segments 1, 3, 4, 9, and 7, respectively (King et al. 2011).

Currently, BTV has 27 serotypes worldwide, with 15 serotypes found in the US (Hofmann et al. 2008, Schwartz-Cornil et al. 2008, Maan et al. 2011a, Maan et al. 2011b, Jenckel et al. 2015). BTV US-endemic serotypes include BTV-2, -10, -11, -13, and -17 (Tabachnick 1996, Walton 2004, Gibbs and Greiner 2017), with exotic serotypes, BTV-1, -3, -5, -6, -9, -12, -14, -19, -22, and -24, also found in this region (Maan et al. 2007, MacLachlan et al. 2007). On the other hand, EHDV has seven serotypes worldwide (Savini et al. 2011), but only three are

within the US: endemic serotypes, EHDV-1 (Chalmers et al. 1964) and EHDV-2 (Shope et al. 1955, Barber and Jochim 1976), and exotic serotype EHDV-6 (Allison et al. 2010).

IIA. Molecular mechanisms of orbivirus replication

Both BTV and EHDV, as orbiviruses, replicate within insect cells through similar mechanisms (Figure 1.2) (King et al. 2011). First, viral protein 2 of the outer capsid attaches to the cell membrane through a hypothesized coreceptor (Bhattacharya and Roy 2010, Zhang, Boyce, et al. 2010). The attached virion then enters the insect cell via clathrin-mediated endocytosis (Forzan et al. 2007). Next, early endosome acidification allows viral protein 5 to act as a fusion protein to permeablize the endosomal membrane (Hassan et al. 2001, Forzan et al. 2004), resulting in the release of the subcore into the cell cytoplasm. The subcore itself can infect *Culicoides* cells (Mertens et al. 1996, Tan et al. 2001) and is transcriptionally active, producing ten positive-sense, single-stranded RNAs (ssRNAs) corresponding to each genome segment (Fukusho et al. 1989). To produce these ssRNAs, dsRNA genome segments are unwound using the helicase activity of viral protein 6 (Kar and Roy 2003), transcribed via viral protein 1, the viral RNA-dependent RNA polymerase (Urakawa et al. 1989, Boyce et al. 2004), and capped by viral protein 4 (Martinez-Costas et al. 1998, Ramadevi, Burroughs, et al. 1998, Ramadevi, Rodriguez, et al. 1998), which are contained within the subcore. These capped, positive-sense, ssRNAs are released through subcore pores (Diprose et al. 2001) and subsequently used as templates for translation and synthesis of the negative-sense RNA strand of each dsRNA genomic segment (Van Dijk and Huismans 1980, 1988, Mertens et al. 1984). In addition, nonstructural protein 1(Ns1), encoded by segment 5, causes the production of tubules, which are required for primary replication of viral proteins, but the exact function within infected cells is unknown (Boyce et al. 2012, Matsuo and Roy 2013).

To assemble the subcore, Ns2, encoded by genomic segment 8, must be phosphorylated to form viral inclusion bodies (VIBs), which are the site for viral assembly (Brookes et al. 1993, Modrof et al. 2005, Kar et al. 2007). Viral proteins 1, 2, 4, and 6 are recruited (Kar et al. 2007), along with the ssRNA segments of the viral genome to the VIBs (Lymperopoulos et al. 2003, 2006, Modrof et al. 2005, Matsuo and Roy 2009). Mature subcores are produced in the VIB, as the subcores can self-assemble (French et al. 1990, Prasad et al. 1992, Mohl and Roy 2014). Viral protein 5 and 2 are then added outside the VIB to form the mature viral particle (VP) through an unknown mechanism (Bhattacharya et al. 2007, Bhattacharya and Roy 2008). Although Ns3 is required for viral egress by interacting with viral proteins 2 and 5 (Bhattacharya et al. 2007, Bhattacharya and Roy 2008, Celma and Roy 2011), along with several cellular proteins, the exact mechanisms behind virion escape are unknown. Of note, both viral release (Wechsler and McHolland 1988, Hyatt et al. 1989, Celma and Roy 2011) and outer capsid proteins 2 and 5 (Mortola et al. 2004) produce a cytopathic effect (CPE) in mammalian cell lines. This virus-induced CPE is due to the induction of cell death, but does not occur within insect cell lines (Mortola et al. 2004).

IIB. Orbiviruses within ruminants

IIBi. Clinical signs

BTV and EHDV infection results in similar clinical signs to varying degrees based on infected host species, geographic area, and infecting virus serotype. Since these viruses cause such similar diseases, referred to as hemorrhagic disease (HD), differentiation is difficult without additional diagnostic testing and are (Karstad, et al. 1961, Thomas et al. 1974). While HD has been reported throughout the US, readily available seroprevalence data for BTV and EHDV of infected ruminants in the US are limited.

Based on infection studies in white tailed deer, three degrees of HD severity have been established: peracute, acute, and chronic HD (Savini et al. 2011, Verwoerd and Erasmus 2016). Peracute HD clinical signs include high fever, hyperemia of the skin and mucosal membranes, weakness, respiratory distress, nasal and oral discharge, swelling of the head and neck caused by edema and petechiae, bloody diarrhea, anorexia, and dehydration, which result in swift and high mortality rates. In severe cases, animals may die without showing clinical signs and/or by lung edema, resulting in death by asphyxiation. Acute HD causes similar clinical signs as listed for peracute HD, but may also result in skin, heart, and/or abdominal hemorrhaging and ulcer development on the tongue, mouth, and nose. Mouth lesions may become necrotic, which causes foul breath, and, in some cases, the tongue swells and turns blue/purple ("blue tongue"), resulting in labored breathing. Similar to peracute HD, acute forms of HD also result in high mortality rates. On the other hand, animals with chronic HD usually recover after several weeks of the clinical signs mentioned above. Muscle degeneration, scars from internal ulcerations, and lameness due to hoof sloughing may still persist after recovery.

The intensity of HD clinical signs is dependent on the species infected and the viral isolate. BTV clinical signs and severe disease tend to manifest themselves most commonly in susceptible sheep herds, causing increased morality (Spruell 1905, Stair et al. 1968, Vosdingh et al. 1968, Erasmus 1975, Howerth et al. 1988, Szmaragd et al. 2007, Sánchez-Cordón et al. 2013). BTV-infected cattle have historically shown subclinical signs, but recent BTV outbreaks have been linked to severe disease and production loss (Thiry et al. 2006, Szmaragd et al. 2007, Wilson and Mellor 2008, Fabiana et al. 2009). While BTV or EHDV infection of white tailed deer or mule deer populations can result in clinical signs, historically, EHDV severe disease, resulting in increased mortality, is most common in susceptible white tailed deer populations

(Shope et al. 1955, Shope et al. 1960, Fletch and Karstad 1971). EHDV infection in cattle can also result in clinical signs, but the mortality rate is lower than in deer (Inaba 1975, House et al. 1998, Ohashi et al. 1999, Garrett et al. 2015, Hirashima et al. 2015). EHDV does not cause clinical signs in sheep (Foster et al. 1980).

Orbivirus infection intensity is not only host-species specific, but also dependent on geographic location, the presence of endemic virus, and the infecting viral strain. EHDV-infected white tailed deer in the Southern US, where EHDV is endemic, usually have chronic infections or minimal signs of disease. In contrast, white tailed deer from the Northeast US, where EHDV is non-endemic, can have intense clinical signs and high mortality rates (Gaydos et al. 2002, 2004, Michigan Department of Natural Resources 2013, Ruder et al. 2015a, Stevens et al. 2015). In addition, susceptible cattle raised in the US and exposed to the endemic US serotype, EHDV-2, usually have subclinical signs (Abdy et al. 1999, Aradaib et al. 2005). On the other hand, severe clinical disease has been observed in Japanese cattle positive for Ibaraki virus (Inaba 1975, Ohashi et al. 1999), a strain of EHDV-2 (Campbell et al. 1975, Anthony et al. 2009, Hirashima et al. 2015). These data indicate that susceptible ruminant species in virus-endemic regions are less likely to develop clinical HD, while animals raised without the natural presence of virus are at high risk for severe HD if exposed to exotic virus serotypes.

IIBii. Economic Impact

BTV and EHDV cause economic burden due to increased mortality, production loss, and trade restrictions (MacLachlan and Osburn 2006). While BTV infection in cattle can manifest in clinical signs, the mortality rates are relatively low. In contrast, BTV-susceptible sheep herds can have as high as 30% mortality rates (MacLachlan and Gard 2008). Infection of EHDV-susceptible white tailed deer populations in EHDV non-endemic areas can result in high

mortality, as observed in a 2012 US outbreak in Michigan that resulted in 14,000 deer deaths (Michigan Department of Natural Resources 2013, Ruder et al. 2015a, Stevens et al. 2015). In addition, production loss during a 2006 BTV outbreak cost the Netherlands 1.63-1.75 million euros, due to reduced milk production of infected cattle (Velthuis et al. 2010). An EHDV outbreak in the same year also resulted in losses between 1.5 -3.4 million dollars to the Israel dairy industry, due to a reduction in milk yield and increased cullings (Kedmi et al. 2010). Furthermore, trade restrictions on cattle exportation from the US cost approximately 144 million dollars annually (Hoar et al. 2003).

IIC. Orbivirus infection within *C. sonorensis*

Viruses ingested by *Culicoides* midges must pass several infection barriers to ensure salivary gland infection and transmission to the next host. First, viruses must access and infect midgut epithelial cells, which are considered to be the first major barrier to infection (mesenteron infection barrier, MIB) (Fu et al. 1999). Amplified, infectious VPs that are released from midgut epithelial cells have successfully escaped the mesenteron escape barrier (MEB). At this stage, the virus must survive the host defenses within the rest of the body (dissemination barrier) (Fu et al. 1999), including hemolymph immune effectors and cellular responses in midge extraintestinal tissues, to arrive at the salivary glands. No salivary gland infection barrier is believed to exist in the midge (Fu et al. 1999).

Overall, the extrinsic incubation period (EIP), the time between ingestion of infectious virus and transmissibility to naive host, for BTV or EHDV is temperature dependent, with EIP shortening as temperature increases (Mullens et al. 1995, Paweska et al. 2002, Wittman et al. 2002, Carpenter et al. 2011, Ruder et al. 2015b). Ruder et al. (2015b) found the EIP of EHDV-1, -2, and -7 to decrease as temperatures increased. Midges fed on EHDV-7 – infected deer and

held at 20°C had a 12 d EIP, while the EIP of midges held at 30°C was shortened to 2 d (Ruder et al. 2015b). Current and future climate changes could permit the expansion of *Culicoides* to previously non-endemic areas. This shortened EIP is a major concern (Ruder et al. 2015b), as earlier virus transmissibility and longer, infectious midge lifespan would result in increased transmission frequency to susceptible ruminants. To understand the dynamics behind EIP, studies focusing on the viral time course of infection within the midge are invaluable. These studies determine the (1) viral titer, (2) infection prevalence, and (3) dissemination of virus throughout the midge over the course of infection. Minimal studies that focus on all three aspects of the infection time course simultaneously are available, but previous studies have worked to provide a basis for each aspect of the infection time course. The studies described below followed temporal changes in viral titer, prevalence, and dissemination during the course of orbivirus infection within the midge.

IICi. Viral titer

To quantify viral titer over the course of infection, most studies summarized here utilized $TCID_{50}$ endpoint dilution assays, which measure the amount of virus that causes CPE in 50% of susceptible, inoculated cells (Table 1.1). While these assays have a limit of detection ranging from $10^{0.75\text{-}2.3}$ $TCID_{50}$/midge (Foster and Jones 1979, Chandler et al. 1985, Fu et al. 1999, Ruder et al. 2012, Ruder et al. 2015b), an ELISA-based approach with a $10^{0.5}$ $TCID_{50}$/midge detection limit has also been used to quantify virus (Veronesi et al. 2013). Early after infection, 0-4 days post-feed (dpf), titers are near or below the limit of detection due to the low number of infectious virus contained in the small volume of blood ingested (Figure 1.3) (Mellor et al. 2008). Viral titer increases to levels above the detection limit between 4-6 dpf when at 25°C; this event is known as the proliferation phase (Figure 1.3). The proliferation phase is temperature-dependent:

high incubation (30°C) hastens the onset of this event to occur as soon as 2-3 dpf, whereas low temperatures (20°C) can delay the event until 12 dpf, as seen during EHDV-1 infection (Ruder et al. 2015b). In most studies, viral titer increases above the threshold for vector competence ($\geq 10^{2.7}$ $TCID_{50}$/midge) during the proliferation phase. Midges with titer above this threshold are likely able to transmit virus to naïve hosts, suggesting competent midges can be observed when this event occurs (Jennings and Mellor 1987, Fu et al. 1999). After the proliferation phase, viral titer varies over the course of infection (Jennings and Mellor 1987), but does not usually fall below the vector competence threshold at later time points (Chandler et al. 1985, Fu et al. 1999, Ruder et al. 2012, Ruder et al. 2015b).

IICii. Infection Prevalence

The number of virus-positive midges in a population (infection prevalence) can be determined when virus titer was below the limit of detection, as prevalence techniques usually have a lower limit of viral detection (Table 1.1) (Fu et al. 1999, Wittman et al. 2002, Ruder et al. 2012, Ruder et al. 2015b). Overall, prevalence of virus-positive midges is high to moderate (50-100% virus positive) immediately after feeding, 0 dpf, on a high virus titer blood meal ($\geq 10^{5.7}$ $TCID_{50}$/ml), due to detection of ingested virus. The initial prevalence after feeding is dependent on the titer of the infectious blood meal, as Ruder et al. (2012) showed 100% of midges were virus-positive at 0 dpf after feeding on EHDV-7-infected, high viremic deer ($10^{7.03-7.6}$ $TCID_{50}$/ml); however, prevalence at 0 dpf was only 33% after midges fed on EHDV-7-infected, low viremic deer ($10^{3.1-3.9}$ $TCID_{50}$/ml). Regardless of initial infection prevalence, any viable VPs should encounter the mesenteron barriers by 2 dpf, as the blood meal is digested this time point. Blood meal digestion can result in as much as a 70% decrease in prevalence between 2-4 dpf when at 25°C, as seen during EHDV-7 infection (Figure 1.3) (Ruder et al. 2015b). This intense

decrease in infection prevalence between 0-4 dpf is called the primary eclipse. Prevalence subsequently increases and plateaus later in infection (Figure 1.3). Prevalence is also temperature-dependent, where increasing temperatures leads to a higher prevalence (>80%) early during infection (1-4 dpf) and low temperatures result in consistently lower prevalence, as observed during infections of either EHDV-1, EHDV-2, or EHDV-7 (Ruder et al. 2015b). Jennings and Mellor (1987) also found BTV-4 infection prevalence in *Culicoides variipennis* to be between 0-51.6% at 8 dpf, demonstrating prevalence variability at this later time point (Jennings and Mellor 1987).

IICiii. Dissemination

Studies monitoring the dissemination of BTV infection in the midge were recorded using an array of detection techniques in a limited number of studies and serotypes (BTV-1, -10, -11, and -17) (Ballinger et al. 1987, Sieburth et al. 1991, Fu et al. 1999, Veronesi et al. 2013). The peritrophic matrix was formed in the midge midgut by 1 d post blood meal ingestion, but did not prevent interaction of BTV-11 with the midgut epithelia early after ingestion (Sieburth et al. 1991). Of note, Sieburth et al. (1991) found BTV-11 virions associated with the midgut epithelia as early as 1 hours post-feed (hpf) and VPs outside the basal lamina by 3 dpf. In competent midges, the MEB was apparently bypassed by BTV-1 as early as 2 dpf, as evidenced by fat body infection (Fu et al. 1999). Data from transcriptomic studies that focused on midge-virus interactions also align with dissemination observations. Since BTV enters insect cells via clathrin-mediated endocytosis (Stevens, Lisa 2015), the presence of up-regulation of clathrin-heavy chain transcripts at 2 dpf may reflect virion entry into midge cells early in infection (Campbell and Wilson 2002, Campbell et al. 2005). Several studies observed virus in extra-

intestinal tissues, including the salivary glands, between 5-7 dpf (Ballinger et al. 1987, Fu et al. 1999, Veronesi et al. 2013).

IICiv. Overall trends in midge infection

These studies summarized above demonstrate the complexity of orbivirus infection time course and events within *Culicoides* midges (Figure 1.3). Nevertheless, we can determine critical time points during infection. The blood meal is present within the midgut from 0-2 dpf, and virus disseminates from the mesenteron barrier between 2-3 dpf (Sieburth et al. 1991, Fu et al. 1999). At these early time points, virus titer is normally below the limit of detection, and the primary eclipse phase in infection prevalence is also observed. Genes and proteins putatively involved in vector-virus interactions at the mesenteron barrier would be expressed or activated between 1-3 dpf. Such interactions are proposed to be the mechanism behind orbivirus infection refractoriness and permissiveness within *Culicoides*. Fu et al. (1999) demonstrated that upon oral infection of BTV-1, midges from the refractory *Culicoides* colony were unable to transmit the virus (Fu et al. 1999). Only after intrathoracic injection of BTV-1 was 100% of the midges from the refractory colony able to transmit the virus (Fu et al. 1999), suggesting the midgut is a key barrier against permissive BTV infections within the midge.

Infection of the salivary glands was not observed until 5 dpf (Ballinger et al. 1987, Fu et al. 1999), which coincided with increasing prevalence and viral proliferation. The proliferation phase normally results in viral titer $\geq 10^{2.7}$ $TCID_{50}$/midge, which suggests that this threshold titer can be used to assess vector competence and associated salivary gland infection. However, because studies have demonstrated that viral titer and prevalence are temperature-dependent (Wittman et al. 2002, Carpenter et al. 2011, Ruder et al. 2015b), the detection of competent

midges (via this threshold titer) and dissemination dynamics could both be impacted by temperatures used during experimental studies.

III. Antiviral defenses

Both field-caught and colonized *Culicoides* show inter-individual variability in vector competence, yet the mechanism underlying refractoriness or permissiveness for virus infection and transmission remains unknown. Selection experiments have generated refractory *Culicoides* lines (Tabachnick 1990), which demonstrate heritable vector competence traits in *Culicoides* (Tabachnick 1991, Fu et al. 1999). Refractoriness may result from selection against midgut receptors for virus entry or selection for robust antiviral defenses. Such antiviral defenses within the midgut epithelia (MIB and MEB) include RNA interference (RNAi), apoptosis, autophagy and JAK/STAT (Janus Kinase/Signal Transducer and Activator of Transcription) pathways. The dissemination barrier also presents multiple antiviral defenses, including hemocytes, prophenoloxidases, and antimicrobial peptides produced by Toll and IMD (Immunodeficiency) pathways (Ip 2005, Calvo et al. 2009, Yordy and Iwasaki 2011, Zhao et al. 2011, Rodriguez-Andres et al. 2012, Sim et al. 2012, Merkling and van Rij 2013, Xiao et al. 2014, Lan et al. 2016). Putative orthologs of components of these major pathways in *Culicoides* are listed (Table 1.2) (Waterhouse et al. 2007, Nayduch et al. 2014b, Nayduch, Lee, et al. 2014c). Further *in vivo* experiments are needed to determine the role of these pathways in *Culicoides* antiviral defense.

IIIA. RNA interference

RNAi is the a prominent antiviral defense mechanism in plants, nematodes, and invertebrates (Li et al. 2002, Keene et al. 2004, Sarkies and Miska 2013, Gammon and Mello 2015). This pathway recognizes viral dsRNAs for targeted dicing of the corresponding

complementary mRNA, effectively hindering viral translation (Figure 1.4B) (Ding 2010, Mongelli and Saleh 2016). The naturally recognized dsRNAs are either generated from the viral genome or synthesized during viral transcription. DsRNAs are recognized by the endoribonuclease, Dicer 2, and spliced into siRNAs (Carthew and Sontheimer 2009, Kim et al. 2009). SiRNAs are approximately 21 nucleotides (nt) long with 2 nt 3' overhangs (Elbashir et al. 2001, Lee et al. 2004) and loaded into an Argonoute 2 (AGO2)-containing RNA-induced silencing complex (RISC) by R2D2 (Carthew and Sontheimer 2009, Kim et al. 2009, Marques et al. 2013, Mirkovic-Hosle and Forstemann 2014). While the RISC complex releases the siRNA "passenger" strand, the "guide" strand remains bound and is subsequently methylated (Horwich et al. 2007, Saito et al. 2007). The "guide" strand recognizes the complementary RNA sequence, leading to the dicing of the target via AGO2 (Figure 1.4B) (Carthew and Sontheimer 2009, Kim et al. 2009).

IIIAi. Antiviral RNAi pathway

The RNAi pathway is a confirmed antiviral response in multiple insects, including mosquitoes. Dengue (DENV), west nile virus (WNV), and Sindbis virus (SINV) infection within mosquitoes resulted in the generation of siRNAs specific to viral transcripts, indicating the induction of the RNAi pathway (Sanchez-Vargas et al. 2009, Brackney et al. 2009, Cirimotich et al. 2009). Member(s) of the RNAi pathway were also targeted for knockdown using RNAi as a molecular tool (Chapter 1. IIIAii - RNAi as a molecular tool), which resulted in an increased viral load within mosquito vectors (Keene et al. 2004, Sanchez-Vargas et al. 2009). These studies confirmed that the RNAi pathway was used as an natural antiviral response within vector mosquitoes.

Viruses also evolved mechanisms to suppress RNAi within their infected host, including: (A) binding long dsRNAs to hide them from Dicer 2, (B) binding siRNAs to prevent loading into RISC, or (C) directly binding either Dicer 2/AGO2 to stop RNAi activity (Bronkhorst and Van Rij 2014). In insects, dsRNA and/or siRNA binding was observed during infection of invertebrate iridescent virus 6 (*Iridoviridae*), Drosophila X virus (*Birnaviridae*), Drosophila C virus (*Dicistroviridae*), and cricket paralysis virus (*Dicistroviridae*) within *Drosophila melanogaster* and Culex Y virus (*Birnaviridae*) within mosquito species (van Rij et al. 2006, Bronkhorst et al. 2012, Mierlo et al. 2014). In addition, direct interference of Dicer 2 or AGO2 was recorded during cricket paralysis virus (*Dicistroviridae*), DENV (*Flaviviridae*), and WNV (*Flaviviridae*) infection within *D. melanogaster, Spodoptera frugiperda*, and *Ae. albopictus*, respectively (Nayak et al. 2010, Schnettler et al. 2012, Kakumani et al. 2013).

Since orbiviruses, such as BTV, are thought to only release single-stranded positive sense mRNAs (Diprose et al. 2001). In addition orbiviruses synthesize the dsRNA genome segments within the viral core (Patel and Roy 2014), and the viral core binds dsRNAs (Diprose et al. 2002). Based on these data, the siRNA machinery may never "see" the dsRNA genome segments necessary for activating this defense pathway. Schnettler et al. (2013) provided BTV-1-infected *Culicoides* cells with exogenous dsRNA specific to BTV-1 Ns1, which reduced viral load compared to controls. These experiments support RNAi as a functional pathway within *Culicoides* cells and a potential antiviral defense. While the RNAi pathway is a critical antiviral defense in other dipterans (Ding 2010, Marques and Imler 2016), its *in vivo* function against orbiviruses, such as BTV and EHDV, in *Culicoides* requires further study.

IIAii. RNAi as a molecular tool

While RNAi is an antiviral mechanism, Fire et al. 1998 were the first to utilize this pathway for targeted mRNA knockdown in *Caenorhabditis elegans* (Fire et al. 1998). RNAi has since been used to study gene function in various organisms, including insects (Huvenne and Smagghe 2010, Scott et al. 2013, Zhang et al. 2013). RNAi can be either cell autonomous, where targeted mRNA dicing occurs only within the introduced cell, or cell non-autonomous, where dsRNA can (A) enter a cell from the environment (environmental RNAi) and/or (B) the silencing signal can be transported to neighboring cells (systemic RNAi, Figure 1.4C) (Huvenne and Smagghe 2010).

DsRNA uptake and subsequent RNAi utilization also varies between insect species. While *C. elegans* receptors required for environmental (systemic RNAi deficient (SID)-2 and -5) and systemic (SID-1) RNAi (Winston et al. 2002, 2007, Hinas et al. 2012) have been identified, few, if any, orthologs of these receptors have been identified in insect species (Huvenne and Smagghe 2010). RNAi within insects seems to be dependent on endocytosis, but the exact mechanisms of dsRNA uptake remain unknown (Scott et al. 2013). The red flower beetle, *Tribolium castaenuem*, is able to utilize environmental RNAi with an intensely robust systemic response (Miller et al. 2012). In contrast, most Dipterans are unable to spread the silencing signal to adjacent cells, but are susceptible to environmental RNAi (Huvenne and Smagghe 2010, Scott et al. 2013). The uptake of exogenous dsRNA from the environment facilitates the use of RNAi as a molecular tool for use in targeted gene knockdown in these insects, including non-model organisms. Indeed, it is suspected that *Culicoides* is able to utilize environmental RNAi, as *Culicoides* cells were able to uptake and use exogenous dsRNA for their own RNAi response (Schnettler et al. 2013).

Targeted gene knockdown can be achieved by injection of exogenous dsRNAs (Blandin et al. 2002, Sant'Anna et al. 2009) into the hemolymph or feeding of target dsRNAs (Baum et al. 2007, Price and Gatehouse 2008, Zhang, Zhang, et al. 2010, Yu et al. 2013). Successful transcript knockdown depends on multiple factors, such as proper dsRNA concentration, base pair length, and target specificity (Scott et al. 2013). In addition, the injected dsRNA should have an optimal length between 300-500 base pairs (Saleh et al. 2006, Kumar et al. 2009) and be designed specific for the target sequence to ensure no knockdown of a non-targeted transcript (Araujo et al. 2006, Baum et al. 2007). In many cases intensity of gene knockdown usually declines over time, suggesting the timing of injection and sample processing is critical for experimental success (Turner et al. 2006, Shakesby et al. 2009).

IIIB. Apoptosis

Apoptosis is the conserved mechanism of programmed cell death and is involved in several multicellular biological processes, such as regulation of embryonic development (Wilson et al. 2002) and proper development and functioning of the immune system (Opferman and Korsmeyer 2003). Programmed cell death also serves as an insect antiviral defense, where infected cells commit self-destruct to inhibit viral replication (Clarke and Clem 2003). Apoptosis occurs through the activation of cysteine proteases called caspases that cleave cellular components at aspartic acid residues, resulting in cell death (Figure 1.4A) (Hengartner 2000, Clem 2016).

IIIBi. Caspases

Caspases are produced as inactive zymogens that contain three domains: the N-terminal prodomain, the large catalytic subunit (p20), and the small catalytic subunit (p10) (Raff 1998, Hengartner 2000). Caspase activation requires the zymogen to be cleaved twice to separate (A)

the prodomain from p20 and (B) p20 from p10 (Cohen 1997, Nicholson 1999). Next, these individual subunits come together to form the active caspase, which is a tetramer composed of two p20/p10 heterodimers with two active sites (Thornberry et al. 1997, Raff 1998, Earnshaw et al. 1999). Of note, not all caspases are involved in apoptosis, such as *D. melanogaster* caspase Dredd (Death-related ced-3/Nedd2-like protein), which is required for AMP expression induced by the IMD pathway (Leulier et al. 2000, Meinander et al. 2012).

Caspases are divided into initiator and effector caspases based on the length of their prodomains, which determine their route of activation. Initiator caspases have a long prodomain, which contains a caspase recruitment domain (CARD) or death effector domain (DED). While initiator caspases are activated by dimerization (Boatright et al. 2003, Donepudi et al. 2003), some initiator caspases can also require the association of a cofactor(s) to these specific domains within the prodomain to be activated (Li et al. 1997, Zou et al. 1999). The *D. melanogaster* initiator caspase involved in apoptosis, Dronc (*Drosophila* Nedd-2-like Caspase), has protein sequence similarity to the mammalian initiator caspase-9 (Dorstyn et al. 1999) and a CARD domain within its prodomain (Dorstyn et al. 1999). The required cofactor, DARK (*Drosophila* Apaf-1-related killer), binds the Dronc CARD domain for auto-processing and activation (Rodriguez et al. 1999, 2002, Quinn et al. 2000). Ectopic expression of *Dronc* within *D. melanogaster* cells resulted in apoptosis, which was inhibited by the addition of caspase-specific inhibitors, suggesting Dronc was involved in caspase-dependent apoptosis (Dorstyn et al. 1999). Later experiments confirmed Dronc as an initiator caspase, as dominant negative *Dronc* mutant flies rescued the apoptosis induced by the pro-apoptotic genes, *reaper, hid* (head involution defect), and/or *grim* (Hawkins et al. 2000, Meier et al. 2000).

Effector caspases have shorter prodomains that are cleaved by initiator caspases for activation, resulting in subsequent cellular substrate cleavage (Raff 1998, Thornberry 1998, Stennicke and Salvesen 2000, Ho and Hawkins 2005, Ho et al. 2005). The effector caspases involved in apoptosis in *D. melanogaster* were determined to be DrICE (*D. melanogaster* interleukin-1 converting enzyme) and DCP-1 (death caspase-1). These effector caspases function like the previously described mammalian effector caspase-3 (Song et al. 1997). *D. melanogaster* cell-line experiments revealed increased apoptosis after DrICE overexpression (Fraser and Evan 1997). In addition, after DrICE immunodepletion, a decrease in apoptosis induced by *reaper* was observed (Fraser et al. 1997). These data, along with observations that DrICE mutations in *D. melanogaster* were resistant to increased apoptosis caused by *reaper, hid,* or *grim* overexpression *in vivo*, confirm DrICE as a key effector caspase involved in cell death (Muro et al. 2006). Furthermore, Xu et al demonstrated that DrICE and DCP-1 have overlapping apoptotic functions as effector caspases (Xu et al. 2006).

IIIBii. Apoptosis regulation: IAP1

Caspase-dependent apoptosis is regulated through several mechanisms, including caspase inhibition by metalloproteins in the inhibitor of apoptosis (IAP) protein family (Figure 1.3A) (Deveraux and Reed 1999, Salvesen and Duckett 2002, Berthelet and Dubrez 2013). IAPs consist of 1-3 baculovirus inhibitor of apoptosis repeat (BIR) domains, containing a zinc binding, Cys/His motif ($GX_2YX_4DX_3CX_2CX_6WX_9HX_{6\text{-}10}C$) (Hinds et al. 1999, Miller 1999, Sun et al. 1999). Of note, not all IAPs are involved in apoptosis regulation, as BIR domains can have distinct protein-binding properties (Eckelman et al. 2008). Specifically, type II BIR domains form a hydrophobic groove that binds IAP binding motifs (IBM), which aids in caspase inhibition (Duckett et al. 1998). Anti-apoptotic IAPs also have a RING (really interesting new

gene) zinc-finger domain at the carboxy terminus, which has E3-ubiquitin ligase activity. This domain is required for auto- and target caspase-ubiquination that leads to proteasome degradation (Joazeiro and Weissman 2000, Yang et al. 2000, Wilson et al. 2002). *D. melanogaster* IAP1 (DIAP1) inhibited apoptosis caused by active DrICE (Kaiser et al. 1998) and Dronc (Hawkins et al. 2000, Meier et al. 2000, Muro et al. 2002).Furthermore, DIAP1 overexpression reduced the cell death induced by the overexpression of *reaper* or *hid* (Hay et al. 1995). Furthermore, inhibition of DIAP1 led to increased caspase-dependent apoptosis (Goyal et al. 2000).

DIAP1 has two BIR domains and a RING domain, which interacts with Dronc, and/or DrICE to inhibit apoptosis (Figure 1.3A). DIAP1 BIR1, a type II BIR domain, is only able to bind active DrICE, as the IBM of DrICE p20 is exposed after activated cleavage (Yan et al. 2004). This binding of DIAP1 to DrICE alone reduces the catalytic activity of this effector caspase (Yan et al. 2004), suggesting DIAP1 binding itself inhibited active DrICE. Similarly, DIAP1 also inhibited DCP-1 activity through binding (Hawkins et al. 1999). In contrast, Dronc does not contain an IBM, but DIAP is able to recognize a five amino acid long sequence in the linker region between the Dronc prodomain and p20 (Chai et al. 2003). While, binding of DIAP1 to this sequence has no effect on Dronc catalytic activity (Yan et al. 2004), Dronc is degraded by the proteasome after ubiquination by the DIAP1 RING domain (Wilson et al. 2002). These interactions between caspases and IAPs are essential for a apoptotic response, and orthologs of these conserved apoptotic pathway members have been identified in multiple mosquito vector species, including *Ae. aegypti* (Waterhouse et al. 2007, Bryant et al. 2008, Liu and Clem 2011, Wang and Clem 2011).

IIIBiii. Antiviral Apoptosis

Activation of caspase-dependent apoptosis has been observed during viral infection within insects. Mims et al. (1966) observed apoptosis within both the midgut and salivary glands upon Semliki Forest virus infection of *Ae. aegypti* mosquitoes, correlating apoptosis with antiviral defenses that prevent persistent viral infection in this species. Infection with SINV and WNV also causes to apoptosis in the salivary glands of their insect vectors, *Aedes albopictus* and *Culex pipiens quinquefasciatus*, respectively (Bowers et al. 2003, Girard et al. 2005, Kelly et al. 2012). These infections correlated with decreased feeding behavior and reduction in viral load (Bowers et al. 2003, Girard et al. 2005, Griard et al. 2007, Kelly et al. 2012).

While these data suggest a link between apoptosis and viral infection responses, later studies directly probed the contribution of apoptosis to antiviral defense through the use of transgenics and targeted gene knockdown via RNAi. After infection of either baculovirus or flock house virus (FHV), Liu et al. (2013) observed transgenic *D. melanogaster* strains with loss of function mutations to pro-apoptotic genes had higher viral titers than wild-type controls. These data indicated that apoptosis limited baculovirus or FHV infection within *D. melanogaster.* In addition, Liu et al. (2013) also observed an increase of *Ae. aegypti* pro-apoptotic gene, *michelob_x*, transcripts after DENV infection, suggesting apoptosis could also be used as an antiviral defense against this virus. Furthermore, Ocampo et al. (2013) used RNAi to knockdown transcripts of the *Ae. aegypti Dronc* ortholog and caspase-16, which resulted in increased DENV infection prevalence in the refractory mosquito line when compared to non-treated controls after oral DENV infection. However, RNAi knockdown of *Ae. aegypti Dronc* and *IAP1* orthologs resulted in reduced and increased SINV titers, respectively, in orally infected mosquitoes (Wang et al 2012). While these data suggest SINV utilizes programmed cell death, Wang et al. (2012) also observed increased mosquito mortality after knockdown of *IAP1* (Wang

et al. 2012). O'Neill et al. (2015) observed reduced infection establishment when comparing mosquitoes fed the pro-apoptotic, *reaper*-expressing SINV when compared to mosquitoes infected with wild-type virus. Furthermore, deep sequencing analyses revealed a strong selection against the *reaper* insertion, indicating apoptosis hinders SINV replication (O'Neill et al. 2015). These studies showcase the variability of caspase-dependent apoptosis as an insect antiviral defense.

In contrast, viruses have also evolved mechanisms to prevent programmed cell death (Hay and Kannourakis 2002, Clem 2007, Richard and Tulasne 2012). Rift Valley fever virus (RVFV) NSm gene is responsible for the inhibition of apoptosis within its vector, *Ae. aegypti* (Won et al. 2007). *Ae. aegypti* mosquitoes infected with a mutant RVFV with a NSm deletion had reduced infection, dissemination, and transmission rates when compared to mosquitoes infected with the wild-type virus (Crabtree et al. 2012, Kading et al. 2014). In addition, Kading et al. observed reduced infection and subsequent dissemination of the NSm-mutated RVFV within the mosquito midgut, as compared to wild-type infections (Kading et al. 2014). These data indicate that apoptosis is detrimental for infection establishment of RVFV and an important aspect of vector competence.

Currently, it is unclear whether apoptosis is used as an antiviral defense in *Culicoides* species. However, apoptosis is induced during orbivirus infection in mammalian cells (Li et al. 2007, Nagaleekar et al. 2007, Mortola and Larsen 2009, Stewart and Roy 2010). Extracellular exposure to BTV outer capsid proteins 2 and 5 resulted in mammalian cell death, but the induced apoptosis was inhibited by endocytosis inhibitors (Mortola et al. 2004). While these data suggest the induction of endocytosis by BTV proteins is sufficient to activate the apoptotic pathway, the target cell membrane receptor and subsequent activating mechanisms behind this response in

mammalian cells remain unclear. Interestingly, *Culicoides* cell lines infected with orbivirus do not display an apoptotic response (Mortola et al. 2004). *In vivo* studies on orbivirus-refractory *Culicoides* species are needed to confirm if apoptosis functions as a successful barrier to infection in these poor-vector species.

IV. Dissertation overview

As summarized in Chapter 1, while *Culicoides* midges vector economically important orbiviruses, there is a lack of data available on (A) midge biology and (B) midge-orbivirus infection dynamics within *Culicoides.* Currently, the immune pathways involved in antiviral defenses against orbiviruses within *C. sonorensis*, including the RNAi and apoptotic pathways, remain unclear, as the absence of molecular tools has prevented the functional analyses of immune pathway members and their potential role as an antiviral defense. In addition, there is a need for infection dynamic studies monitoring infection prevalence, viral load, and viral dissemination within the midge, simultaneously, as these data are required for accurate epidemiological modeling to determine the intensity of potential outbreaks and for the design of effective experiments focusing on vector-virus interactions within *C. sonorensis*. Overall, there is a clear gap in knowledge within the *Culicoides* field that could be filled by the development of molecular tools and comprehensive infection studies focusing on the vector.

To fill the deficit of next generation resources and tools available to study *Culicoides* (Nayduch et al. 2014a), this dissertation aimed to establish RNAi as a reverse genetic tool for targeted gene knockdown in the vector, *C. sonorensis*, and, in the process, increase the understand of the RNAi pathway in this organism. As previously mentioned in this chapter, exogenous dsRNA induced an RNAi response in *Culicoides* cell lines (Schnettler et al. 2013),

and multiple studies demonstrated that related dipteran vectors are able to utilize environmental RNAi (Blandin et al. 2002, Sant'Anna et al. 2009). Based on these studies we tested the hypotheses that the RNAi machinery exists within *C. sonorensis* and is inducible through uptake of exogenous dsRNA triggers provided in the hemolymph by intrathoracic injection of the adult midge. The establishment of RNAi in *C. sonorensis* would allow for the study of both midge biology and vector competence through targeted gene knockdown.

Due to the lack of data available on orbivirus infection within *C. sonorensis* outlined within this chapter, this dissertation reported the EHDV-2 infection dynamics, by monitoring infection prevalence, viral load, and viral dissemination simultaneously during EHDV-2 infection within *C. sonorensis*. Based on previous orbivirus studies (Fu et al. 1999, Veronesi et al. 2013, Wittman et al. 2002, Ruder et al. 2012, Ruder et al. 2015b), we hypothesized that EHDV-2 infection would result in both non-permissive and permissive infections within the exposed *C. sonorensis* population. Additionally, we also hypothesized that the EIP of EHDV-2 would be similar to the findings observations by Ruder et al. (2015b) that EHDV-2 had an EIP of 6 dpf when held at 25°C. These data would fill an important gap in the *Culicoides* vector field, and provide needed information for epidemiological models for the proper preparation against EHDV-2 outbreaks. In addition, this dissertation would confirmed key time points encompassing EHDV-2 passage of the MIB and MEB and the infection of the salivary glands.

Acknowledgments

Part of this chapter was published in 2017 by Elsevier in the journal Current Opinion in Insect Science, volume 22, from pages 7-15, and titled "*Culicoides*-virus interactions: infection

barriers and possible factors underlying vector competence" (DOI:

https://doi.org/10.1016/j.cois.2017.05.003).

References

(OIE-Listed diseases 2016: OIE - World Organisation for Animal Health) . **n.d.** OIE-Listed diseases 2016: OIE - World Organisation for Animal Health. (http://www.oie.int/en/animal-health-in-the-world/oie-listed-diseases-2016/).

Abdy, M., E. W. Howerth, and D. E. Stallknecht. **1999**. Experimental infection of calves with epizootic hemorrhagic disease virus. Am. J. Vet. Res. Artic. 60: 621–626.

Allison, A. B., V. H. Goekjian, A. C. Potgieter, W. C. Wilson, D. J. Johnson, P. P. C. Mertens, and D. E. Stallknecht. **2010**. Detection of a novel reassortant epizootic hemorrhagic disease virus (EHDV) in the USA containing RNA segments derived from both exotic (EHDV-6) and endemic (EHDV-2) serotypes. J. Gen. Virol. 91: 430–439.

Anthony, S. J., S. Maan, N. Maan, L. Kgosana, K. Bachanek-Bankowska, C. Batten, K. E. Darpel, G. Sutton, H. Attoui, and P. P. C. Mertens. **2009**. Genetic and phylogenetic analysis of the outer-coat proteins VP2 and VP5 of epizootic haemorrhagic disease virus (EHDV): comparison of genetic and serological data to characterise the EHDV serogroup. Virus Res. 145: 200–210.

Aradaib, I. E., R. A. Mederos, and B. I. Osburn. **2005**. Evaluation of epizootic haemorrhagic disease virus infection in sentinel calves from the San Joaquin Valley of California. Vet. Res. Commun. 29: 447–451.

Araujo, R., A. Santos, F. Pinto, M. Lehane, and M. Pereira. **2006**. RNA Interference of the salivary gland nitrophorin 2 in the Triatomine Bug *Rhodnius Prolixus* (Hemiptera: Reduviidae) by dsRNA ingestion or injection. Insect Biochem. Mol. Biol. 36: 683–693.

Ballinger, M. E., R. H. Jones, and B. J. Beaty. **1987**. The comparative virogenesis of three serotypes of bluetongue virus in *Culicoides variipennis* (Diptera: Ceratopogonidae). J. Med. Entomol. 24: 61–65.

Barber, T. L., and M. M. Jochim. **1976**. Serotyping bluetongue and epizootic hemorrhagic disease virus strains. Proc. Am. Assoc. Vet. Lab. Diagn. 18: 149–157.

Barnard, D. R., and R. H. Jones. **1980**. *Culicoides variipennis*: seasonal abundance, overwintering, and voltinism in northeastern Colorado. Environ. Entomol. 9: 709–712.

Baum, J. A., T. Bogaert, W. Clinton, G. R. Heck, P. Feldmann, O. Ilagan, S. Johnson, G. Plaetinck, T. Munyikwa, M. Pleau, T. Vaughn, and J. Roberts. **2007**. Control of Coleopteran insect pests through RNA interference. Nat. Biotechnol. 25: 1322–1326.

Becker, M. E., W. K. Reeves, S. K. Dejean, M. P. Emery, E. N. Ostlund, and L. D. Foil. **2010**. Detection of bluetongue virus RNA in field-collected *Culicoides*, spp. (Diptera: Ceratopogonidae) following the discovery of bluetongue virus serotype 1 in white-tailed deer and cattle in Louisiana. J. Med. Entomol. 47: 269–273.

Berthelet, J., and L. Dubrez. **2013**. Regulation of apoptosis by inhibitors of apoptosis (IAPs). Cells. 2: 163–187.

Bhattacharya, B., R. J. Noad, and P. Roy. **2007**. Interaction between bluetongue virus outer capsid protein VP2 and vimentin is necessary for virus egress. Virol. J. 4: 1–12.

Bhattacharya, B., and P. Roy. **2008**. Bluetongue virus outer capsid protein VP5 interacts with membrane lipid rafts via a SNARE domain. J. Virol. 82: 10600–10612.

Bhattacharya, B., and P. Roy. **2010**. Role of lipids on entry and exit of bluetongue virus, a complex non-enveloped virus. Viruses. 2: 1218–1235.

Blackwell, A., A. J. Mordue Luntz, and W. Mordue. **1994**. Identification of bloodmeals of the Scottish biting midges, *Culicoides impuctatus*, by indirect enzyme-linked immunosorbent assay (ELISA). Med. Vet. Entomol. 8: 20–24.

Blandin, S., L. F. Moita, T. Köcher, M. Wilm, F. C. Kafatos, and E. A. Levashina. **2002**. Reverse genetics in the mosquito *Anopheles gambiae*: targeted disruption of the *Defensin* gene. EMBO Rep. 3: 852–856.

Boatright, K. M., M. Renatus, F. L. Scott, S. Sperandio, H. Shin, I. M. Pedersen, J. Ricci, W. A. Edris, D. P. Sutherlin, D. R. Green, G. S. Salvesen, S. Diego, D. N. A. Way, and S. S. Francisco. **2003**. A unified model for apical caspase activation. Mol. Cell. 11: 529–541.

Borkent, A. 2005. The Biting Midges, the Ceratopogonidae (Diptera), pp. 113–126. *In* Marquardt, W.H. (ed.), Biol. Dis. Vectors. Academic Press.

Borkent, A., and W. L. Grogan. **2009**. Catalog of the New World biting midges north of Mexico (Diptera: Ceratopogonidae). Zootaxa. 2273: 1–48.

Bowers, D. F., C. Coleman, and D. T. Brown. **2003**. Sindbis virus-associated pathology in *Aedes albopictus* (Diptera: Culicidae). J. Med. Entomol. 40: 698–705.

Boyce, M., C. C. P. Celma, and P. Roy. **2012**. Bluetongue virus non-structural protein 1 is a positive regulator of viral protein synthesis. Virol. J. 9: 1–11.

Boyce, M., J. Wehrfritz, R. Noad, and P. Roy. **2004**. Purified recombinant bluetongue virus VP1 exhibits RNA replicase activity. J. Virol. 78: 3994–4002.

Bronkhorst, A. W., K. W. R. Van Cleef, and N. Vodovar. **2012**. The DNA virus Invertebrate iridescent virus 6 is a target of the *Drosophila* RNAi machinery. Proc. Natl. Acad. Sci. U. S. A. 109: 2604–3603.

Bronkhorst, A. W., and R. P. Van Rij. **2014**. The long and short of antiviral defense: Small RNA-based immunity in insects. Curr. Opin. Virol. 7: 19–28.

Brookes, S. M., A. D. Hyatt, and B. T. Eaton. **1993**. Characterization of virus inclusion bodies in bluetongue virus-infected cells. J. Gen. Virol. 74: 525–530.

Bryant, B., C. D. Blair, K. E. Olson, and R. J. Clem. **2008**. Annotation and expression profiling of apoptosis-related genes in the yellow fever mosquito, *Aedes aegypti*. Insect Biochem. Mol. Biol. 38: 331–345.

Calvo, E., V. Pham, O. Marinotti, J. Andersen, and J. Ribeiro. **2009**. The salivary gland transcriptome of the neotropical malaria vector *Anopheles darlingi* reveals accelerated evolution of genes relevant to hematophagy. BMC Genomics. 10: 1–27.

Campbell, C. H., S. S. Breese Jr, and P. D. McKercher. **1975**. Antigenic and morphologic comparisons of Ibaraki and bluetongue viruses. Can. J. Microbiol. 21: 2098–2102.

Campbell, C. L., K. A. Vandyke, G. J. Letchworth, B. S. Drolet, T. Hanekamp, and W. C. Wilson. **2005**. Midgut and salivary gland transcriptomes of the arbovirus vector *Culicoides sonorensis* (Diptera: Ceratopogonidae). Insect Mol. Biol. 14: 121–136.

Campbell, C. L., and W. C. Wilson. **2002**. Differentially expressed midgut transcripts in *Culicoides sonorensis* (Diptera: Ceratopogonidae) following orbivirus (*Reoviridae*) oral feeding. Insect Mol. Biol. 11: 595–604.

Carpenter, S., A. Wilson, J. Barber, E. Veronesi, P. Mellor, G. Venter, and S. Gubbins. **2011**. Temperature dependence of the extrinsic incubation period of orbiviruses in *Culicoides* biting midges. PLoS One. 6: e27987.

Carthew, R. W., and E. J. Sontheimer. **2009**. Review origins and mechanisms of miRNAs and siRNAs. Cell. 136: 642–655.

Celma, C. C. P., and P. Roy. **2011**. Interaction of calpactin light chain (S100A10/p11) and a

viral NS protein is essential for intracellular trafficking of nonenveloped bluetongue virus. J. Virol. 85: 4783–4791.

Chai, J., N. Yan, J. R. Huh, J. Wu, W. Li, B. A. Hay, and Y. Shi. **2003**. Molecular mechanism of Reaper-Grim-Hid-mediated suppression of DIAP1-dependent Dronc ubiquitination. Nat. Struct. Biol. 10: 892–898.

Chalmers, G. A., H. N. Vance, and G. J. Mitchell. **1964**. An outbreak of epizootic hemorrhagic disease in wild ungulates in Alberta. Wildl. Dis. 42: 1–6.

Chandler, L. J., M. E. Ballinger, R. H. Jones, and B. J. Beaty. **1985**. The virogenesis of bluetongue virus in *Culicoides variipenis*. Prog. Clin. Biol. Res. 178: 245–253.

Clarke, T. E., and R. J. Clem. **2003**. Insect defenses against virus infection: the role of apoptosis. Int. Rev. Immunol. 22: 401–24.

Clem, R. J. 2007. Baculoviruses and apoptosis: a diversity of genes and responses. Curr. Drug Targets. 8: 1069–1074.

Clem, R. J. 2016. Arboviruses and apoptosis: the role of cell death in determining vector competence. J. Gen. Virol. 97: 1033–1036.

Cohen, G. M. 1997. Caspases: the executioners of apoptosis. Biochem. J. 326: 1–16.

Crabtree, M. B., R. J. K. Crockett, B. H. Bird, S. T. Nichol, B. R. Erickson, B. J. Biggerstaff, K. Horiuchi, and B. R. Miller. **2012**. Infection and transmission of Rift Valley fever viruses lacking the NSs and/or NSm genes in mosquitoes: potential role for NSm in mosquito infection. PLoS Negl. Trop. Dis. 6: 1–8.

Deveraux, Q. L., and J. C. Reed. **1999**. IAP family proteins-suppressors of apoptosis. Genes Dev. 13: 239–252.

Van Dijk, A. A., and H. Huismans. **1980**. The in vitro activiation and further characterization of the bluetongue virus-associated transcriptase. Virology. 104: 347–356.

Van Dijk, A. A., and H. Huismans. **1988**. In vitro transcription and translation of bluetongue virus mRNA. J Gen Virol. 69: 573–581.

Ding, S. W. 2010. RNA-based antiviral immunity. Nat Rev Immunol. 10: 632–644.

Diprose, J. M., J. N. Burroughs, G. C. Sutton, A. Goldsmith, P. Gouet, R. Malby, I. Overton, S. Zintara, P. P. C. Mertens, D. I. Stuart, and J. M. Grimes. **2001**. Translocation portals for the substrates and products of a viral transcription complex: the

bluetongue virus core. EMBO J. 20: 7229–7239.

Diprose, J. M., J. M. Grimes, G. C. Sutton, J. N. Burroughs, A. Meyer, S. Maan, P. P. Mertens, and D. I. Stuart. **2002**. The core of bluetongue virus binds double-stranded RNA. J. Virol. 76: 9533–9536.

Donepudi, M., A. Mac Sweeney, C. Briand, and M. G. Gru. **2003**. Insights into the regulatory mechanism for caspase-8 activation. Mol. Cell. 11: 543–549.

Dorstyn, L., P. A. Colussi, L. M. Quinn, H. Richardson, and S. Kumar. **1999**. DRONC, an ecdysone-inducible *Drosophila* caspase. Proc. Natl. Acad. Sci. U. S. A. 96: 4307–4312.

Duckett, C. S., F. Li, Y. U. Wang, K. J. Tomaselli, C. B. Thompson, and R. C. Armstrong. **1998**. Human IAP-like protein regulates programmed cell death downstream of Bcl-xL and cytochrome *c*. Mol. Cell Biol. 18: 608–615.

Earnshaw, W. C., L. M. Martins, and S. H. Kaufmann. **1999**. Mammalian caspases: structure, acitvation, substrates, and functions during apoptosis. Ann. Rev. Biochem. 68: 383–424.

Eckelman, B., M. Drag, S. Snipas, and G. S. Salvesen. **2008**. The mechanism of peptide-binding specificity of IAP BIR domains. Cell Death Differ. 15: 920–928.

Elbashir, S. M., W. Lendeckel, and T. Tuschl. **2001**. RNA interference is mediated by 21- and 22-nucleotide RNAs. Genes Dev. 15: 188–200.

Elbers, A. R. W., C. J. M. Koenraadt, and R. Meiswinkel. **2015**. Mosquitoes and *Culicoides* biting midges: vector range and the influence of climate change. Rev. Sci. Tech. l'OIE. 34: 123–137.

Erasmus, B. J. 1975. Bluetongue in sheep and goats. Aust. Vet. J. 51: 165–170.

Fabiana, D. P., S. Claude, and T. Etienne. **2009**. Bovine infection with bluetongue virus with special emphasis on European serotype 8. Vet. J. 182: 142–151.

Ferraguti, M., J. Martínez-de la Puente, S. Ruiz, R. Soriguer, and J. Figuerola. **2013**. On the study of the transmission networks of blood parasites from SW Spain: diversity of avian haemosporidians in the biting midge *Culicoides circumscriptus* and wild birds. Parasit. Vectors. 6: 1–7.

Fire, A., S. Xu, M. K. Montgomery, S. A. Kostas, S. E. Driver, and C. C. Mello. **1998**. Potent and specific genetic interference by double-stranded RNA in *Caenorhabditis elegans*. Nature. 391: 806–811.

Fletch, A. L., and L. H. Karstad. **1971**. Studies on the pathogenesis of experimental epizootic hemorrhagic disease of white-tailed deer. Can. J. Comp. Med. 35: 224–229.

Forzan, M., M. Marsh, and P. Roy. **2007**. Bluetongue virus entry into cells. J. Virol. 81: 4819–4827.

Forzan, M., C. Wirblich, and P. Roy. **2004**. A capsid protein of nonenveloped bluetongue virus exhibits membrane fusion activity. Proc. Natl. Acad. Sci. U S A. 101: 2100–2105.

Foster, N. M., R. D. Breckon, A. J. Luedke, and R. H. Jones. **1977**. Transmission of two strains of epizootic hemorrhagic disease virus in deer by *Culicoides variipennis*. J. Wildl. Dis. 13: 9–16.

Foster, N. M., and R. H. Jones. **1979**. Multiplication rate of bluetongue virus in the vector *Culicoides variipennis* (Diptera: Ceratopogonidae) infected orally. J. Med. Entomol. 15: 302–303.

Foster, N. M., R. H. Jones, and B. R. McCrory. **1963**. Preliminary investigations on insect transmission of bluetongue virus in sheep. Am. J. Vet. Res. 24: 1195–1200.

Foster, N., H. Metcalf, T. Barber, R. H. Jones, and A. Luedke. **1980**. Bluetongue and epizootic hemorrhagic disease virus isolation from vertebrate and invertebrate hosts at a common geographic site. J. Am. Vet. Med. Assoc. 176: 126–129.

Fraser, A. G., and G. I. Evan. **1997**. Identification of a *Drosophila melanogaster* ICE/CED-3-related protease, drICE. EMBO J. 16: 2805–2813.

Fraser, A. G., N. J. Mccarthy, and G. I. Evan. **1997**. drICE is an essential caspase required for apoptotic activity in *Drosophila* cells. EMBO J. 16: 6192–6199.

French, T. J., J. J. Marshall, and P. Roy. **1990**. Assembly of double-shelled, viruslike particles of bluetongue virus by the simultaneous expression of four structural proteins. J. Virol. 64: 5695–5700.

Fu, H., C. J. Leake, P. P. Mertens, and P. S. Mellor. **1999**. The barriers to bluetongue virus infection, dissemination and transmission in the vector, *Culicoides variipennis* (Diptera: Ceratopogonidae). Arch. Virol. 144: 747–61.

Fukusho, A., Y. Yu, S. Yamaguchi, and P. Roy. **1989**. Completion of the sequence of bluetongue virus serotype 10 by the characterization of a structural protein, VP6, and a non-structural protein, NS2. J. Gen. Virol. 70: 1677–1689.

Gammon, D., and C. C. Mello. **2015**. RNA interference-mediated antiviral defense in insects.

Curr. Opin. Insect. Sci. 8: 111–120.

Garrett, E. F., E. Po, E. R. Bichi, S. K. Hexum, R. Melcher, and A. M. Hubner. **2015**. Clinical disease associated with epizootic hemorrhagic disease virus in cattle in Illinois. J. Am. Vet. Med. Assoc. 247: 190–195.

Gaydos, J. K., J. M. Crum, W. R. Davidson, S. S. Cross, S. F. Owen, and D. E. Stallknecht. **2004**. Epizootiology of an epizootic hemorrhagic disease outbreak in West Virginia. J. Wildl. Dis. 40: 383–393.

Gaydos, J. K., W. R. Davidson, F. Elvinger, D. G. Mead, E. W. Howerth, D. E. Stallknecht, and F. O. Elvinger. **2002**. Innate resistance to epizootic hemorrhagic disease in white-tailed deer. J. Wildl. Dis. Wildl. Dis. Assoc. 38: 713–719.

Gerry, A. C., B. A. Mullens, N. J. Maclachlan, and J. O. Mecham. **2001**. Seasonal transmission of bluetongue virus by *Culicoides sonorensis* (Diptera: Ceratopogonidae) at a southern California dairy and evaluation of vectorial capacity as a predictor of bluetongue virus transmission. J. Med. Entomol. 38: 197–209.

Gibbs, E. P. J., and E. C. Greiner. **2017**. The epidemiology of bluetongue. Comp. Immunol. Microbiol. Infect. Dis. 17: 201–220.

Girard, Y. A., V. Popov, J. Wen, V. C. Han, and Higgs. **2005**. Ultrastructural study of west nile virus pathogenesis in *Culex pipiens quinquefasciatus* (Diptera: Culicidae). J. Med. Entomol. 42: 429–444.

Girard, Y. A., B. S. Schneider, C. E. McGee, J. Wen, V. C. Han, V. Popov, P. W. Mason, and S. Higgs. **2007**. Salivary gland morphology and virus transmission during long-term cytopathologic west nile virus infection in *Culex* mosquitoes. Am. J. Trop. Med. Hyg. 76: 118–128.

Goyal, L., K. McCall, J. Agapite, E. Hartwieg, and H. Steller. **2000**. Induction of apoptosis by *Drosophila reaper, hid* and *grim* through inhibition of IAP function. EMBO J. 19: 589–97.

Hassan, S. H., C. Wirblich, M. Forzan, and P. Roy. **2001**. Expression and functional characterization of bluetongue virus VP5 protein: role in cellular permeabilization. J. Virol. 75: 8356–8367.

Hawkins, C. J., S. L. Wang, and B. a Hay. **1999**. A cloning method to identify caspases and their regulators in yeast: identification of *Drosophila* IAP1 as an inhibitor of the *Drosophila* caspase DCP-1. Proc. Natl. Acad. Sci. U. S. A. 96: 2885–90.

Hawkins, C. J., S. J. Yoo, E. P. Peterson, S. L. Wang, S. Y. Vernooy, and B. A. Hay. **2000**. The *Drosophila* caspase DRONC cleaves following glutamate or aspartate and is regulated by DIAP1, HID, and GRIM. J. Biol. Chem. 275: 27084–27093.

Hay, B. A., D. A. Wassarman, and G. M. Rubin. **1995**. *Drosophila* homologs of baculovirus inhibitor of apoptosis proteins function to block cell death. Cell. 83: 1253–1262.

Hay, S., and G. Kannourakis. **2002**. A time to kill: viral manipulation of the cell death program. J. Gen. Virol. 83: 1547–1564.

Hengartner, M. O. 2000. The biochemistry of apoptosis. Nature. 407: 770–776.

Hinas, A., A. J. Wright, and C. P. Hunter. **2012**. Report SID-5 is an endosome-associated protein required for efficient systemic RNAi in *C. elegans*. Curr. Biol. 22: 1938–1943.

Hinds, M. G., R. S. Norton, D. L. Vaux, and C. L. Day. **1999**. Solution structure of a baculoviral inhibitor of apoptosis (IAP) repeat. Nat. Struct. Biol. 6: 648–651.

Hirashima, Y., T. Kato, M. Yamakawa, H. Shirafuji, R. Okano, and T. Yanase. **2015**. Reemergence of Ibaraki disease in southern Japan in 2013. J. Vet. Med. Sci. 77: 1253–1259.

Ho, P., and C. J. Hawkins. **2005**. Mammalian initiator apoptotic caspases. FEBS J. 272: 5436–5453.

Ho, P., A. M. Jabbour, P. G. Ekert, and C. J. Hawkins. **2005**. Caspase-2 is resistant to inhibition by inhibitor of apoptosis proteins (IAPs) and can activate caspase-7. FEBS J. 272: 1401–1414.

Hoar, B. R., T. E. Carpenter, R. S. Singer, and I. A. Gardner. **2003**. Regional risk of exporting cattle seropositive for bluetongue virus from the United States. Am. J. Vet. Res. 64: 520–529.

Hofmann, M. A., S. Renzullo, M. Mader, V. Chaignat, G. Worwa, and B. Thuer. **2008**. Genetic characterization of Toggenburg orbivirus, a new bluetongue virus, from goats, Switzerland. Emerg. Infect. Dis. 14: 1855–1861.

Holbrook, F. R., W. J. Tabachnick, E. T. Schmidtmann, C. N. McKinnon, R. J. Bobian, and W. L. Grogan. **2000**. Sympatry in the *Culicoides variipennis* complex (Diptera: Ceratopogonidae): a taxonomic reassessment. J. Med. Entomol. 37: 65–76.

Hopken, M. W., B. M. Ryan, K. P. Huyvaert, and A. J. Piaggio. **2017**. Picky eaters are rare: DNA-based blood meal analysis of *Culicoides* (Diptera: Ceratopogonidae) species from the United States. Parasit. Vectors. 10: 1–9.

Horwich, M. D., C. Li, C. Matranga, V. Vagin, G. Farley, P. Wang, and P. D. Zamore. **2007**. The *Drosophila* RNA methyltransferase, DmHen1, modifies germline piRNAs and single-stranded siRNAs in RISC. Curr. Biol. 17: 1265–1272.

House, C., L. Shipman, and G. Weybright. **1998**. Serological diagnosis of epizootic hemorrhagicdisease in cattle in the USA with lesions suggestive of vesicular disease. Ann. New York Acad. 849: 497–500.

Howerth, E. W., C. E. Greene, and A. K. Prestwood. **1988**. Experimentally induced bluetongue virus infection in white-tailed deer: coagulation, clinical pathologic, and gross pathologic changes. Am. J. Vet. Res. 49: 1906–1913.

Huvenne, H., and G. Smagghe. **2010**. Mechanisms of dsRNA uptake in insects and potential of RNAi for pest control: a review. J. Insect Physiol. 56: 227–235.

Hyatt, A. D., B. T. Eaton, and S. M. Brookes. **1989**. The release of bluetongue virus from infected cells and their suuperinfection by progeny virus. Virology. 173: 21–34.

Inaba, Y. 1975. Ibaraki disease and its relationship to bluetongue. Aust. Vet. J. 54: 178–185.

Ip, Y. T. 2005. *Drosophila* innate immunity goes viral. Nat. Immunol. 6: 863–864.

Jenckel, M., E. Bréard, C. Schulz, C. Sailleau, C. Viarouge, B. Hoffmann, D. Höper, M. Beer, and S. Zientara. **2015**. Complete coding genome sequence of putative novel bluetongue virus serotype 27. Genome Announc. 3: e00016-15.

Jennings, D. M., and P. S. Mellor. **1987**. Variation in the responses of *Culicoides variipennis* (Diptera, Ceratopogonidae) to oral infection with bluetongue virus. Arch. Virol. 95: 177–182.

Joazeiro, C. A. P., and A. M. Weissman. **2000**. RING finger proteins: mediators of ubiquitin ligase activity. Cell. 102: 549–552.

Kading, R. C., M. B. Crabtree, B. H. Bird, S. T. Nichol, B. R. Erickson, K. Horiuchi, B. J. Biggerstaff, and B. R. Miller. **2014**. Deletion of the NSm virulence gene of Rift Valley fever virus inhibits virus replication in and dissemination from the midgut of *Aedes aegypti* mosquitoes. PLoS Negl. Trop. Dis. 8: 17–18.

Kaiser, W. J., V. Domagoj, and L. K. Miller. **1998**. The *Drosophila* inhibitor of apoptosis D-IAP1 suppresses cell death induced by the caspase drICE. FEBS Lett. 440: 243–248.

Kakumani, P. K., S. Ponia, K. S. Rajgokul, V. Sood, M. Chinnappan, and A. C. Banerjea. **2013**. Role of RNA Interference (RNAi) in dengue virus replication and identification of

NS4B as an RNAi suppressor. J. Virol. 87: 8870–8883.

Kar, A. K., B. Bhattacharya, and P. Roy. **2007**. Bluetongue virus RNA binding protein NS2 is a modulator of viral replication and assembly. BMC Mol. Biol. 8: 1–13.

Kar, A. K., and P. Roy. **2003**. Defining the structure-function relationships of bluetongue virus helicase protein VP6. J. Virol. 77: 11347–56.

Karstad, L., Winter, A., and D. O. Trainer. **1961**. Pathology of epizootic hemorrhagic disease of deer. Am. J. Vet. Res. 22: 227–235.

Kedmi, M., M. Van Straten, E. Ezra, N. Galon, and E. Klement. **2010**. Assessment of the productivity effects associated with epizootic hemorrhagic disease in dairy herds. J. Dairy Sci. 93: 2486–2495.

Keene, K. M., B. D. Foy, I. Sanchez-Vargas, B. J. Beaty, C. D. Blair, and K. E. Olson. **2004**. RNA interference acts as a natural antiviral response to O'nyong-nyong virus (Alphavirus; Togaviridae) infection of *Anopheles gambiae*. Proc. Natl. Acad. Sci. U. S. A. 101: 17240–17245.

Kelly, E. M., D. C. Moon, and D. F. Bowers. **2012**. Apoptosis in mosquito salivary glands: Sindbis virus-associated and tissue homeostasis. J. Gen. Virol. 93: 2419–2424.

Kim, V. N., J. Han, and M. C. Siomi. **2009**. Biogenesis of small RNAs in animals. Nat. Rev. Mol. Cell Biol. 10: 126–139.

King, A., E. Lefkowitz, M. Adams, and E. Carstens. **2011**. Family-*Reoviridae*, pp. 395–404. *In* King, A.M., Lefkowitz, E., Adams, M.J., Carstens, E.B. (eds.), Virus Taxon. Ninth Rep. Int. Comm. Taxon. Viruses. Elsevier.

Kumar, M., G. Prasad, and M. Venkat. **2009**. Silencing of acetylcholinesterase gene of *Helicoverpa armigera* by siRNA affects larval growth and its life cycle. J. Insect Physiol. 55: 273–278.

Lan, H., H. Chen, Y. Liu, C. Jiang, Q. Mao, D. Jia, Q. Chen, and T. Wei. **2016**. Small interfering RNA pathway modulates initial viral infection in midgut epithelium of insect after ingestion of virus. J. Virol. 90: 917–929.

Lee, Y. S., K. Nakahara, J. W. Pham, K. Kim, Z. He, E. J. Sontheimer, and R. W. Carthew. **2004**. Distinct roles for *Drosophila* Dicer-1 and Dicer-2 in the siRNA / miRNA silencing pathways. Cell. 117: 69–81.

Leulier, F., A. Rodriguez, R. S. Khush, J. M. Abrams, and B. Lemaitre. **2000**. The

Drosophila caspase Dredd is required to resist gram-negative bacterial infection. EMBO Rep. 1: 353–358.

Li, H., W. X. Li, and S. W. Ding. **2002**. Induction and suppression of RNA silencing by an animal virus. Science. 296: 1319–1321.

Li, P., D. Nijhawan, I. Budihardjo, S. M. Srinivasula, M. Ahmad, E. S. Alnemri, and X. Wang. **1997**. Cytochrome c and dATP-dependent formation of Apaf-1/Caspase-9 complex initiates an apoptotic protease cascade. Cell. 91: 479–489.

Li, Q., H. Li, B. J. Blitvich, and J. Zhang. **2007**. The *Aedes albopictus* inhibitor of apoptosis 1 gene protects vertebrate cells from bluetongue virus-induced apoptosis. Insect Mol. Biol. 16: 93–105.

Linley, J. R. 1985. Biting midges (Diptera: Ceratopogonidae) as vectors of nonviral animal pathogens. J. Med. Entomol. 22: 589–599.

Liu, B., S. K. Behura, R. J. Clem, A. Schneemann, J. Becnel, D. W. Severson, and L. Zhou. **2013**. P53-mediated rapid induction of apoptosis conveys resistance to viralinfection in *Drosophila melanogaster*. PLoS Pathog. 9: e1003137.

Liu, Q., and R. J. Clem. **2011**. Defining the core apoptosis pathway in the mosquito disease vector *Aedes aegypti*: the roles of *iap1, ark, dronc,* and effector caspases. Apoptosis. 16: 105–113.

Lymperopoulos, K., R. Noad, S. Tosi, S. Nethisinghe, I. Brierley, and P. Roy. **2006**. Specific binding of bluetongue virus NS2 to different viral plus-strand RNAs. Virology. 353: 17–26.

Lymperopoulos, K., C. Wirblich, I. Brierley, and P. Roy. **2003**. Sequence specificity in the interaction of bluetongue virus non-structural protein 2 (NS2) with viral RNA. J. Biol. Chem. 278: 31722–31730.

Lysyk, T. J., and T. Danyk. **2007**. Effect of temperature on life history parameters of adult *Culicoides sonorensis* (Diptera: Ceratopogonidae) in relation to geographic origin and vectorial capacity for bluetongue virus. J. Med. Entomol. 44: 741–751.

Maan, S., N. S. Maan, K. Nomikou, C. Batten, F. Antony, M. N. Belaganahalli, A. M. Samy, A. A. Reda, S. A. Al-Rashid, M. el Batel, C. A. L. Oura, and P. P. C. Mertens. **2011**. Novel bluetongue virus serotype from Kuwait. Emerg. Infect. Dis. 17: 886–889.

Maan, S., N. S. Maan, K. Nomikou, E. Veronesi, K. Bachanek-Bankowska, M. N. Belaganahalli, H. Attoui, and P. P. C. Mertens. **2011**. Complete genome characterisation of a novel 26th bluetongue virus serotype from Kuwait. PLoS One. 6: e26147.

Maan, S., N. S. Maan, A. R. Samuel, S. Rao, H. Attoui, and P. P. C. Mertens. **2007**. Analysis and phylogenetic comparisons of full-length VP2 genes of the 24 bluetongue virus serotypes. J. Gen. Virol. 88: 621–630.

MacLachlan, N. J., and G. Gard. **2008**. Clinical signs and pathology, pp. 285–294. *In* Mellor, P., Baylis, M., Mertens, P.P.C. (eds.), Bluetongue. Elsevier, London, U. K.

MacLachlan, N. J., and B. I. Osburn. **2006**. Impact of bluetongue virus infection on the international movement and trade of ruminants. J. Am. Vet. Med. Assoc. 228: 1346–1349.

MacLachlan, N. J., S. Zientara, D. E. Stallknecht, J. D. Boone, V. H. Goekjian, C. Sailleau, and U. B. Balasuriya. **2007**. Phylogenetic comparison of the S10 genes of recent isolates of bluetongue virus from the United States and French Martinique Island. Virus Res. 129: 236–240.

Marques, J., and J.-L. Imler. **2016**. The diversity of insect antiviral immunity: Insights from viruses. Curr. Opin. Microbiol. 32: 71–76.

Marques, J. T., J. Wang, X. Wang, K. Pollyanna, V. De Oliveira, C. Gao, E. Roberto, G. Rocha, N. Jafari, and R. W. Carthew. **2013**. Functional specialization of the mmall interfering RNA pathway in response to virus infection. PLoS Pathog. 9: e1003579.

Martinez-Costas, J., G. Sutton, N. Ramadevi, and P. Roy. **1998**. Guanylyltransferase and RNA 5′-triphosphatase activities of the purified expressed VP4 protein of bluetongue virus. J. Mol. Biol. 180: 859–866.

Matsuo, E., and P. Roy. **2009**. Bluetongue virus VP6 acts early in the replication cycle and can form the basis of chimeric virus formation. J. Virol. 83: 8842–8.

Matsuo, E., and P. Roy. **2013**. Minimum requirements for bluetongue virus primary replication in vivo. J. Virol. 87: 882–889.

McDermott, E. G., and B. A. Mullens. **2014**. Desiccation tolerance in the eggs of the primary North American bluetongue virus vector, *Culicoides sonorensis,* (Diptera: Ceratopogonidae), and implications for vector persistence. J. Med. Entomol. 51: 1151–1158.

Meier, P., J. Silke, S. J. Leevers, and G. I. Evan. **2000**. The *Drosophila* caspase DRONC is regulated by DIAP1. EMBO J. 19: 598–611.

Meinander, A., C. Runchel, T. Tenev, L. Chen, C. Kim, P. S. Ribeiro, M. Broemer, F. Leulier, M. Zvelebil, N. Silverman, and P. Meier. **2012**. Ubiquitylation of the initiator caspase DREDD is required for innate immune signalling. EMBO J. 31: 2770–2783.

Mellor, P. S., J. Boorman, and M. Baylis. **2000**. *Culicoides* biting midges: their role as arbovirus vectors. Annu. Rev. Entomol. 45: 307–340.

Mellor, P. S., S. Carpenter, and D. M. White. **2008**. Bluetongue virus in the insect host., pp. 295–320. *In* Mertens, P., Baylis, M., Mellor, P. (eds.), Biol. Anim. Infect. Bluetongue. Academic Press.

Merkling, S. H., and R. P. van Rij. **2013**. Beyond RNAi: Antiviral defense strategies in *Drosophila* and mosquito. J. Insect Physiol. 59: 159–170.

Mertens, P. P. C., F. Brown, and D. Sangar. **1984**. Assignment of the genome segments of bluetongue virus type 1 to the proteins which they encode. Virology. 135: 207–217.

Mertens, P. P. C., J. N. Burroughs, A. Walton, M. Wellby, H. Fu, R. O'Harra, S. M. Brookes, and P. S. Mellor. **1996**. Enhanced infectivity of modified bluetongue virus particles for two insect cell lines and for two *Culicoides* vector species. Virology. 217: 582–593.

Michigan Department of Natural Resources. **2013**. Epizootic hemorrhagic disease (EHD) in white-tailed deer. (http://www.michigan.gov/dnr/0,1607,7-153-10370_12150-26647--,00.html).

Mierlo, T. Van, P. Miesen, G. J. Overheul, K. W. R. Van Cleef, J. Fros, S. Schuster, M. Marklewitz, G. P. Pijlman, S. Junglen, and R. P. Van Rij. **2014**. Mosquito and *Drosophila* entomobirnaviruses suppress dsRNA- and siRNA-induced RNAi. Nucleic Acids Res. 42: 8732–8744.

Miller, L. K. 1999. An exegesis of IAPs: salvation and surprises from BIR motifs. Trends Cell Biol. 9: 323–328.

Miller, S. C., K. Miyata, S. J. Brown, and Y. Tomoyasu. **2012**. Dissecting systemic RNA interference in the Red Flour Beetle *Tribolium castaneum*: parameters affecting the efficiency of RNAi. PLoS One. 7: e47431.

Mills, M. K., D. Nayduch, and K. Michel. **2015**. Inducing RNA interference in the arbovirus vector, *Culicoides sonorensis*. Insect Mol. Biol. 24: 105–14.

Mims, C. A., M. F. Day, and I. D. Marshall. **1966**. Cytopathic effect of Semliki forest virus in the mosquito, *Aedes aegypti*. Am. J. Trop. Med. Hyg. 15: 775–784.

Mirkovic-Hosle, M., and K. Forstemann. **2014**. Transposon defense by endo-siRNAs, piRNAs and somatic pilRNAs in *Drosophila*: contributions of Loqs-PD. PLoS One. 9: e84994.

Modrof, J., K. Lymperopoulos, and P. Roy. **2005**. Phosphorylation of bluetongue virus nonstructural protein 2 is essential for formation of viral inclusion bodies phosphorylation of bluetongue virus nonstructural protein 2 is essential for formation of viral inclusion bodies. J. Virol. 79: 10023–10031.

Mohl, B.-P., and P. Roy. **2014**. Bluetongue virus capsid assembly and maturation. Viruses. 6: 3250–3270.

Mongelli, V., and M.-C. Saleh. **2016**. Bugs are not to be silenced: small RNA pathways and antiviral responses in insects. Annu. Rev. Virol. 3: 573–589.

Mortola, E., and A. Larsen. **2009**. Bluetongue virus infection: signaling pathway activated during apoptosis. Rev. Argent. Microbiol. 41: 134–140.

Mortola, E., R. Noad, and P. Roy. **2004**. Bluetongue virus outer capsid proteins are sufficient to trigger apoptosis in mammalian cells. J. Virol. 78: 2875–83.

Mullens, B. A., and D. A. Rutz. **1983**. Development of immature *Culicoides variipennis* (Diptera: Ceratopogonidae) at constant laboratory temperatures. Ann. Entomol. Soc. Am. 76: 747–751.

Mullens, B. A., and E. T. Schmidtmann. **1982**. The gonotrophic cycle of *Culicoides variipennis* (Diptera: Ceratopogonidae) and its implications in age-grading field populations in New York State, USA. J. Med. Entomol. 19: 340–349.

Mullens, B. A., W. Tabachnick, F. R. Holbrook, and L. Thompson. **1995**. Effects of temperature on virogenesis of bluetongue serotype 11 in *Culicoides varripennis sonorensis*. Med. Vet. Entomol. 9: 71–76.

Muro, I., D. L. Berry, J. R. Huh, C. H. Chen, H. Huang, S. J. Yoo, M. Guo, E. H. Baehrecke, and B. A. Hay. **2006**. The *Drosophila* caspase Ice is important for many apoptotic cell deaths and for spermatid individualization, a nonapoptotic process. Development. 3315: 3305–3315.

Muro, I., B. A. Hay, and R. J. Clem. **2002**. The *Drosophila* DIAP1 protein is required to prevent accumulation of a continuously generated, processed form of the apical caspase DRONC. J. Biol. Chem. 277: 49644–49650.

Nagaleekar, V. K., A. K. Tiwari, R. S. Kataria, M. V. Bais, P. V. Ravindra, and S. Kumar. **2007**. Bluetongue virus induces apoptosis in cultured mammalian cells by both caspase-dependent extrinsic and intrinsic apoptotic pathways. Arch. Virol. 152: 1751–1756.

Nayak, A., B. Berry, M. Tassetto, M. Kunitomi, A. Acevedo, C. Deng, A. Kruchinsky, J.

Gross, and C. Antoniewski. **2010**. Cricket paralysis virus (CrPV) antagonizes Argonaute 2 to modulate antiviral defense in *Drosophila*. Nat. Struct. Biol. 17: 547–554.

Nayduch, D., L. W. Cohnstaedt, C. Saski, D. Lawson, P. Kersey, M. Fife, and S. Carpenter. **2014a**. Studying *Culicoides* vectors of BTV in the post-genomic era: resources, bottlenecks to progress and future directions. Virus Res. 182: 43–49.

Nayduch, D., M. B. Lee, and C. A. Saski. **2014b**. The reference transcriptome of the adult female biting midge (*Culicoides sonorensis*) and differential gene expression profiling during teneral, blood, and sucrose feeding conditions. PLoS One. 9: e98123.

Nayduch, D., M. B. Lee, and C. A. Saski. 2014c. Gene discovery and differential expression analysis of humoral immune response elements in female *Culicoides sonorensis* (Diptera: Ceratopogonidae). Parasit. Vectors. 7: 388-405.

Nicholson, D. W. 1999. Caspase structure, proteolytic substrates, and function during apoptotic cell death. Cell Death Differ. 6: 1028–1042.

O'Neill, K., B. J. S. C. Olson, N. Huang, D. Unis, and R. J. Clem. **2015**. Rapid selection against arbovirus-induced apoptosis during infection of a mosquito vector. Proc. Natl. Acad. Sci. U. S. A. E1152-2261.

Ocampo, C. B., P. A. Caicedo, G. Jaramillo, R. Ursic Bedoya, O. Baron, I. M. Serrato, D. M. Cooper, and C. Lowenberger. **2013**. Differential expression of apoptosis related genes in selected strains of *Aedes aegypti* with different susceptibilities to dengue virus. PLoS One. 8: e61187.

Ohashi, S., K. Yoshida, Y. Watanabe, and T. Tsuda. **1999**. Identification and PCR-restriction fragment length polymorphism analysis of a variant of the Ibaraki virus from naturally infected cattle and aborted fetuses in Japan. J. Clin. Microbiol. 37: 3800–3803.

Opferman, J. T., and S. J. Korsmeyer. **2003**. Apoptosis in the development and maintenance of the immune system. Nat. Immunol. 4: 410–415.

Patel, A., and P. Roy. **2014**. The molecular biology of bluetongue virus replication. Virus Res. 182: 5–20.

Paweska, J. T., G. J. Venter, and P. S. Mellor. **2002**. Vector competence of South African *Culicoides* species for bluetongue virus serotype 1 (BTV-1) with special reference to the effect of themperature on the rate of virus replication in *C. imicola* and *C. bolitinos*. Med. Vet. Entomol. 16: 10–21.

Pfannenstiel, R. S., B. A. Mullens, M. G. Ruder, L. Zurek, L. W. Cohnstaedt, and D.

Nayduch. **2015**. Management of North American *Culicoides* biting midges: current knowledge and research needs. Vector Borne Zoonotic Dis. 15: 374–384.

Pinheiro, F. P., A. P. Travassos da Rosa, M. L. Gomes, J. W. LeDuc, and A. L. Hoch. **1982**. Transmission of Oropouche virus from man to hamster by the midge *Culicoides paraensis*. Science. 215: 1251–1253.

Prasad, B. V. V., S. Yamaguchi, and P. Roy. **1992**. Three-dimensional structure of single-shelled bluetongue virus. J. Virol. 66: 2135–2142.

Price, D. R. G., and J. A. Gatehouse. **2008**. RNAi-mediated crop protection against insects. Trends Biotechnol. 26: 393–400.

Purse, B. V, S. Carpenter, G. J. Venter, G. Bellis, and B. A. Mullens. **2015**. Bionomics of temperate and tropical *Culicoides* midges: knowledge gaps and consequences for transmission of *Culicoides*-borne viruses. Annu. Rev. Entomol. 60: 373–392.

Purse, B. V, P. S. Mellor, D. J. Rogers, A. R. Samuel, P. P. C. Mertens, and M. Baylis. **2005**. Climate change and the recent emergence of bluetongue in Europe. Nat. Rev. Microbiol. 3: 171–181.

Quinn, L. M., L. Dorstyn, K. Mills, P. A. Colussi, P. Chen, M. Coombe, J. Abrams, S. Kumar, and H. Richardson. **2000**. An essential role for the caspase Dronc in developmentally programmed cell death in *Drosophila*. J. Biol. Chem. 275: 40416–40424.

Raff, M. 1998. Cell suicide for beginners. Nature. 396: 119–122.

Ramadevi, N., N. J. Burroughs, P. P. Mertens, I. M. Jones, and P. Roy. **1998**. Capping and methylation of mRNA by purified recombinant VP4 protein of bluetongue virus. Proc. Natl. Acad. Sci. U. S. A. 95: 13537–13542.

Ramadevi, N., J. Rodriguez, and P. Roy. **1998**. A leucine zipper-like domain is essential for dimerization and encapsidation of bluetongue virus nucleocapsid protein VP4. J. Virol. 72: 2983–2990.

Richard, A., and D. Tulasne. **2012**. Caspase cleavage of viral proteins, another way for viruses to make the best of apoptosis. Cell Death Dis. 3: e277.

van Rij, R. P., M. Saleh, B. Berry, C. Foo, A. Houk, C. Antoniewski, and R. Andino. **2006**. The RNA silencing endonuclease Argonaute 2 mediates specific antiviral immunity in *Drosophila melanogaster*. Genes Dev. 2985–2995.

Rodriguez-Andres, J., S. Rani, M. Varjak, M. E. Chase-Topping, M. H. Beck, M. C.

Ferguson, E. Schnettler, R. Fragkoudis, G. Barry, A. Merits, J. K. Fazakerley, M. R. Strand, and A. Kohl. **2012**. Phenoloxidase activity acts as a mosquito innate immune response against infection with Semliki forest virus. PLoS Pathog. 8: e1002977.

Rodriguez, A., P. Chen, H. Oliver, and J. M. Abrams. **2002**. Unrestrained caspase-dependent cell death caused by loss of *Diap1* function requires the *Drosophila* Apaf-1 homolog, *Dark*. EMBO J. 21: 2189–2197.

Rodriguez, A., H. Oliver, H. Zou, P. Chen, X. Wang, J. M. Abrams, H. Hughes, S. Medical, and H. H. Boulevard. **1999**. Dark is a *Drosophila* homologue of Apaf-1/CED-4 and functions in an evolutionarily conserved death pathway. Nat. Cell Biol. 1: 272–279.

Ruder, M. G., E. W. Howerth, D. E. Stallknecht, A. B. Allison, D. L. Carter, B. S. Drolet, E. Klement, and D. G. Mead. **2012**. Vector competence of *Culicoides sonorensis* (Diptera: Ceratopogonidae) to epizootic hemorrhagic disease virus serotype 7. Parasit. Vectors. 5: 1–8.

Ruder, M. G., T. J. Lysyk, D. E. Stallknecht, L. D. Foil, D. J. Johnson, C. C. Chase, D. A. Dargatz, and E. P. J. Gibbs. **2015a**. Transmission and epidemiology of bluetongue and epizootic hemorrhagic disease in North America: current perspectives, research gaps, and future Directions. Vector-Borne Zoonotic Dis. 15: 348–363.

Ruder, M. G., D. E. Stallknecht, E. W. Howerth, D. L. Carter, R. S. Pfannenstiel, A. B. Allison, and D. G. Mead. **2015b**. Effect of temperature on replication of epizootic hemorrhagic disease viruses in *Culicoides sonorensis* (Diptera: Ceratopogonidae). J. Med. Entomol. 52: 1050–1059.

Saito, K., Y. Sakaguchi, T. Suzuki, and T. Suzuki. **2007**. Pimet, the *Drosophila* homolog of HEN1, mediates 2-O-methylation of Piwi-interacting RNAs at their 3' ends. Genes Dev. 21: 1603–1608.

Saleh, M. C., R. P. van Rij, A. Hekele, A. Gillis, E. Foley, P. H. O'Farrell, and R. Andino. **2006**. The endocytic pathway mediates cell entry of dsRNA to induce RNAi silencing. Nat. Cell Biol. 8: 793–802.

Salvesen, G. S., and C. S. Duckett. **2002**. IAP proteins: blocking the road to death's door. Nat. Rev. Mol. Cell Biol. 3: 401–410.

Sánchez-Cordón, P. J., F. J. Pleguezuelos, A. C. Pérez de Diego, J. C. Gómez-Villamandos, J. M. Sánchez-Vizcaíno, J. J. Cerón, F. Tecles, B. Garfia, and M. Pedrera. **2013**. Comparative study of clinical courses, gross lesions, acute phase response and coagulation disorders in sheep inoculated with bluetongue virus serotype 1 and 8. Vet. Microbiol. 166: 184–194.

Sant'Anna, M. R., H. Diaz-Albiter, M. Mubaraki, R. J. Dillon, and P. a Bates. **2009**. Inhibition of trypsin expression in *Lutzomyia longipalpis* using RNAi enhances the survival of *Leishmania*. Parasit. Vectors. 2: 62.

Santiago-Alarcon, D., P. Havelka, H. M. Schaefer, and G. Segelbacher. **2012**. Bloodmeal analysis reveals avian *Plasmodium* infections and broad host preferences of *Culicoides*. PLoS One. 7: e31098.

Sarkies, P., and E. A. Miska. **2013**. RNAi pathways in the recognition of foreign RNA: antiviral responses and host–parasite interactions in nematodes. Biochem. Soc. Trans. 41: 876–880.

Savini, G., A. Afonso, P. Mellor, I. Aradaib, H. Yadin, M. Sanaa, W. Wilson, F. Monaco, and M. Domingo. **2011**. Epizootic heamorragic disease. Res. Vet. Sci. 91: 1–17.

Schnettler, E., M. Ratinier, M. Watson, A. E. Shaw, M. McFarlane, M. Varela, R. M. Elliott, M. Palmarini, and A. Kohl. **2013**. RNA interference targets arbovirus replication in *Culicoides* cells. J. Virol. 87: 2441–2454.

Schnettler, E., M. G. Sterken, J. Y. Leung, S. W. Metz, C. Geertsema, R. W. Goldbach, and J. M. Vlak. **2012**. Noncoding flavivirus RNA displays RNA interference suppressor activity in insect and mammalian cells. J. Virol. 86: 13486–13500.

Schwartz-Cornil, I., P. P. C. Mertens, V. Contreras, B. Hemati, F. Pascale, E. Br??ard, P. S. Mellor, N. James MacLachlan, S. Zientara, E. Bréard, P. S. Mellor, N. J. MacLachlan, and S. Zientara. **2008**. Bluetongue virus: virology, pathogenesis and immunity. Vet Res. 39: 1–16.

Scott, J. G., K. Michel, L. C. Bartholomay, B. D. Siegfried, W. B. Hunter, G. Smagghe, K. Y. Zhu, and A. E. Douglas. **2013**. Towards the elements of successful insect RNAi. J Insect Physiol. 59: 1212–1221.

Shakesby, A., I. Wallace, H. Isaacs, J. Pritchard, D. Roberts, and A. Douglas. **2009**. A water-specific aquaporin involved in aphid osmoregulation. Insect Biochem. Mol. Biol. 39: 1–10.

Shope, R. E., L. G. MacNamara, and R. Mangold. **1955**. Report on the deer mortality, epizootic hemorrhagic disease of deer. New Jersey outdoors. 6: 17–21.

Shope, R. E., L. G. MacNamara, and R. Mangold. **1960**. A virus-induced epizootic hemorrhagic disease of the Virginia white-tailed deer (*Odocoileus virginianus*). J. Exp. Med. 11: 155–170.

Sieburth, P. J., C. E. Nunamaker, J. Ellis, and R. A. Nunamaker. **1991**. Infection of the midgut of *Culicoides variipennis* (Diptera: Ceratopogonidae) with bluetongue virus. J. Med. Entomol. 28: 74–85.

Sim, S., J. L. Ramirez, and G. Dimopoulos. **2012**. Dengue virus infection of the *Aedes aegypti* salivary gland and chemosensory apparatus induces genes that modulate infection and blood-feeding behavior. PLoS Pathog. 8: e1002631.

Smith, K. E., and D. E. Stallknecht. **1996**. *Culicoides* (Diptera:Ceratopogonidae) collected during epizootics of hemorrhagic disease among captive white-tailed deer. J. Med. Entomol. 33: 507–510.

Song, Z., K. Mccall, and H. Steller. **1997**. DCP-1, a *Drosophila* cell death protease essential for development. Science. 275: 536–540.

Spruell, J. 1905. Malarial catarrhal fever (bluetongue) of sheep in South Africa. J. Comp. Pathol. Ther. 18: 321–337.

Stair, E. L., R. M. Robinson, and L. P. Jones. **1968**. Spontaeous bluetongue in Texas white-tailed deer. Pathol. Vet. 5: 164–173.

Stennicke, H. R., and G. S. Salvesen. **2000**. Caspases–controlling intracellular signals by protease zymogen activation. Biochim. Biophys. Acta (BBA)-Protein Struct. Mol. Enzymol. 1447: 299–306.

Stevens, Lisa, M. 2015. Understanding the early events in bluetongue virus cell entry.

Stevens, G., B. McCluskey, A. King, E. O'Hearn, and G. Mayr. **2015**. Review of the 2012 epizootic hemorrhagic disease outbreak in domestic ruminants in the United States. PLoS One. 10: 1–11.

Stewart, M. E., and P. Roy. **2010**. Role of cellular caspases, nuclear factor-kappa B and interferon regulatory factors in bluetongue virus infection and cell fate. Virol. J. 7: 362.

Sun, C., M. Cai, A. H. Gunasekera, R. P. Meadows, H. Wang, J. Chen, H. Zhang, W. Wu, N. Xu, S. Ng, and S. W. Fesik. **1999**. Cell culture inhibitor-of-apoptosis protein XIAP. Nature. 401: 818–822.

Szmaragd, C., A. Wilson, S. Carpenter, P. P. C. Mertens, P. S. Mellor, and S. Gubbins. **2007**. Mortality and case fatality during the recurrence of BTV-8 in northern Europe in 2007. Vet. Rec. 161: 571–572.

Tabachnick, W. J. 1990. Genetic variation in laboratory and field populations of the vector of

bluetongue virus, *Culicoides variipennis* (Diptera: Ceratopogonidae). J. Med. Entomol. 27: 24–30.

Tabachnick, W. J. 1991. Genetic control of oral susceptibility to infection of *Culicoides variipennis* with bluetongue virus. Am. J. Trop. Med. Hyg. 45: 666–671.

Tabachnick, W. J. 1996. *Culicoides variipennis* and bluetongue-virus epidemiology in the United States. Annu. Rev. Entomol. 41: 23–43.

Tan, B. H., E. Nason, N. Staeuber, W. R. Jiang, K. Monastryrskaya, and P. Roy. **2001**. RGD tripeptide of bluetongue virus VP7 protein is responsible for core attachment to *Culicoides* cells. J. Virol. 75: 3937–3947.

Tanya, V. N., E. C. Greiner, and E. P. Gibbs. **1992**. Evaluation of *Culicoides insignis* (Diptera: Ceratopogonidae) as a vector of bluetongue virus. Vet Microbiol. 32: 1–14.

Thiry, E., C. Saegerman, H. Guyot, P. Kirten, B. Losson, F. Rollin, M. Bodmer, G. Czaplicki, J. Toussaint, K. De Clercq, J.-M. Dochy, J. Dufey, J.-L. Gilleman, and K. Messeman. **2006**. Bluetongue in northern Europe. Vet. Rec. 159: 327.

Thomas, F. C., N. Willis, and G. Ruckerbrauer. **1974**. Identification of viruses involved in the 1971 outbreak of hemorrhagic disease in southeastern United States white-tailed deer. J. Wildl. Dis. 10: 187–189.

Thornberry, N. A. 1998. Caspases: key mediators of apoptosis. Chem. Biol. 5: 97–103.

Thornberry, N. A., T. A. Rano, E. P. Peterson, D. M. Rasper, T. Timkey, M. Garcia-calvo, V. M. Houtzager, P. A. Nordstrom, S. Roy, J. P. Vaillancourt, K. T. Chapman, and D. W. Nicholson. **1997**. A combinatorial approach defines specificities of members of the caspase family and granzyme B. J. Biol. Chem. 272: 17907–17911.

Turner, C., M. Davy, R. MacDiarmid, K. M. Plummer, N. P. Birch, and R. D. Newcomb. **2006**. RNA interference in the light brown apple moth, *Epiphyas postvittana* (Walker) induced by double-stranded RNA feeding. Insect Mol. Biol. 15: 383–391.

Urakawa, T., D. Ritter, and P. Roy. **1989**. Expression of largest RNA segment and synthesis of VPI protein of bluetongue virus in insect cells by recombinant baculovirus: association of VPI protein with RNA polymerase activity. Nucleic Acids Res. 17: 7395–7402.

Velthuis, A. G. J., H. W. Saatkamp, M. C. M. Mourits, A. A. de Koeijer, and A. R. W. Elbers. **2010**. Financial consequences of the Dutch bluetongue serotype 8 epidemics of 2006 and 2007. Prev. Vet. Med. 93: 294–304.

Veronesi, E., F. Antony, S. Gubbins, N. Golding, A. Blackwell, P. P. Mertens, J. Brownlie, K. E. Darpel, P. S. Mellor, and S. Carpenter. **2013**. Measurement of the infection and dissemination of bluetongue virus in *Culicoides* biting midges using a semi-quantitative rt-PCR assay and isolation of infectious virus. PLoS One. 8: e70800.

Verwoerd, D. W., and B. J. Erasmus. **2016**. Bluetongue, pp. 1201–1220. *In* Infect. Dis. Livest.

Viennet, E., C. Garros, I. Rakotoarivony, X. Allène, L. Gardès, J. Lhoir, I. Fuentes, R. Venail, D. Crochet, R. Lancelot, M. Riou, C. Moulia, T. Baldet, and T. Balenghien. **2012**. Host-seeking activity of bluetongue virus vectors: endo/exophagy and circadian rhythm of *Culicoides* in Western Europe. PLoS One. 7: e48120.

Vigil, S. L., J. C. Wlodkowski, J. Parris, S. E. De Vargas, D. Shaw, C. Cleveland, W. L. Grogan, and J. L. Corn. **2014**. New records of biting midges of the genus *Culicoides latreille* from the southeastern United States (Diptera: Ceratopogonidae). Insecta mundi. 394: 1–14.

Vosdingh, R. A., D. O. Trainer, and B. C. Easterday. **1968**. Experimental bluetongue disease in white-tailed deer. Can. J. Comp. Med. Vet. Sci. 32: 382–387.

VotÝpka, J., P. Synek, and M. SvobodovÁ. **2009**. Endophagy of biting midges attacking cavity-nesting birds. Med. Vet. Entomol. 23: 277–280.

Walton, T. E. 2004. The history of bluetongue and a current global overview. Vet. Ital. 40: 31–38.

Wang, H., C. D. Blair, K. E. Olson, and R. J. Clem. **2008**. Effects of inducing or inhibiting apoptosis on Sindbis virus replication in mosquito cells. J. Gen. Virol. 89: 2651–2661.

Wang, H., and R. J. Clem. **2011**. The role of IAP antagonist proteins in the core apoptosis pathway of the mosquito disease vector *Aedes aegypti*. Apoptosis. 16: 235–248.

Wang, H., T. Gort, D. L. Boyle, and R. J. Clem. **2012**. Effects of manipulating apoptosis on Sindbis virus infection of *Aedes aegypti* mosquitoes. J. Virol. 86: 6546–6554.

Waterhouse, R. M., E. V Kriventseva, S. Meister, Z. Xi, K. S. Alvarez, L. C. Bartholomay, C. Barillas-mury, G. Bian, S. Blandin, B. M. Christensen, Y. Dong, H. Jiang, M. R. Kanost, A. C. Koutsos, E. A. Levashina, J. Li, P. Ligoxygakis, R. M. Maccallum, G. F. Mayhew, A. Mendes, K. Michel, M. A. Osta, S. Paskewitz, S. W. Shin, and D. Vlachou. **2007**. Evolutionary dynamics of immune-related genes and pathways in disease-vector mosquitoes. Science. 316: 1738–1743.

Wechsler, S. J., and L. E. McHolland. **1988**. Susceptibilities of 14 cell lines to bluetongue

virus infection. J. Clin. Microbiol. 26: 2324–2327.

Wilson, A., and P. Mellor. **2008**. Bluetongue in Europe: vectors, epidemiology and climate change. Parasitol. Res. 104: 489.

Wilson, R., L. Goyal, M. Ditzel, A. Zachariou, D. A. Baker, J. Agapite, H. Steller, and P. Meier. **2002**. The DIAP1 RING finger mediates ubiquitination of Dronc and is indispensable for regulating apoptosis. Nat. Cell Biol. 4: 445–450.

Winston, W. M., C. Molodowitch, and C. P. Hunter. **2002**. Systemic RNAi in *C. elegans* requires the putative transmembrane protein SID-1. Science. 295: 2456–2459.

Winston, W. M., M. Sutherlin, A. J. Wright, E. H. Feinberg, and C. P. Hunter. **2007**. *Caenorhabditis elegans* SID-2 is required for environmental RNA interference. Proc. Natl. Acad. Sci. U. S. A. 104: 10565–10570.

Wittman, E. J., P. S. Mellor, and M. Baylis. **2002**. Effect of temperature on the transmission of arboviruses by the biting midge, *Culicoides sonorensis*. Med. Vet. Entomol. 16: 147–156.

Won, S., T. Ikegami, C. J. Peters, and S. Makino. **2007**. NSm Protein of Rift Valley fever virus suppresses virus-induced apoptosis. J. Virol. 81: 13335–13345.

Xiao, X., Y. Liu, X. Zhang, J. Wang, Z. Li, X. Pang, P. Wang, and G. Cheng. **2014**. Complement-related proteins control the Flavivirus infection of *Aedes aegypti* by inducing antimicrobial peptides. PLoS Pathog. 10: e10042027.

Xu, D., Y. Wang, Z. Chen, T. Ding, and A. Bergmann. **2006**. The effector caspases drICE and dcp-1 have partially overlapping functions in the apoptotic pathway in *Drosophila*. Cell Death Differ. 13: 1697–1706.

Yan, N., J. Wu, J. Chai, W. Li, and Y. Shi. **2004**. Molecular mechanisms of DrICE inhibition by DIAP1 and removal of inhibition by Reaper, Hid and Grim. Nat. Struct. Mol. Biol. 11: 420–428.

Yang, Y., S. Fang, J. P. Jensen, A. M. Weissman, and J. D. Ashwell. **2000**. Ubiquitin protein ligase activity of IAPs and their degradation in proteasomes in response to apoptotic stimuli. Science. 288: 874–877.

Yordy, B., and A. Iwasaki. **2011**. Autophagy in the control and pathogenesis of viral infection. Curr. Opin. Virol. 1: 196–203.

Yu, N., O. Christiaens, J. Lio, J. Niu, K. Cappelle, S. Caccia, H. Huvenne, and G. Smagghe. **2013**. Delivery of dsRNA for RNAi in insects: an overview and future directions. Insect

Sci. 20: 4–14.

Zhang, H., H. C. Li, and X. X. Miao. **2013**. Feasibility, limitation and possible solutions of RNAi-based technology for insect pest control. Insect Sci. 20: 15–30.

Zhang, X., M. Boyce, B. Bhattacharya, X. Zhang, S. Schein, P. Roy, and Z. H. Zhou. **2010**. Bluetongue virus coat protein VP2 contains sialic acid-binding domains, and VP5 resembles enveloped virus fusion proteins. Proc. Natl. Acad. Sci. U. S. A. 107: 6292–6297.

Zhang, X., J. Zhang, and K. Y. Zhu. **2010**. Chitosan/double-stranded RNA nanoparticle-mediated RNA interference to silence chitin synthase genes through larval feeding in the African malaria mosquito (*Anopheles gambiae*). Insect Mol. Biol. 19: 683–693.

Zhao, P., Z. Lu, M. R. Strand, and H. Jiang. **2011**. Antiviral, antiparasitic, and cytotoxic effects of 5, 6-dihydroxyindole (DHI), a reactive compound generated by phenoloxidase during insect immune response. Insect Biochem. Mol. Biol. 41: 645–652.

Zou, H., Y. Li, X. Liu, and X. Wang. **1999**. An APAF-1 cytochrome c multimeric complex is a functional apoptosome that activates procaspase-9. J. Biol. Chem. 274: 11549–11556.

Tables and Figures – Chapter 1

Table 1.1 Summary of orbivirus transmission dynamics within *C. sonorensis*

		Experimental Setup			Viral Titer	Prevalence	
						Primary Eclipse	
Paper	Virus	Infecting Dose §	Temp [°C]	Detection limit §§	Proliferation Phase [dpi]	dpi	% decrease
Foster and Jones 1979	BTV**	6	23	NA	4	-	-
Chandler et al. 1985	BTV-11	6.5	27	NA	5	-	-
Fu et al. 1999	BTV-1	6.7	24	0.75	1	2.5	14.3
Wittman et al. 2002	EHDV-1	5.7-6.5	20	1.4	-	2	20
			25		-	1	10
			30		-	3*	20*
	BTV-10	5.7-6.5	20	1.4	-	4	20
			25		-	1	10
			30		-	4*	10*
	BTV-16	5.7-6.5	20	1.4	-	4	20
			25		-	5	10
			30		-	1	50
Ruder et al. 2012	EHDV-7	7.03-7.6	22	2.3	6	-	-
		3.1-3.9	22	2.3	-	-	-
Veronesi et al. 2013	BTV-1	≥6	25	0.5	4	3	52
Ruder et al. 2015	EHDV-1	7	20	2.3	(13-20)	3	70
			25		6	3	30
			30		(2-6)	3	20
	EHDV-2	6.8	20	2.3	(16-20)	1	40
			25		6	4	10
			30		(4-12)	3	20
	EHDV-7	7	20	2.3	12	3	50
			25		6	4	20
			30		3	(2-3)*	20*
	EHDV-7	6.2	20	2.3	12	(2-3)*	60*
			25		4	(2-3)*	60*
			30		(2-6)	2	62

§ $\log_{10}TCID_{50}$/ml
§§ $\log_{10}TCID_{50}$/midge
*initial 10% decrease at 1 dpi
**serotype not listed
NA detection limit not listed

Table 1.2 Heritable factors of vector competence identified from *C.sonorensis* transcriptome

Pathway	Description	Members	Accession No.	Reference No.	e value
IMD AMPs	Receptors	Peptidoglycan Recognition Protein (Long; PGRP-LC)	GAWM01004359	AAEL013112	4.49E-23
		PGRP-LC	GAWM01003592	AAEL014640	1.9E-40
		PGRP-LC	GAWM01011033	AAEL014640	1.9E-40
		PGRP-LC	GAWM01011035	AAEL014640	1.9E-40
		PGRP-LC	GAWM01011037	AAEL014640	7.24E-43
		PGRP-LC	GAWM01011039	AAEL014640	1.9E-40
		PGRP-LC	GAWM01000194	AAEL014989	1.3E-22
	Signaling	DREDD (Caspase-8)	GAWM01000519	AAEL014148	4.93E-66
		Inhibitor of apoptosis (IAP)	GAWM01008211	AAEL006633	4.4E-146
		tak1-associated binding protein (TAB)	GAWM01006076	CPIJ000820	5.27E-21
		tak1 (MAP3K)	GAWM01010356	AAEL007035	3.82E-62
		tak1 (MAP3K)	GAWM01012184	AAEL012659	8.2E-54
		I-Kappa-B Kinase 2 (IKK2, IKK-gamma), key/kenny	GAWM01018250	AAEL012510	2.02E-43
		I-Kappa-B Kinase 1 (IKK1, IKK-beta), ird5	GAWM01013537	AAEL003245	0
	Transcription	NF-kappaB transcription factor, Relish	GAWM01014884	AAEL007624	5.09E-52
		NF-kappaB transcription factor, Relish	GAWM01014885	AAEL007624	2.64E-27
	AMPs	attacin-like AMP	GAWM01008443	n/a	0.000000353
		attacin	GAWM01017969	AAEL003389	1.39E-22
		defensin	GAWM01019039	n/a	0.000146
		defensin	GAWM01019040	n/a	5.14E-08
		cecropin	GAWM01000005	n/a	3.93E-14
	Regulators	Caudal homeobox protein poor imd response upon knock-in (PIRK); PIMS; RUDRA	GAWM01004228	AAEL014557	1.83E-82
		FAS-associated factor 1, caspar	GAWM01010231	CPIJ014088	3.27E-09
		Peptidoglycan Recognition Protein (Short form); PGRPSC2/SC3	GAWM01012793	AAEL003579	0
			GAWM01018647	AAEL007039	4.37E-84
Toll	Upstream signaling	Peptidoglycan Recognition Protein (Short); PGRP-SA	GAWM01018051	AAEL009474	6.18E-17
		Gram-Negative Binding Protein (GNBP), or Beta-1,3-Glucan Binding Protein (BGBP); GNBP-1	GAWM01002165	AAEL009176	3.81E-90
		GNBP-1/BGBP-1	GAWM01003712	AAEL009176	3.81E-90
		GNBP-1/BGBP-1	GAWM01004143	AAEL009176	3.81E-90
		GNBP-3/BGBP-3	GAWM01011997	AAEL000652	2.96E-38
		Spaetzle-like cytokine, Spz3	GAWM01001358	AAEL014950	3.56E-129
		Spaetzle-like cytokine, Spz5	GAWM01006049	AAEL001929	1.29E-44
		Spaetzle-like cytokine, Spz6	GAWM01012721	AAEL012164	2.42E-37
		Spaetzle-like cytokine, Spz1?	GAWM01015015	AAEL000499	1.59E-35
	Receptors	Toll receptor	GAWM01015594	AAEL009551	5.73E-106
		Toll receptor	GAWM01019001	AAEL000633	0
		Toll receptor	GAWM01015706	AAEL009551	4.24E-152

		Toll receptor	GAWM01013057	AAEL002583	0
		Toll receptor	GAWM01013058	AAEL002583	0
	Cell signaling	myeloid differentiation primary response protein 88 (MYD88)	GAWM01018790	AAEL007768	1.44E-46
		Ser/Thr Kinase, Pelle (IRAK1)	GAWM01001221	AAEL006571	1.62E-92
		Ser/Thr Kinase, Pelle (IRAK1)	GAWM01011117	AAEL006571	1.62E-92
		Tube (IRAK4)	GAWM01007838	AAEL007642	1.93E-42
		cactus (IkappaB)	GAWM01009580	AAEL001584	1.95E-16
	Transcription	dorsal/dif (REL1)	GAWM01010293	AAEL014821	4.73E-95
		dorsal/dif (REL1)	GAWM01010294	AAEL014821	4.73E-95
		dorsal/dif (REL1)	GAWM01010296	AAEL014821	4.73E-95
		dorsal/dif (REL1)	GAWM01010297	AAEL014821	4.73E-95
JAK-STAT	Receptors	Domeless (Dome)	GAWM01016058	AAEL012471	4.38E-85
			GAWM01016156	AAEL012471	4.38E-85
	Cell signalling	Hopscotch janus kinase (Hop)	GAWM01005626	AAEL012553	0
	Transcription	Signal transducer and activator of transcription (STAT)	GAWM01007780	AAEL013265	1.01E-43
			GAWM01011778	AAEL013265	1.01E-43
			GAWM01013279	AAEL013265	1.01E-43
	Regulators	suppressor of cytokine signaling 5 (SOCS36E?)	GAWM01008465	AAEL000393	5.7E-102
		suppressor of cytokine signaling (SOCS7?)	GAWM01008657	AAEL006949	1.62E-104
		protein inhibitor of activated stat; PIAS, sumo ligase	GAWM01011450	AAEL015099	1.66E-150
			GAWM01011451	AAEL015099	1.66E-150
Apoptosis	Regulators	IAP1	GAWM01009039	AAEL009074	1.00E-112
		IAP2	GAWM01008211	AAEL006633	6.00E+150
		IAP5	GAWM01018859	AAEL014251	1.00E-54
		IAP6	GAWM01016583	AAEL012446	0.00E+00
	Caspases	Dronc	GAWM01016707	AAEL011562	1.00E-46
		DrICE	GAWM01000206	AAEL012143	1.00E-108
			GAWM01002195	AAEL014348	1.00E-31
Melanization	Prophenoloxidaes	PPO3	GAWM01010754	AAEL011763	0
		PPO6	GAWM01004196	AAEL014544	9.00E-97
			GAWM01015170	AAEL014545	0
			GAWM01004197	AAEL014546	0
Complement		TEP/MCR	GAWM01009528	AAEL012267	0
Autophagy		APG12	GAWM01007498	AAEL009089	4.00E-42
		APG18A	GAWM01006903	AAEL013063	3.00E-173
		APG18B	GAWM01014186	AAEL013995	0
		APG2	GAWM01013097	AAEL003799	0
		APG4A	GAWM01008772	AAEL010516	0
		APG4B	GAWM01004413	AAEL007228	5.00E-150
			GAWM01004412	AAEL007229	5.00E-151
		APG5	GAWM01004821	AAEL002286	2.00E-141
		APG6	GAWM01004552	AAEL010427	0
		APG7A	GAWM01018401	AAEL010641	0
		APG7B	GAWM01011557	AAEL012306	0
		APG8	GAWM01004039	AAEL007162	2.00E-23
			GAWM01012322	AAEL007163	2.00E-81
		APG9	GAWM01011616	AAEL009105	0
	Regulators	BUFFY	GAWM01016181	AAEL001521	3.00E-105
		DEBCL	GAWM01000607	AAEL001515	7.00E-73
		TOR	GAWM01000709	AAEL000693	0

RNAi		AGO2	GAWM01012834	AAEL017251	5.00E-49
			GAWM01012835	AAEL017251	2.00E-133
			GAWM01012837	AAEL017251	4.00E-48
		Dicer2	GAWM01016560	AAEL006794	0
		R2D2	GAWM01013568	AAEL011753	1.00E-53
			GAWM01017705	AAEL011753	1.00E-21
Other	Neural protein	AaHig	GAWM01013591	AAEL004725	0
			GAWM01013592	AAEL004725	0

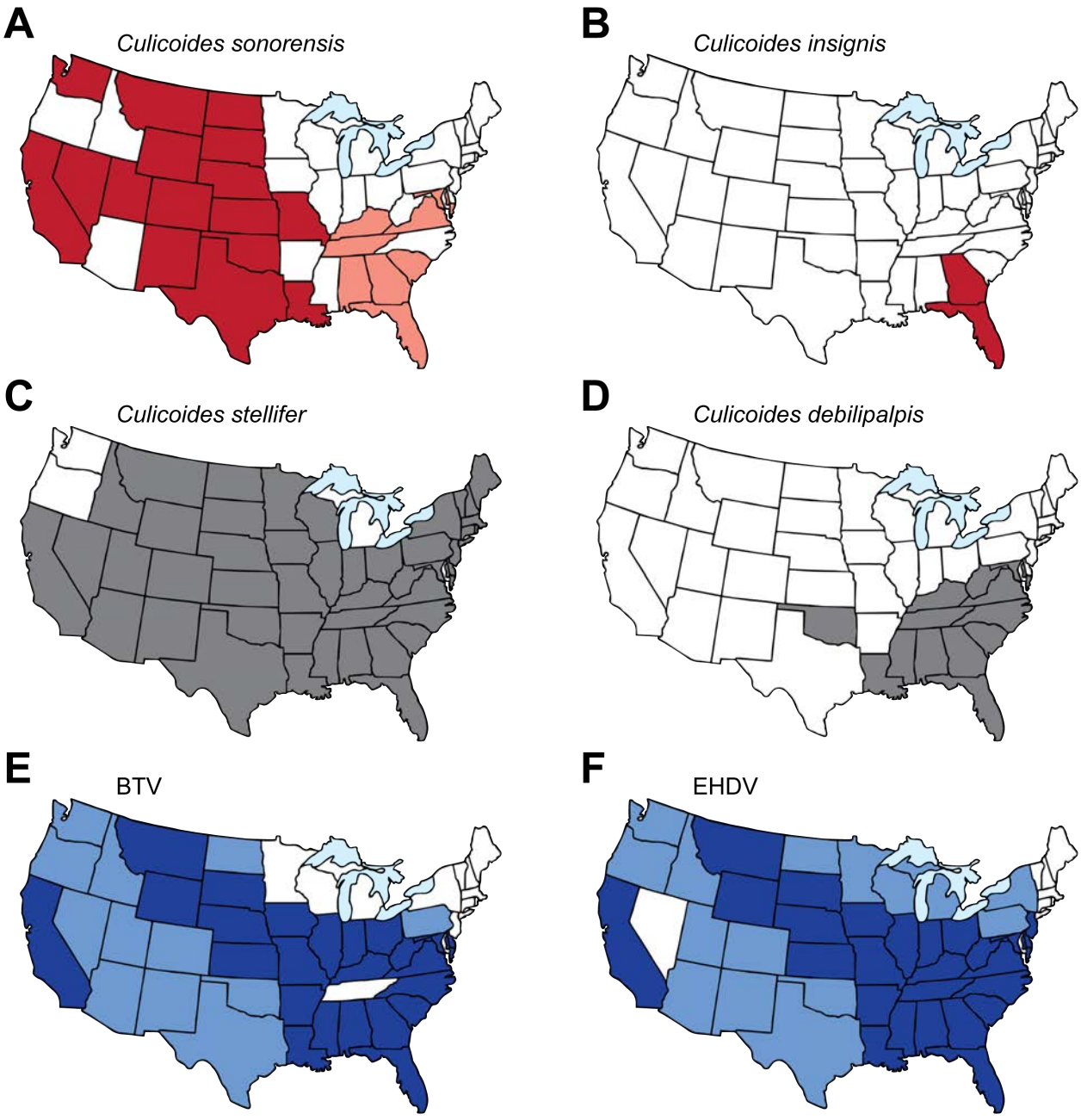

Figure 1.1 Geographic Distribution of *Culicoides* and HD throughout the US

This figure depicts the geographic distribution *Culicoides* species that are confirmed orbivirus vectors (red), (**A**) *C. sonorensis* and (**B**) *C. insignis,* or suspected orbivirus vectors (grey), (**C**) *C. stellifer* and (**D**) *C. debilipalpis.* (**A-D**) These *Culicoides* distributions are based on work complied by Blandon and Wirth (1979*) (**A**) *C. sonorensis* midges, while distributed throughout

the US, are not commonly (<10% of trap collections) found in field collections in the eastern US (Kramer et al. 1985*, Mellor et al. 2000*, Vigil et al. 2014*), as denoted by the different shades of red (dark red: more common, light red: less common). In addition, this figure provides the distribution of (**E**) BTV or (**F**) EHDV isolated from ruminants per state throughout the US from 1974-2012, with intensity of HD reports from wild ruminants denoted by different shades of blue. States colored blue (regardless of shade) denote the confirmed isolation of (**E**) BTV or (**F**) EHDV by Veterinary Services Laboratories (USDA-APIS-VS) or the Southeastern Cooperative Wildlife Disease Study (University of Georgia). States with ≥50% of their counties reporting HD of wild ruminants are denoted by dark blue, while states with ≤50% of their counties reporting HD of wild ruminants are denoted by light blue. HD intensity data was adapted from complied HD reports by the Southeastern Cooperative Wildlife Disease Study (University of Georgia). The data presented in this figure is adapted from published data from Ruder et al (2015b).

A

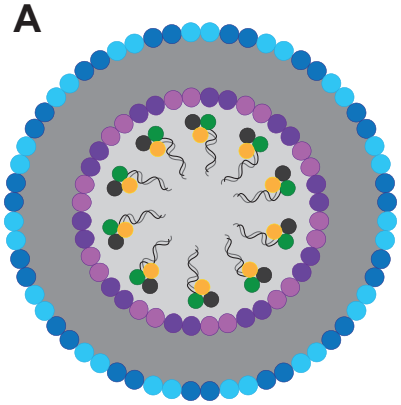

Viral Protein	Genome Segment (S)	Function
VP1	S1	RNA dependent RNA polymerase
VP2	S2	Outer capsid structure, cell attachment
VP3	S3	Inner capsid structure
VP4	S4	RNA capping enzyme
VP5	S6	Outer capsid structure, release of inner capsid
VP6	S9	Helicase
VP7	S7	Inner capsid structure
Ns1	S5	Enhances viral translation
Ns2	S8	Recruits viral components to VIBs
Ns3	S10	Aids in viral egress (exit)

B

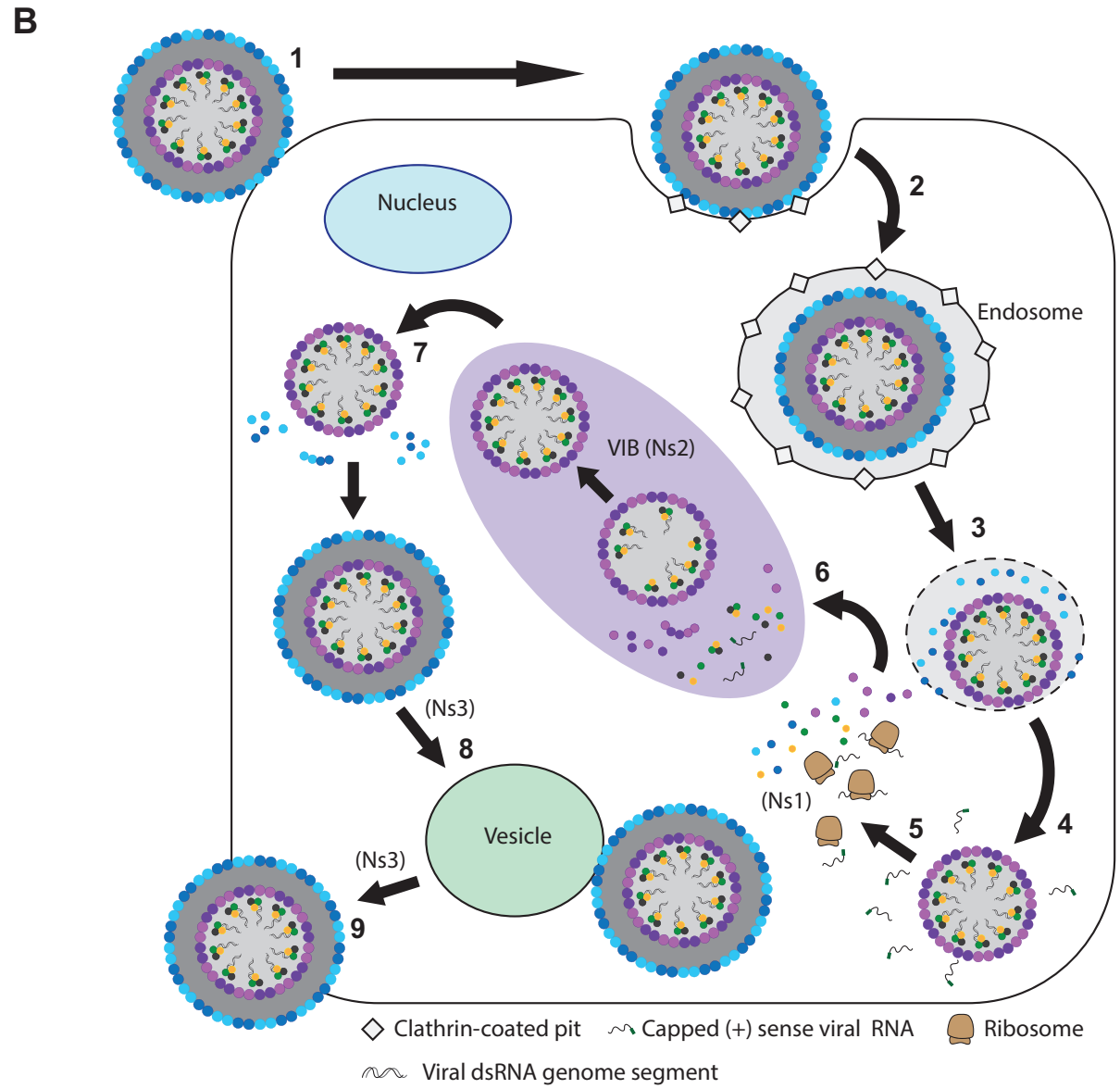

Figure 1.2 Orbivirus replication in insect cells

Figure 1.1 Orbivirus replication in insect cells

Graphical representation of the (**A**) orbivirus mature viral particle with viral proteins and corresponding genome segments and functions listed and (**B**) the steps of replication of orbivirus within the insect cell. (**1**) VP2 attaches to the insect cell and (**2**) induces clathrin-mediated endocytosis to enter the cell. (**3**) Acidification promotes permeabilization of the endosome by VP5. (**4**) Endosome permeablilization leads to the release of the transcriptionally active, inner capsid. Each of the ten dsRNA genome segments is transcribed using VP1, VP4, and VP6, and capped, positive-sense ssRNAs are released into the cytosol. (**5**) Promoted by Ns1, the released viral ssRNAs are used as template for the translation of viral proteins by host ribosomes. (**6**) Viral ssRNAs and proteins, VP1, VP3, VP4, VP6, and VP7, are recruited to viral inclusion bodies (VIB) created by NS2. These components self assemble into the inner capsid, and each viral ssRNA is used as a template for the synthesis of the corresponding dsRNA genome segment. (**7**) Inner capsids are released from the VIB, where they associate with outer capsid proteins, VP2 and VP5. (**8**) With the assistance of Ns3, the mature viral particle then associates with host vesicles and (**9**) leaves the cell by unknown mechanisms.

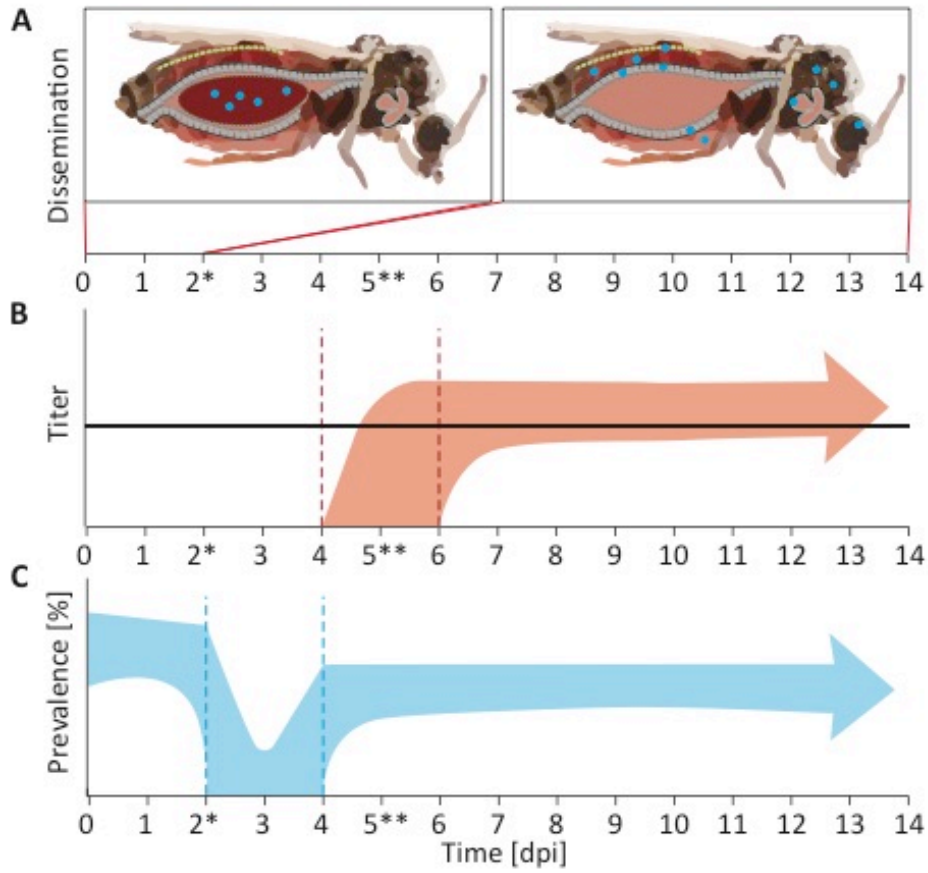

Figure 1.3 Proposed temporal proliferation dynamics of orbivirus infection within *C. sonorensis* at 25°C.

This figure summarize typical findings from previous experimental BTV and EHDV infections listed in Table 2 and compare dissemination (**A**), viral load (**B**), and prevalence (**C**) at 25°C. (**A**) After ingestion of the infected blood meal, the mesenteron escape barrier (MEB) is passed as early as 2 dpi (*) in competent midges, but salivary gland infection does not occur until 5 dpi (**). (**B**) Upon initial infection, viral load remains at or below the limit of detection until the proliferation phase (4–6 dpi). Viral load continues to fluctuate along the competence threshold (black line), but overall increases/plateaus over time. (**C**) Prevalence of virus-positive midges is stable early in infection, but undergoes a primary eclipse between 2–4 dpi. Afterwards,

prevalence increases and plateaus over the course of infection. Additional environmental and host factors can also significantly impact this scenario.

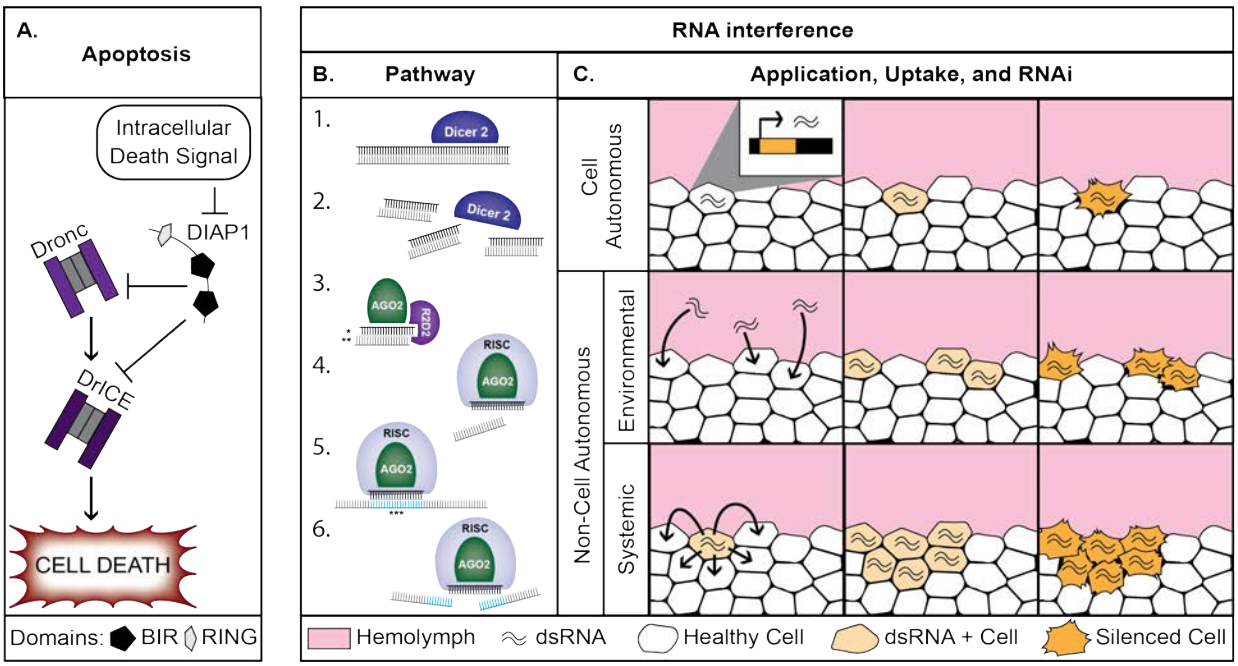

Figure 1.4 Heritable antiviral defenses, apoptosis and RNAi pathways in *Drosophila*

Graphical representation of the apoptosis (**A**) and RNAi (**B-C**) pathways. (**A**) Apoptosis is induced by the activation of the initiator caspase, Dronc, which, in turn, activates the effector caspase, DrICE, to cleave cellular substrates and lead to cell death. DIAP1 inhibits both Dronc and DrICE, and inhibition of DIAP1 initiates cell death. (**B**) The RNAi pathway is activated by the recognition of dsRNA by Dicer 2 (1), and subsequent cleavage of the bound dsRNA into siRNAs (2). These siRNAs, consisting of the guide strand (*) and passenger strand (**), are loaded into the AGO2 by R2D2 (3). After releasing the passenger strand from the guide strand (4), the RISC complex recognizes the sequence complementary to the guide strand (light blue, ***, 4) and cleaves the complementary sequence (6). (**C**) The siRNA pathway can be used as a reverse genetic tool for targeted gene knockdown (RNAi). Exogenous dsRNAs can be directly delivered to the target cell through a transgenic approach (cell autonomous), taken up by cells from the environment (environmental RNAi), or the silencing signal can be amplified to neighboring calls after the initial silencing signal is received (systemic RNAi).

Chapter 2 - Inducing RNA interference in the arbovirus vector, *Culicoides sonorensis*

Abstract

Biting midges in the genus *Culicoides* are important vectors of arboviral diseases, including epizootic hemorrhagic disease, bluetongue, and likely Schmallenberg, which cause significant economic burden worldwide. Research on these vectors has been hindered by the lack of a sequenced genome, the difficulty of consistent culturing of certain species, and the absence of molecular techniques such as RNA interference (RNAi). Here, we report the establishment of RNAi as a research tool for the adult midge, *Culicoides sonorensis*. Based on previous research and transcriptome analysis, which revealed putative siRNA pathway member orthologs, we hypothesized that adult *C. sonorensis* midges have the molecular machinery needed to preform RNA silencing. The development of an injection protocol allowed for double-stranded RNA (dsRNA) microinjection into the hemocoel of adult female midges. Using CO_2 exposure as a means to immobilize adult midges, injection of control dsRNA, ds*GFP*, into 2-3 day old adult female midges resulted in survival curves that support virus transmission. DsRNA injection targeting the newly identified *C. sonorensis* inhibitor of apoptosis protein 1 (CsIAP1) ortholog, resulted in increased mortality rates, with median survival shortened to less than eight days compared to 30 days in ds*GFP*-injected controls. *CsIAP1* transcript levels were decreased by 33% five days post-injection. These results reveal the conserved function of IAP1. Importantly, they also demonstrate the feasibility of RNAi by dsRNA injection in adult midges, which will greatly facilitate studies of the underlying mechanisms of vector competence in *C. sonorensis*.

Introduction

Biting midge species within the genus *Culicoides* (family: Cetratopogonidae) vector economically significant arboviruses, including bluetongue virus (BTV, orbivirus), epizootic hemorhagic disease virus (EHDV, orbivirus), and Schmallenberg virus (Bunyaviridae). While not affecting human health, these viral diseases cause fatalities in several ruminant species including cattle, sheep and goat livestock (Garigliany et al., 2012; Mellor et al., 2000). Disease control is focused on host-based methods, including vaccinations against BTV/EHDV, as well as control of livestock movement and housing (Maclachlan and Mayo, 2013). In addition, several potential vector-based control strategies, such as breeding site removal, repellents, traps, and insecticides have been evaluated (summarized in Carpenter et al., 2008). Despite the positive impact of surveillance and preventative measures on disease transmission, the potential economic losses due to a BTV outbreak would be substantial and could benefit significantly from long-term cost-effective vector control strategies (Calistri et al., 2004; Giovannini et al., 2004).

Novel control strategies, based on detailed molecular understanding of vector-pathogen interactions or biology of the vector species, have been proposed and are being implemented for Culicidae (e.g. Fu et al., 2010; Hoffmann et al., 2011). However, similar molecular studies into the biology and vector competence of *Culicoides* midges are hindered by many factors. These factors include lack of laboratory colonies for the vast majority of *Culicoides* vector species, sequence information, and molecular and genetic protocols. In addition, their minute size severely limits the amount of protein or nucleic acids that can be obtained from an individual, and challenges their fine-scale manipulations. This knowledge gap can be shortened, most easily, in *C. sonorensis*, the major vector of BTV in North America (Tabachnick, 1996), as it is one of

the two species for which robust colonies and cell lines exist (Nayduch et al., 2014a). In addition, a number of transcriptome studies have been published (Campbell et al., 2005; Campbell and Wilson, 2002), most recently using RNAseq data (Nayduch et al., 2014b). Some of these *C. sonorensis* gene products are potential targets for new vector control strategies, but require gene function analysis on the molecular level.

A central molecular tool to study gene function in non-model organisms is targeted gene knockdown by RNA interference (RNAi), which degrades mRNAs through the endogenous small interfering RNA (siRNA) pathway in a sequence-specific manner. Reverse genetic analyses by so-called environmental RNAi depends on the ability of tissues to take up an exogenous molecular trigger, either long dsRNA or siRNAs (Winston et al., 2007), and the function of Dicer2, R2D2 and AGO2 (most recently reviewed in Wilson and Doudna, 2013). A recent study revealed that RNAi can be induced by exogenous dsRNA in a larval cell line of *C. sonorensis* (Schnettler et al., 2013). However, based on studies in other insect species (Terenius et al., 2011) these results may not be a good predictor of environmental RNAi success in the whole organism. This study therefore aims to test the efficacy of RNAi in adult female *C. sonorensis* midges by assessing the knockdown phenotype of the *Culicoides* ortholog of *inhibitor of apoptosis (IAP)1*. Knockdown of this conserved gene in other insect species results in increased apoptosis and decreased lifespan (Hay et al., 1995; Walker III and Allen, 2011; Wang et al., 2012), and thus is a potential target to interrupt viral transmission in *C. sonorensis*.

Materials and Methods

Insect rearing and maintenance

The *C. sonorensis* AK strain was reared as described previously (Jones and Foster, 1974). At 1-3 d post-eclosion, midges were immobilized with CO_2 (Flypad, Flowbuddy Benchtop Regulator; Genesee Scientific, San Diego, CA, USA) then counted and sexed. Adults were maintained on sugar water (8% fructose in 2.5 mM 4-aminobenzoic acid) at 21-25°C and 70% relative humidity, with a photoperiod of 12:12 (L:D) h. Midges were allowed to recover for 1-2 d before performing experiments, and returned to the rearing conditions described above.

Sequence alignment, phylogenetic analysis, and protein domain identification

Amino acid sequence alignments were performed in MEGA 6.0 (Tamura et al., 2013) using ClustalW (Larkin et al., 2007) with default settings. To reconstruct the phylogenetic relationships, Maximum likelihood trees were generated using MEGA 6.0, with the following settings: Bootstrap method with 1,000 iterations, Jones-Taylor-Thorton substitution model, complete gap deletions, and nearest-neighbor-interchange. Protein domains were identified by means of the ScanProsite tool (http://prosite.expasy.org/scanprosite/; de Castro et al., 2006).

Total RNA extraction

Midges were frozen and stored at -80 °C prior to RNA extraction. Frozen midges (n=20) were homogenized in 200 µl homogenized Trizol (Ambion, Life Technologies, Carlsbad, CA, USA), and total RNA was extracted using a final volume of 1 ml Trizol according to manufacturer instructions. Pellets were air dried and resuspended in 100 µl RNAse-free water (Fisher Scientific, Waltham, MA, USA). RNA was purified with the RNeasy mini kit (Qiagen, Valencia, CA, USA) using the standard protocol and eluted in 50 µl RNAse-free water. RNA integrity was verified by agarose gel electrophoresis and concentration determined by Nanodrop

(Thermo Fisher Scientific, Waltham, MA, USA). On average, 17-21 ng of total RNA was obtained per midge.

cDNA synthesis

C. sonorensis cDNA was synthesized from 100 ng of purified total RNA with iScript cDNA synthesis kit (Biorad, Hercules, CA, USA), using oligo(dT) and random hexamer primers, in a total reaction volume of 20 µl, following manufacturer's protocol.

DsRNA synthesis

Template for dsRNA synthesis was generated by two-round PCR initially using 100 ng of cDNA. Primers for first round PCR (25 µl total reaction volume) were as follows: dsCsIAP1_F 5′-TAATACGACTCACTATAGGGAGTTGAAGAACACTTGAGATGG -3′; dsCsIAP1_R 5′-TAATACGACTCACTATAGGGGCCAATCTTCATACGACACC-3′. The resulting PCR product was purified by gel extraction (QIAquick Gel Extraction Kit; Qiagen). Next, 1 µl of first round PCR product was then amplified in a 50 µl second round PCR reaction using T7 primers: T7_F 5′-TAATACGACTCACTATAGGG-3′; T7_R 5′-TAATACGACTCACTATAGGG-3′. PCR product from these reactions was precipitated using 1 volume of isopropanol and resuspended in deionized water.

Ds*GFP* (An et al., 2010) and ds*CsIAP1* were synthesized as described previously (An et al., 2010) using 1 µg of second round PCR template in a total reaction volume of 20 µl. Purified dsRNA was resuspended in RNase-free water at a final concentration of 3 µg/µl.

Injection of adult female *C. sonorensis*

Midges were anesthetized under a constant flow of CO_2 (7 l/min). Female midges (n=100 per treatment and replicate) were injected with 50 nl H_2O, ds*GFP*, or ds*CsIAP1* under the wing base using a nanoinjector (Nanoject II, Drummond Scientific, Broomall, PA, USA). Injection

needles were made from borosilicate capillaries (3.5", outer diameter = 1.143 mm, inner diameter = 0.0531 mm, Drummond Scientific) using a Micropipette Puller (P-97, Sutter Instrument Co., Novato, CA, USA) and following pulling protocol: H* = 546, V =160, P = 170, T = 133 (*setting specific to each filament; instrument). Needles were opened by clipping the tip with scissors, and dsRNA was front-filled using the nanoinjector.

Survival analysis

After injection, survival was monitored daily until all midges within the experiment had died. Resulting data were analyzed and graphed using Kaplan-Meier and compared using the Log-rank (Mantel-Cox) Test and Hazard ratios. Median survival data were evaluated statistically with 1-way ANOVA followed by Tukey's Multiple Comparison post test. Biological replicates for CO_2 exposure (N = 3), injection (N = 6), and ds*CsIAP1* knockdown (N = 5) were performed. All statistical analyses were performed using Graphpad Prism software version 5.01 (GraphPad Software Inc., La Jolla, CA, USA).

Quantitative (q)RT-PCR

Female midges (n = 20 per treatment and replicate) were collected 5 d post-injection (dpi) for expression analysis. QRT-PCR was performed using iQ SYBR Green Supermix (Biorad) according to manufacturer's protocol with 1 µl of diluted cDNA (1:2) as template for each 20 µl volume reaction. QPCRs were executed on the StepOnePlus RT-PCR System and analyzed with the StepOne Software 2.0 (Life Technologies) with the following amplification protocol: initial cycle of 5 min at 95°C, followed by 40 cycles of 15 s at 95°C, 1 min at 59°C, and 1 min at 72°C (detection). Primers, designed using the Beacon Design 8 (Premier Biosoft International, Palo Alto, CA, USA), were as follows: CsIAP1_F 5′-TTGTGGACATATTATTGCCTGTG-3′;

CsIAP1_R 5′-CATGACTTTCGTGAATGGTTGT- 3′; EF1b_F 5′-ATCCGTGAAGAACGTCTCAAA- 3′; EF1b_R 5′-CATGGCTTAACTTCGAGGATG-3′.

Fold change for each treatment (ds*GFP* or ds*CsIAP1*) was assessed using a modified DDCt method (Pfaffl, 2001), which takes potentially different primer efficiencies (Figure A.1) into account. All qRT-PCRs were performed with 3 technical and four biological replicates. Untreated controls were used as the calibrator in each biological replicate. Expression data between ds*GFP* and ds*CsIAP1* treatments were compared statistically with Student's t-test. Statistical analyses were performed using GraphPad Prism software version 5.01 (GraphPad Software Inc., La Jolla, CA, USA).

Results

Adult midges encode and express components of the siRNA pathway

Previous work demonstrated that a *C. sonorensis* cell line was capable of environmental RNAi, and provided support for the potential application of reverse genetics in this species (Schnettler et al. 2013). As the first step to examine whether a functional siRNA pathway exists in adult *C. sonorensis*, we queried the recently published transcriptome (Nayduch et al., 2014b). Using *Aedes aegypti* siRNA pathway protein sequences as queries, multiple *C. sonorensis* transcripts with sequence similarity to *AGO2, Dicer2,* and *R2D2* were identified by best reciprocal BLAST hits. Overall, this analysis identified three *AGO2*, one *Dicer2*, and two *R2D2* putative orthologous sequences (Table 1).

Each of the three partial transcripts identified as AGO2 mapped to amino acids 242-786 of the *Ae. aegypti* ortholog (AAEL017251-RA). The amino acid sequence identity between the three *C. sonorensis* AGO2 sequences was very high, ranging from 88-97 %. In contrast, both

sequences orthologous to R2D2 spanned the entire *Ae. aegypti* R2D2 protein sequence (AAEL011753-RA), and showed sequence divergence between them, with only 36% sequence identity and a unique N-terminal extension of 21 amino acids encoded by the GAWM1017705 transcript. Finally, the *in silico* translated single putative *C. sonorensis Dicer2* transcript aligned to the complete *Ae. aegypti* Dicer2 protein (AAEL006794-RA), with 46% amino acid identity. Taken together, these data suggested strongly that a functional siRNA pathway is present in adult midges that may be exploited for RNA interference by provision of exogenous dsRNA.

Delivery of dsRNA into adult *C. sonorensis*

Intrathoracic injection is the most direct means of dsRNA delivery and has been used successfully in multiple insect species to induce RNAi (recently reviewed in Scott et al. 2013). Injection requires immobilization of insects by either cold treatment (Harris et al., 1965) or exposure to CO_2 (Blandin et al., 2002).

Despite several attempts of cold treatment using either a cold plate or ice, we were unable to immobilize *C. sonorensis* females sufficiently to allow for injection. Placement of adult female midges on a Flypad (Figure 2.1A) and exposure to constant CO_2 levels at 7 l/min immobilized adult midges within 30 s. After CO_2 exposure, all midges recovered completely and were motile within 10 min. To determine possible long term detrimental effects of CO_2 exposure on midge survival, 2-4 d old adult *C. sonorensis* were placed under a constant flow of 7 l/min CO_2 for a duration of 0, 10, 20, 30, and 40 min. Analysis of survival by Kaplan-Meier revealed statistically significant differences based on CO_2 exposure (Log-Rank test, $P<0.0001$; Figure 2.1B, see Figure A.2 for individual replicates). However, these differences were small with hazard ratios of 1.316 (1.153-1.501 95% CI) when comparing the longest CO_2 exposures to untreated controls. In addition, CO_2 treatment did not affect median survival (One-way

ANOVA, P=0.2348, Tukey's post test, P>0.05; Figure 2.1C). Given these results, we deemed CO_2 exposure as the method of choice for *C. sonorensis* injection.

Next, we examined the intrathoracic injection volume delivered into adult midges using a hand-held microinjector. Injected volumes of up to 50 nl lead to complete fluid retention using a single injection under the wing base (Figure 2.1D). To determine the extent of injury through the injection process, a control dsRNA, ds*GFP*, or its vehicle, ddH_2O, were injected into adult midges. Survival was analyzed by Kaplan-Meier, revealing accelerated mortality in both treatment groups as compared to untreated controls (Log Rank test, P<0.0001; Figure 2.1E, see Figure A.3 for individual replicates). Injection also shortened median survival by 6-8 d (One-way ANOVA, P=0.2348, Tukey's post test, P<0.05; Figure 2.1F). Hazard ratios of 1.433 (1.229-1.581 95% CI) due to ds*GFP* injection and 2.159 (1.912-2.438 95% CI) due to H_2O injection indicated that increased mortality rates, in part, were caused by injury and potentially exacerbated by the vehicle due to osmotic shock (Figure A.3). Nevertheless, average lifespan of ds*GFP*-injected midges exceeded 17 days and demonstrated the feasibility of this dsRNA injection protocol using ds*GFP* as a reliable negative control.

Identification of *C. sonorensis* IAP1 ortholog

Drosophila inhibitor of apoptosis 1 (IAP1) regulates apoptosis by inhibiting caspases, which are essential for cell death (Figure 2.3A). Since inhibition of IAP1 results in increased cell death and mortality, this protein has been discussed as a potential target for insect pest control by RNAi (Zhang et al., 2013). To identify an ortholog of IAP1 in *C. sonorensis,* Dipteran IAP protein sequences were obtained from ImmunoDB (http://cegg.unige.ch/Insecta/immunodb) and used to query the *C. sonorensis* transcriptome. We recovered five full-length transcripts that encoded putative IAPs. To determine orthology, their deduced amino acid sequences and known

IAPs from *Ae. aegypti* (Aa), *An. gambiae* (Ag)*, Culex quinquefasciatus* (Cq), and *D. melanogaster* (Dm) were used to reconstruct their phylogenetic relationships by maximum likelihood (Figure 2.2A, see Figure A.4 for sequences). In general, the tree topology for IAP1, 2, 5, and 6 mirrored the phylogenetic relationships among the five species (Wiegmann et al., 2011). Clusters for IAP2, 5, and 6 contained a single protein from each species, while two potential *C. sonorensis* IAP1 orthologs were found (CsIAP1A, CsIAP1B). Similar results were obtained after performing the phylogenetic analysis using alignments of the individual BIR domains (Figure A.5, see Figure A.6 for sequences). Protein domain analysis further corroborated the phylogenetic analysis and identified the expected number and location of BIRs, RINGs and Ubiquitin-conjugating domains required for the function of each protein (Figure 2.2B).

To further discriminate between the two putative orthologs of IAP1 in *C. sonorensis*, alignments of CsIAP1A/B were inspected. CsIAP1B lacks the DXXD motif and contains a truncated linker region between BIR1 and BIR2 (Figure 2.2B, and Figure A.7), which are required for IAP1 function (Ditzel et al., 2003; Sun et al., 1999). Based on these findings, CsIAP1A (GAWM01009039; CsIAP1) was chosen as the target for further analysis.

Targeted knockdown of *CsIAP1* by dsRNA injection in adult midges

IAP1 regulates apoptosis by inhibiting initiator and effector caspases, called DRONC and DRICE in *D. melanogaster* (Figure 2.3A), for which we identified putative orthologs in the *C. sonorensis* transcriptome (Figure A.8). Depletion of IAP1 by RNAi was shown previously to increase mortality in *Lygus lineolaris* and *Ae. aegypti* (Walker III and Allen, 2011; Wang et al., 2012). To test if GAWM01009039 is indeed IAP1, dsRNA targeting *CsIAP1* (ds*CsIAP1*) was injected into adult midges, and survival was monitored daily. As expected, injection of ds*CsIAP1* resulted in a significant increase in mortality rates and decreased life span when compared to

both untreated and ds*GFP*-injected midges (Log-Rank test, $P<0.0001$; Figure 2.3B, see Figure A.9 for individual replicates). Ds*CsIAP1*-injected midges were twice as likely to die as compared to ds*GFP*-treated controls (Log Rank test, $P<0.0001$; Hazard ratio=2.098), and their median survival was reduced three-fold to 7 days post-injection (1-Way ANOVA, $P<0.0001$, Tukey's post test $P<0.05$, Figure 2.3C). Transcript levels of *CsIAP1* were determined by qRT-PCR 5 dpi. *Elongation factor 1b* (*EF1b*, GAWM01010754) was used as the reference gene, as its expression remains constant during multiple physiological processes (Nayduch et al., 2014b). *CsIAP1* expression was reduced by 33% in ds*CsIAP1*-treated midges relative to ds*GFP*-injected midges, but the combination of increased variation and lowered reduction in transcript levels resulted in a loss of the originally reported statistical significance (Student's t-test, P=0.07; Figure 2.4). These decreased transcript levels specific to ds*CsIAP1*-injection demonstrate that dsRNA-targeted knockdown can be utilized in adult *C. sonorensis*.

Discussion

Over the last 15 years, RNAi has become the standard genetic tool for gene function analysis in non-model insect species and also harbors the promise of highly species-specific insect control both for agricultural and public health purposes. The canonical siRNA pathway is characterized by three key proteins: Dicer2 and R2D2, which are required to process long dsRNA into 21 nt siRNAs, as well as AGO2, which forms the protein core of the RISC complex and cleaves the single-stranded target (recently reviewed in Wilson and Doudna, 2013). Based on available transcriptome data, we identified their putative orthologs in *C. sonorensis*. The high percent identities amongst the three putative AGO2 proteins strongly suggest that these transcripts are from a single gene, and sequence differences are likely the result of haplotype variation within

the midge laboratory strain. In contrast, R2D2 has potentially undergone gene duplication in the midge lineage. Of the two putative R2D2 proteins, we hypothesize that GAWM01013568 has retained function required for siRNA pathway activity.

To develop RNAi as a molecular tool for *C. sonorensis*, we chose dsRNA injection as the delivery method to avoid inconsistent dose uptake due to variable feeding volumes or degradation by digestive enzymes (Arimatsu et al., 2007). In addition, injection disseminates dsRNA through hemolymph circulation, allowing direct contact between dsRNA and all midge tissues. Immobilization for intrathoracic injection is essential and can be achieved in insects through cold treatment or CO_2 exposure (Harris et al., 1965). The inability of adult *C. sonorensis* to be immobilized by cold plate was an interesting observation, and may be a result of their ability to overwinter at low temperatures as larvae (Barnard and Jones, 1980). In contrast, CO_2 exposure immobilized adult midge effectively and over prolonged periods of time with barely measureable adverse effects on their survival.

Not surprisingly, injury due to injection accelerated midge mortality rates. However, increased mortality rates were usually limited to the first three to five days post-injection, suggesting that by five days the surviving midges had overcome initial injury by wound healing. This period was followed by decreased daily mortality rates as compared to untreated controls, which resulted in roughly similar median survival between injected and control groups. Importantly, the lifespan of ds*GFP*-injected midges supports the BTV intrinsic incubation period, which is between 4-20 days depending on temperature (Foster et al., 1968; Purse et al., 2005). This protocol thus enables the study of the molecular basis of arbovirus-midge interactions by reverse genetics.

As proof of principle, we targeted *CsIAP1* for knockdown by dsRNA injection in adult female midges. IAP1 is a key regulator of apoptosis (Hay et al., 1995; Tenev et al., 2007), which functions in persistent viral infection as well as antiviral defense in insects (reviewed in Clarke and Clem, 2003). Apoptosis affects virus replication in multiple insect cell lines (Settles and Friesen, 2008; Wang et al., 2008). Furthermore, cytopathic apoptosis in a mammalian cell line caused by BTV infection is hindered by expression of recombinant *Ae. aegypti* IAP1 (Li et al., 2007). These published data suggest that regulation of apoptosis could be integral for persistent virus infection within the midge vector. Putative orthologs of both initiator and effector caspases inhibited by IAP1 are expressed in adult midges, further supporting that the core of the apoptosis pathway is conserved in *C. sonorensis*.

As expected, injection of ds*CsIAP1* into adult female midges led to accelerated mortality rates, a conserved phenotype observed previously in hemiptera (Walker III and Allen, 2011) and mosquitoes (Wang et al., 2012). Given that *CsIAP1* transcript levels were significantly and specifically reduced, this phenotype is in all likelihood the result of RNAi triggered by the injection of long dsRNAs. In some cases, the RNAi trigger is amplified and propagated through endogenous production and release of siRNAs (Winston et al., 2002). However, very few insect species are capable of this so-called systemic RNAi (Tomoyasu et al., 2008). The 33% transcript reduction of *CsIAP1* induced by a comparatively high dose of dsRNA (Miller et al., 2012) suggests that the initial RNAi trigger is not amplified in *C. sonorensis* and is likely not taken up by all tissues. Similar results have been obtained from closely related Culicidae (Blandin et al., 2002; Zhu et al., 2003). In addition, we observed considerable variation in overall transcript reduction levels between biological replicates. Nevertheless, our data clearly demonstrate that environmental RNAi in *C. sonorensis* can be exploited for gene function analysis. Determining

average transcript reduction levels across other *C. sonorensis* genes requires further empirical assessment, as knockdown levels are influenced by a multitude of factors, including species, tissue, target gene, as well as temperature (recently reviewed in Scott et al., 2013).

RNAi has evolved as a fundamental antiviral immune response and affects virus replication in insect vectors (Keene et al., 2004; Olson et al., 1996). The demonstration of an active siRNA pathway in adult female midges dictates that replication of arboviruses with dsRNA genomes, such as BTV and EHDV must overcome this defense mechanism. One hypothesis is that during infection, BTV escapes RNA silencing due to the release of only positive-sense capped mRNA transcripts into the cytosol and sequestration of dsRNA genome to the inner viral capsid (Roy, 2008). In addition, the BTV core has a high affinity for dsRNA, effectively trapping and concealing it from host detection (Diprose et al., 2002). Nevertheless, engineered dsRNA specific for BTV non-structural protein 1 limits virus replication in a *C. sonorensis* cell line (Schnettler et al., 2013). Studies are currently underway to determine the contribution of the siRNA pathway to biting midge vector competency *in vivo.*

Taken together, this study provides the first demonstration of RNAi in adult *C. sonorensis* midges providing a much needed means to study this important arbovirus vector species. With the development of an intrathoracic injection protocol and delivery of long dsRNAs, we verify the conserved function of *CsIAP1* as a negative regulator of cell death in adult midges. The decreased life span of ds*CsIAP1*-treated midges ablates virus transmission, and thus may be exploited for novel disease control strategies targeting the vector. In addition, we provide annotation of siRNA and apoptosis pathway components in *C. sonorensis* enabling future studies on their role in vector competence for arboviruses.

Acknowledgments

The authors thank Dr. Lee Cohnsteadt, Mr. James A. Kempert, and Mr. William E. Yarnell at the Arthropod-Borne Animal Disease Research Unit, USDA-ARS, Manhattan, KS for provision of all adult *C. sonorensis* midges and housing materials used in this study. We further thank Drs. Rollie Clem and W. Bart Bryant, Division of Biology, Kansas State University, for helpful discussions on IAP1. This project was supported by Specific Cooperative Agreement 58-5430-1360 to K. M. from the USDA Agricultural Research Service. This chapter was published in 2015 by Elsevier in the journal Insect Molecular Biology, volume 24, issue 1, from pages 105-114, and titled "Inducing RNA interference in the arbovirus vector, *Culicoides sonorensis*" (DOI: 10.1111/imb.12139). A corrigendum to the published manuscript was included in this chapter. The corrigendum was published in 2015 by Elsevier in the journal of Insect Molecular Biology, volume 24, issue 5, and on page 502 (DOI: 10.1111/imb.12178).

References

An, C., A. Budd, M.R. Kanost, and K. Michel. 2010. Characterization of a regulatory unit that controls melanization and affects longevity of mosquitoes. Cell. Mol. Life Sci. 68: 1929-1939.

Arimatsu, Y., E. Kotani, Y. Sugimura, and T. Furusawa. 2007. Molecular characterization of a cDNA encoding extracellular dsRNase and its expression in the silkworm, *Bombyx mori*. Insect Biochem. Mol. Biol. 37: 176-183.

Barnard, D.R. and R.H. Jones. 1980. *Culicoides variipennis*: seasonal abundance, overwintering, and voltinism in northeastern Colorado. Environmental Entomol. 9: 709-712.

Blandin, S., L.F. Moita, T. Kocher, M. Wilm, F.C. Kafatos, and E.A. Levashina. 2002. Reverse genetics in the mosquito *Anopheles gambiae*: targeted disruption of the Defensin gene. EMBO Rep. 3: 852-856.

Calistri, P., A. Giovannini, A. Conte, D. Nannini, U. Santucci, C. Patta, S. Rolesu, and V. Caporale. 2004. Bluetongue in Italy: Part I. Vet. Italiana. 40: 243-251.

Campbell, C.L., K.A.Vandyke, G.J. Letchworth, B.S. Drolet, T. Hanekamp, and W.C. Wilson. 2005. Midgut and salivary gland transcriptomes of the arbovirus vector *Culicoides sonorensis* (Diptera: Ceratopogonidae). Insect Mol. Biol. 14: 121-136.

Campbell, C.L. and W.C. Wilson. 2002. Differentially expressed midgut transcripts in *Culicoides sonorensis* (Diptera: Ceratopogonidae) following orbivirus (*Reoviridae*) oral feeding. Insect Mol. Biol. 11: 595-604.

Carpenter, S., P.S. Mellor, and S.J. Torr. 2008. Control techniques for *Culicoides* biting midges and their application in the U.K. and northwestern Palaearctic. Med. Vet. Entomol. 22: 175-187.

Clarke, T.E. and R.J. Clem. 2003. Insect defenses against virus infection: the role of apoptosis. Int. Rev. Immunol. 22: 401-424.

de Castro, E., C.J. Sigrist, A. Gattiker, V. Bulliard, P.S. Langendijk-Genevaux, E. Gasteiger, A. Bairoch, and N. Hulo. 2006. ScanProsite: detection of PROSITE signature matches and ProRule-associated functional and structural residues in proteins. Nucleic Acids Res. 34: W362-365.

Diprose, J.M., J.M. Grimes, G.C. Sutton, J.N. Burroughs, A. Meyer, S. Maan, P.P. Mertens, P.P., and D.I. Stuart. 2002. The core of bluetongue virus binds double-stranded RNA. J. Virol. 76: 9533-9536.

Ditzel, M., R. Wilson, T. Tenev, A. Zachariou, A. Paul, E. Deas, and P. Meier. 2003. Degradation of DIAP1 by the N-end rule pathway is essential for regulating apoptosis. Nat Cell Biol. 5: 467-473.

Foster, N.M., R.H. Jones, and A.J. Luedke. 1968. Transmission of attenuated and virulent bluetongue virus with *Culicoides variipennis* infected orally via sheep. Am. J. Vet. Res. 29: 275-279.

Fu, G., R.S. Lees, D. Nimmo, D Aw, L. Jin, P. Gray, T.U. Berendonk, H. White-Cooper, S. Scaife, H. Kim Phuc, O. Marinotti, N. Jasinskiene, A.A. James, and L. Alphey. 2010. Female-specific flightless phenotype for mosquito control. Proc. Natl. Acad. Sci. U. S. A. 107: 4550-4554.

Garigliany, M.M., C. Bayrou, D. Kleijnen, D. Cassart, S. Jolly, A. Linden, and D. Desmecht. 2012. Schmallenberg virus: a new Shamonda/Sathuperi-like virus on the rise in Europe. Antiviral. Res. 95: 82-87.

Giovannini, A., P. Calistri, D. Nannini, C. Paladini, U. Santucci, C. Patta, and V. Caporale. 2004. Bluetongue in Italy: Part II. Vet. Italiana: 40: 252-259.

Harris, R.L., R.A. Hoffman, and E.D. Frazar 1965. Chilling vs. other methods of immobilizing flies. J. Econ. Entomol. 58: 379-380.

Hay, B.A., D.A. Wassarman, and G.M. Rubin. 1995. *Drosophila* homologs of baculovirus inhibitor of apoptosis proteins function to block cell death. Cell. 83: 1253-1262.

Hoffmann, A.A., B.L. Montgomery, J. Popovici, I. Iturbe-Ormaetxe, P.H. Johnson, F. Muzzi, M. Greenfield, M. Durkan, Y.S. Leong, Y. Dong, H. Cook, J. Axford, A.G. Callahan, N. Kenny, C. Omodei, E.A. McGraw, P.A. Ryan, S.A. Ritchie, M. Turelli, and S.L. O'Neill. 2011. Successful establishment of *Wolbachia* in *Aedes* populations to suppress dengue transmission. Nature. 476; 454-457.

Jones, R.H. and N.M. Foster. 1974. Oral infection of *Culicoides variipennis* with bluetongue virus: development of susceptible and resistant lines from a colony population. J. Med. Entomol. 11: 316-323.

Keene, K.M., B.D. Foy, I. Sanchez-Vargas, B.J. Beaty, C.D. Blair, and K.E. Olson. 2004. RNA interference acts as a natural antiviral response to O'nyong-nyong virus (Alphavirus; Togaviridae) infection of *Anopheles gambiae*. Proc. Natl. Acad. Sci. U. S. A. 101: 17240-17245.

Larkin, M.A., G. Blackshields, N.P. Brown, R. Chenna, P.A. McGettigan, H. McWilliam, F. Valentin, I.M. Wallace, A. Wilm, R. Lopez, J.D. Thompson, T.J. Gibson, and D.G. Higgins .2007. Clustal W and Clustal X version 2.0. Bioinformatics. 23: 2947-2948.

Li, Q., H. Li, B.J. Blitvich, and J. Zhang. 2007. The *Aedes albopictus inhibitor of apoptosis 1* gene protects vertebrate cells from bluetongue virus-induced apoptosis. Insect. Mol. Biol. 16: 93-105.

Maclachlan, N.J. and C.E. Mayo. 2013. Potential strategies for control of bluetongue, a globally emerging, *Culicoides*-transmitted viral disease of ruminant livestock and wildlife. Antiviral. Res. 99: 79-90.

Mellor, P.S., J. Boorman, and M. Baylis. 2000. *Culicoides* biting midges: their role as arbovirus vectors. Annu. Rev. Entomol. 45; 307-340.

Miller, S.C., K. Miyata, S.J. Brown, and Y. Tomoyasu. 2012. Dissecting systemic RNA interference in the red flour beetle *Tribolium castaneum*: parameters affecting the efficiency of RNAi. PloS One. 7: e47431.

Nayduch, D., L.W. Cohnstaedt, C. Saski, D. Lawson, P. Kersey, M. Fife, and S. Carpenter. 2014a. Studying *Culicoides* vectors of BTV in the post-genomic era: resources, bottlenecks to progress and future directions. Virus. Res. 182; 43-49.

Nayduch, D., M.B. Lee, and C. Saski. 2014b. The reference transcriptome of the adult female biting midge (*Culicoides sonorensis*) and differential gene expression profiling during teneral, blood, and sucrose feeding conditions. PloS One. 9: e98123.

Olson, K.E., S. Higgs, P.J. Gaines, A.M. Powers, B.S. Davis, K.I. Kamrud, J.O. Carlson, C.D. Blair, and B.J. Beaty. 1996. Genetically engineered resistance to dengue-2 virus transmission in mosquitoes. Science. 272: 884-886.

Pfaffl, M.W. 2001. A new mathematical model for relative quantification in real-time RT-PCR. Nucleic Acids Res. 29: e45.

Purse, B.V., M.S. Mellor, D.J. Rogers, A.R. Samuel, P.P Mertens, and M. Baylis. 2005. Climate change and the recent emergence of bluetongue in Europe. Nat. Rev. Microbiol. 3: 171-181.

Roy, P. 2008. Functional mapping of bluetongue virus proteins and their interactions with host proteins during virus replication. Cell Biochem. Biophys. 50: 143-157.

Schnettler, E., M. Ratinier, M. Watson, A.E. Shaw, M. McFarlane, M. Varela, R.M. Elliott, M. Palmarini, and A. Kohl. 2013. RNA interference targets arbovirus replication in *Culicoides* cells. J. Virol. 87: 2441-2454.

Scott, J.G., K. Michel, L.C. Bartholomay, B.D. Siegfried, W.B. Hunter, G. Smagghe, K.Y. Zhu, and A.E. Douglas. 2013. Towards the elements of successful insect RNAi. J. Insect. Physiol. 59: 1212-1221.

Settles, E.W., and P.D. Friesen. 2008. Flock house virus induces apoptosis by depletion of *Drosophila* inhibitor-of-apoptosis protein DIAP1. J. Virol. 82: 1378-1388.

Sun, C., M. Cai, A.H. Gunasekera, R.P. Meadows, H. Wang, J. Chen, H. Zhang, W. Wu, N. Xu, S.C. Ng, and S.W Fesik. 1999. NMR structure and mutagenesis of the inhibitor-of-apoptosis protein XIAP. Nature. 401: 818-822.

Tabachnick, W.J. 1996. *Culicoides variipennis* and bluetongue-virus epidemiology in the United States. Annu. Rev. Entomol. 41: 23-43.

Tamura, K., G. Stecher, D. Peterson, A. Filipski, and S. Kumar. 2013. MEGA6: Molecular Evolutionary Genetics Analysis version 6.0. Mol. Biol. Evol. 30: 2725-2729

Tenev, T., M. Ditzel, A. Zachariou, and P. Meier. 2007. The antiapoptotic activity of insect IAPs requires activation by an evolutionarily conserved mechanism. Cell Death Differ. 14: 1191-1201.

Terenius, O., A. Papanicolaou, J.S. Garbutt, I. Eleftherianos, H. Huvenne, S. Kanginakudru, M. Albrechtsen, C. An, J.L. Aymeric, A. Barthel, P. Bebas, K. Bitra, A. Bravo, F. Chevalier, D.P. Collinge, C.M. Crava, R.A. de Maagd, B. Duvic, M. Erlandson, I. Faye, G. Felfoldi, H. Fujiwara, R. Futahashi, A.S. Gandhe, H.S. Gatehouse, L.N. Gatehouse, J.M. Giebultowicz, I. Gomez, C.J. Grimmelikhuijzen, A.T. Groot, F. Hauser, D.G. Heckel, D.D. Hegedus, S. Hrycaj, L. Huang, J.J. Hull, K. Iatrou, M. Iga, M.R. Kanost, J. Kotwica, C. Li, J. Li, J. Liu, M. Lundmark, S. Matsumoto, M. Meyering-Vos, P.J. Millichap, A. Monteiro, N. Mrinal, T. Niimi, D. Nowara, A. Ohnishi, V. Oostra, K. Ozaki, M. Papakonstantinou, A. Popadic, M.V. Rajam, S. Saenko, R.M. Simpson, M. Soberon, M.R. Strand, S. Tomita, U. Toprak, P. Wang, C.W. Wee, S. Whyard, W. Zhang, J. Nagaraju, R.H. Ffrench-Constant, S. Herrero, K. Gordon, L. Swevers, and G. Smagghe. 2011. RNA interference in Lepidoptera: an overview of successful and unsuccessful studies and implications for experimental design. J. Insect. Physiol. 57: 231-245.

Tomoyasu, Y., S.C. Miller, S. Tomita, M. Schoppmeier, D. Grossmann, and G. Bucher. 2008. Exploring systemic RNA interference in insects: a genome-wide survey for RNAi genes in *Tribolium*. Genome Biol. 9: R10.

Walker III, W.B., and M.L. Allen. 2011. RNA interference-mediated knockdown of IAP in *Lygus lineolaris* induces mortality in adult and pre-adult life stages. Entomol. Exp. Appl. 138: 83-92.

Wang, H., C.D. Blair, K.E. Olson, and R.J. Clem. 2008. Effects of inducing or inhibiting apoptosis on Sindbis virus replication in mosquito cells. J. Gen. Virol. 89: 2651-2661.

Wang, H., T. Gort, D.L. Boyle, and R.J Clem. 2012. Effects of manipulating apoptosis on Sindbis virus infection of *Aedes aegypti* mosquitoes. J. Virol. 86: 6546-6554.

Wiegmann, B.M., M.D. Trautwein, I.S. Winkler, N.B. Barr, J.W. Kim, C. Lambkin, M.A. Bertone, B.K. Cassel, K.M. Bayless, A.M. Heimberg, B.M., Wheeler, K.J. Peterson, T. Pape, B.J. Sinclair, J.H. Skevington, V. Blagoderov, J. Caravas, S.N. Kutty, U. Schmidt-Ott, G.E. Kampmeier, F.C. Thompson, D.A. Grimaldi, A.T. Beckenbach, G.W. Courtney, M. Friedrich, R. Meier, and D.K. Yeates. 2011. Episodic radiations in the fly tree of life. Proc. Natl. Acad. Sci. U. S. A. 108: 5690-5695.

Wilson, R.C. and J.A. Doudna. 2013. Molecular mechanisms of RNA interference. Annu. Rev. Biophys. 42: 217-239.

Winston, W.M., C. Molodowitch, and C.P. Hunter. 2002. Systemic RNAi in *C. elegans* requires the putative transmembrane protein SID-1. Science. 295: 2456-2459.

Winston, W.M., M. Sutherlin, A.J. Wright, E.H. Feinberg, and C.P. Hunter. 2007. *Caenorhabditis elegans* SID-2 is required for environmental RNA interference. Proc. Natl. Acad. Sci. U. S. A. 104; 10565-10570.

Zhang, H., H. C.Li, and X.X. Miao. 2013. Feasibility, limitation and possible solutions of RNAi-based technology for insect pest control. Insect Sci. 20: 15-30.

Zhu, J., L. Chen, and A.S. Raikhel. 2003. Posttranscriptional control of the competence factor betaFTZ-F1 by juvenile hormone in the mosquito *Aedes aegypti*. Proc. Natl. Acad. Sci. U. S. A. 100: 13338-13343.

Tables and Figures – Chapter 2

Table 2.1 Putative *C. sonorensis* siRNA pathway members

Protein	*Culicoides sonorensis*	Length [AA]	*Anopheles gambiae*	Length [AA]	*Aedes aegypti*	Length [AA]
AGO2	GAWM01012834	269	AGAP011537-PA	841	AAEL017251-RA	992
	GAWM01012835	633				
	GAWM01012837	254				
Dicer2	GAWM01016560	1679	AGAP012289-PA	1673	AAEL006794-RA	1659
R2D2	GAWM01013568	295	AGAP009887-PA	325	AAEL011753-RA	319
	GAWM01017705	334				

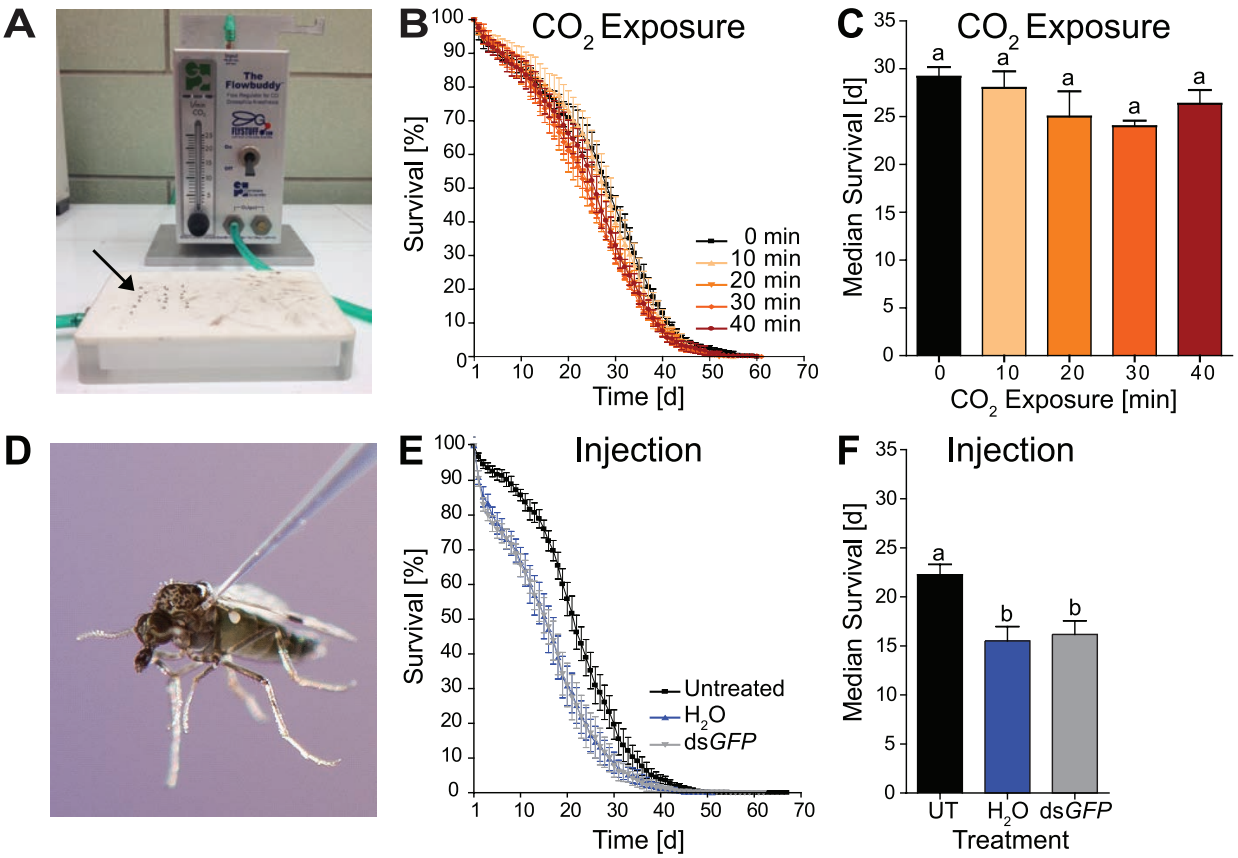

Figure 2.1 Delivery of dsRNA by microinjection to adult midges

(**A-C**) Effects of CO_2 exposure on *C. sonorensis* adults. (**A**) Midges (arrow) were immobilized using a Flypad. (**B**) Survival curves of midges after exposure to CO_2 at indicated time intervals. (**C**) Comparison of median survival after CO_2 exposures. Lettering denotes lack of statistically significant differences (Tukey's post test, $P>0.05$). Data were combined from three biological replicates (Figure A.2), and are presented as mean ± one standard error of the mean (S.E.M.). **(D-F**) Effects of injection on *C. sonorensis* adult females. (**D**) Female midges were injected intrathoracically into the soft cuticle between wing base and the second pleural sclerite. (**E**) Graph depicts survival curves of midges after no, H_2O, or ds*GFP* injection. (**F**) Midge median survival after injection treatments. Statistically significant differences are indicated by different

letters (Tukey's post test, $P<0.05$). All data are presented as mean ± one S.E.M. from six biological replicates (Figure A.3). UT; untreated control.

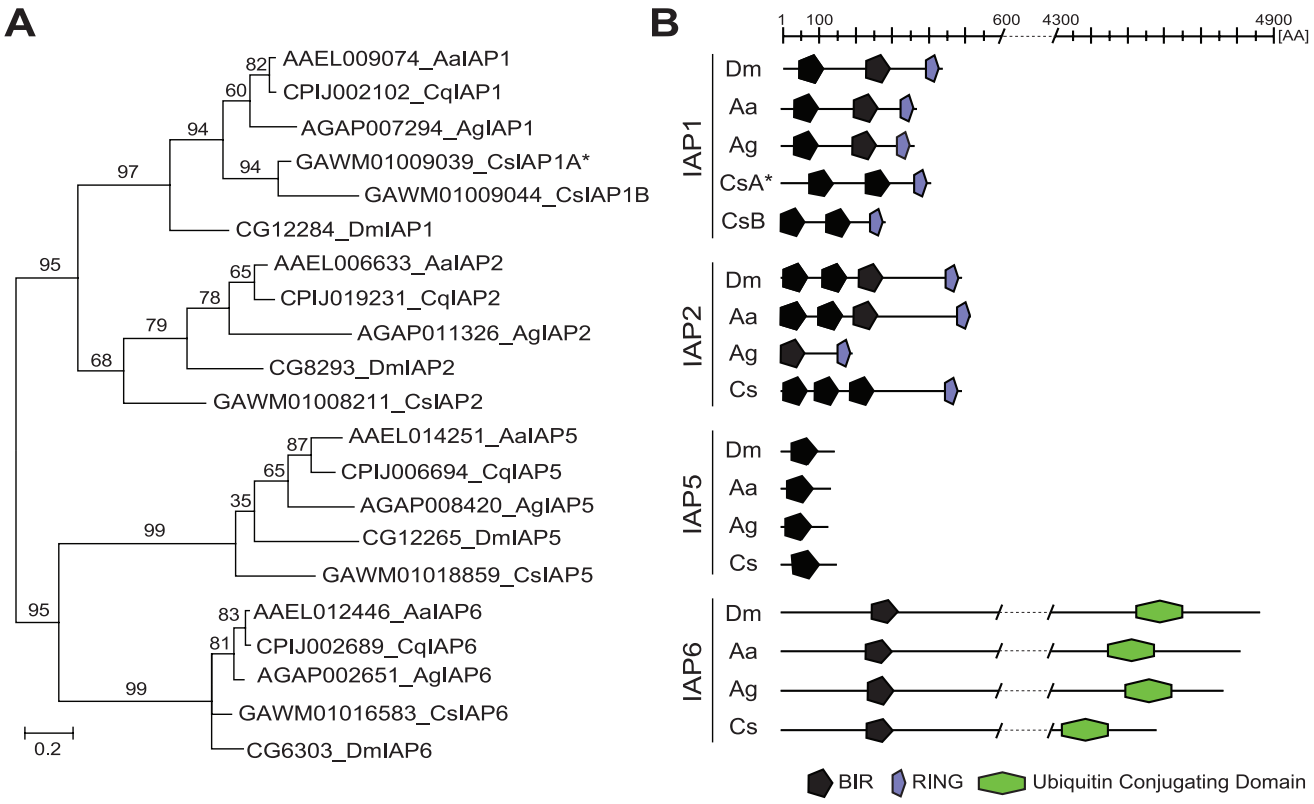

Figure 2.2 Identification of *Culicoides* IAP1 orthologs

(**A**) Maximum Likelihood phylogenetic tree of Dipteran IAPs. IAPs are identified by their accession number, species abbreviation, and IAP subfamily. (**B**) Schematic representation of IAP proteins indicating the length and location of functional domains including BIR (black pentagon), RING (purple narrow pentagon), and Ubiquinin Conjugating domain (green hexagon). Corresponding total protein sequences are listed in Figure A.4, and BIR domain sequences are listed in Figure A.6.

Aa, *Ae. aegypti*; Ag, *An. gambiae*; Cq, *Culex quinquefasciatus*; Cs, *C. sonorensis*; Dm, *D. melanogaster;* * putative functional ortholog of IAP1 in *C. sonorensis* used for further analysis.

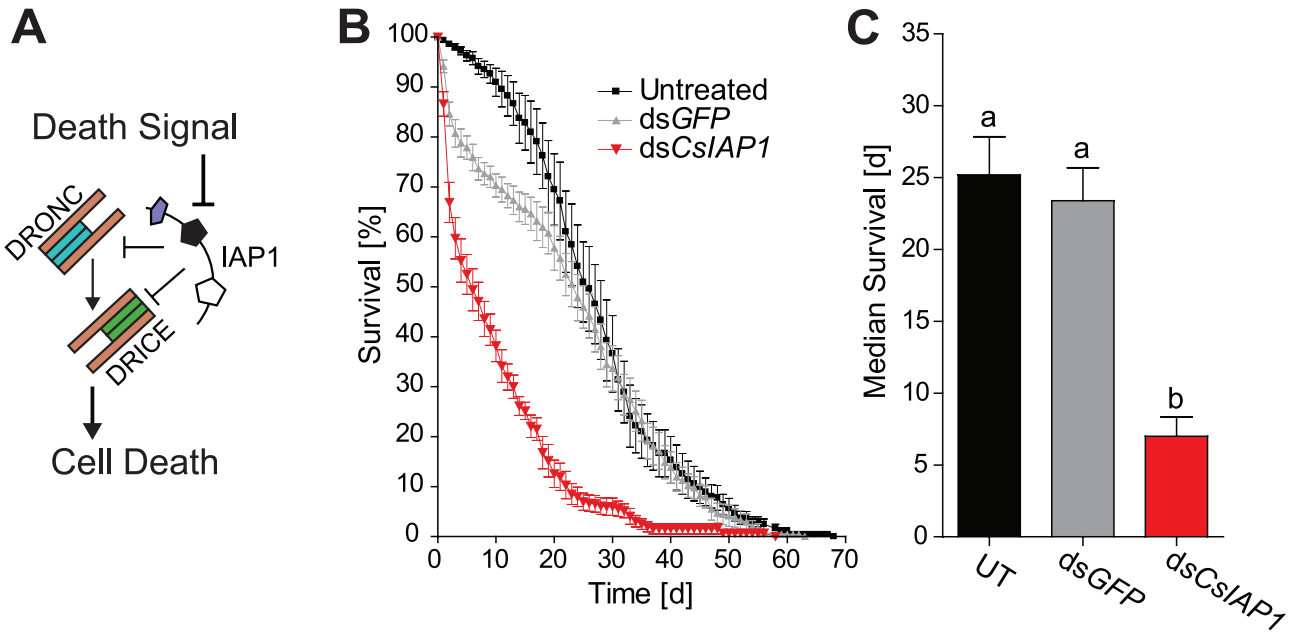

Figure 2.3 Effects of ds*CsIAP1* injection on female *C. sonorensis* mortality

A) Illustration of the IAP1's regulatory function of apoptosis through caspase (*D. melanogaster* Dronc and DrICE) inhibition. B) Graph represents percent survival of midges after no, ds*GFP*, or ds*CsIAP1* injection. C) Median survival of midges after corresponding treatments. Statistically-significant differences are indicated by different letters (Tukey's post test, $P<0.05$). Data are presented as mean ± one S.E.M. from five biological replicates (Figure A.9). UT; untreated control.

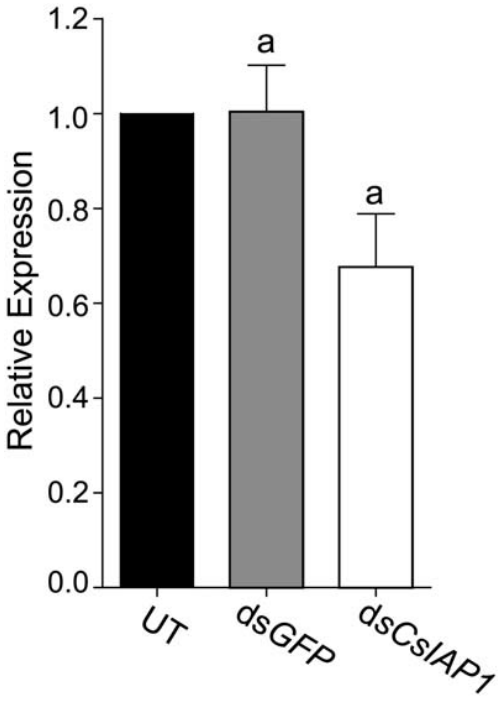

Figure 2.4 Relative expression of *CsIAP1* transcripts after dsRNA injection

Graph depicts *CsIAP1* mean transcript levels at 5 dpi for ds*GFP* and ds*CsIAP1*-injected midges relative to untreated controls. RT-qPCR results were analyzed using *EF1b* as reference gene and untreated midges as calibrator condition. On average, mRNA levels of *CsIAP1* were unaffected by ds*GFP* injection, and reduced by 33% after ds*CsIAP1* treatment compared to untreated controls (UT). However, expression levels between ds*GFP* and ds*CsIAP1*- treated midges were not statistically significantly different (Student's t-test, $P = 0.07$). Data are presented as mean ± one S.E.M., from four biological replicates (Figure A.2).

Chapter 3 - Functional validation of apoptosis genes *IAP1* and *Dronc* in the biting midge *Culicoides sonorensis* by RNAi

Abstract

Culicoides biting midges transmit multiple ruminant viruses, including bluetongue virus and epizootic hemorrhagic disease virus, causing significant economic burden worldwide. To further enhance current control techniques, understanding vector-virus interactions within the midge is critical. We developed previously a double-stranded RNA (dsRNA) delivery method to induce RNA interference (RNAi) for targeted gene knockdown in adult *Culicoides sonorensis*. Here, we confirm the *C. sonorensis* inhibitor of apoptosis 1 (CsIAP1) as an anti-apoptotic functional ortholog of IAP1 in *Drosophila*, identify the ortholog of the *Drosophila* initiator caspase Dronc (CsDRONC), and demonstrate that injection of dsRNA into the hemocoel can be used for targeted knockdown in the midgut in *C. sonorensis*. We observed *CsIAP1* transcript reduction in whole midges, with highest transcript reduction in midgut tissues. *IAP1*knockdown (kd) resulted in pro-apoptotic caspase activation in midgut tissues. In *IAP1*kd midges, midgut tissue integrity and size was severely compromised. This phenotype, as well as reduced longevity, was partially reverted by co-RNAi suppression of *CsDRONC* and *CsIAP1*. Therefore, RNAi can be directed to the midgut of *C. sonorensis*, the initial site of virus infection, using dsRNA injection into the hemocoel. In addition, we provide evidence that the core apoptosis pathway is conserved in *C. sonorensis*, and can be experimentally activated in the midgut to reduce longevity in *C. sonorensis*. This study thus paves the way for future reverse genetic analyses of midgut-virus interactions in *C. sonorensis*, including the putative antiviral properties of RNAi and apoptosis pathways.

Introduction

Culicoides midges are hematophagous insects, able to biologically transmit arboviruses of international importance, such as bluetongue virus (BTV) and epizootic hemorrhagic disease virus (EHDV). Both viruses belong to the genus orbivirus with segmented dsRNA genomes, and cause hemorrhagic fevers with significant economic impact worldwide, due to livestock production loss and trade restrictions, as well as negatively impacting wildlife populations (Purse et al. 2015). Current control methods against these diseases focus on vaccines, which are currently only available for BTV, livestock management, and vector control (*USDA-ARS workshop report.* 2013). Over the last years, knowledge of host-virus-vector interactions for orbiviruses has increased significantly (Coetzee and Venter 2015). However, significant knowledge gaps remain, especially with regards to virus-vector interactions and molecular underpinnings that determine *Culicoides* vector competence to orbiviruses (Drolet et al. 2015).

Besides abiotic factors such as temperature, transmission of arboviruses is influenced by biotic factors within their insect vector (Hardy et al. 1983, Carpenter et al. 2015, Franz et al. 2015). Both EHDV and BTV must successfully infect and escape the midgut, ultimately infect the salivary glands, and escape into the saliva to be passed horizontally to the next host (Mellor 1990, Sieburth et al. 1991, Fu et al. 1999). The midgut is the first physical barrier to infection against ingested pathogens, and was confirmed as the major barrier to infection and dissemination against BTV in the principal North American vector, *Culicoides sonorensis* (Diptera: Ceratopogonidae) (Fu et al. 1999).

In insects, innate cellular anti-viral mechanisms exist including RNA interference (RNAi) and programmed cell death (Kingsolver et al. 2013, Lamiable and Imler 2014). RNAi functions as an anti-viral pathway by detecting viral double-stranded RNA (dsRNA), cleaving it into 21-23

nucleotide small interfering RNA (siRNA), which are then used as templates to detect and degrade viral transcripts by base complementarity (Wilson and Doudna 2013). Not surprisingly, several viral mechanisms exist to counter RNAi, including expression of RNAi suppressors and/or sequestration of viral dsRNA to prevent detection (Zhou and Rossi 2011). Several studies indicate that BTV utilizes the latter strategy, as its dsRNA genome is sequestered to its inner viral capsid and only positive sense capped RNA transcripts are released into the cytosol (Mohl and Roy 2014). Furthermore, the BTV core has a high affinity for dsRNA, effectively shielding the BTV genome from host detection (Diprose et al. 2002). Nevertheless, a recent study demonstrated that RNAi in cell lines can limit BTV infection when cells are provided with an external RNAi trigger of dsRNA specific to BTV nonstructural protein 1 (Schnettler et al. 2013). Therefore, if RNAi triggers can target viral transcripts in the *Culicoides* midgut, this immune response could be boosted experimentally to strengthen the initial infection barrier against BTV and possibly EHDV, and ultimately integrated into control strategies to reduce bluetongue and EHD burden.

Apoptosis, a type of programed cell death, has also been demonstrated to act as an antiviral mechanism in several insect species including vectors of arboviruses, such as *Aedes aegypti* (L.) and *Culex quinquefasciatus* Say (most recently reviewed in (Clem 2016)). Apoptosis is controlled by a conserved and continuously expressed regulatory network (Zmasek et al. 2013), which upon activation initiates a core proteolytic cascade consistent of cysteine-dependent aspartate-directed proteases of the caspase family. Apoptosis is primarily regulated through the anti-apoptotic Inhibitor of Apoptosis 1 (IAP1), which binds to inactive caspase zymogens, preventing activation and subsequent cell death. Inhibition of IAP1-caspase binding results in the dimerization causing auto-activation of initiator caspases, such as *Drosophila*

Nedd2-like caspase (Dronc) (Liu and Clem 2011) and the death-related ced-3/Nedd2-like gene (DREDD) (Chen et al. 1998). Initiator caspases then activate executioner caspases through proteolytic cleavage and subsequent dimerization. Executioner caspases mediate proteolysis of multiple cellular proteins and ultimately cause cell death (Zmasek et al. 2013). Putative orthologs of the core apoptosis pathway were detected in the *C. sonorensis* reference transcriptome (Nayduch et al. 2014), suggesting that the pathway is intact. Apoptosis in animals is correlated with viral infection but not necessarily antiviral (Richard and Tulasne 2012). However, recent work established apoptosis as an antiviral response to arbovirus infection in mosquitoes (Clem 2016), for instance RNAi silencing of initiator caspase *Dronc* increased infection prevalence of dengue virus in *Aedes aegypti* mosquitoes (Ocampo et al. 2013).

The role of apoptosis in insect vectors during orbivirus infection has yet to be elucidated. While BTV and EHDV infections cause apoptosis that contributes to the pathology in ruminant hosts (Mortola et al. 2004, Li et al. 2007, Schwartz-Cornil et al. 2008, Shai et al. 2013), there was no detection of apoptosis induction after BTV infection of three insect cell lines, including the hemocyte-like embryonic KC cell line from *C. sonorensis* (Mortola et al. 2004). However, comparable *in vivo* data from infected midges have yet to be performed.

To enable molecular studies on the intrinsic factors underlying vector competence in *Culicoides* midges, we previously established a dsRNA delivery method for targeted gene knockdown by RNAi in *C. sonorensis* (Mills et al. 2015). Injection of dsRNA specific to the putative ortholog of IAP1 (CsIAP1) into the thorax of adult midges resulted in significantly reduced target transcripts and caused increased mortality rates. However, the level of RNAi penetrance in different *Culicoides* tissues and whether the induction of apoptosis underlies the observed mortality phenotype remained unclear. Here we demonstrate that dsRNA does indeed

induce knockdown in the target midgut tissue. We also confirm that both *CsIAP1* and *CsDRONC* function as anti-apoptotic and pro-apoptotic orthologs of *Drosophila* IAP1 and Dronc in *C. sonorensis*.

Materials and Methods

Insect rearing and injection of adult female *C. sonorensis*

The *C. sonorensis* AK strain was reared and injected as described previously (Mills et al. 2015). In all experiments, female midges were injected with 50 nl of total dsRNA (4 µg/µl in RNAse-free water). For single kd experiments, females were injected only with either ds*GFP* or ds*CsIAP1*, while midges used for co-injection experiments were injected with a 1:1 dsRNA ratio with combinations of ds*GFP*, ds*IAP1*, and ds*DRONC*. Throughout all experiments, all midges were fed sugar *ad libitum* and were not provided a blood meal.

DsRNA synthesis

All dsRNA products were synthesized as previously described. Ds*GFP* (154 bp in length, bp 107-261 in the enhanced GFP gene sequence) and ds*CsIAP1* (343 bp in length, bp 381-724 in GAWM01009039) were synthesized using published primers (An et al. 2011, Mills et al. 2015). Ds*CsDRONC* (283 bp in length, bp 394-658 in GAWM01016707) was synthesized using the following primers for first round PCR: ds*CsDRONC* _F 5′-TAATACGACTCACTATAGGGGGCAGAGGTTGATAAAGAGAGA-3′; ds*CsDRONC* _R 5′-TAATACGACTCACTATAGGGGTTTACCAATCAAATGTGT-3′. Purified dsRNA was resuspended in RNase-free water at a final concentration of 4 µg/µl. *CsIAP* sequences can be also be viewed as previously described (Mills et al. 2015).

Sample collection, total RNA extraction, and cDNA synthesis

Whole midges were frozen and stored at -80°C prior to RNA extraction. For midgut and remaining carcass collection, midguts were dissected in ice-cold PBS on ice, immediately flash-frozen in liquid nitrogen, and stored at -80°C at 2 and 5 days post-injection (dpi). For single kd experiments, RNA from frozen midges and/or midguts and carcasses (n = 20-40 per treatment and replicate) was extracted using the RNeasy Micro Kit standard protocol (Qiagen, Valencia, CA, USA) and eluted in 10 µl RNAse-free water (Fisher Scientific, Waltham, MA, USA). For all co-injection experiments, RNA was extracted from frozen midges (n=20) using a phenol: chloroform protocol as described previously (Mills et al. 2015).

C. sonorensis cDNA was synthesized from 100 ng of purified total RNA with the iScript cDNA synthesis kit (Biorad, Hercules, CA, USA).

RT-qPCR

For single kd experiments, female midges and/or midguts (n = 20-40 per treatment and replicate) were collected 2 and 5 dpi, and RT-qPCR was performed as described previously using *elongation factor 1b* as the reference gene (Mills et al. 2015). Females (n = 20 per treatment group) were collected at 5 dpi for dkd experiments, and RT-qPCR analyses were performed using published *CsIAP1* primers (Mills et al. 2015) and the following *CsDRONC* primers: CsDRONC_F 5′- CTGAACATGCACATGATACC-3′; CsDRONC_R 5′-CTGAGCAAACTTGTTTGTATTC-3′.

RT-qPCR analyses for co-injection experiments were performed using iQ SYBR Green Supermix (Bio-Rad) according to the manufacturer's protocol with 6 µl undiluted cDNA as template for each 20 µl volume reaction. All RT-qPCR analyses used the same amplification

protocol (Mills et al., 2015), and were performed with 3 technical replicates. Biological replicates (n) for kd (2 dpi, n = 4; 5 dpi, n = 3) and dkd (n = 3) experiments were performed.

Fold changes between treatments were calculated using the Pfaffl method (Pfaffl 2001), with a primer efficiency of E=1.79 for *CsDRONC* (Figure B1), using *Elongation factor 1b* as the reference gene and untreated (UT) controls as the calibrator condition (Mills et al. 2015). Expression data between kd treatments and control were compared statistically using unpaired t-tests, while co-injection expression data were analyzed using 1-way ANOVA, followed by Tukey's Multiple Comparison post-test. All statistical analyses were performed using Graphpad Prism software version 6 (GraphPad Software Inc., La Jolla, CA, USA).

Immunostaining

Midgut tissues were dissected into 1X phosphate buffer saline (PBS) and immediately fixed in 4% paraformaldehyde in PBS for 30 min at room temperature (RT). Tissues were washed in PBS with 0.3% Triton X-100 (PBST) four times at RT. Midguts were transferred into blocking buffer [1% bovine serum albumin in PBST] and incubated for 30 min at RT. Tissues were incubated with monoclonal rabbit anti-cleaved caspase-3 (Asp175) (D3E9) primary antibody (1:500 in PBST, Cell Signaling Technology, Catalog# 9579, Danvers, MA, USA) overnight at 4°C. Midguts were washed four times for 30 min each in PBST at RT, and subsequently incubated with Alexa594-conjugated goat anti-rabbit secondary antibodies (1:1000 in PBST, Invitrogen, Carlsbad, CA, USA) for two hours at RT. Tissues were washed thrice for 30 min in PBST, then incubated with DAPI (5 ng/ml in PBST) for 30 min at RT. Midguts were mounted in Vectashield mounting medium containing DAPI (Vector Laboratories, Burlingame, CA, USA), sealed with nail polish, and stored at 4°C until imaging.

Confocal microscopy and measurement of midgut area

Representative images were acquired using a LSM700 Confocal Microscope (Zeiss, Oberkochen, Germany) with identical laser and microscope settings between samples. Images were processed in ZEN 2010 software (Zeiss, Oberkochen, Germany) and figures were prepared using Photoshop and Illustrator software (Adobe Systems, San Jose, CA, USA). The area of each midgut (n = 6 per treatment) was determined by using the contour tool (Figure B.2) of the ZEN 2010 software (Zeiss, Jena, Germany). Data passed the Kolmogorov-Smirnov normality test, and were analyzed statistically using 2-way ANOVA (time, treatment) followed by Tukey's Multiple Comparison post-test. All statistical analyses were performed using Graphpad Prism software version 6 (GraphPad Software Inc., La Jolla, CA, USA).

Caspase activity assay

Assays were performed as described previously (Wang et al. 2012). Midges were collected 2 dpi, flash frozen, and stored at -80ºC until further analysis. Frozen midges were homogenized with a motorized pestle in 30 µl lysis buffer (25 mM Tris-HCl, pH 8, 50 mM NaCl) and subjected to four freeze-thaw cycles using liquid nitrogen to free cellular contents. Resulting homogenates were centrifuged for 10 min at 16,000 x g in 4°C. Supernatants were transferred to new tubes and stored at -80ºC until further analyses. Protein concentration was determined using the Pierce BCA Assay Protein Assay Kit standard protocol (Fisher Scientific, Waltham, MA, USA), and adjusted to 50 µg protein per sample in a total volume of 48 µl lysis buffer. Samples were added to 50 µl reaction buffer (100 mM HEPES buffer, pH 7.4, 2 mM DTT, 0.1% CHAPS, 1% sucrose) with 200 µM Ac-DEVD-AFC caspase substrate (MP Biomedical, Santa Ana, CA, USA) and incubated at 37°C for 15 min. Relative fluorescence was monitored for 15 min to determine caspase activity [Δ relative fluorescent units per minute].

Experiments were performed in four biological replicates using n=10 midges per replicate, and caspase activity for each sample was measured in duplicate. Data were analyzed statistically using Kruskal-Wallis, followed by Dunn's Multiple Comparison post-test.

Midgut classification

Midgut morphology was deemed 'altered' if dissections revealed one or more of the following morphological changes: (i) no clear midgut was identifiable, (ii) midgut size was visibly reduced by at least one third compared to the average size of midguts observed in the control group, and (iii) loss of posterior to anterior tapering of the midgut. If none of the morphological changes were observed, midguts were classified as 'normal'. Experiments were performed with four biological replicates using 30 to 40 midguts per replicate. Data were analyzed statistically using the contingency table chi-square test followed by Tukey's Multiple Comparison post-test.

Sequence alignment and phylogenetic anaylsis

Amino acid sequence alignments were performed in MEGA 6.0 (Tamura et al. 2013) using ClustalW (Larkin et al. 2007) with default settings. To reconstruct the phylogenetic relationships, Maximum likelihood trees were generated using MEGA 6.0, with the following settings: Bootstrap method with 1,000 iterations, Jones-Taylor-Thorton substitution model, complete gap deletions, and nearest-neighbor-interchange.

Survival analysis

After dsRNA injection, survival was assessed every 24 h until all midges within the experiment were dead. Survival experiments were performed with four biological replicates using 100 midges per replicate. Resulting data were analyzed and graphed using Kaplan-Meier and compared using the Log-rank (Mantel-Cox) Test and Hazard ratios. Median survival data

were evaluated statistically with Kruskal-Wallis test followed by Dunn's Multiple Comparison post-test. Percent daily mortality was defined as the percentage of dead midges out of the total population between two consecutive days and evaluated statistically using Kruskal-Wallis, followed by Dunn's Multiple Comparison post-test.

Results

Delineating RNAi knockdown persistence of *CsIAP1* transcripts in midgut and carcass tissues

To determine the efficacy and longevity of RNAi knockdown following haemocoel injection of dsRNA, we examined the time period and midgut penetrance of transcript knockdown (kd). Adult female midges were injected with 80 ng of dsRNA specific to CsIAP1 (ds*CsIAP1*). Whole body or dissected midguts and remaining carcasses were collected for reverse transcription - quantitative PCR (RT-qPCR) analysis at 2 and 5 days post-injection (dpi) (Figure 3.1). Similar to previous findings (Mills et al. 2015), *CsIAP1* transcripts were significantly reduced by 30% in whole ds*CsIAP1* kd (*IAP1*kd) midges at both time points when compared to ds*GFP*-injected controls (Unpaired t-test; day 2: df = 4, $t = 3.098$, $P = 0.021$; day 5: df = 4, $t = 4.301$, $P = 0.013$; Figure 3.1A and D). Transcript reduction levels were even higher when midge midguts were examined. Midguts dissected from *IAP1*kd midges exhibited a statistically significantly transcript reduction of 50 % at 2 dpi, while the corresponding carcasses showed statistically significant kd levels of 45 % (Unpaired t-test, midguts t = 6.132, df = 5, $P = 0.002$; carcasses t = 3,568, df = 5, $P = 0.016$; Figure 3.1B and C). In addition, *IAP1*kd midguts at 5 dpi showed a 66 % transcript reduction which was not statistically significantly different compared to ds*GFP*-treated midguts, due to high variation between the biological replicates (Figure 3.1F; Unpaired t-

test, $t = 2.55$, df = 4, $P = 0.063$). Moreover, the small 20 % *CsIAP1* transcript reduction in carcasses from dsCs*IAP1*-injected midges at 5 dpi was also not statistically significant (Figure 3.1F; Unpaired t-test, $t = 1.418$, df = 4, $P = 0.229$).

Overall, dsRNAs injected into the hemocoel of *C. sonorensis* females function as an efficient trigger of RNAi as early as 2 dpi and persists for at least 5 dpi. These data further demonstrate that uptake of the RNAi trigger is successful in midgut tissues, as targeted transcript reduction was even more efficient in the midgut as compared to the remainder of the midge body.

IAP1 kd induces increased caspase activity and apoptosis

Based on phylogenetic evidence supporting CsIAP1 as an evolutionarily conserved inhibitor of initiator and executioner caspases in the apoptosis pathway (Hay et al. 1995, Tenev et al. 2007, Mills et al. 2015), we hypothesized that *IAP1*kd would cause an increase in overall caspase activity and, consequently, apoptosis. To test this hypothesis, caspase activity assays were performed on whole midges at 2 dpi using the fluorescent substrate of human executioner caspase 3, which can be cleaved by insect caspases, such as DrICE and Dronc (Hawkins et al. 2000, Wang et al. 2012). Extracts from *IAP1*kd midges showed a statistically significant increase in caspase activity when compared to untreated (UT) and ds*GFP*-injected controls (Kruskal Wallis: H (2) = 7.423, $P = 0.013$; Dunn's multiple comparisons post-test, $P < 0.01$; Figure 3.2).

Given *IAP1*kd was most pronounced in the midgut, we used an independent experimental method to demonstrate that increased caspase activity could be observed specifically in this tissue. Midguts were dissected at 2 dpi and stained with anti-cleaved human executioner caspase-3 antibody (Figure 3.3) that is a marker for activated caspase-3 in evolutionarily distant dipteran species (Buchon et al. 2009, Heerman et al. 2015). *IAP1*kd resulted in strong staining of midgut

tissues with anti-cleaved caspase-3 antibodies (Figure 3.3C and D), while midguts dissected from ds*GFP*-injected (Figure 3.3G and H) and UT (Figure B.3) midges showed virtually no staining. This staining signal was specific to the anti-cleaved caspase-3 antibody, as no staining was observed in midguts from all treatments that were only incubated with the secondary antibody (Figure B.4). In addition to strong anti-cleaved caspase-3 staining, several epithelial cells in *IAP1*kd-midguts also contained fragmented nuclei (Figure 3.3B and Figure B.5), which are a hallmark of apoptosis (Umansky 1982). While antibody staining and nuclear fragmentation varied in intensity and region between midguts isolated from different midges, we did not identify specific areas of the midgut that were targeted preferentially. Nucleus fragmentation was not observed in midguts dissected from ds*GFP*-injected or UT midges. In summary, these results demonstrate that CsIAP1 functions as a caspase inhibitor and attenuates apoptosis in *C. sonorensis.*

Increased caspase activity due to *IAP1*kd negatively affects midgut morphology

Next, we investigated the possible influence of increased caspase activity and apoptosis after ds*IAP1* injection on the overall morphology of the midgut. Visual examination of midguts from *IAP1*kd midges at 2 and 5 dpi revealed strong size differences between the treatment group and controls (Figure 3.4A-D). To quantify these changes, we determined average midgut size by measuring the area of individual midguts from each treatment group by microscopy at 2 dpi (Figure B.2). The average area of midguts was significantly affected by *IAP1*kd, and did not vary according to time (2-way ANOVA, Treatment: $F_{(2, 34)} = 19.07$, $P < 0.0001$; Time: $F_{(1, 34)} = 0.138$, $P = 0.712$: Figure 3.4E). On average, midgut size of *IAP1*kd midges was reduced by more than 50 % when compared to UT and ds*GFP*-injected controls at 2 dpi (Tukey's post test, $P < 0.01$, Figure 3.4E).

In addition to the significant size decrease, we frequently observed additional morphological changes decreasing overall midgut tissue integrity. Midguts from *IAP1*kd midges were more fragile, and some midguts lacked the typical distinction between narrow anterior and wider posterior midgut sections (Figure 3.4C-D). Furthermore, in some cases, the alimentary canal could only be identified through the presence of a crop and Malpighian tubules and seemingly did not contain a discernible midgut. To quantify these changes after *IAP1*kd, we determined the frequency of altered midgut morphologies in the treatment vs. control groups. Any of the altered morphologies described above were only observed in *IAP1*kd midges, and nearly two-thirds of all *IAP1*kd midguts exhibited one or more morphological alterations (Figure 3.2F; Table B.1; Contingency table, $\chi^2 = 426.4$, df = 4, $P < 0.0001$). The frequency of altered midgut morphology in the *IAP1*kd midges remained equally high at 2 and 5 dpi (Chi square test; $\chi^2 = 1.914$, df = 1, $P = 0.1666$). These results show that the presence of *IAP1*kd in the midgut of *C. sonorensis* leads to altered tissue morphology that disturbs and ultimately destroys its structural integrity.

The initiator caspase Dronc is required for *IAP1*kd-induced phenotypic changes

To determine whether initiator caspases are conserved and can be targeted in *C. sonorensis*, we next looked for an ortholog of the initiator caspase Dronc and tested if it was required for the *IAP1*kd-induced phenotypes. Specifically, we hypothesized that co-injection of two dsRNAs targeting *CsDRONC* and *CsIAP1* would revert the *IAP1*kd-induced phenotypes, similar to work completed in *Ae. aegypti* (Wang et al. 2012). To identify putative orthologs of initiator caspase(s), we mined the *C. sonorensis* transcriptome data (Nayduch, et al. 2014) by BLAST analysis using reference sequences from ImmunoDB (http://cegg.unige.ch/Insecta/immunodb) (Figure B.6). One sequence with accession number

GAWM01016707 was identified by best reciprocal Blast hit using *Ae. aegypti* Dronc (AAEL011562, Figure B.6). Sequence alignment of the deduced amino acid sequence of GAWM01016707 with known initiator caspases from *Ae. aegypti*, *Anopheles gambiae* Giles, and *D. melanogaster* confirmed the presence of the critical residues required for caspase function (Fuentes-Prior and Salvesen 2004, Bryant et al. 2010, Figure B.7). Next, we used the sequence alignment to reconstruct the phylogenetic relationship of GAWM01016707 with the known Dipteran initiator caspases by maximum likelihood. The tree topology of the initiator caspases mirrored the phylogenetic relationships of these Dipteran species (Wiegmann et al. 2011), and identified GAWM01016707 as the ortholog of the initiator caspase Dronc and not DREDD in *C. sonorensis* (Figure B.8). We therefore named this gene CsDRONC.

To functionally confirm CsDRONC as an initiator caspase, we performed experiments where midges were co-injected with 40 ng of each dsRNA specific to *CsIAP1* and *CsDRONC* (ds*IAP1/dsDRONC*), which is half the dose previously used for *IAP1*kd. For single-dsRNA treatment controls, either dsRNA was replaced with equal amount of ds*GFP* (ds*GFP*/*dsIAP1*, ds*GFP*/ds*DRONC*). Knockdown levels were assessed for each transcript using RT-qPCR. Average transcript reduction in whole midges was specific to the dsRNA injected (Figure B.9) and reduction levels were similar between ds*IAP1/dsDRONC*-injected midges and single-dsRNA treatment controls, respectively. However, transcript reduction of neither *CsIAP1* nor Cs*DRONC* was statistically significant as compared to ds*GFP*-treated controls (One-way ANOVA: *CsDRONC, P*=0.325; *CsIAP1*, *P*=0.4661), and we observed substantial variation of *CsIAP1* and *CsDRONC* transcript levels observed in the ds*GFP*-injected controls. Interestingly, using a dose of 40 ng of ds*CsIAP1* led to an average transcript reduction of 25% in whole midges 5 dpi, as

compared to the 40 % reduction observed previously using an 80 ng dsRNA dose (Figure B.9, Figure 3.1A).

We next assessed the effect of ds*IAP1*/ds*DRONC* injection on decreased tissue integrity of midguts induced by *IAP1*kd. Nearly three quarters of all midguts from *dsGFP*/*dsIAP1*-injected midges showed one or more signs of altered morphology (Figure 3.5, Table B.2). Midgut morphology was partially restored in ds*IAP1*/ds*DRONC*-injected midges (Contingency Table, df=1, χ^2=9.889, P = 0.0017), demonstrating that midgut damage due to *IAP1*kd is at least partially dependent on CsDRONC.

We previously reported that *IAP1*kd significantly accelerated mortality in adult female midges (Mills et al. 2015). We confirmed our previous results and also observed this phenotype after ds*GFP*/ds*CsIAP1* injection (Figure 3.6, Figure B.10) with median survival reduced by 50 % (Kruskal-Wallis, $H_{(4)}$ = 11.68, P = 0.0199; Dunn's post-test, $P < 0.05$ when comparing ds*GFP*/ds*CsIAP1* and *dsGFP/dsGFP*-injected treatments). In addition, daily mortality doubled two days after ds*GFP*/ds*CsIAP1* as compared to ds*GFP/dsGFP*-injected controls (Kruskal-Wallis, $H_{(4)}$ = 15.15, P = 0.004; Dunn's post-test, $P < 0.05$; Figure 3.6B and C, Figure B.10). However, the survival phenotype observed in these midges injected with 40 ng of ds*IAP1* was dampened as compared to our previous results, which used a ds*IAP1* dose of 70 ng (Figure B.11).

Injection of ds*IAP1*/ds*DRONC* partially reverted the ds*GFP*/ds*IAP1*-induced mortality phenotype (Figure 3.5A): Median survival of ds*IAP1*/ds*DRONC*-injected midges was intermediate to ds*GFP*/ds*IAP1* and ds*GFP/dsGFP*-injected controls, respectively, and not statistically significantly different from either of these treatment groups (Kruskal-Wallis, $H_{(4)}$ = 11.68, P = 0.0199; Dunn's post-test, $P < 0.05$). Phenotypic rescue was especially pronounced

early in the time course, as the ds*GFP*/ds*IAP1*-dependent mortality at 2 dpi was fully reverted by ds*IAP1*/ds*DRONC* injection Kruskal-Wallis, $H_{(4)} = 15.15$, $P = 0.004$; Dunn's post-test, $P < 0.05$; Figure 3.6B and C, Figure B.10). Thus, both *IAP1*kd phenotypes of decreased midgut tissue integrity, and increased mortality rates seem dependent on the initiator caspase CsDRONC.

Discussion

The overarching hypothesis tested by this study was that apoptosis is inducible in the midgut of adult female *C. sonorensis* by injecting an RNAi trigger into the hemocoel. Our data demonstrate that injection of long dsRNAs against *IAP1* into the thorax indeed triggers apoptosis and ablates the midgut tissue. Our work also extends the use of RNAi in this important vector species, as we demonstrate that simultaneous injection of ds*IAP1* and ds*DRONC* partially reverts the phenotype induced by *IAP1*kd.

We previously reported that ds*CsIAP1* injection resulted in increased mortality of *C. sonorensis* (Mills et al. 2015). This study now provides clear evidence that this shortened life span is due to increased apoptosis and tissue damage, especially in the midgut. Multiple methods to detect apoptosis are available, including the presence of nucleus fragmentation (Umansky 1982). In dipterans, caspase activity assays (Wang and Clem 2011, Wang et al. 2012) and immunofluorescence analyses with anti-cleaved caspase-3 antibody (Buchon et al. 2009, Heerman et al. 2015, Dong et al. 2016) were utilized previously to detect apoptosis. Indeed, we observed caspase-mediated apoptosis after *IAP1*kd, by all three methods, verifying CsIAP1 (GAWM01009039) as the ortholog of IAP1 in *C. sonorensis.*

CsIAP1 transcript reduction was pronounced in midge midguts and presumably the cause for the observed morphological changes. This midgut damage was linked to increased caspase-

dependent apoptosis as observed through the presence of fragmented nuclei and anti-cleaved caspase-3 staining, indicating a large number of midgut cells undergoing apoptosis at 2 dpi. The increase in apoptosis resulted in the loss of midgut epithelial cells, causing reduced midgut size and increased fragility observed in *IAP1*kd midguts. Similar to results in *Ae. aegypti* and *D. melanogaster* with the kd of *IAP1* (Wang et al. 2012) and *hand* (Lo et al. 2007), respectively, these altered midgut morphologies were linked to increased mortality, as these alterations very likely prevent the uptake of essential nutrients, resulting in starvation.

In addition to confirming the functional ortholog of IAP1, we identified the initiator caspase Dronc in *C. sonorensis*. Since activation of Dronc was previously demonstrated to be essential for apoptosis (Daish et al 2004), we hypothesized the simultaneous kd of *CsDRONC* and *CsIAP1* would inhibit *IAP1*kd-phenotypes, similar to experiments in *Ae. aegypti* (Wang et al. 2012). We mined the *C. sonorensis* transcriptome (Nayduch et al. 2014), and based on phylogenetic analyses, identified GAWM01016707 as the ortholog of the initiator caspase Dronc. Co-injection of ds*IAP1* and ds*DRONC* required us to lower the dose for each dsRNA, which led to transcript kd levels just outside of statistical significance. In addition, the protein half-life of Dronc is about 4.3 fold higher than that of IAP1 in *D. melanogaster*, which may also contribute to the incomplete rescue of *IAP1*kd-phenotypes (Yoo et al. 2002). Future experiments are needed to test whether these limitations can be overcome using sequential injections of individual RNAi triggers. Nevertheless, the results from the reverse genetic experiments strongly suggest that *CsDRONC* is required for *IAP1*kd-phenotypes, as simultaneous injection of ds*IAP1* and ds*DRONC* partially rescued the *IAP1*kd-induced mortality and altered midgut morphology phenotypes. Together, these data demonstrate *CsDRONC* (GAWM01016707) as an initiator caspase in the midge and the conserved nature of the core apoptosis pathway in *C. sonorensis.*

In addition to further characterizing apoptosis in *C. sonorensis*, this study extends our understanding of RNAi in this species. First, our data demonstrate that long dsRNAs injected into the hemocoel provide the trigger for RNAi in multiple tissues, as transcript reduction was not only detected in dissected midguts, but also in the remaining carcasses of adult females. Second, the results from the co-injection experiments show that the expression of at least two genes can be targeted simultaneously. Transcript reduction was specific to the dsRNA injected, as injection of ds*CsDRONC* reduced transcript levels of its target by up to 30 %, while not affecting *CsIAP1* transcript levels, and vice versa. Although transcript level reduction was not statistically significantly different from control levels, the partial rescue of *IAP1*kd-mortality and midgut phenotypes provides strong evidence that *Culicoides* midges are able to utilize multiple dsRNA triggers for simultaneous transcript kd.

Finally, the analysis of transcript levels after dsRNA injection revealed that RNA interference in *C. sonorensis* mainly, if not solely relies on environmental RNAi. The hallmark of environmental RNAi is that the RNAi trigger is taken up by the cells individually and, in contrast to systemic RNAi, is not amplified or propagated between cells (Huvenne and Smagghe 2010). As a result, kd levels can be titrated, where RNAi trigger dose correlates positively with transcript kd levels (Whyard et al. 2009). We observed similar results in our co-injection experiments. Midges in these experiments were injected with half the dsRNA dose per target transcript than in single kd experiments due to viscosity and injection volume limitations. This lowered dsRNA dose resulted in less pronounced transcript reduction and lessened severity of the mortality phenotype in ds*GFP/*ds*IAP1*-injected midges when compared to our previous single kd experiments (Mills et al. 2015). Similar results were obtained in other Dipteran species,

suggesting that environmental RNAi is a trait common to all Dipterans, and the ability to propagate the RNAi trigger was lost at the base of this insect order (Scott et al. 2013).

RNAi has revolutionized our ability to study vector-pathogen interactions in non-model Dipteran insects including mosquitoes (Blandin et al. 2002, Xi et al. 2008), tsetse flies (Wang et al. 2009), and sand flies (Sant'anna et al. 2009, Coutinho-Abreu and Ramalho-Ortigao 2010). Similar to these vector species, the results presented here pave the way for future reverse genetic analyses of midgut-virus interactions within in the biting midge *C. sonorensis*, including the putative antiviral properties of RNAi and apoptosis pathways.

Acknowledgments

Thanks go to Dr. Lee Cohnsteadt, Mr. James A. Kempert, and Mr. William E. Yarnell at the Arthropod-Borne Animal Disease Research Unit, USDA-ARS, Manhattan, KS for provision of all adult *C. sonorensis* midges and housing materials used in this study. Additional thanks go to Matthew Herman and Dr. Marcelo Ramalho-Ortigao at Kansas State University, Manhattan, KS for the use of the anti-cleaved caspase-3 antibodies and the Confocal Microscopy and Molecular Biology Cores funded by KSU-CVM for use of their facilities. Research reported in this publication was supported by NIAID of the National Institutes of Health under award number R01AI095842 (K.M.), and by Specific Cooperative Agreements 58-5430-1360 and 58-5430-4-022 to K. M. from the USDA Agricultural Research Service. The content is solely the responsibility of the authors and does not necessarily represent the official views of the funding agencies. This is contribution no. 16-312-J from the Kansas Agricultural Experiment Station. This chapter was published in 2016 by Oxford University Press in the Journal of Medical Entomology in volume 54, issue 3, from pages 559-567, and titled "Functional Validation of

Apoptosis Genes IAP1 and DRONC in Midgut Tissue of the Biting Midge *Culicoides sonorensis* (Diptera: Ceratopogonidae) by RNAi" (DOI: https://doi.org/10.1093/jme/tjw225).

References

(USDA-ARS) U.S. Department of Agriculture, Agricultural Research Service, Washington, DC. 2013. Orbiviruses, bluetongue and epizootic hemmorhagic disease: gap analysis workshop report. U.S. Dep. Agric. Agric. Res. Serv. Washington, DC.

An, C., A. Budd, M. R. Kanost, and K. Michel. 2011. Characterization of a regulatory unit that controls melanization and affects longevity of mosquitoes. Cell. Mol. Life. Sci. 68: 1929–1939.

Blandin, S., L. F. Moita, T. Kocher, M. Wilm, F. C. Kafatos, and E. A. Levashina. 2002. Reverse genetics in the mosquito *Anopheles gambiae*: targeted disruption of the *Defensin* gene. EMBO Rep. 3: 852–856.

Bryant, B., M. C. Ungerer, Q. Liu, R. M. Waterhouse, and R. J. Clem. 2010. A caspase-like decoy molecule enhances the activity of a paralogous caspase in the yellow fever mosquito, *Aedes aegypti*. Insect Biochem. Mol. Biol. 40: 516–523.

Buchon, N., N. A. Broderick, S. Chakrabarti, W. Lee, and B. Lemaitre. 2009. Invasive and indigenous microbiota impact intestinal stem cell activity through multiple pathways in *Drosophila*. Genes Dev. 23: 2333–2344.

Carpenter, S., E. Veronesi, B. Mullens, and G. Venter. 2015. Vector competence of *Culicoides* for arboviruses: three major periods of research, their influence on current studies and future directions. Rev. Sci. Tech. 34: 97–112.

Chen, P., A. Rodriguez, R. Erskine, T. Thach, and J. M. Abrams. 1998. Dredd, a novel effector of the apoptosis activators reaper, grim, and hid in *Drosophila*. Dev. Biol. 201: 202–16.

Clem, R. J. 2016. Arboviruses and apoptosis: the role of cell death in determining vector competence. J. Gen. Virol. 97: 1033–1036.

Coetzee, P., and E. H. Venter. 2015. Recent advances in knowledge of BTV-host-vector interaction. Vet. Ital. 51: 301–11.

Coutinho-Abreu, I. V, and M. Ramalho-Ortigao. 2010. Transmission blocking vaccines to

control insect-borne diseases: a review. Mem. Inst. Oswaldo. Cruz. 105: 1–12.

Daish, T.J., Mills, K. and S. Kumar. 2004. *Drosophila* caspase DRONC is required for specific developmental cell death pathways and stress-induced apoptosis. Dev. cell. 7: 909-915.

Diprose, J. M., J. M. Grimes, G. C. Sutton, J. N. Burroughs, A. Meyer, S. Maan, P. P. Mertens, and D. I. Stuart. 2002. The core of bluetongue virus binds double-stranded RNA. J. Virol. 76: 9533–9536.

Dong, S., Kantor, A. M., Lin, J., Passarelli, A. L., Clem, R. J., and A.W. Franz. 2016. Infection pattern and transmission potential of chikungunya virus in two New World laboratory-adapted *Aedes aegypti* strains. Scientific reports. 6: 1-13.

Drolet, B. S., P. van Rijn, E. W. Howerth, M. Beer, and P. P. Mertens. 2015. A review of knowledge gaps and tools for orbivirus research. Vector-Borne Zoonotic Dis. 15: 339–47.

Franz, A. W. E., A. M. Kantor, A. L. Passarelli, and R. J. Clem. 2015. Tissue barriers to arbovirus infection in mosquitoes. Viruses. 7: 3741–3767.

Fu, H., C. J. Leake, P. P. C. Mertens, and P. S. Mellor. 1999. The barriers to bluetongue virus infection, dissemination and transmission in the vector, *Culicoides variipennis* (Diptera: Ceratopogonidae). Arch. Virol. 144: 747–761.

Fuentes-Prior, P., and G. S. Salvesen. 2004. The protein structures that shape caspase activity, specificity, activation and inhibition. Biochem. J. 384: 201–232.

Hardy, J. L., E. J. Houk, L. D. Kramer, and W. C. Reeves. 1983. Intrinsic factors affecting vector competence of mosquitoes for arboviruses. Annu. Rev. Entomol. 28: 229–262.

Hawkins, C.J., Yoo, S.J., Peterson, E.P., Wang, S.L., Vernooy, S.Y. and B.A. Hay 2000. The *Drosophila* caspase DRONC cleaves following glutamate or aspartate and is regulated by DIAP1, HID, and GRIM. J. Biol. Chem. 275: 27084-27093.

Hay, B. A., D. A. Wassarman, and G. M. Rubin. 1995. *Drosophila* homologs of baculovirus inhibitor of apoptosis proteins function to block cell death. Cell. 83: 1253–1262.

Heerman, M., J.-L. Weng, I. Hurwitz, R. Durvasula, and M. Ramalho-Ortigao. 2015. Bacterial infection and immune responses in *Lutzomyia longipalpis* sand fly larvae midgut. PLoS Negl. Trop. Dis. 9: e0003923.

Huvenne, H., and G. Smagghe. 2010. Mechanisms of dsRNA uptake in insects and potential of RNAi for pest control: a review. J. Insect Physiol. 56: 227–235.

Kingsolver, M. B., Z. Huang, and R. W. Hardy. 2013. Insect antiviral innate immunity: pathways, effectors, and connections. J. Mol. Biol. 425: 4921–4936.

Lamiable, O., and J. L. Imler. 2014. Induced antiviral innate immunity in Drosophila. Curr. Opin. Microbiol. 20: 62–68.

Larkin, M. A., G. Blackshields, N. P. Brown, R. Chenna, P. A. McGettigan, H. McWilliam, F. Valentin, I. M. Wallace, A. Wilm, R. Lopez, J. D. Thompson, T. J. Gibson, and D. G. Higgins. 2007. Clustal W and Clustal X version 2.0. Bioinformatics. 23: 2947–2948.

Li, Q., H. Li, B. J. Blitvich, and J. Zhang. 2007. The *Aedes albopictus inhibitor of apoptosis 1* gene protects vertebrate cells from bluetongue virus-induced apoptosis. Insect Mol. Biol. 16: 93–105.

Liu, Q., and R. Clem. 2011. Defining the core apoptosis pathway in the mosquito disease vector *Aedes aegypti*: the roles of iap1, ark, dronc, and effector caspases. Apoptosis. 16: 105–13.

Lo, P. C. H., S. Zaffran, S. Sénatore, and M. Frasch. 2007. The *Drosophila Hand* gene is required for remodeling of the developing adult heart and midgut during metamorphosis. Dev. Biol. 311: 287–296.

Mellor, P. 1990. Replication of bluetongue virus in *Culicoides* vectors. Curr. Top. Microbiol. Immunol. 162: 143–161.

Mills, M. K., D. Nayduch, and K. Michel. 2015. Inducing RNA interference in the arbovirus vector, *Culicoides sonorensis*. Insect Mol. Biol. 24: 105–14.

Mohl, B.-P., and P. Roy. 2014. Bluetongue virus capsid assembly and maturation. Viruses. 6: 3250–3270.

Mortola, E., R. Noad, and P. Roy. 2004. Bluetongue virus outer capsid proteins are sufficient to trigger apoptosis in mammalian cells. J. Virol. 78: 2875–2883.

Nayduch, D., M. B. Lee, and C. A. Saski. 2014. The reference transcriptome of the adult female biting midge (*Culicoides sonorensis*) and differential gene expression profiling during teneral, blood, and sucrose feeding conditions. PLoS One. 9: e98123.

Ocampo, C. B., P. A. Caicedo, G. Jaramillo, R. Ursic Bedoya, O. Baron, I. M. Serrato, D. M. Cooper, and C. Lowenberger. 2013. Differential expression of apoptosis related genes in selected strains of *Aedes aegypti* with different susceptibilities to dengue virus. PLoS One. 8: e61187.

Pfaffl, M. W. 2001. A new mathematical model for relative quantification in real-time RT-PCR.

Nucleic Acids Res. 29: e45.

Purse, B. V., S. Carpenter, G. J. Venter, G. Bellis, and B. A. Mullens. 2015. Bionomics of temperate and tropical *Culicoides* midges: knowledge gaps and consequences for transmission of *Culicoides*-borne viruses. Annu. Rev. Entomol. 60: 373–392.

Richard, A., and D. Tulasne. 2012. Caspase cleavage of viral proteins, another way for viruses to make the best of apoptosis. Cell Death Dis. 3: e277.

Sant'anna, M. R., H. Diaz-Albiter, M. Mubaraki, R. J. Dillon, and P. a Bates. 2009. Inhibition of trypsin expression in *Lutzomyia longipalpis* using RNAi enhances the survival of *Leishmania*. Parasit. Vectors. 2: 62.

Schnettler, E., M. Ratinier, M. Watson, A. E. Shaw, M. McFarlane, M. Varela, R. M. Elliott, M. Palmarini, and A. Kohl. 2013. RNA interference targets arbovirus replication in *Culicoides* cells. J. Virol. 87: 2441–2454.

Schwartz-Cornil, I., P. P. C. Mertens, V. Contreras, B. Hemati, F. Pascale, E. Breard, P. S. Mellor, N. James MacLachlan, S. Zientara, E. Bréard, P. S. Mellor, N. J. MacLachlan, and S. Zientara. 2008. Bluetongue virus: virology, pathogenesis and immunity. Vet. Res. 39: 46.

Scott, J. G., K. Michel, L. C. Bartholomay, B. D. Siegfried, W. B. Hunter, G. Smagghe, K. Y. Zhu, and A. E. Douglas. 2013. Towards the elements of successful insect RNAi. J. Insect Physiol. 59: 1212–1221.

Shai, B., E. Schmukler, R. Yaniv, N. Ziv, G. Horn, V. Bumbarov, H. Yadin, N. I. Smorodinsky, E. Bacharach, R. Pinkas-Kramarski, and M. Ehrlich. 2013. Epizootic hemorrhagic disease virus induces and benefits from cell stress, autophagy, and apoptosis. J. Virol. 87: 13397–408.

Sieburth, P. J., C. E. Nunamaker, J. Ellis, and R. A. Nunamaker. 1991. Infection of the midgut of *Culicoides variipennis* (Diptera: Ceratopogonidae) with bluetongue virus. J. Med. Entomol. 28: 74–85.

Tamura, K., G. Stecher, D. Peterson, A. Filipski, and S. Kumar. 2013. MEGA6: Molecular Evolutionary Genetics Analysis version 6.0. Mol. Biol. Evol. 30: 2725–2729.

Tenev, T., M. Ditzel, A. Zachariou, and P. Meier. 2007. The antiapoptotic activity of insect IAPs requires activation by an evolutionarily conserved mechanism. Cell Death Differ. 14: 1191–201.

Umansky, S. R. 1982. The genetic program of cell death. hypothesis and some applications:

Transformation, carcinogenesis, ageing. J. Theor. Biol. 97: 591–602.

Wang, H., and R. J. Clem. 2011. The role of IAP antagonist proteins in the core apoptosis pathway of the mosquito disease vector *Aedes aegypti*. Apoptosis. 16: 235–248.

Wang, H., T. Gort, D. L. Boyle, and R. J. Clem. 2012. Effects of manipulating apoptosis on Sindbis virus infection of *Aedes aegypti* mosquitoes. J. Virol. 86: 6546–54.

Wang, J., Y. Wu, G. Yang, and S. Aksoy. 2009. Interactions between mutualist *Wigglesworthia* and tsetse peptidoglycan recognition protein (PGRP-LB) influence trypanosome transmission. Proc. Natl. Acad. Sci. U. S. A. 106: 12133–8.

Whyard, S., A. D. Singh, and S. Wong. 2009. Ingested double-stranded RNAs can act as species-specific insecticides. Insect Biochem. Mol. Biol. 39: 824–832.

Wiegmann, B. M., M. D. Trautwein, I. S. Winkler, N. B. Barr, J.-W. Kim, C. Lambkin, M. A. Bertone, B. K. Cassel, K. M. Bayless, A. M. Heimberg, B. M. Wheeler, K. J. Peterson, T. Pape, B. J. Sinclair, J. H. Skevington, V. Blagoderov, J. Caravas, S. N. Kutty, U. Schmidt-Ott, G. E. Kampmeier, F. C. Thompson, D. A. Grimaldi, A. T. Beckenbach, G. W. Courtney, M. Friedrich, R. Meier, and D. K. Yeates. 2011. Episodic radiations in the fly tree of life. Proc. Natl. Acad. Sci. U. S. A.108: 5690–5695.

Wilson, R. C., and J. A. Doudna. 2013. Molecular mechanisms of RNA interference. Annu. Rev. Biophys. 42: 217–239.

Xi, Z. Y., J. L. Ramirez, and G. Dimopoulos. 2008. The *Aedes aegypti* toll pathway controls dengue virus infection. PLoS Pathog. 4: e1000098.

Yoo, S.J., Huh, J.R., Muro, I., Yu, H., Wang, L., Wang, S.L., Feldman, R.R., Clem, R.J., Müller, H.A.J. and B.A. Hay. 2002. Hid, Rpr and Grim negatively regulate DIAP1 levels through distinct mechanisms. Nature Cell Biol. 4: 416-424.

Zhou, J., and J. J. Rossi. 2011. Antiviral RNAi, 1st ed. Humana Press.

Zmasek, C. M., A. Godzik, J. Silke, P. Meier, and F. K. Chan. 2013. Evolution of the animal apoptosis network. Cold Spring Harb. Perspect. Biol. 5.

Figures – Chapter 3

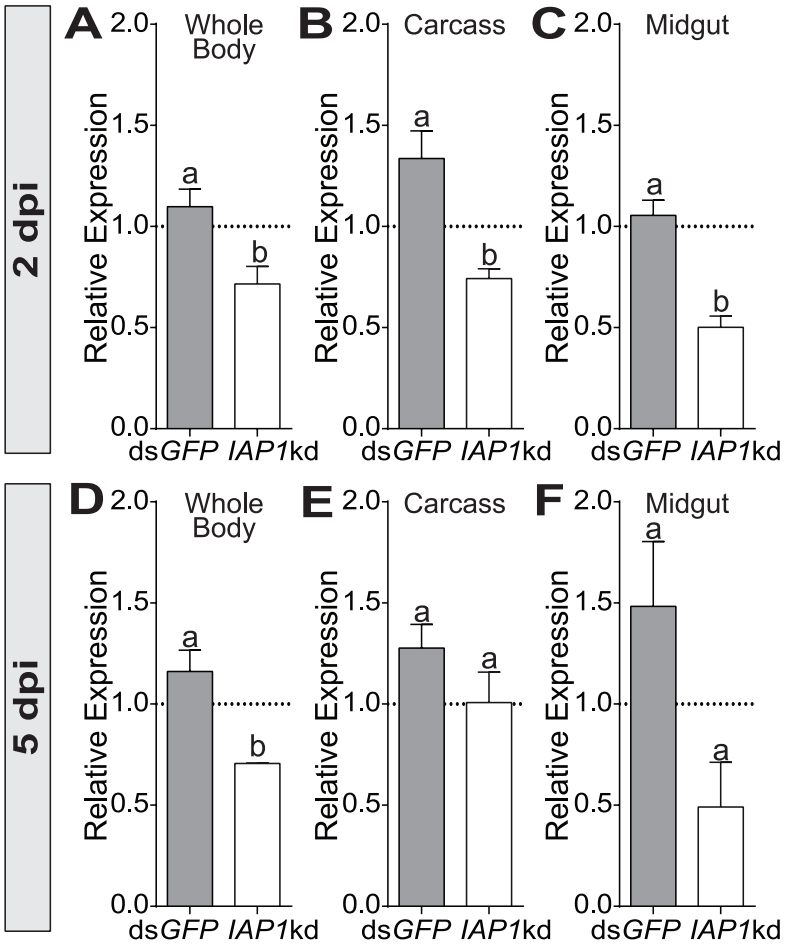

Figure 3.1 Temporospatial analysis of *CsIAP1* transcript levels after dsRNA injection

Graphs depict mean transcript levels at 2 (**A-C**) and 5 (**D-E**) dpi. Graphs show relative expression in whole midges (**A** and **D**), carcass (**B** and **E**), and corresponding midguts (**C** and **F**). All data were calibrated relative to UT controls (dotted line), and quantitative RT-PCR results were calculated using elongation factor 1b as the reference gene. Data are presented as mean ± SEM from multiple biological replicates (2 dpi, N = 4; 5 dpi, N = 3). Statistically significant differences between samples from ds*IAP1* and ds*GFP*-treated midges are denoted by different letters (Unpaired T-test, $P < 0.05$).

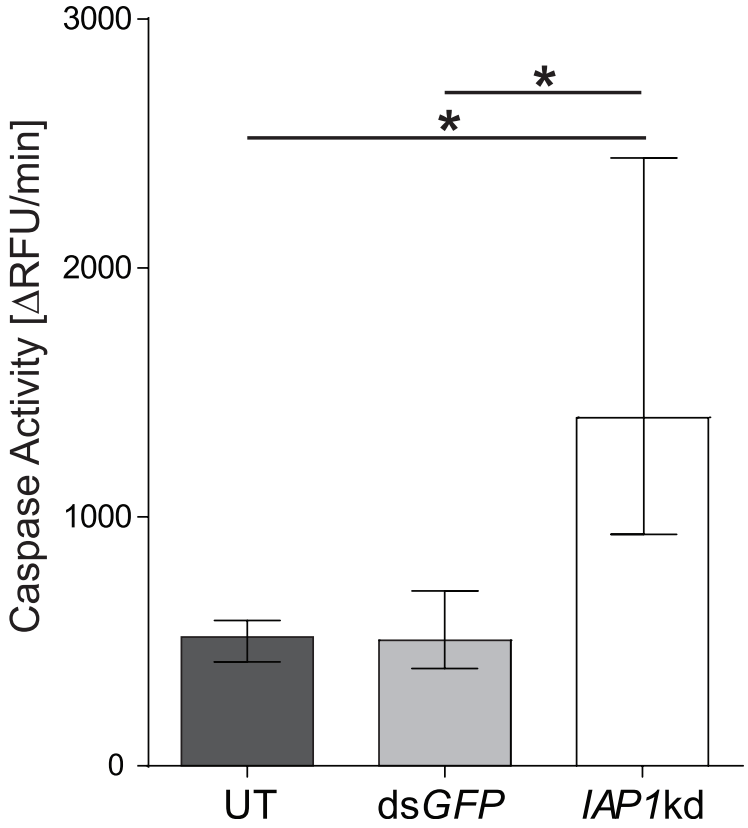

Figure 3.2 *In vitro* caspase activity of whole female midge extracts

Midges were collected at 2 dpi and pooled (n = 10 per biological replicate) for caspase activity assessment. Caspase activity was determined using the caspase substrate Ac-DEVD-AFC. Statistical significance is denoted by asterisks (Kruskal-Wallis followed by Dunn's multiple comparisons test, $P < 0.05$). Data are presented as the median with interquartile range from four biological replicates.

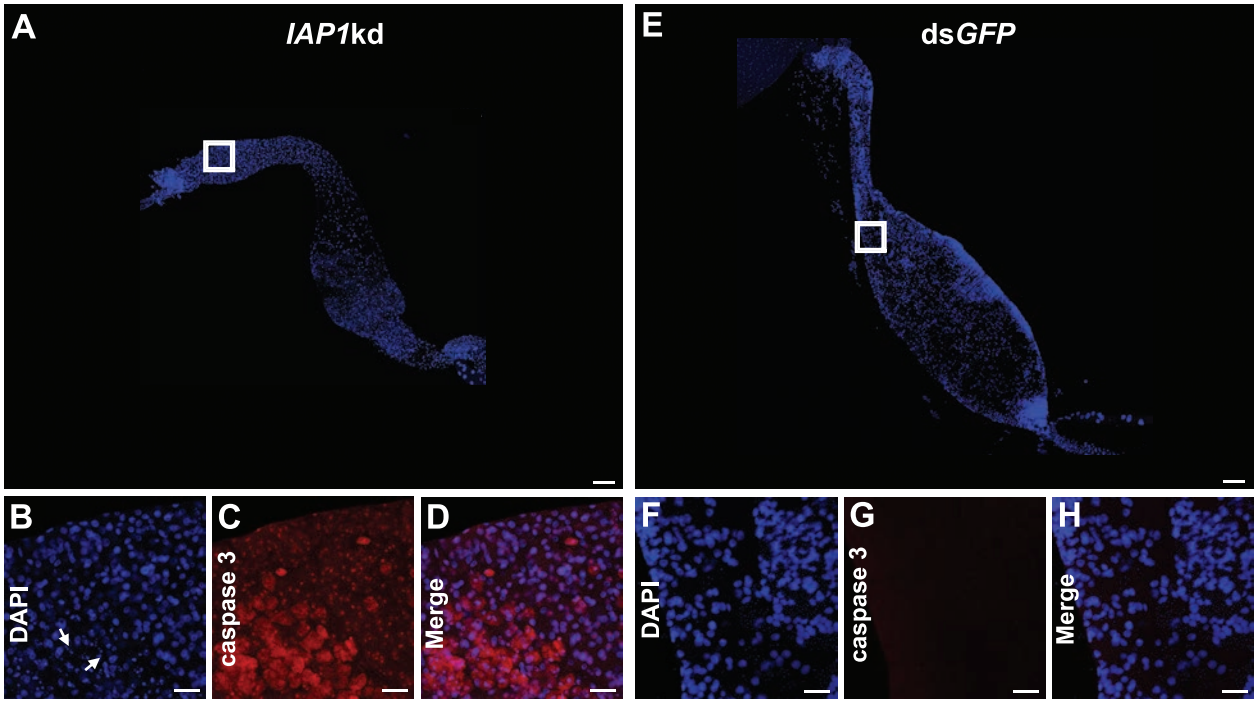

Figure 3.3 Active caspase staining of midge midguts

(**A** and **E**) Representative images of whole midge midgut at 2 dpi via DAPI stain (blue). Scale bar, 100 nm. (**B-D**) Ds*CsIAP1* injection led to increased fluorescence related to anti-cleaved caspase-3 antibody staining (red) compared to UT (Additional file 1: Figure A.1) and ds*GFP* (**F-H**) controls. Images (**B-D** and **F-H**) were taken from midgut location denoted by white squares. Scale bar, 20 nm.

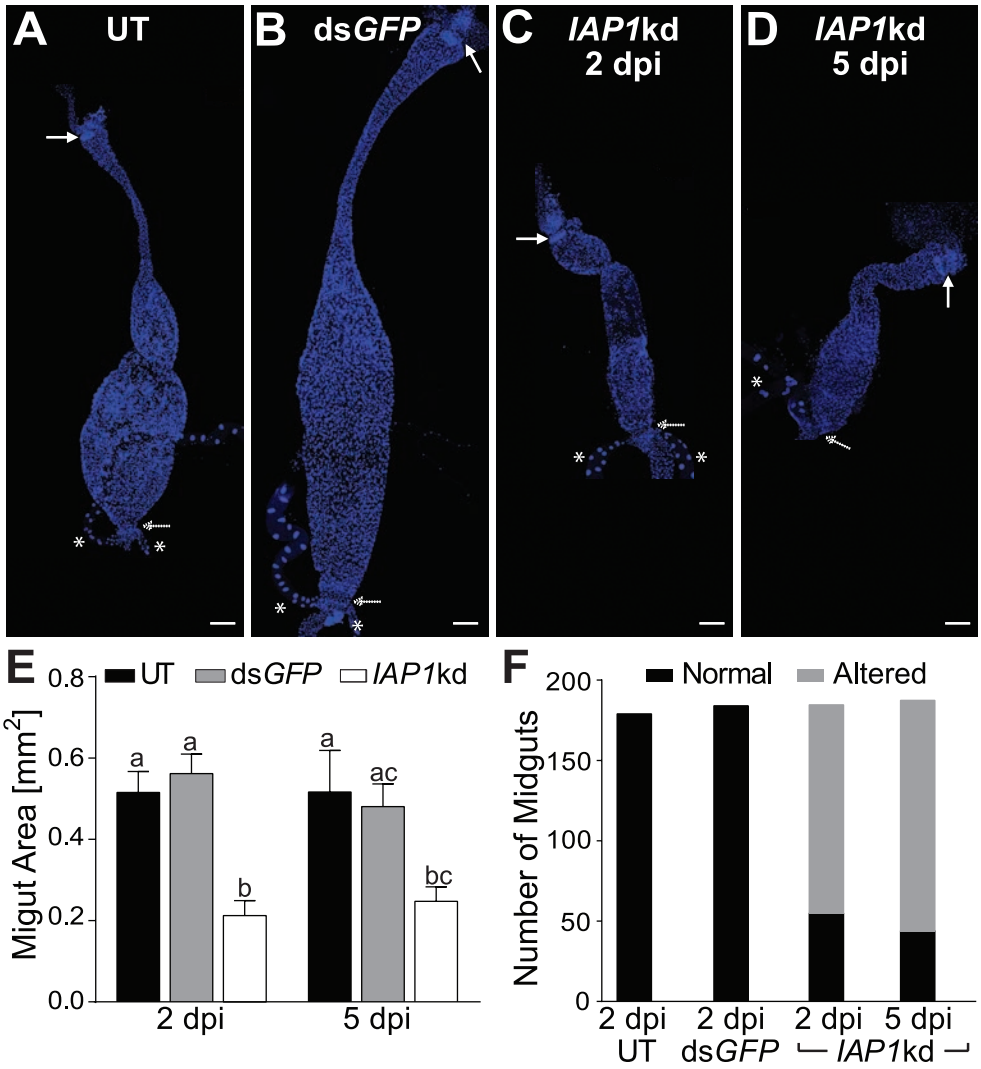

Figure 3.4 Altered midgut morphologies in *IAP1*kd midges

(**A-D**) Representative images depicting midge midguts with DAPI stain (blue). UT and ds*GFP*-injected midguts (**A-B**) are considered to have "normal" morphology, while dsCs*IAP1*-injected midguts (**C-D**) are deemed "altered" based on criteria detailed in Materials and Methods section 4.8. (**E**) The mean area per midgut from UT and ds*GFP*-injected controls were compared to *IAP1*kd midges at 2 and 5 dpi. Midgut areas from UT and ds*GFP*-injected midges are shown for 2 dpi only (for numbers at 5 dpi, see Additional file 5: Table S1). Statistically significant differences in midgut area are denoted by different letters (Two-way ANOVA; Tukey's post-test,

$P < 0.05$). Data are presented as the mean ± SEM (n = 6 midguts per treatment). (**F**) Graph depicts the number of midguts observed with either the normal or altered morphology at indicated time points. Data are presented as the combined number of midguts from five biological replicates. Scale bar, 100 nm.

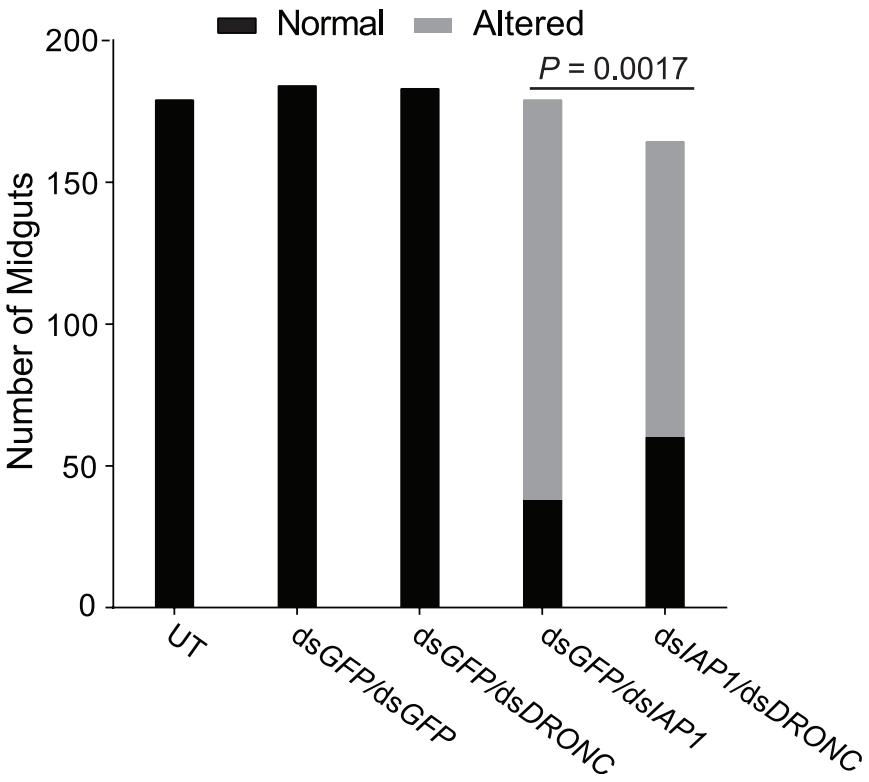

Figure 3.5 *IAP1*kd-mediated changes in midgut morphology are dependent on CsDRONC

Graph depicts the number of midguts observed with either normal or altered morphology at 5 dpi. Data are presented as the total midgut number combined from six biological replicates. Statistically significantly different treatment groups are denoted by *P* value. (Contingency Table, $P = 0.0017$).

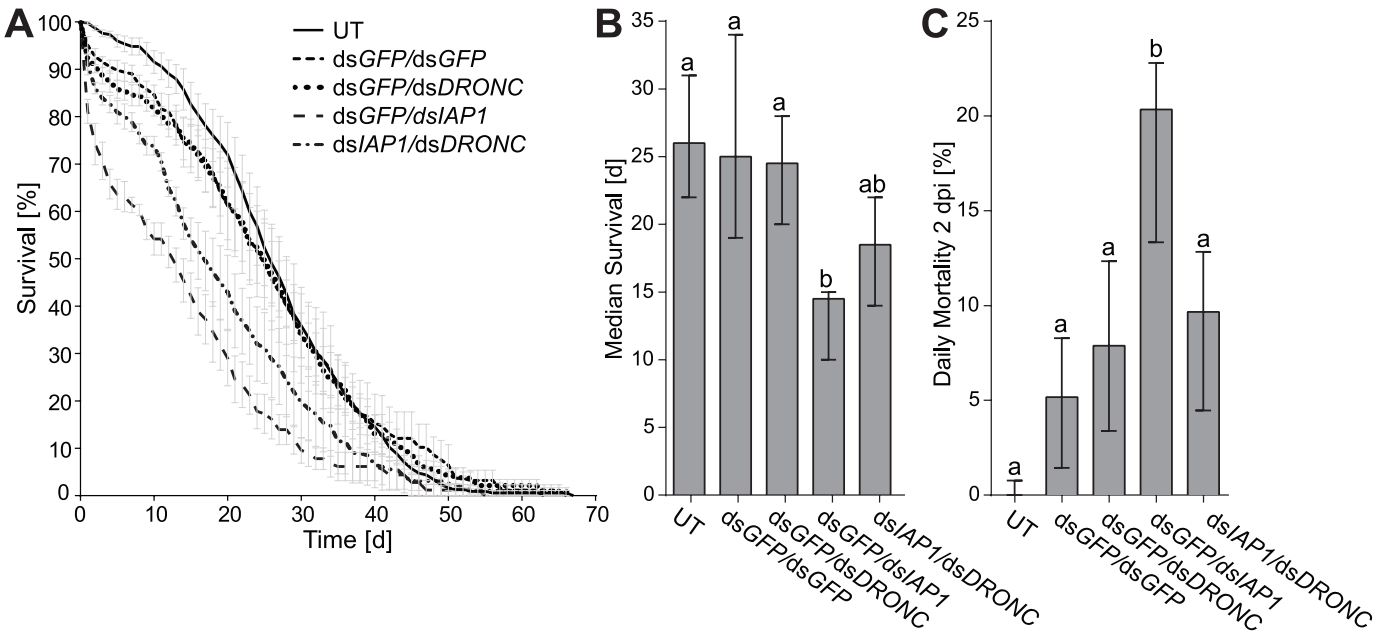

Figure 3.6 CsDRONC partially mediates *IAP1*kd-induced lethality

(**A**) Survival curves of midges after injection of dsRNA specific to one gene of interest (*IAP1*kd or *DRONC*kd), both genes of interest (*IAP1*/*DRONC*dkd), and ds*GFP* controls. Additional graphs depict corresponding median survival (**B**) and daily mortality rates at 2 dpi (**C**). Data were combined from four biological replicates (shown individually in Figure B.10). Different letters represent statistically significant differences (Kruskal Wallis, Dunn's multiple comparison post-test, $P < 0.05$). Median survival and Daily mortality rates are represented as median with interquartile range.

Chapter 4 - Dynamics of epizootic hemorrhagic disease virus serotype 2 infection within the vector, *Culicoides sonorensis*

Abstract

Culicoides sonorensis biting midges are confirmed vectors of epizootic hemorrhagic disease virus (EHDV), which causes mortality in white-tailed deer and ruminant populations. Currently, of the seven EHDV serotypes, only 1, 2, and 6 are present in the USA, and very few studies have focused on the infection time course of these serotypes within the midge. The objective of this current research was to characterize EHDV-2 infection within the midge by measuring infection prevalence, virus dissemination, and viral load over the course of infection. Midges were fed a blood meal containing $10^{6.9}$ PFU/ml EHDV-2, collected every 12 h from 0-2 days post-feeding (dpf) and daily from 3-10 dpf, and processed using several techniques. Cytopathic effect assays and quantitative (q)PCR were used to determine infection prevalence, revealing a 50% infection rate by 10 dpf using both methods. Using immunohistochemistry, EHDV-2 infection was detectable at 5 dpf, and shown to disseminate from the midgut to other tissues, including fat body, eyes, and salivary glands by 5 dpf. Stain intensity increased from 5-8 dpf, indicating replication of EHDV-2 in secondary infection sites after dissemination. This finding is also supported by trends in viral load over time, determined by plaque assays and qPCR. An increase in titer between 4-5 dpf correlated with viral replication in the midgut as seen with staining at day 5, while the subsequent gradual increase in viral load from 8-10 dpf suggested viral replication in midges with disseminated infection. Overall, the data presented herein suggest that EHDV-2 is likely to disseminate via the hemolymph to secondary infection sites throughout the midge and that virus transmission by *C. sonorensis* may occur as early as 5 dpf.

Introduction

Culicoides midges are hematophagous dipterans in the family Ceratopogonidae. Due to their need to blood feed for egg production, these insects are considered nuisance biters and capable of vectoring a variety of pathogens (Linley 1986), including arboviruses (Mellor et al. 2000). *Culicoides sonorensis* is a confirmed vector of the orbivirus (family *Reoviridae*) epizootic hemorrhagic disease (EHD) virus (EHDV) in the USA (Foster et al. 1977, Jones et al. 1977). EHDV can cause disease in susceptible ruminant species, resulting in economic losses due to increased mortality within infected herds, production loss, and trade restrictions (MacLachlan and Osburn 2006, Ruder et al. 2015a). Historically, the geographic range of orbiviruses and their known *Culicoides* vectors was limited to between 35°S and 40°N; however, climate change has likely resulted in *Culicoides* range expansions worldwide (Purse et al. 2005, 2015, Zuliani et al. 2015). In the USA, this range expansion has possibly played a role in more severe EHD outbreaks in susceptible herds from previously non-endemic areas, including a 2012 EHD outbreak in Michigan which resulted in the deaths of over 14,000 white-tailed deer (Michigan Department of Natural Resources 2013, Ruder, Lysyk, et al. 2015, Stevens et al. 2015). In contrast, EHDV infection of white-tailed deer in the EHDV-endemic southern USA often results in mild infections with minimal incidence of mortality (Gaydos et al. 2004).

Despite this increase in sporadic EHD outbreaks, relatively little is known of the EHDV infection dynamics in *C. sonorensis*. Based on studies of *C. sonorensis* and bluetongue virus (BTV), orbivirus infection in *Culicoides* is limited by multiple barriers in its vector that have to be overcome for transmission to occur (Fu et al. 1999). While BTV serotype 1 (BTV-1) was detected at 1 day post-feeding (dpf) in all midges that had taken up a virus-containing blood meal, only a proportion of these midges developed persistent infection in the midgut, and only a

small proportion of those midges with persistent midgut infections had BTV in their saliva. Thus, BTV encounters a midgut infection barrier (MIB) that limits virus entry and/or replication within the midgut epithelium and a midgut escape barrier (MEB), which the virus must overcome to disseminate to the salivary glands (Fu et al. 1999). BTV was shown to penetrate the midge MEB as soon as 3 dpf (Sieburth et al. 1991, Fu et al. 1999), disseminate throughout the hemolymph, and infect the salivary glands as early as 5-7 dpf (Fu et al. 1999, Veronesi et al. 2013). While a salivary gland barrier has been observed in multiple mosquito species (Beaty et al. 1981, Grimstad et al. 1985, Romoser et al. 2005), BTV-1 does not appear to encounter such a barrier in *C. sonorensis* midges, as intrathoracic inoculation led to salivary gland infection in all midges (Fu et al. 1999).

Of the three EHDV serotypes within the USA (EHDV-1, -2, and -6) (Shope et al. 1955, Barber and Jochim 1976, Allison et al. 2010), temperature effects on infection dynamics of EHDV-1, and -2 have been reported in a single study that determined infectious titer by $TCID_{50}$ (Ruder et al. 2015b). Ruder et al. (2015) fed *C. sonorensis* midges a blood meal spiked with approximately $10^{7.0}$ $TCID_{50}$/ml of EHDV-1,-2 and -7. EHDV-1 and -7 infected females had a high infection prevalence of approximately 90% throughout the experiment. In contrast, EHDV-2 infected midges had infection rates ranging from 25-30% at 1-2 dpf and 75-80% at 8-12 dpf (Ruder et al. 2015b). Titers $\geq 10^{2.7}$ $TCID_{50}$/midge, the calculated viral infection threshold for successful transmission (Jennings and Mellor 1987, Fu et al. 1999, Ruder et al. 2012), were first observed at 6 dpf in EHDV-2 infected females at 25°C, and from 2-4 dpf at 30°C (Ruder et al. 2015b). Overall, this study suggested that the extrinsic incubation period (EIP) required for these viruses to be transmitted after being ingested by the insect vector was highly temperature

dependent (Ruder et al. 2015b). This trend is similar to what has been reported for BTV, where the EIP decreases with increasing temperatures (Wittman et al. 2002, Carpenter et al. 2011).

While the study by Ruder et al. has provided initial insight into the replication dynamics of EHDV within *Culicoides* midges (Ruder et al. 2015b), fundamental questions of EHDV infection dynamics, including tissue tropism, infection progression, and routes of dissemination remain unresolved. To that end, we conducted an EHDV-2 time-course infection study of *C. sonorensis* to examine virus infection dynamics by molecular, viral, and immunohistochemical techniques.

Materials and Methods

C. sonorensis maintenance and EHDV-2 infections

All experiments were performed with *C. sonorensis* females from the Ausman colony, which were reared using established protocols (Jones and Foster 1974, Tabachnick 1990). EHDV-2 virus stock (ID no. CC12-304) was prepared from the spleen of an infected white-tailed deer from Kansas in 2012. The virus was isolated in calf pulmonary artery endothelial (CPAE; American Type Culture Collection, Manassas, VA, USA) cells and passed twice in baby hamster kidney (BHK; American Type Culture Collection) cells before purification by centrifugation through a 25% sucrose cushion at 28,000 g for 1 h. For oral infections, adult female midges (3-4 d post-eclosion) were allowed to feed for 1 h on a mixture of equal volumes of commercial defibrinated sheep blood (Lampire, Everett, PA, USA) and EHDV-2 virus suspension ($10^{7.2}$ PFU/ml in 199E cell culture medium) using an artificial feeding apparatus with parafilm as a membrane. Engorged females were separated immediately and placed into cages in groups of 80 per cage.

To provide positive controls for immunohistochemical analysis, infections were also performed by intrathoracic (IT) inoculation. For IT inoculation, 3-4 day old female midges were injected as described previously (Mills et al. 2015) with 50 nl of the same EHDV-2 virus suspension. Orally or IT infected midges, along with negative control midges that received a non-infectious blood meal, were kept at 25°C and fed 10 % sucrose solution ad libitum.

Sequential insect sampling

Orally infected midges (n = 20 per time point and assay) were collected every 12 h from 0-2 dpf and daily from 3-10 dpf, and processed for immunohistochemistry (IHC), virus isolation and plaque assays, and qPCR. For IHC, females were IT injected with 50 nl EM grade 10%

formalin (Thermo Fisher Scientific, Waltham, MA, USA). Subsequently, wings were removed with scissors, and midges were placed overnight in 1.5 ml microcentrifuge tubes containing 500 µl 10% buffered formalin (Thermo Fisher Scientific). Midges were transferred to Tissue-Loc HistoScreen cassettes (two midges per cassette, Thermo Fisher Scientific) and held in 10% buffered formalin (Thermo Fisher Scientific) for at least 24 h at room temperature until further processing. For virus isolation and plaque assays, female midges were collected and placed individually into 500 µl of midge viral transport medium (199E cell culture medium, 200 U/ml penicillin, 200 µg/ml streptomycin, 100 µg/ml gentamycin, 100 µg/ml gentamycin, and 5 µg/ml amphotericin B) (Nunamaker et al. 2000). Samples were frozen immediately and stored at -80ºC until further processing. For qPCR analyses, midges were collected and placed individually in 300 µl Trizol (Ambion, Life Technologies, Carlsbad, CA, USA). Samples were frozen immediately and stored at -80ºC until further processing as detailed below.

Embedding and Sectioning

Midges for IHC analyses were embedded in paraffin wax as described previously (Drolet et al. 2005), and stored at room temperature. Embedded midges were serially cut in 5 µm sagittal sections using a Leica RM2235 microtome (Leica, Wetzlar, Germany) with MX35 Premier blades (Thermo Fisher Scientific). Sections were mounted onto positively charged microscope slides (Premiere, C&A Scientific, Manassas, VA, USA) and kept on a slide warmer at 40°C overnight. Midges fed a non-infectious blood meal and IT-infected midges were used as negative and positive controls, respectively, and processed in parallel to the experimental samples.

IHC

IHC staining was performed by modification of a protocol established previously (Drolet et al. 2005). Briefly, midge sections were deparaffinized and hydrated with phosphate buffer

saline (PBS). Antigens were retrieved by submerging sections in citrate-EDTA buffer (10mM citric acid, 2 mM EDTA, 0.05% Tween®20, at pH 6.2) at 65°C for 30 min. Sections were allowed to cool at room temperature and blocked with 6% casein (Sigma-Aldrich, St. Louis, MO, USA) in PBS for 1 h. Sections were incubated at room temperature for 1 h with a 1:1,000 dilution of a polyclonal rabbit EHDV-2 primary antibody. Sections were then sequentially incubated at room temperature for 1 h with biotinylated rabbit anti-mouse secondary antibody and avidin-biotin alkaline phosphatase, according to manufacturer's instruction (VECTASTAIN ABC-AP Staining kit, Vector Laboratories, Burlingame, CA, USA). Between each incubation step, samples were washed twice with PBST (PBS, 0.05% Tween®20) for 5 min. Sections were incubated with Vector Red chromagen substrate (Vector Laboratories) for 20 min, and counterstained with Meyer's hematoxylin (Sigma-Aldrich) for 3 min. Sections were covered with CC Mount (Sigma-Aldrich) and air-dried. Coverslips were added using Vectamount (Vector Laboratories).

Image acquisition and processing

IHC slides were examined for virus-positive (red) staining by light microscopy using a Nikon Eclipse 80i microscope (Nikon, Minato, Tokyo, Japan). Representative images were taken using Leica DFC 7000T camera (Leica), using identical exposure settings across all treatment and control samples. Images were processed in Adobe Photoshop CC 2017 (Adobe Systems, San Jose, CA, USA) using the white balance tool across all treatment and control samples.

Cytopathic effect and plaque assays

To isolate infectious virus, midges stored in midge viral transport medium were homogenized individually using a MM40 bead beater (Retsch, Haan, Germany) at 28 beats per second for 2 min with two hollow titanium beads. Samples were centrifuged at 9,615 × g for 4

min and sonicated at 100 A for 5 second bursts, pulsing every 2 seconds for 35 seconds (Q700 Sonicator, Qsonica, Newtown, CT, USA). Sonicated samples were filtered through 0.45 µm DISMIC:13CP filters (Advantec MFS Inc., Toyo Roshi Kaisha Ltd., Bunkyo-ku, Tokyo, Japan). For each sample, 200 µl of undiluted filtered homogenate was added to a monolayer of Vero cells in a 12-well format and incubated at 37ºC for 10-14 days. Observation of cytopathic effects (CPE) after one passage was used as an indicator of infectious virus within that sample. Infection prevalence was calculated as the percent of midges whose homogenate showed CPE out of the total number of midges assayed at each corresponding time point.

All homogenates that were virus positive in the CPE assays were analyzed further to determine infectious virus particle (VP) titer by standard plaque assay using Vero cells, with plates incubated at 37ºC for 10 days. Because of the dilutions used in this assay, the minimum detectable titer was $10^{1.39}$ Plaque Forming Units (PFU)/midge.

RNA extraction and cDNA synthesis

To isolate total RNA from single infected midges sampled over time, midges stored in 300 µl Trizol were homogenized using a motorized pestle and brought to a final volume of 500 µl Trizol. Samples were centrifuged at 9,615 × g for 4 min, and the supernatant was transferred to a 2 ml Heavy Phase Lock Gel tube (5prime, Thermo Fisher Scientific), which was centrifuged for 2 min at 9,615 × g. Next, 60 µl 1-bromo-3chloropropane (BCP) were added to each tube, and samples were centrifuged at 21,100 × g for 15 min. A further 40 µl BCP were added, and samples were centrifuged again at 21,100 × g for 15 min. The aqueous layer was transferred to a fresh 1.5 ml RNAse-free tube and mixed with an equal volume of isopropanol. Samples were incubated for 30 min at room temperature and centrifuged at 21,100 × g for 30 min. The supernatant was removed, and the remaining RNA pellet was washed with 800 µl of 70%

ethanol. Pellets were air-dried for 3-4 min, and each pellet was dissolved in 10 µl RNAse-free water. DNA was removed with PerfeCTa DNase I (Quantabio, Beverly, MA, USA) per manufacturer's instructions, and DNAseI was subsequently heat denatured at 80ºC for 15 min. Complementary DNA (cDNA) was synthesized using the qScript XLT cDNA SuperMix (Quantabio) with 200 ng of total RNA as template and a mixture of random hexamers and oligo(dT) primers in a total reaction volume of 20 µl, following the manufacturer's protocol.

qPCR

To quantify EHDV-2 load by viral genomic equivalents (GE), qPCR reactions were performed using primers that anneal to the negative sense strand of genomic segment 10 of EHDV-2, which is translated into non-structural protein 3 (Ns3). Using iQ SYBR Green Supermix (Bio-Rad, Hercules, CA, USA), 5 µl-undiluted cDNA was used as template for each 20 µl reaction. Primers were designed based on published EHDV-2 *Ns3* complete coding DNA sequence (GenBank accession No. KU140932.1) as follows: Ns3_F 5'-CTACCACAGCCGCAATTA-3', Ns3_R 5'- GCATGTAAACGAGCAAGTATT-3'. To ensure high quality of the extracted total RNA, midge *Elongation Factor 1b* (*EF1b,* GAWM01010754) transcripts were detected using our previously established protocol (Mills et al. 2015). All qPCRs were performed with 3 technical replicates per sample and primer set, using previously described PCR parameters (Mills et al. 2015). Samples were deemed virus-positive by this method if (1) *EF1b* amplification resulted in a threshold cycle (C_t) between 21-25, and (2) the viral amplicon from at least two out of three technical replicates produced a smooth, single-peak melt curve, with a fluorescence maximum at 80°C.

Calculating total VPs from qPCR

Total RNA from the EHDV-2 stock was extracted in 750 µl Trizol as described previously (Mills et al. 2015) and resuspended in 40 µl RNAse-free water. To precipitate single-stranded RNA, an equal volume of 4 M LiCl was added to each sample and incubated for 1 h at -20°C. Samples were centrifuged at 21,100 × g for 1 h at 4°C, and the supernatant was transferred to a new tube. To precipitate viral genomic dsRNA from the supernatant, an equal volume of 8 M LiCl was added to each sample and incubated at -20°C for 1 h. Samples were centrifuged 21,100 × g for 1 h at 4°C, supernatants were removed, and pellets were washed with 800 µl 70% ethanol. Pellets were air-dried for 3-5 min and resuspended in 50 µl RNase-free water. Complementary DNA was synthesized using the qScript XLT cDNA SuperMix (Quantabio) with 200 ng of viral genomic dsRNA as template and a mixture of random hexamers and oligo(dT) primers in a total reaction volume of 20 µl, following the manufacturer's protocol. The resulting cDNA was serially diluted in RNase-free water [undiluted, 1:2, 1:10, 1:20, 1:50, $1:10^2$, $1:10^3$, $1:10^4$, $1:10^5$].

To obtain a standard curve, the serially diluted cDNA was used as template in qPCR reactions with Ns3 primers as described above. The standard curve was generated by plotting the natural log of the dsRNA amount against the observed C_t values for each dilution (Figure C.1). Data were analyzed by linear regression, yielding an equation of $y = (-1.253)x + 22.63$ (Graphpad Prism 6, GraphPad Software Inc., La Jolla, CA, USA). This equation was used to convert C_t values obtained from experimental midge samples to total viral dsRNA per sample, which was further converted to total number of VPs using the ratio published by Huismans et al. (0.1 fg viral dsRNA: viral genome equivalents of 6 VPs) (Huismans et al. 1979).

Results

Tissue tropism of EHDV-2 in *C. sonorensis*

To identify the tissues susceptible to EHDV-2 infection within *C. sonorensis*, infected midges underwent sagittal sectioning and IHC staining, with representative images taken of infected midge tissues after dissemination (Figure 4.1). In disseminated infections, IHC staining of EHDV-2 was observed in the neural lamella of the cerebral ganglia (Figure 4.1B), salivary glands (Figure 4.1C), posterior midgut (Figure 4.1D), Johnston's organ (antenna; Fig 1F), optic ganglia and ommatidia of the eye (Figure 4.1G), and fat body (Figure 4.1H). Interestingly, apparent degradation of the photoreceptor cluster of the ommatidia was associated with EHDV-2 staining in the eye (Figure 4.1G). No staining was observed in the muscle, anterior midgut, hindgut, and rectum, which suggest these tissues may be refractory to EHDV-2 infection. While tracheal epithelial cells, lumen, and tinidea did not stain for EHDV-2, IHC-positive staining was detected in the tracheoles (Figure C.2). In the ovary, EHDV-2 positive staining was localized to the ovarian sheath but absent in the ovariolar sheath, ovarioles, follicular epithelium, oocytes, and nurse cells (Figure 4.1E). Epithelial cells of the spermatheca were positive, but neither the sperm, nor the reservoir lumen, which contains the sperm, were positively stained by IHC (Figure 4.1I).

Temporal progression of EHDV-2 within *C. sonorensis*

To identify the temporal patterns of EHDV-2 infection within the susceptible *C. sonorensis* tissues, IHC were performed on midges processed daily 3-10 dpf. We focused on infection progression in the midgut, the primary site of infection following viral ingestion (Figure 4.2A-C), and the salivary gland, as these organs are responsible for bite transmission (Figure 4.2D-F). In addition, images were taken of tissues that confirmed dissemination: fat body

(Figure 4.2G-I) and eye (Figure 4.2J-L). Following digestion of the blood meal at 2-3 dpf, staining for EHDV-2 was first observed at 5 dpf in foci of the midgut epithelium (Figure 4.2B). At the same time point, EHDV-2 staining was also observed in salivary glands, fat bodies, and eyes, specifically the ommatidia and optic ganglia (Figure 4.2E, H, and K). In all midges that were positive for EHDV-2 infection at 5 dpf, staining was more pronounced in the midgut than in other infected tissues (Figure 4.2B). At time points sampled daily between 6-10 dpf, overall staining intensity was more pronounced in all tissues when compared to staining patterns at 5 dpf (Figure 4.2C, F, I, and L), with the fat body having the strongest and most homogeneous tissue staining (Figure 4.2I). The midgut and salivary glands both had foci of intense staining, where strongly positive cells were located near non- or weakly-stained cells of the same tissue (Figure 4.2C and F).

EHDV-2 infection prevalence and titer throughout *C. sonorensis* infection

Total and infectious VPs within the sampled midge population were determined throughout the infection time course to reveal trends in EHDV-2 prevalence and virus load (Table 4.1). At 0 dpf, VPs were detected in 30% and 13% of sampled midges, as determined by CPE and qPCR, respectively. This percentage generally increased through 4 dpf to 53 and 56% of midges, when VPs were isolated and detected by qPCR, respectively. Prevalence levels, measured by either method, appeared to decrease to 20-37% between 5 and 6 dpf and increase again to 50-60% by 10 dpf. At individual time points, up to two-fold differences in prevalence were observed by the two detection methods. Nevertheless, these differences were non-directional, and neither method was consistently more sensitive at detecting EHDV-2.

For each EHDV-2-positive midge, the number of total and infectious VPs was determined (Figure 4.3). Based on the average *Culicoides* blood meal size of 100 nl (Mellor et al.

2008), and titer of the EHDV-2 stock in the infectious blood meal, each midge on average ingested approximately 40 infectious VPs from the EHDV-2 spiked blood meal. Between 0-1.5 dpf, infectious VP load was at or below this average ingestion titer, with VP titers during the first 12 h of infection below the detection limit of $10^{1.39}$ PFU/midge. Viral load varied across the time course of infection with similar trends observed for total and infectious VP load/midge. Peaks in total VP load were observed at 2, 4, and 10 dpf, and infectious VP titers peaked at 5 and 8-10 dpf. Both total and infectious VPs increased steadily from 7 dpf, until reaching their maximum at 10 dpf. Throughout the infection time course, total VP load as calculated by qPCR amplification of genomic RNA was consistently greater than infectious VP titer, as calculated by plaque assay, at the corresponding time point. Total VP load ranged from $10^{7.0}$ to $10^{8.6}$ GE/midge, while infectious VP titer ranged from $10^{1.88}$ to $10^{5.48}$ PFU/midge. These data suggest that qPCR not only detects released VPs, but also incomplete core particles trapped within infected cells (Stuart and Grimes 2006).

Discussion

There are inherent challenges to studying virus-vector interactions such as variation in blood meal virus uptake, variation between individuals within and across biological replicates, as well as detection limits of the assays available. Acknowledging these challenges, we used a multidisciplinary approach to analyze the EHDV-2 infection time course in its competent vector *C. sonorensis*. The time course infection prevalence, dissemination, and viral titer results presented herein provide the first insight into the overall infection dynamics of EHDV-2 in *C. sonorensis* midges. Driven by the small blood meal size, midges take up very few EHDV-2 VPs, at least some of which must escape the blood meal during digestion to infect the midgut epithelium. Replication of virus in this first site of infection occurs by 48 h, the first time point at

which we measured an increase in total VP numbers by qPCR. While histological sections showed the blood meal was digested and cleared from *C. sonorensis* midguts by 2-3 dpf, infectious VP titers remained below the detectable limit for an additional two days, suggesting that virus replication is likely limited and restricted to the midgut epithelial cells. This low viral titer also corresponded with a lack of EHDV-2 staining before 5 dpf. At this time point, infection prevalence reached a temporary plateau that matched endpoint prevalence. EHDV-2 subsequently exited the midgut epithelium and disseminated throughout the body of the midge. Infection of secondary tissues was first detected at 5 dpf, confirming midgut escape and dissemination prior to this time point. Virus replication was observed at all secondary infection sites, reflected in increases in IHC staining and virus titers from 7 dpf onwards. These trends are similar to previous reports that monitored orbivirus load and infection prevalence in *C. sonorensis* (Mills et al. 2017). Our observations are further supported by published IHC analyses, which detected BTV within the midgut epithelium by 3 dpf (Sieburth et al. 1991, Fu et al. 1999), and within the salivary glands and saliva between 5-7 dpf (Fu et al. 1999, Veronesi et al. 2013).

Of the *C. sonorensis* midges that ingested a virus-spiked blood meal, only 50% were positive for infectious EHDV-2 at 10 dpf, indicating that in the other 50% of midges the viral inoculum titer ingested was too low to establish infection or was cleared by various innate antiviral responses. This 50% infection rate was also observed prior to complete blood meal digestion (1.5 dpf) and dissemination (2-4 dpf), suggesting that in some cases EHDV-2 may be cleared in the meal before establishing infection. These trends are distinct from the infection prevalence data observed for BTV-1 (Fu et al. 1999) and EHDV-7 (Ruder et al. 2015b). In these studies, initial infection prevalence at 0 dpf was closer to 100%, and a decrease in infection rates was observed between 0 dpf and 3-4 dpf (Fu et al. 1999, Ruder et al. 2015b). The function of

MIB and MEB as barriers during BTV-1 and EHDV-7 infection was clearly correlated to the sharp decrease in infection prevalence between 0 dpf and 3-4 dpf. In contrast, Ruder et al. (2015) observed a low EHDV-2 infection prevalence of 25% at 0 dpf with no subsequent, intense decrease in infection rate (Ruder et al. 2015b). These data suggest that EHDV-2 overall infection rates are partially dependent on the amount of virus taken up during hematophagy. The role of the MIB and MEB as barriers to EHDV-2 infection was more reflected in the decreasing trend in viral titers observed at days 3 and 6, respectively, than in the prevalence data of this study.

Orbivirus EIP in *C. sonorensis* has been measured previously as the time period between virus uptake and an infectious virus titer larger than $10^{2.7}$ $TCID_{50}$/midge. This is considered the threshold for vector competence (Jennings and Mellor 1987, Fu et al. 1999, Ruder et al. 2012), and is substantiated by detecting VPs in the salivary glands/saliva (Fu et al. 1999, Veronesi et al. 2013). We observed EHDV-2 in the salivary gland epithelia as early as 5 dpf, the same time point at which infectious VP titers crossed the vector competence threshold for the first time. These data suggest an EHDV-2 EIP in *C. sonorensis* at or below 5 days at 25ºC, which is slightly shorter than EIPs reported previously for EHDV-1, -2, and -7 (6 dpf) (Ruder et al. 2015b). As the lengths of orbivirus EIP and other arboviruses are temperature dependent (Wittman et al. 2002, Carpenter et al. 2011), the short EIP seen in this study could become even more reduced at higher temperatures. Climate change is predicted to precipitate such a phenomenon in *C. sonorensis* throughout large regions of their geographic range in the USA (Zuliani et al. 2015).

Arboviruses utilize a variety of routes to disseminate from the midgut to susceptible secondary tissues in the insect including the tracheal network, neural network, or hemolymph (Hardy et al. 1983, Blanc et al. 2014, Franz et al. 2015). Based on the observed infection time course of these secondary tissues, EHDV-2 disseminates from the midgut via the hemolymph to

infect all susceptible secondary tissues, including the salivary glands, at approximately the same rate. Equivalent EHDV-2 staining was observed across all secondary tissues with no evidence of a specific sequential infection throughout the midge. In contrast, routes of arbovirus dissemination via the tracheal or neural networks result in a characteristic, sequential infection of host tissues over time (Franz et al. 2015). For example, vesicular stomatitis virus (VSV) was detected in *C. sonorensis* midges, sequentially along the alimentary canal from foregut to midgut to Malpighian tubules before dissemination via hemolymph. Additionally, VSV was shown to disseminate rapidly from midgut epithelial cells to abdominal node neural cell bodies via retrograde axonal transport and progress sequentially down axons to other node cell bodies via anterograde transport (Drolet et al. 2005). However, EHDV-2 staining was not associated with the neuronal ganglia, and infection was limited to the neural lamella, which serves as the insect blood brain barrier by lining neuronal tissues (Hindle and Bainton 2014). Furthermore, a tracheal route for EHDV-2 dissemination is unlikely, as EHDV-2 staining was not detected in tracheal epithelia or lumen and limited only to tracheoles. Together, these observations strongly suggest that EHDV-2, similar to BTV-1 (Fu et al. 1999), relies on the hemolymph to reach susceptible secondary tissues.

Tissue tropism can be used to infer physiological consequences of virus infection. EHDV-2 staining was observed in the midge ommatidia, optic ganglia, and Johnston's organ, which provide visual and auditory perception (Land 1997, Boekhoff-Falk 2005). EHDV-2 infection and replication was associated with damage to the ommatidia, which could result in impaired function and subsequent behavioral changes of *C. sonorensis.* Previous studies observed BTV-1 and -17 infected *C. sonorensis* ommatidia (Fu et al. 1999, McDermott et al. 2015) and light aversion behavior was attributed to infection of these vision organs (McDermott

et al. 2015). Some impact of virus infection on vector behavior, such as host-seeking, has also been suggested for mosquito-borne viruses including dengue (Putnam and Scott 1995, Linthicum et al. 1996, Platt et al. 1997). Future studies are required to examine EHDV-2 infection-related damage of sensory tissues and determine the potential consequences on altered sensory perception in *C. sonorensis* host-seeking behavior.

Analysis of viral tissue tropism also revealed EHDV-2 infection of *C. sonorensis* female reproductive organs. EHDV-2 staining was associated with the epithelia of the *C. sonorensis* spermatheca, which is structurally similar to other dipteran vectors (Pascini et al. 2012, Pascini and Martins 2013, Laghezza Masci et al. 2015). In the ovaries, EHDV-2 staining was limited to the ovarian sheath, which does not come into direct contact with the developing oocyte (Büning 1994), and was absent from the ovariolar sheath, ovarioles, follicular epithelium, oocytes, and nurse cells. These observations suggest a barrier to EHDV-2 infection of *C. sonorensis* ovaries. Previous studies detected BTV in the ovarian sheath, within the immature yolk bodies and vitelline membrane of the developing *Culicoides* oocyte, as well as on eggs oviposited by BTV-infected females (Jones and Foster 1971, Chandler et al. 1985, Nunamaker et al. 1990, Osborne et al. 2015). Nevertheless, these studies found no evidence for vertical transmission of BTV by *Culicoides* (Jones and Foster 1971, Chandler et al. 1985, Nunamaker et al. 1990, Osborne et al. 2015). Considering our findings along with these published data, it is unlikely that vertical transmission of EHDV-2 occurs in its vector, *C. sonorensis.* Given the role of the spermatheca in sperm survival and reproductive success (Degner and Harrington 2016), future studies should investigate the potential effects of EHDV-2 spermathecal epithelium infection on reproduction.

In summary, this study was the first to examine EHDV-2 infection dissemination, infection prevalence, and viral titer simultaneously within *C. sonorensis* over the course of

infection. The viral titer and infection prevalence data reported here showed similar trends in EHDV-2 infection observed by Ruder et al. (Ruder et al. 2015b), and linked these trends with the temporal-spatial fate of the virus. Similar to BTV-1, EHDV-2 disseminates through the hemolymph of *C. sonorensis* to the salivary glands by 5 dpf, suggesting an EIP of 5 d or shorter. In addition, this study is the first to identify the physiological basis for the lack of EHDV-2 vertical transmission in its insect vector. Overall trends in VP load and infection prevalence were similar between qPCR and plaque assays, confirming that the molecular assay, described herein, can be used to monitor EHDV-2 infection progression in its vector over time. Together, these findings fill important gaps in our knowledge of EHDV interactions with its vector. This knowledge will facilitate future studies aiming to identify the molecular mechanisms that underlie EHDV-2 vector competence in *C. sonorensis.*

Acknowledgments

Thanks go to Dr. Lee Cohnstaedt and Mr. William E. Yarnell at the Arthropod-Borne Animal Diseases Research Unit, USDA-ARS, Manhattan, KS for provision of all adult C. sonorensis midges and housing materials used in this study. Research reported in this publication was supported by the USDA-ARS National Programs 103 & 104 (B.S.D., D. N.) and through USDA-ARS Specific Cooperative Agreement 58-5430-4-022 (K.M.). Mention of trade names or commercial products in this publication is solely for the purpose of providing specific information and does not imply recommendation or endorsement by the U.S. Department of Agriculture. Any opinions, findings, conclusion, or recommendations expressed in this publication are those of the author(s) and do not necessarily reflect the view of the U.S. Department of Agriculture. This is contribution 17-393-J from the Kansas Agricultural

Experiment Station. This chapter is submitted to PLoS ONE for publication in 2017 and titled "Dynamics of epizootic hemorrhagic disease virus serotype 2 infection within the vector, *Culicoides sonorensis* (Diptera: Ceratopogonidae)".

References

Allison, A. B., V. H. Goekjian, A. C. Potgieter, W. C. Wilson, D. J. Johnson, P. P. C. Mertens, and D. E. Stallknecht. **2010**. Detection of a novel reassortant epizootic hemorrhagic disease virus (EHDV) in the USA containing RNA segments derived from both exotic (EHDV-6) and endemic (EHDV-2) serotypes. J. Gen. Virol. 91: 430–439.

Barber, T. L., and M. M. Jochim. **1976**. Serotyping bluetongue and epizootic hemorrhagic disease virus strains. Proc. Am. Assoc. Vet. Lab. Diagn. 18: 149–157.

Beaty, A. B. J., M. Holterman, W. Tabachnick, R. E. Shope, E. J. Rozhon, and L. Bishop. **1981**. Molecular basis of Bunyavirus transmission by mosquitoes: role of the middle-sized RNA segment. Science. 211: 1433–1435.

Blanc, S., M. Drucker, and M. Uzest. **2014**. Localizing viruses in their insect vectors. Annu. Rev. Phytopathol. 52: 403–425.

Boekhoff-Falk, G. 2005. Hearing in *Drosophila*: development of Johnston's organ and emerging parallels to vertebrate ear development. Dev. Dyn. 232: 550–558.

Büning, J. 1994. The insect ovary: ultrastructure, previtellogenic growth and evolution. Springer Science & Business Media.

Carpenter, S., A. Wilson, J. Barber, E. Veronesi, P. Mellor, G. Venter, and S. Gubbins. **2011**. Temperature dependence of the extrinsic incubation period of orbiviruses in *Culicoides* biting midges. PLoS One. 6: e27987.

Chandler, L. J., M. E. Ballinger, R. H. Jones, and B. J. Beaty. **1985**. The virogenesis of bluetongue virus in *Culicoides variipenis*. Prog. Clin. Biol. Res. 178: 245–253.

Degner, E. C., and L. C. Harrington. **2016**. A mosquito sperm's journey from male ejaculate to egg: Mechanisms, molecules, and methods for exploration. Mol. Reprod. Dev. 83: 897–911.

Drolet, B. S., C. L. Campbell, M. A. Stuart, and W. C. Wilson. **2005**. Vector competence of

Culicoides sonorensis (Diptera: Ceratopogonidae) for vesicular stomatitis virus. J. Med. Entomol. 42: 409–418.

Foster, N. M., R. D. Breckon, A. J. Luedke, and R. H. Jones. **1977**. Transmission of two strains of epizootic hemorrhagic disease virus in deer by *Culicoides variipennis*. J. Wildl. Dis. 13: 9–16.

Franz, A. W. E., A. M. Kantor, A. L. Passarelli, and R. J. Clem. **2015**. Tissue barriers to arbovirus infection in mosquitoes. Viruses. 7: 3741–3767.

Fu, H., C. J. Leake, P. P. Mertens, and P. S. Mellor. **1999**. The barriers to bluetongue virus infection, dissemination and transmission in the vector, *Culicoides variipennis* (Diptera: Ceratopogonidae). Arch. Virol. 144: 747–61.

Gaydos, J. K., J. M. Crum, W. R. Davidson, S. S. Cross, S. F. Owen, and D. E. Stallknecht. **2004**. Epizootiology of an epizootic hemorrhagic disease outbreak in West Virginia. J. Wildl. Dis. 40: 383–393.

Grimstad, P. R., S. L. Paulson, and G. B. Craig Jr. 1985. Vector competence of *Aedes hendersoni* (Diptera: Culicidae) for La Crosse virus and evidence of a salivary-gland escape barrier. J. Med. Entomol. 22: 447–453.

Hardy, J. L., E. J. Houk, L. D. Kramer, and W. C. Reeves. **1983**. Intrinsic factors affecting vector competence of mosquitoes for arboviruses. Annu. Rev. Entomol. 28: 229–262.

Hindle, S. J., and R. J. Bainton. **2014**. Barrier mechanisms in the *Drosophila* blood-brain barrier. Front. Neurosci. 8: 1–12.

Huismans, H., C. W. Bremer, and T. L. Barber. **1979**. The nucleic acid and proteins of epizootic haemorrhagic disease virus. J. Vet. Res. 46: 95–104.

Jennings, D. M., and P. S. Mellor. **1987**. Variation in the responses of *Culicoides variipennis* (Diptera, Ceratopogonidae) to oral infection with bluetongue virus. Arch. Virol. 95: 177–182.

Jones, R., and N. Foster. **1971**. Transovarian transmission of bluetongue virus unlikely for *Culicoides sonorensis*. Mosq. News. 31: 434–437.

Jones, R. H., and N. M. Foster. **1974**. Oral infection of *Culicoides variipennis* with bluetongue virus: development of susceptible and resistant lines from a colony population. J. Med. Entomol. 11: 316–323.

Jones, R. H., R. D. Roughton, N. M. Foster, and B. M. Bando. **1977**. *Culicoides*, the vector of

epizootic hemorrhagic disease in white-tailed deer in Kentucky in 1971. J. Wildl. Dis. 13: 2–8.

Laghezza Masci, V., M. Di Luca, G. Gambellini, A. R. Taddei, M. C. Belardinelli, L. Guerra, M. Mazzini, and A. M. Fausto. **2015**. Reproductive biology in Anophelinae mosquitoes (Diptera, Culicidae): fine structure of the female accessory gland. Arthropod Struct. Dev. 44: 378–387.

Land, M. F. 1997. Visual Acuity in Insects. Annu. Rev. Entomol. 42: 147–177.

Linley, J. R. 1986. The effect of salinity on oviposition and egg hatching in *Culicoides variipennis sonorensis* (Diptera: Ceretopogonidae). J. Am. Mosq. Control Assoc. 2: 79–82.

Linthicum, K., K. B. Platt, K. S. Myint, K. Lerdthusnee, B. L. Innis, and D. W. Vaughn. **1996**. Dengue 3 virus distribution in the mosquito *Aedes aegypti*: an immunocytochemical study. Med. Vet. Entomol. 10: 97–92.

MacLachlan, N. J., and B. I. Osburn. **2006**. Impact of bluetongue virus infection on the international movement and trade of ruminants. J. Am. Vet. Med. Assoc. 228: 1346–1349.

McDermott, E. G., C. E. Mayo, A. C. Gerry, D. Laudier, N. J. MacLachlan, and B. A. Mullens. **2015**. Bluetongue virus infection creates light averse *Culicoides* vectors and serious errors in transmission risk estimates. Parasit. Vectors. 8: 2–9.

Mellor, P. S., J. Boorman, and M. Baylis. **2000**. *Culicoides* biting midges: their role as arbovirus vectors. Annu Rev Entomol. 45: 307–340.

Mellor, P. S., S. Carpenter, and D. M. White. **2008**. Bluetongue virus in the insect host., pp. 295–320. *In* Mertens, P., Baylis, M., Mellor, P. (eds.), Biol. Anim. Infect. Bluetongue. Academic Press.

Michigan Department of Natural Resources. **2013**. Epizootic hemorrhagic disease (EHD) in white-tailed deer. (http://www.michigan.gov/dnr/0,1607,7-153-10370_12150-26647--,00.html).

Mills, M. K., K. Michel, R. S. Pfannenstiel, M. G. Ruder, E. Veronesi, and D. Nayduch. **2017**. *Culicoides*–virus interactions: infection barriers and possible factors underlying vector competence. Curr. Opin. Insect Sci. 22: 7–15.

Mills, M. K., D. Nayduch, and K. Michel. **2015**. Inducing RNA interference in the arbovirus vector, *Culicoides sonorensis*. Insect Mol. Biol. 24: 105–14.

Nunamaker, R. A., A. A. Peréz De León, C. L. Campbell, and S. M. Lonning. **2000**. Oral

infection of *Culicoides sonorensis* (Diptera: Ceratopogonidae) by vesicular stomatitis virus. J. Med. Entomol. 37: 784–786.

Nunamaker, R. A., P. J. Sieburth, V. C. Dean, J. G. Wigington, C. E. Nunamaker, and J. O. Mecham. **1990**. Abscence of transovarial transmission of bluetongue virus in *Culicoides variipennis*: immunogold labeling of bluetongue virus antigen in developing oocytes from *Culicoides variipennis* (Coquillett). Comp. Biochem. Physiol. 96: 19–31.

Osborne, C. J., C. E. Mayo, B. A. Mullens, E. G. McDermott, A. C. Gerry, W. K. Reisen, and N. J. Maclachlan. **2015**. Lack of evidence for laboratory and natural vertical transmission of bluetongue virus in *Culicoides sonorensis* (Diptera: Ceratopogonidae). J. Med. Entomol. 52: 274–277.

Pascini, A. T. V, and G. F. Martins. **2013**. The fine structure of the spermatheca in *Anopheles aquasalis* (Diptera: Culicidae). Ann. Entomol. Soc. Am. 106: 857–867.

Pascini, T. V., M. Ramalho-Ortigão, and G. F. Martins. **2012**. Morphological and morphometrical assessment of spermathecae of *Aedes aegypti* females. Mem. Inst. Oswaldo Cruz. 107: 705–712.

Platt, K. B., K. J. Linthicum, K. S. Myint, B. L. Innis, K. Lerdthusnee, and D. W. Vaughn. **1997**. Impact of dengue virus infection on feeding behavior of *Aedes aegypti*. Am. J. Trop. Med. Hyg. 57: 119–125.

Purse, B. V, S. Carpenter, G. J. Venter, G. Bellis, and B. A. Mullens. **2015**. Bionomics of temperate and tropical *Culicoides* midges: knowledge gaps and consequences for transmission of *Culicoides*-borne viruses. Annu. Rev. Entomol. 60: 373–392.

Purse, B. V, P. S. Mellor, D. J. Rogers, A. R. Samuel, P. P. C. Mertens, and M. Baylis. **2005**. Climate change and the recent emergence of bluetongue in Europe. Nat. Rev. Microbiol. 3: 171–181.

Putnam, J. L., and T. W. Scott. **1995**. Blood-feeding behavior of dengue-2 virus-infected *Aedes aegypti*. Am. J. Trop. Med. Hyg. 52: 225–227.

Romoser, W. S., M. Turell, K. Lerdthusnee, M. Neira, D. Dohm, G. Ludwig, and L. Wasieloski. **2005**. Pathogenesis of Rift Valley fever virus in mosquitoes- tracheal conduits & the basal lamina as an extra-cellular barrier. Arch. Virol. 19: 89–100.

Ruder, M. G., E. W. Howerth, D. E. Stallknecht, A. B. Allison, D. L. Carter, B. S. Drolet, E. Klement, and D. G. Mead. **2012**. Vector competence of *Culicoides sonorensis* (Diptera: Ceratopogonidae) to epizootic hemorrhagic disease virus serotype 7. Parasit Vectors. 5: 1–8.

Ruder, M. G., T. J. Lysyk, D. E. Stallknecht, L. D. Foil, D. J. Johnson, C. C. Chase, D. A. Dargatz, and E. P. J. Gibbs. **2015a**. Transmission and epidemiology of bluetongue and epizootic hemorrhagic disease in North America: current perspectives, research gaps, and future directions. Vector-Borne Zoonotic Dis. 15: 348–363.

Ruder, M. G., D. E. Stallknecht, E. W. Howerth, D. L. Carter, R. S. Pfannenstiel, A. B. Allison, and D. G. Mead. **2015b**. Effect of temperature on replication of epizootic hemorrhagic disease viruses in *Culicoides sonorensis* (Diptera: Ceratopogonidae). J. Med. Entomol. 52: 1050–1059.

Shope, R. E., L. G. MacNamara, and R. Mangold. **1955**. Report on the deer mortality, epizootic hemorrhagic disease of deer. New Jersey outdoors. 6: 17–21.

Sieburth, P. J., C. E. Nunamaker, J. Ellis, and R. A. Nunamaker. **1991**. Infection of the midgut of *Culicoides variipennis* (Diptera: Ceratopogonidae) with bluetongue virus. J. Med. Entomol. 28: 74–85.

Stevens, G., B. McCluskey, A. King, E. O'Hearn, and G. Mayr. **2015**. Review of the 2012 epizootic hemorrhagic disease outbreak in domestic ruminants in the United States. PLoS One. 10: 1–11.

Stuart, D. I., and J. M. Grimes. **2006**. Structural studies on orbivirus proteins and particles, pp. 221–244. *In* Reoviruses Entry, Assem. Morphog. Springer Science & Business Media.

Tabachnick, W. J. 1990. Genetic variation in laboratory and field populations of the vector of bluetongue virus, *Culicoides variipennis* (Diptera: Ceratopogonidae). J. Med. Entomol. 27: 24–30.

Veronesi, E., F. Antony, S. Gubbins, N. Golding, A. Blackwell, P. P. Mertens, J. Brownlie, K. E. Darpel, P. S. Mellor, and S. Carpenter. **2013**. Measurement of the infection and dissemination of bluetongue virus in *Culicoides* biting midges using a semi-quantitative rt-PCR assay and isolation of infectious virus. PLoS One. 8: e70800.

Wittman, E. J., P. S. Mellor, and M. Baylis. **2002**. Effect of temperature on the transmission of arboviruses by the biting midge, *Culicoides sonorensis*. Med. Vet. Entomol. 16: 147–156.

Zuliani, A., A. Massolo, T. Lysyk, G. Johnson, S. Marshall, K. Berger, and S. C. Cork. **2015**. Modelling the Northward Expansion of *Culicoides sonorensis* (Diptera: Ceratopogonidae) under Future Climate Scenarios. PLoS One. 10: 1–23.

Tables and Figures – Chapter 4

Table 4.1 Infection prevalence and viral load throughout EHDV-2 infection within the midge

	Infectious VP		Total VP	
dpf	% CPE positive*	PFU per midge** (n)	% qPCR positive*	Viral Genome Equivalents per midge**
0	30 (6/20)	<1.39 (6)	13 (2/15)	7.81, 8.27
0.5	35 (7/20)	<1.39 (7)	18 (3/17)	6.66, 6.70, 7.10
1	40 (8/20)	<1.39 (7), 2.70	28 (5/18)	7.15, 7.23, 7.27, 7.60, 7.69
1.5	55 (11/20)	<1.39 (10), 2.40	39 (7/18)	6.91, 7.07, 7.32, 7.78, 7.54, 8.03, 8.11
2	39 (7/18)	<1.39 (7)	50 (10/20)	6.56, 7.47, 7.63, 8.11, 8.30, 9.32, 10.10, 11.17, 11.85, 12.61
3	50 (10/20)	<1.39 (10)	41 (7/17)	6.62, 6.74, 7.00, 7.35, 7.72, 8.33, 12.32
4	53 (9/17)	<1.39 (8), 1.88	56 (10/18)	6.72, 7.01, 7.34, 7.42, 7.63, 7.96, 8.28, 11.88, 12.06, 13.85
5	20 (4/20)	<1.39 (1), 2.60, 3.53, 4.01	37 (7/19)	6.38, 6.88, 7.20, 7.29, 7.54, 7.83, 15.41
6	30 (6/20)	<1.39 (6)	31 (5/16)	6.60, 6.73, 7.03, 7.51, 7.64
7	65 (13/20)	<1.39 (13)	56 (9/17)	6.45 ,6.87, 6.93, 7.11, 7.18, 7.22, 7.78, 12.36, 15.48
8	35 (7/20)	<1.39 (3), 2.85, 3.68, 5.18, 5.48	45 (8/20)	6.87, 6.94, 7.18, 7.22, 7.78, 12.36, 15.42, 15.48
9	45 (9/20)	<1.39 (7), 4.28, 5.10	90 (18/20)	7.04, 7.11, 7.21, 7.30, 7.38, 7.40, 7.52, 7.62, 7.69, 7.89, 8.05, 8.08, 8.17, 8.26, 8.61, 9.22, 14.34, 14.85
10	50 (10/20)	<1.39 (7), 2.72, 4.90, 5.10	62.5 (5/8)	6.66, 7.53, 8.59, 9.26, 14.49

*no. positive/n

** Log_{10}/midge; n is denoted if n > 1. Conversion of C_t values to total viral genome equivalents is based on calculation ratios published by Huismans et al. where 0.1 fg viral dsRNA is the genomic equivalent of 6 VPs (Huismans et al. 1979).

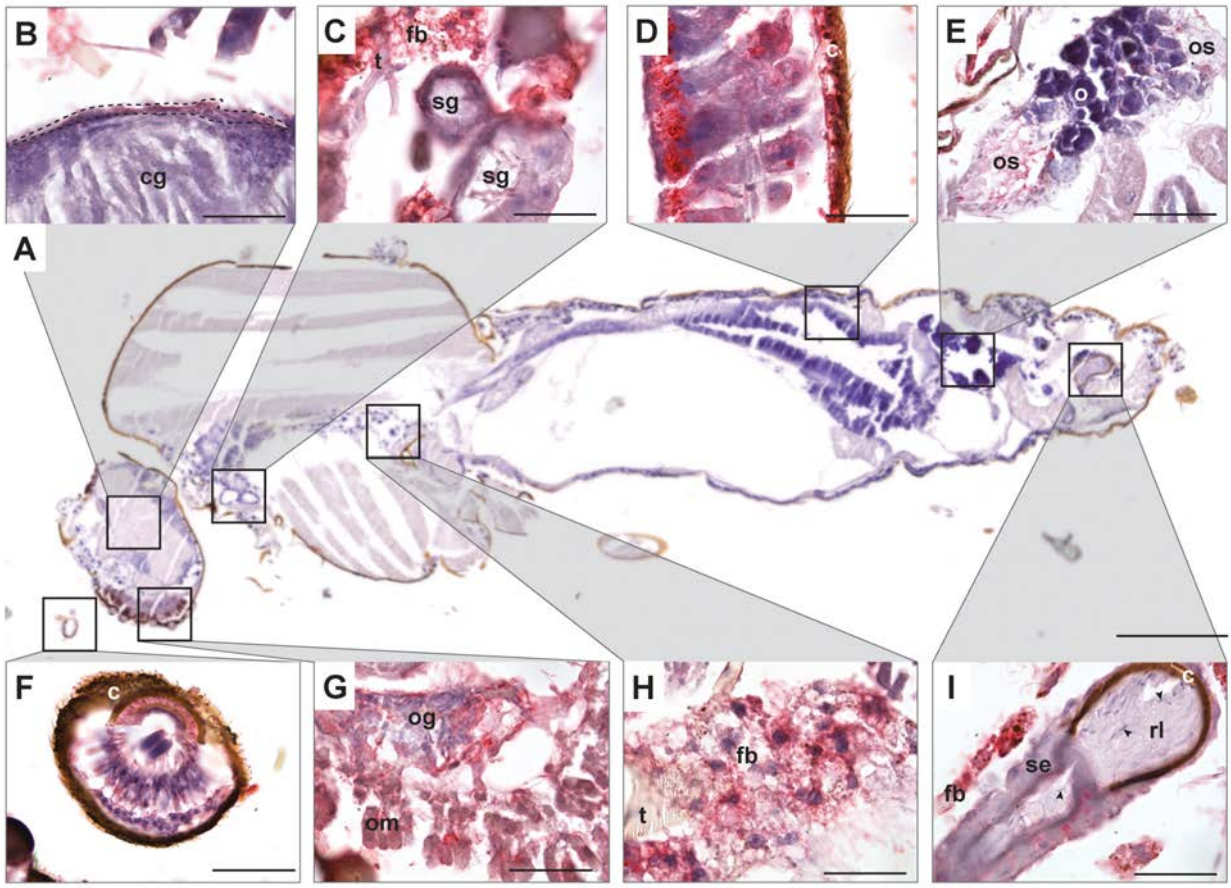

Figure 4.1 IHC staining of EHDV-2 infected tissues throughout *C. sonorensis*

Representative images were taken from orally infected midges at 7-10 dpf. (**A**) The internal anatomy of *C. sonorensis* revealed by a hematoxylin-stained sagittal section of the whole midge. No staining for EHDV-2 is provided in this section. Boxes indicate locations of tissues positive for EHDV-2 by IHC staining (red). (**B**) the neural lamella (dotted line) of the cerebral ganglia (cg); (**C**) salivary gland (sg), fat body (fb), trachea (t); (**D**) posterior midgut, cuticle (c); (**E**) ovarian sheath (os), ovariole (o); (**F**) Johnston's organ (antenna); (**G**) eye containing the ommatidia (om) and optical ganglia (og); (**H**) fat body (fb); and (**I**) spermatheca, which contains the spermathecal epithelia (se), reservoir lumen (rl), and sperm (arrow). All sections were

counterstained with hematoxylin (blue) to reveal overall tissue structure. Scale bars: (A) = 200 μm, (B-D and F-I) = 25 μm, and (E) = 50 μm.

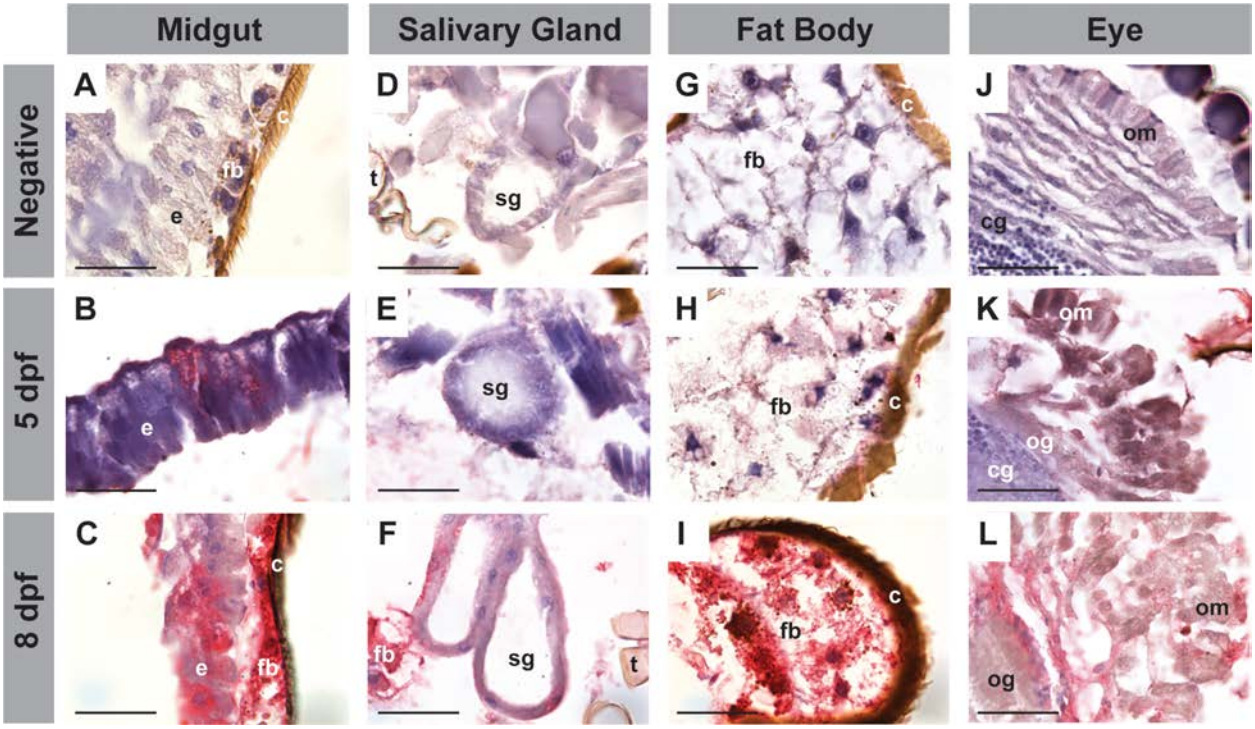

Figure 4.2 EHDV-2 postitive staining pattern in *C. sonorensis* by IHC over the course of infection.

Increasing intensity of IHC staining (red) showing progression of EHDV-2 infection in tissues over time, with representative images taken at 5 dpf (**B, E, H,** and **K**) and 8 dpf (**C, F, I,** and **L**), compared to negative controls tissues (**A, D, G,** and **J**). This increase was observed in all infected tissues: (**A-C**) the midgut [midgut epithelium (e), fat body (fb), cuticle (c)]; (**D-F**) salivary glands (sg), [trachea (t)]; (**G-I**) fat body (fb); and (**J-L**) eye containing the ommatidia (om) and optic ganglia (og) [cerebral ganglia (cg)]. All sections were counterstained with hematoxylin (blue) to reveal overall tissue structure. Scale bars = 25 μm.

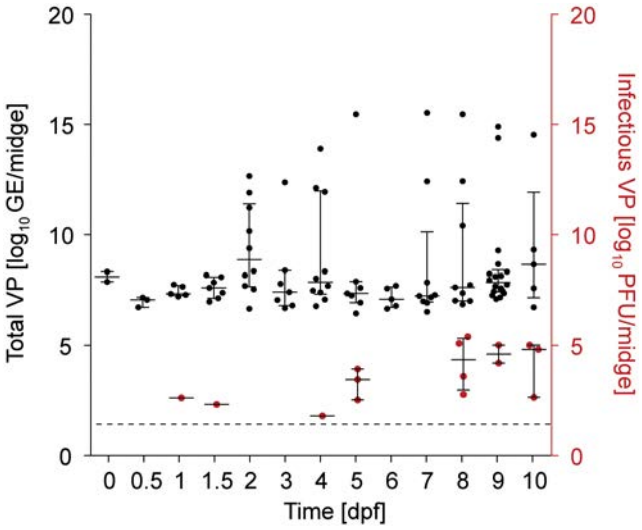

Figure 4.3 Whole body viral titer over the course of EHDV-2 infection within *C. sonorensis*

Graph depicts the viral load per midge over the infection time course. Total VPs (black), were estimated by calculating genome equivalents (GE) by qPCR, and infectious VPs (red with $10^{1.39}$ PFU/midge limit of detection: dotted line) were calculated by plaque assay. All samples are represented as median and interquartile range. Corresponding raw values are presented in Table 1.

Chapter 5 - Conclusions

This chapter provides an overview of the major findings of this dissertation which contributed critical information to our understanding of host-pathogen interactions within *Culicoides sonorensis.* The following sections highlight these major findings in the context of the current literature and give a brief outlook on the future studies focusing on vector-virus interactions of *C. sonorensis* that are now enabled by this research. The work presented in this dissertation was completed to (**A**) establish the function and utilization of RNAi in *Culicoides sonorensis* adults and (**B**) determine the infection dynamics of epizootic hemorrhagic disease virus serotype 2 (EHDV-2) in *C. sonorensis*.

A. Establishing the function and utilization of RNAi in *C. sonorensis* adults

Molecular and functional studies in vector biology were revolutionized by genomic and RNA interference (RNAi) technologies. Using RNAi as a molecular tool, studies were able to evaluate the contributions of molecular pathways to host-pathogen interactions, such as the apoptotic and RNAi pathways. In addition, epistatic analyses can be completed to determine gene interactions and pathway regulators (Phillips 2008). RNAi has been used in multiple non-model, vector species for targeted gene knockdown (Brown et al. 1999, Blandin et al. 2002, Sant'Anna et al. 2009). However, research on *C. sonorensis*, an important vector of economically important orbiviruses (Mellor et al. 2000), has been hindered due to the difficulty of culturing certain species and the absence of molecular tools, such as RNAi (Nayduch et al. 2014a). A previous study revealed RNAi could function as an antiviral pathway in a *Culicoides*

cell line (Schnettler et al. 2013), indicating that *Culicodies* have the molecular machinery required for this pathway to be induced.

The work in Chapter 2 hypothesized that RNAi was inducible with an external dsRNA trigger in adult *C. sonorensis* and further confirmed the RNAi knockdown of target transcripts by phenotype and relative transcript abundance. The *C. sonorensis* ortholog to *inhibitor of apoptosis 1* (*CsIAP1*) was chosen as the target transcript for knockdown in the midge, after identification through phylogenic and protein domain analyses. Similar to previous studies of increased mortality after RNAi knockdown of *IAP1* in other insect species (Hay et al. 1995, Allen and Walker 2012, Wang et al. 2012), injection of double-stranded RNA (dsRNA) to *CsIAP1* (ds*CsIAP1*) resulted in increased mortality in adult midges, when compared to controls. Further, ds*CsIAP1*-injected midges had a significantly decreased median survival, with a statistically significant increase of daily mortality observed at 2 days post ds*CsIAP1* injection. This increased mortality phenotype correlated with a 33% decrease in *CsIAP1* transcript levels at 5 days post ds*CsIAP1*-injection, confirming RNAi is inducible within the adult *C. sonorensis* midge by injection of an exogenous dsRNA trigger into the hemolymph.

Building on the work from Chapter 2, experiments in Chapter 3 tested the hypothesis that RNAi could be used for (1) single knockdown of *CsIAP1* in the midgut and (2) double knockdown.of both *CsIAP1* and the *C. sonorensis* Dronc ortholog (*CsDRONC*). Injection of ds*CsIAP1* into adult midges resulted in higher reduction of *CsIAP1* transcripts in the midgut, as compared to the midge carcass, and increased caspase activity in this tissue. This increased apoptosis in the midgut resulted in a loss of midgut tissue integrity and reduction in midgut size, which also observed after IAP1 knockdown in *Aedes aegypti* mosquitoes (Wang et al. 2012). Wang et al. (2012) also observed double knockdown of both the initiator caspase, Dronc, and

IAP1 orthologs in *A. aegypti* mosquitoes resulted in rescue of the increased morality phenotype (Wang et al. 2012). Similarly, these longevity and altered midgut phenotypes were partially rescued after co-injection of dsRNA specific to the *CsIAP1* and *CsDRONC*, identified through phylogenetic analyses. Of note, the total concentration of ds*CsIAP1* injected had to be reduced during the double knockdown experiments, which resulted in the dampening of the intensity of the increased mortality phenotype. Similar to observations in mosquitoes, these data suggest that RNAi in the midge is dose-dependent (Boisson et al. 2006, Meleshkevitch et al. 2013). Overall, the work in Chapter 3 supported the hypothesis that RNAi functional in the *C. sonorensis* midgut and can be used to simultaneously knockdown multiple transcripts. The proper function of the RNAi pathway within the midge midgut suggests that RNAi response may contribute to the midgut barrier in non-permissible infections, as the RNAi pathway has been confirmed as an important antiviral response within insects, such as mosquitoes (Cirimotich et al. 2009, Brachney et al. 2009, Morazzani et al. 2012).

Together, the work from Chapter 2 and Chapter 3 are the first to provide biological insights into both the apoptosis and RNAi pathways. These experiments confirmed the functional orthologs of IAP1 and Dronc in *C. sonorensis*, demonstrating the conserved nature of this pathway. This work provides confirmed apoptotic pathway members as targets for later RNAi experiments focusing on determining the importance of the apoptosis in orbivirus infection, as programmed cell death was confirmed as a crucial antiviral pathway in insects (Griard et al. 2007, Ocampo et al. 2015). In addition, the work from these chapters demonstrated that *C. sonorensis* uses environmental RNAi, as the RNAi pathway was induces after the exogenous dsRNA trigger was provided into the hemolymph, similar to other dipteran vectors (Blandin et al. 2002, Sant-Anna et al. 2009).

The efficacy of the dsRNA trigger to induce RNAi in *C. sonorensis* was dose dependent and varied across different tissues. Similar observations have been made in mosquitoes and other insects (Boisson et al. 2006, Lycette et al. 2006, Meleshkevitch et al. 2013). Several mechanisms behind these observations have been proposed, including dsRNAases within the hemolymph, differential uptake of the dsRNA trigger by different cell types, or the differential processing of the dsRNA trigger (Wang et al. 2016, Shukla et al. 2016). While these trends have been observed in previous studies, the exact mechanism behind these differences remains unclear and should be addressed in future studies.

The experiments in Chapter 2 and Chapter 3 also provide RNAi as a molecular tool to increase our understanding of midge biology and vector-virus relationships. RNAi can now be used to determine the relative contribution of immune pathways outlined from the midge transcriptome as antiviral defenses at the midgut during non-permissive and permissive orbivirus infections in *C. sonorensis* (Nayduch et al. 2014b, Nayduch et al. 2014c). These pathways may be probed using single or double knockdown experiments. Since double knockdown experiments can be used for epistatic analyses in the midge, these experiments would allow the direct testing of the relationships between phenotypes and their causal pathways (Phillips 2008). The ability to induce RNAi for targeted gene knockdown in the *C. sonorensis* life stage (adult) and tissue (midgut), which are critical to the vector competence of the midge, solved a serious bottleneck in *C. sonorensis* research.

B. Determining the infection dynamics of EHDV-2 in *C. sonorensis*

Understanding infection dynamics and vector biology are critical for adequate preparation against vector-borne disease outbreaks through the use of epidemiological modeling

(Brand et al. 2016). Specifically, infection dynamic studies provide important information, such as the pathogen extrinsic incubation period (EIP), number of infected vectors in a population (infection prevalence), and/or viral tissue tropism, which determine the probability of pathogen transmission by the vector population at a given time. EIP, the time it takes a vector to become infectious after feeding on an infected individual, is a major concern, as short EIPs result in earlier virus transmissibility in a larger proportion of the vector population. While epidemiological modeling (Brand et al. 2016) and infection dynamic studies within *C. sonorensis* (Fu et al. 1999, Veronesi et al. 2013, Ballinger et al. 1985) have been completed on the orbivirus, bluetongue virus (BTV), only limited data were available on the EHDV infection time course within the midge (Ruder et al. 2015a). While EHDV causes serve mortality in white tailed deer populations (Savini et al. 2011, Ruder et al. 2015b, Stevens et al. 2015), EHDV EIP and infection prevalence thus far has been based on viral load data (Ruder et al. 2015a). As EHDV-2 is one of the three EHDV serotypes present in the US (Shope et al. 1955, Chalmers et al. 1964, Barber and Jochim 1976, Allison et al. 2010), it is important to understand infection dynamics of this virus within the vector, *C. sonorensis.*

EHDV-2 infection dynamics recorded in Chapter 4 provided the infection prevalence, EIP, and route of transmission for this virus within *C. sonorensis.* Approximately 50% of *C. sonorensis* midges were positive for EHDV-2 by 10 dpf, indicating only half of the exposed midge population are likely to develop a permissive EHDV-2 infection, similar to previously reported data (Ruder et al. 2015a). Regardless of the percentage infected and/or infective, IHC and titer experiments determined that the EIP for EHDV-2 in *C. sonorensis* was as short as 5 d. *C. sonorensis* could survive to transmit EHVD-2 during multiple blood meals due to their maximum lifespan varying between 28 d at 30°C to 84 d at 10°C when reared under laboratory

conditions (Lysyk et al. 2007, Mullens and Schmidtmann et al. 1982). In addition, IHC also confirmed the lack of vertical transmission of EHDV-2 by *C. sonorensis*, as EHDV-2 was limited to the somatic cells of the ovarian sheath and spermathecal epithelia. Similarly, vertical transmission was not observed during BTV infection within the midge (Jones and Foster 1971, Chandler et al. 1985, Nunamaker et al. 1990, Osborne et al. 2015). These data confirm that only horizontal transmission is possible by *C. sonorensis*, which limit the potentially infected vectors to those which blood feed on an infected host.

The IHC experiments in Chapter 4 also provided insights into EHDV-2 tissue tropism, including the infection of sensory and reproductive tissues. The loss of ommatidia architecture was solely associated with EHDV-2 infection, suggesting the orbivirus-associated behavioral changes observed by McDermott et al. (2015) may be due to pathological effects caused by orbivirus infection of the ommatidia. While, EHDV-2 infection of the Johnston's organ was not associated with pathology, infection of this tissue could also play a role in these behavioral changes (McDermott et al. 2015), as BTV also infected the Johnston's organ (Fu et al. 1999). These behavioral changes could limit or enhance the probability of transmission by affecting the detection of hosts by the infected vector. If EHDV-2 infection is confirmed to affect midge behavior, *Culicoides* surveying techniques must be updated to ensure the proper sampling of orbivirus-infected midges, which would provide more accurate data for the modeling of and preparation for potential orbivirus outbreaks. In addition, these experiments were the first to observed orbivirus staining within the spermathecal epithelium, which is responsible for sperm health (Degner and Harrington 2016).

These experiments also revealed time points critical for EHDV-2 infection establishment within *C. sonorensis,* which coincided important viral bottlenecks during infection. The findings

from Chapter 4, in addition to studies reporting BTV beyond the midge midgut by 3 dpf (Fu et al. 1999, Sieburth et al. 1991), identified the time points between 2-5 dpf as critical to orbivirus infection establishment. These time points span the (1) infection of the midgut, (2) viral dissemination into secondary tissues, and (3) infection of the salivary glands, allowing for the focused study of *Culicoides*-EHDV-2 interactions. Furthermore, observations that the hemolymph is the route of EHDV-2 dissemination to secondary tissues throughout the midge support the midgut as a key barrier to orbivirus infection within *C. sonorensis.* These data confirm the importance of studying the midgut and provide the time points that should be focused on to determine vector-virus interactions within *C. sonorensis.*

Future directions

The work within this dissertation provides a foundation for the study of orbivirus interactions within *C. sonorensis.* By utilizing the putative orthologs of antiviral pathways reviewed in Chapter 1, the RNAi protocols developed in Chapters 2 and 3, and the time points during EHDV-2 infection identified in Chapter 4, future *Culicoides* studies can probe specific immune pathways to determine their role during orbivirus infection.

Future experiments should determine the role of the RNAi pathway as an antiviral defense against orbivirus infection within the midge. Work completed by Schnettler et al. (2013a) *in vitro* demonstrated that the RNAi pathway could be induced after addition of an exogenous dsRNA trigger specific to a viral genome segment. In addition, previous studies have confirmed the antiviral function of the RNAi pathway *in vivo* through the knockdown of RNAi pathway members (Keene et al. 2004, Sanchez-Vargas et al. 2009, Franz et a. 2006). Future *in vivo* studies should be completed to determine if the RNAi pathway recognizes and limits

EHDV-2 infection within *C. sonorensis* through the knockdown of RNAi pathway members, such as Arognaute 2 or Dicer 2, using RNAi methodology outlined in this dissertation. If the RNAi pathway acts as an antiviral defense against EHDV-2, RNAi knockdown of RNAi pathway member(s) would result in an increase in overall EHDV-2 infection prevalence and/or in the increase of EHDV-2 titer. In contrast, if the knockdown of midge RNAi pathway member(s) led to no change in titer or prevalence, this pathway is likely not induced during EHDV-2 infection. These experiments would be of great interest, as orbiviruses are thought to "hide" their dsRNA genome segments to avoid detection by the RNAi pathway (Diprose et al. 2001, Diprose et al. 2002, Patel and Roy 2014). To verify if EHDV-2 inhibits or "hides" from the RNAi pathway, future studies may also provide exogenous dsRNA to a viral genome segment, such as nonstructural protein 1. If there is no RNAi response is induced upon introduction of the viral dsRNA trigger, as noted by no change in titer and/or infection prevalence, EHDV-2 likely inhibits the RNAi pathway.

Additional studies may focus on the role of apoptosis during EHDV-2 infections by monitoring for active caspases during both permissive and non-permissive infections. The techniques developed in this dissertation could be used to identify the presence or absence of apoptosis throughout orbivirus infection (Mills et al. 2017a, Mills et al. 2017b), as previous work observed increased apoptosis associated with decreased transmission (Griard et al. 2007). Increased caspase activity at the primary site of infection or the salivary glands during orbivirus infection with *Culicoides* species considered "poor-vectors," such as *Culicoides nubeculosus* (Jennings and Mellor 1988), could provide the first indication that apoptosis serves as a natural antiviral defense. Previous work confirmed that apoptosis was a crucial antiviral defense against DENV within the mosquito, through the RNAi knockdown of the *Aedes* Dronc ortholog during

DENV infection, which resulted in increased infection prevalence in the refractory mosquito colony (Ocampo et al. 2013). Future studies can also knockdown *CsDRONC* and/or *CsIAP1* to further confirm if apoptosis is able to limit orbivirus infection within the midge. If apoptosis were used as an antiviral response against EHDV-2, knockdown of *CsIAP1* would result in a reduction in EHDV-2 infection prevalence and/or titer. In contrast, knockdown of *CsDRONC* should result in increased EHDV-2 titer and/or infection rates. The techniques and observations documented in this dissertation will allow future work to determine and confirm the role these pathways play during EHDV-2 infection.

Furthermore, studies should be completed to understanding the potential effects of EHDV-2 infection on sensory and reproductive tissues of *C. sonorensis*. McDermott et al. (2015) demonstrated that BTV-positive midges had an aversion to UV light, which is currently used, along with CO_2, to collect *Culicoides* midges. Future studies are needed to determine if EHDV-2 infection results in changes in midge behavior, as these changes could alter the perception and/or detection of the host by the infected vector. These studies should test if UV light and or CO_2 deter EHDV-2 infected midges. Since these UV light and CO_2 are associated with typical *Culicoides* traps, the data generated from these studies would be critical for proper surveillance of midges. Follow-up studies are also necessary to determine if BTV also infects the spermathecal epithelia to confirm if this tissue tropism is EHDV-2- or orbivirus-specific. Additional studies are also needed to determine if EHDV-2 infection lowers the reproductive output of *C. sonorensis* through infection of the spermathecal epithelia. Such studies should monitor the success of eggs laid and hatched, as these data should be added to orbivirus infection models to better predict the potential transmission frequency in an infected area.

Together, the work in this dissertation allow the field of midge vector biology to take a large step forward. The development of RNAi as a molecular tool provides the field a means to assess the importance of pathways involved in both midge biology and vector-virus interactions. Finally, this dissertation provided critical data that allow for more precise quantification of EHDV-2 transmission by *C. sonorensis* in the field.

References

Allen, M. L., and W. B. Walker. **2012**. Saliva of *Lygus lineolaris* digests double stranded ribonucleic acids. J. Insect Physiol. 58: 391–396.

Allison, A. B., V. H. Goekjian, A. C. Potgieter, W. C. Wilson, D. J. Johnson, P. P. C. Mertens, and D. E. Stallknecht. **2010**. Detection of a novel reassortant epizootic hemorrhagic disease virus (EHDV) in the USA containing RNA segments derived from both exotic (EHDV-6) and endemic (EHDV-2) serotypes. J. Gen. Virol. 91: 430–439.

Ballinger, M. E., R. H. Jones, and B. J. Beaty. **1987**. The comparative virogenesis of three serotypes of bluetongue virus in *Culicoides variipennis* (Diptera: Ceratopogonidae). J. Med. Entomol. 24: 61–65.

Barber, T. L., and M. M. Jochim. **1976**. Serotyping bluetongue and epizootic hemorrhagic disease virus strains. Proc. Am. Assoc. Vet. Lab. Diagn. 18: 149–157.

Blandin, S., L. F. Moita, T. Köcher, M. Wilm, F. C. Kafatos, and E. A. Levashina. **2002**. Reverse genetics in the mosquito *Anopheles gambiae*: targeted disruption of the *Defensin* gene. EMBO Rep. 3: 852–856.

Boisson, B., Jacques, J. C., Choumet, V., Martin, E., Xu, J., Vernick, K., and C. Bourgouin. 2006. Gene silencing in mosquito salivary glands by RNAi. FEBS Letters. 580: 1988-1992.

Brackney, D. E., Beane, J. E., and G. D. Ebel. 2009. RNAi targeting of west nile virus in mosquito midguts promotes virus diversification. PLoS Patho. 5: e1000502.

Brand, S.P.C., Rock, K.S., and M. J. Keeling. 2016. The interaction between vector life history and short vector life in vector-borne disease transmission and control. PLoS Comp. 4: 1-21.

Brown, S. J., J. P. Mahaffey, M. D. Lorenzen, R. E. Denell, and J. W. Mahaffey. **1999**. Using RNAi to investigate orthologous homeotic gene function during development of distantly related insects. Evol. Dev. 1: 11–5.

Chalmers, G. A., H. N. Vance, and G. J. Mitchell. **1964**. An outbreak of epizootic hemorrhagic disease in wild ungulates in Alberta. Wildl. Dis. 42: 1–6.

Chandler, L. J., M. E. Ballinger, R. H. Jones, and B. J. Beaty. **1985**. The virogenesis of bluetongue virus in *Culicoides variipenis*. Prog. Clin. Biol. Res. 178: 245–253.

Cirimotich, C. M., Scott, J. C., Phillips, A. T., Geiss, B. J., and K. E. Olson. 2009. Suppression of RNA interference increases alphavirus replication and virus-associated mortality in *Aedes aegypti* mosquitoes. B. M. C. Microbiol. 9: 1-13.

Degner, E. C., and L. C. Harrington. **2016**. A mosquito sperm's journey from male ejaculate to egg: Mechanisms, molecules, and methods for exploration. Mol. Reprod. Dev. 83: 897–911.

Diprose, J. M., J. N. Burroughs, G. C. Sutton, A. Goldsmith, P. Gouet, R. Malby, I. Overton, S. Zintara, P. P. C. Mertens, D. I. Stuart, and J. M. Grimes. **2001**. Translocation portals for the substrates and products of a viral transcription complex: the bluetongue virus core. EMBO J. 20: 7229–7239.

Diprose, J. M., J. M. Grimes, G. C. Sutton, J. N. Burroughs, A. Meyer, S. Maan, P. P. Mertens, and D. I. Stuart. **2002**. The core of bluetongue virus binds double-stranded RNA. J. Virol. 76: 9533–9536.

Franz, A. W. E., Sanchez-Vargas, I., Piper, J., Smith, M. R., James, A. A., and K. E. Olson. 2009. Stability and loss of a virus resistance phenotype over time in transgenic mosquitoes harbouring an antiviral effector gene. Insect. Molec. Biol. 5: 661-672.

Fu, H., C. J. Leake, P. P. Mertens, and P. S. Mellor. **1999**. The barriers to bluetongue virus infection, dissemination and transmission in the vector, *Culicoides variipennis* (Diptera: Ceratopogonidae). Arch. Virol. 144: 747–61.

Girard, Y. A., B. S. Schneider, C. E. McGee, J. Wen, V. C. Han, V. Popov, P. W. Mason, and S. Higgs. **2007**. Salivary gland morphology and virus transmission during long-term cytopathologic west nile virus infection in *Culex* mosquitoes. Am. J. Trop. Med. Hyg. 76: 118–128.

Hay, B. A., D. A. Wassarman, and G. M. Rubin. **1995**. *Drosophila* homologs of baculovirus inhibitor of apoptosis proteins function to block cell death. Cell. 83: 1253–1262.

Jennings, D. M. and P. S. Mellor. 1988. The vector potential of British *Culicoides* species for bluetongue virus. Vet. Microbiol. 17: 1-10.

Jones, R., and N. Foster. **1971**. Transovarian transmission of bluetongue virus unlikely for *Culicoides sonorensis*. Mosq. News. 31: 434–437.

Keene, K. M., Foy, B. D., Sanchez-Vargas, I., Beaty, B. J., Blair, C. D., and K. E. Olson. 2004. RNA interference acts as a natural antiviral response to O'nyong-nyong virus (Alphavirus; Togaviridae) infection of *Anopheles gambiae.* Proc. Natl. Acad. Sci. U. S. A. 101: 17240-17245.

Lycett, G. J., McLaughlin, L. A., Ranson, H., Hemingway, J., Kafatos, F. C., Loukeris, T. G., and M. J. I. Paine. 2006 *Anopheles gambiae* P450 reductase is highly expressed in oenocytes and in vivo knockdown increases permethrin susceptibility. Insect Mol. Biol. 3: 321-327.

Lysyk, T. J., and T. Danyk. **2007**. Effect of temperature on life history parameters of adult *Culicoides sonorensis* (Diptera: Ceratopogonidae) in relation to geographic origin and vectorial capacity for bluetongue virus. J. Med. Entomol. 44: 741–751.

McDermott, E. G., C. E. Mayo, A. C. Gerry, D. Laudier, N. J. MacLachlan, and B. A. Mullens. **2015**. Bluetongue virus infection creates light averse *Culicoides* vectors and serious errors in transmission risk estimates. Parasit. Vectors. 8: 2–9.

Meleshkevitch, E. A., Voronov, D., Miller, M., Penneda, M., Fox, J., Metzler, R., and Y. B. Dmitri. 2013. A novel eukaryotic Na+ Methionine selective symporter is essential for mosquito development. Insect Biochem. Mol. Biol. 43: 755-767.

Mellor, P. S. 1990. The replication of bluetongue virus in *Culicoides* vectors. Curr. Top. Microbiol. Immunol. 162: 143–161.

Mellor, P. S., J. Boorman, and M. Baylis. **2000**. *Culicoides* biting midges: their role as arbovirus vectors. Annu. Rev. Entomol. 45: 307–340.

Mills, M. K., Michel, K., Pfannenstiel, R. S., Ruder, M. G., Veronesi, E., and D. Nayduch 2017a. *Culicoides* – virus interactions: infection barriers and possible factors underlying vector competence. Curr. Opin. Insect Science. 22: 7-15.

Mills, M. K,. Nayduch, D., Mcvey, D. S., and K. Michel. 2017b. Functional validation of apoptosis genes *IAP1* and *DRONC* in midgut tissue of the biting midge *Culicoides sonorensis* (Diptera: Ceratopogonidae) by RNAi. J. Med. Entomol. 54: 559-567.

Morazzani, E. M., Wiley, M. R., Murreddu, M. G., Adelman, Z. N., and K. M. Myles. 2012. Production of virus-derived ping-pong-dependent piRNA-like small RNAs in the mosquito

soma. PLoS Patho. 8: e1002470.

Mullens, B. A. and E. T. Schmidtmann. 1982. The gonotrophic cycle of *Culicoides variipennis* (Diptera: Ceratopogonidae) and its implications in age-grading field populations in New York State, USA. J. Med. Entomol. 19: 340-349.

Nayduch, D., L. W. Cohnstaedt, C. Saski, D. Lawson, P. Kersey, M. Fife, and S. Carpenter. **2014a**. Studying *Culicoides* vectors of BTV in the post-genomic era: resources, bottlenecks to progress and future directions. Virus Res. 182: 43–49.

Nayduch, D., M. B. Lee, and C. A. Saski. **2014b**. The reference transcriptome of the adult female biting midge (*Culicoides sonorensis*) and differential gene expression profiling during teneral, blood, and sucrose feeding conditions. PLoS One. 9: e98123.

Nayduch, D., M. B. Lee, and C. A. Saski. 2014c. Gene discovery and differential expression analysis of humoral immune response elements in female *Culicoides sonorensis* (Diptera: Ceratopogonidae). Parasit. Vectors. 7: 388-405.

Nunamaker, R. A., P. J. Sieburth, V. C. Dean, J. G. Wigington, C. E. Nunamaker, and J. O. Mecham. **1990**. Abscence of transovarial transmission of bluetongue virus in *Culicoides variipennis*: immunogold labeling of bluetongue virus antigen in developing oocytes from *Culicoides variipennis* (Coquillett). Comp. Biochem. Physiol. 96: 19–31.

Ocampo, C. B., P. A. Caicedo, G. Jaramillo, R. Ursic Bedoya, O. Baron, I. M. Serrato, D. M. Cooper, and C. Lowenberger. **2013**. Differential expression of apoptosis related genes in selected strains of *Aedes aegypti* with different susceptibilities to dengue virus. PLoS One. 8: e61187.

Osborne, C. J., C. E. Mayo, B. A. Mullens, E. G. McDermott, A. C. Gerry, W. K. Reisen, and N. J. Maclachlan. **2015**. Lack of evidence for laboratory and natural vertical transmission of bluetongue virus in *Culicoides sonorensis* (Diptera: Ceratopogonidae). J. Med. Entomol. 52: 274–277**.**

Patel, A., and P. Roy. **2014**. The molecular biology of bluetongue virus replication. Virus Res. 182: 5–20.

Phillips, P. C. 2008. Epistasis—the essential role of gene interactions in the structure and evolution of genetic systems. Nat. Rev. Genetics, 9: 855-867..

Ruder, M. G., D. E. Stallknecht, E. W. Howerth, D. L. Carter, R. S. Pfannenstiel, A. B. Allison, and D. G. Mead. **2015a**. Effect of temperature on replication of epizootic hemorrhagic disease viruses in *Culicoides sonorensis* (Diptera: Ceratopogonidae). J. Med. Entomol. 52: 1050–1059.

Ruder, M. G., T. J. Lysyk, D. E. Stallknecht, L. D. Foil, D. J. Johnson, C. C. Chase, D. A. Dargatz, and E. P. J. Gibbs. **2015b**. Transmission and epidemiology of bluetongue and epizootic hemorrhagic disease in North America: current perspectives, research gaps, and future Directions. Vector-Borne Zoonotic Dis. 15: 348–363.

Sánchez-Vargas, I., Scott, J. C., Poole-Smith, B. K., Franz, A. W., Barbosa-Solomieu, V., Wilusz, J., Olson, K. E., and C. D. Blair. 2009. Dengue virus type 2 infections of *Aedes aegypti* are modulated by the mosquito's RNA interference pathway. PLoS Patho. 5: e1000299.

Sant'Anna, M. R., H. Diaz-Albiter, M. Mubaraki, R. J. Dillon, and P. a Bates. **2009**. Inhibition of trypsin expression in *Lutzomyia longipalpis* using RNAi enhances the survival of *Leishmania*. Parasit. Vectors. 2: 62.

Savini, G., A. Afonso, P. Mellor, I. Aradaib, H. Yadin, M. Sanaa, W. Wilson, F. Monaco, and M. Domingo. **2011**. Epizootic heamorragic disease. Res. Vet. Sci. 91: 1–17.

Schnettler, E., M. Ratinier, M. Watson, A. E. Shaw, M. McFarlane, M. Varela, R. M. Elliott, M. Palmarini, and A. Kohl. **2013**. RNA interference targets arbovirus replication in *Culicoides* cells. J. Virol. 87: 2441–2454.

Shope, R. E., L. G. MacNamara, and R. Mangold. **1955**. Report on the deer mortality, epizootic hemorrhagic disease of deer. New Jersey outdoors. 6: 17–21.

Shukla, J. N., Kalsi, M., Sethi, A., Narva, K. E., Fishilevich, E., Singh, S., Mogilicherla, K., and S. R. Palli. 2016. Reduced stability and intracellular transport of dsRNA contribute to poor RNAi response in lepidopteran insects. RNA Biol. 13: 656-669.

Sieburth, P. J., C. E. Nunamaker, J. Ellis, and R. A. Nunamaker. **1991**. Infection of the midgut of *Culicoides variipennis* (Diptera: Ceratopogonidae) with bluetongue virus. J. Med. Entomol. 28: 74–85.

Stevens, G., B. McCluskey, A. King, E. O'Hearn, and G. Mayr. **2015**. Review of the 2012 epizootic hemorrhagic disease outbreak in domestic ruminants in the United States. PLoS One. 10: 1–11.

Veronesi, E., F. Antony, S. Gubbins, N. Golding, A. Blackwell, P. P. Mertens, J. Brownlie, K. E. Darpel, P. S. Mellor, and S. Carpenter. **2013**. Measurement of the infection and dissemination of bluetongue virus in *Culicoides* biting midges using a semi-quantitative rt-PCR assay and isolation of infectious virus. PLoS One. 8: e70800.

Wang, H., T. Gort, D. L. Boyle, and R. J. Clem. **2012**. Effects of manipulating apoptosis on Sindbis virus infection of *Aedes aegypti* mosquitoes. J. Virol. 86: 6546–6554.

Wang, K, Peng, Y., Pu, J., Fu, W., Wang, J., and Z. Han. 2016. Variation in RNAi efficacy among insect species is attributable to dsRNA degradation in vivo. Insect. Biochem. Molec. Biol. 77: 1-9.

Appendix A - Supplemental data for Chapter 2

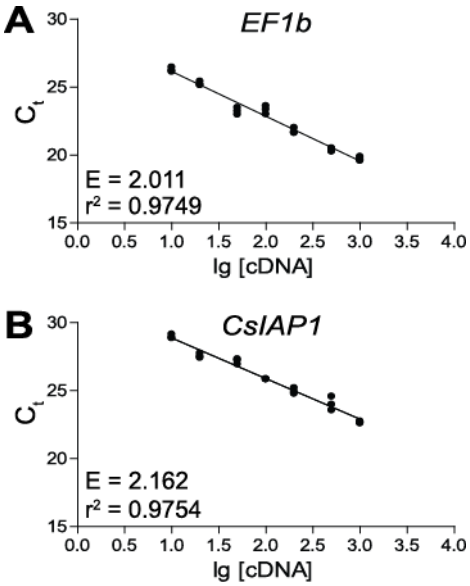

Figure A.5.1 Primer efficiencies for qRT-PCR analysis

(**A-B**) Primer efficiencies measured using dilutions of the cDNA stock for qRT-PCR analysis. Graphs show lg values for the dilution ratio plotted against Ct values for the reference gene, *EF1b* (**A**), and the gene of interest, *CsIAP1* (**B**).r^2, goodness of fit; E, calculated primer efficiency.

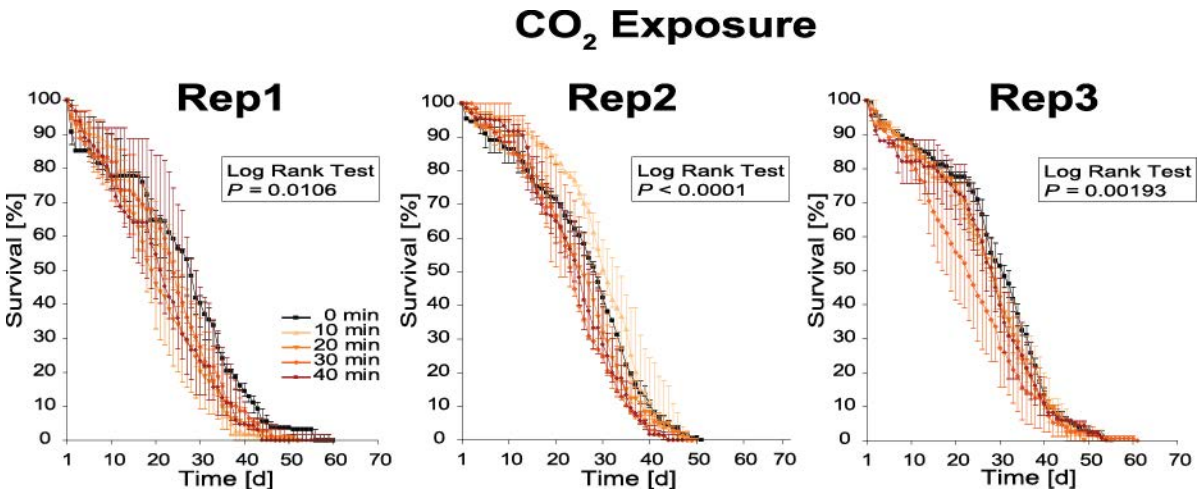

Figure A.5.2 Survival analysis of female midges after CO_2 exposure

(**Rep1-3**) Individual biological replicates of CO_2 exposure shown in Figure 1B-C. Survival curves of midges after exposure to CO_2 at indicated time intervals are presented as mean ± range of two technical replicates within each biological replicate (n=50 per technical replicate). Statistical significant differences between survival curves was assessed by Log Rank Test, resulting *P* values are indicated in figure.

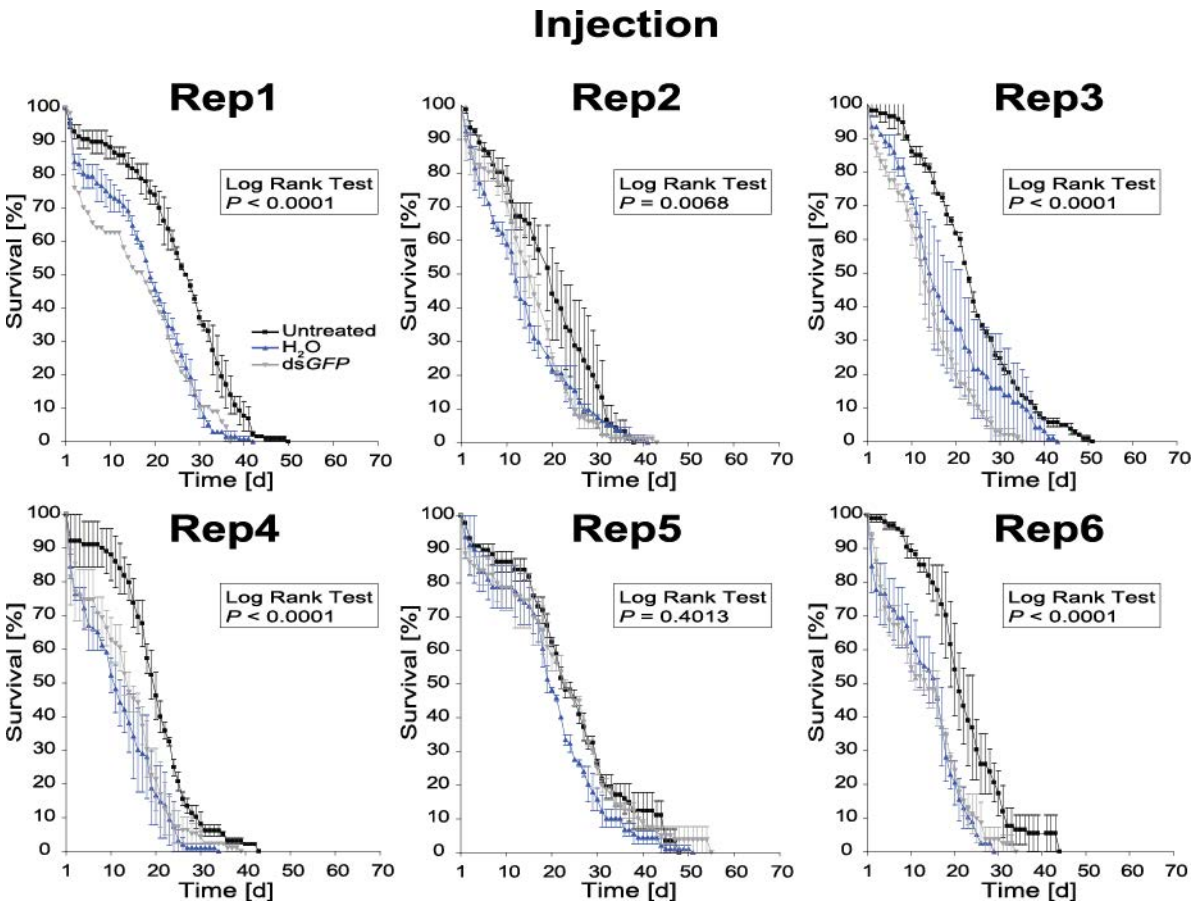

Figure A.5.3 Survival analysis of female midges after intrathorasic injection

(**Rep1-6**) Individual biological replicates of survival curves after no, H_2O, or ds*GFP* injection shown in Figure 1E-F. Survival curves are presented as mean ± range of two technical replicates for each biological replicate (n=50 per technical replicate). Statistical significant differences between survival curves was assessed by Log Rank Test, resulting *P* values are indicated in figure.

>GAWM01016583_CsIAP6

NNNMADAKYLKEDDYLNVSEDTCNIIYHPTLNVILLFTKSGDVKVLDVNSGLILHSCSLLVDNQLPKAKFLPEQEKV

LFWNNATLGLRGDYNGVLLLDTILQTPIVQADDTIRLELLLSEAMLFLQSIQSLEQQGLENTADVTNELLLKIEQAR

QNNKKGIKAQRWETICLELPHSSIKMVASSVALTLKRLGRQIPALAIASAINERLTDLIVGGRVVDSENVQRFHMYS

EAARRQTFEQWPHMDYKWALPDQMAQAGFYHQPGESGGDRAMCFTCNVCLVCWEKTDEPWSEHERHSPDCAFVKGEY

TQNVPLTVTYATNPAAATNRFTIISNGYQTNIICTGNRVAEVNVWNIERQLQKVHQFNIDTQAIQQKFDMANCKHDI

ELTALSTYCVISGGKNGQGNTGAMKKHVSLSSKAKMLGSKIVAGVSVVRQIDQMEQNSENCDIEKKLLLIVYQLKDI

SDKNNSNKQETSNTATKKSSSSTLSTIEERFEDDEFMKFLASETDLQQLQLLEDYIDNIDTTTSSEKIAELACKNLF

STNSSSNVSNEESKNDDQKISKLKAFNHMSNPSKWAWSQNDSIASSTSSTVTVASSKQEQNINPENYKSVSIASEKM

TSVMNCGSQIQSSPVQFVSVVPFLSDDYEIDEIIPSCDTKFLLVVLRRCTQLEGTSFADDDMETDIPKDNSNVQLIL

YSIEENGMLDEVAVCVRILEEKDSPLEFCMLPKYEGKRRVFEGPDTENGIFAMTCVDGSLKIISLSSLKTISEAKVD

TGNFVSVTYCKSLERICACTDKGSLHFYSFYEFDADSSDDRDDDQCFSNLITDPLTAMGRCSKSNIIYDAMPSTSSQ

TPLAQGNKQETELIAYKNNLTLNDLKILYSLTLFEELPLTYNAEVPGCWSELIQAQKQRRHPNHLRPGDDSNLTRTW

RLHNDATTWDEHLIELNVPKSVTQTIGHIDFKFSLYQPCTNPPAIQVTLLKQKSLGICSRRKIGSKSFDENSDMNSG

CSDNKDSCENPVLSDEFLQARSAEILRLETYQNWPVSFIQPADLARAGFYYINRSDQVKCAWCQRVIGEWEVLDDPV

TEHLKFSPACQKARVGPIELSSCMDLSEQGGVVTLTSPKLLKTKSRNFLLHIKTVADMSKDGQGKTRGCDWLHEISI

TVRAAKHIHKVPNERIQRLVMLESNQLLDNLLKLVATDQRMLMQNLAFDILNWISSIRLMRYRSPIPTMCKWSAKNA

AKNPNSAALDPNEQQNECAMIIGNNLGEIVKNCMVLNNRSIAHKCSKLILASLDGAQNLLHADICQAFEEKLKMAIV

NALPHMIRCEHAGALKWFTLLISGTSALDSQNEISEQSIKLLIEIAGEMVHRYNPLGLLLRSRFGLYGLPFEPELFD

AELPNLSKSGNLIYTYVPATKPGIQVGNQPMDLKSFCVSDGSELRVLPFQLRRKGIGSHFKGALEVEPLHFICTGTS

EATRLENTDSAMVQSGHIIDDIMLETPINNLDSGTAMTSGGGSKKETGDKENLDDDMMNNVKNILVDKIIYSAIKKN

KLKEEIKEAAKSFDLEVSVLSGYNEPDTNDEWGPPEPRVVFLTNNSANNENSDGISEDTTTTSASLTNKIQEFFEES

NANEDAAFQWHKILSTPPKQTIVVDRMHSGARRYVILDFGQPTMLTDLIIPAYPDLASISIDIWCFEEEADSVRLVV

SQDIGAKSLVLSDLQPPPICRYLKITFTGRYGMTGTRCKIPMGAFFGHVVIVEKEGYADPVMKYMKNKKSNTAIQLK

VLNALFEDVHCRYCLSSSKLSEYLQPFLNNETSNMSHMQAFLNKNKESDESNQGYTKIYATYEECIYFQYQLNLIKR

VIDRIESISPNPIPMQIEHESVQTLCTDKLRVLSESLIEILLHCIISNGSNAMNDATLTALMNQNVCSLLFETIIVS

GDTHTQLATCSLLVRLCGAQPWWGDFIASNFNKLYSSKNTQIFPQDRIFFLLTYLGRKSISMGVSRTRVIDSILKAI

AELLVPLSTSVDAGLGIWPNTDLTQLSWLLLFLSVCSDDGTEKKDTATYRWDFMSGEGDMAKSRLSMCSNNSRTFSR

SFKKRYIQNKTTTTSHLPEKYYISDALNLVGNGDMLTIKQQADHLKKLQNSMKGKLQSFGDYFNEITTKKQLRAQAE

SSRAFQSTSTQSGSETPIDTDTVFDKGLKTIKTQNIIVVIRGLIGLILNMDFTCNMDLFLLTCKIIARLVIACRPSI

QLTKIITSNQLLQLLRIAVWENQQQPWAVHAISCLLQDILDADKNYKNAELDDEGMEVDAAFEREDSVLGQDACSSN

SSGGSSSVAHSSSIQLSSAGMDISSNSADSIFKPIQFHNPPPPATYTTTSYADAVKGKLPCLMECEDTEMDELLDNL

LEREKLRNKKEPVPSQAQRSSGSGLTILYRAVSSAMDARLEHGLDMSTEITLRRLTMRSSVTLFACLPQNLLQGSCT

QAVSLEPESWPSELLESWSSPEYNARVETNTMLVEAFDNIFYDLNLKETWLDLEKIMQLWLTLNGEVVEQTNGNGFG

HNAYKPKIPFGERAMNGLLKTLATSPIVKLRTWCLGFQCLIMACKPPVDLFDSSLNNTQEKVCRRMGQLLTEDVNFE

RVLVRFFSGTDRCMSSIENSRYAGPTICKLLVELFGCVASKCGCKQQLKEILMRVLMNLVEPNGAIATQQGPIDAQS

QLVKELLKYTFDKNDLGVAMNLIQHISQLVYTNIANEERIYCKKSSENGSTNNVFGSLFATVLGSESSRHCKTVTDN

TLHVSLLKLSLILIKTKIPRPGEEFPGHDDPMSDQDTINESQTDEIKAEQQGFDQISSRQKIPCFADTILQHSPTMN

RLLSSLSGCSNSSFAMLVASSLYTSCSSESKNAISEPQNVADAVFQLLIALTKTATQQQFVVKPLYDFLSSSANQAY

ALPKLQLSEPFLWFILKVLESPESVNTFAQLGGVRVLCQSLVRSNRSLINSQPSLVSMIMQHISRTSGSLQSNLTGT

IKKSNVPAVKNEEGLINFAPYCTISSDNPTAQPADVLIQNPIASHRRARTPAWTYLFYPNESHVDLTITLPAAILLK

EIQLQPHVSTLASCPSAVAVEITRDNNLGPIPISQPIATIGMTCIRLKFNQPEIATSVVIRLYRPTDSTNMGLTQIL

VLGSTTFSENANQPNGKLNEIGNSDDELQSKSSLGWLRILSQCFNVATFNAPSDPTEQNLVISQAAEVTGFLEACVS

LLSVPCPNPNYAISNLETVLLKLGLYSRDLGLQLIDSLLRQAIPQSLKHNNDAVSDLLYILCTTQDNYTRDRIETML

RWVEGMYQHGDQYALEPVSGHIKCLASVLWQAYAITLIPDLPNMITKSLFESLYKWRQSLDTDAPMQKAIDSMLCSV

CCIRPELFTILLRRMNVLVPNLSNDLSASISDDRKEDAEPMSEDTNEEWYSHLSIQDLSKLDLTSAQLNTISMACQS

PLAIQLLIDSGLPALFTSAILEFCHREMSKNGLEIESEVVETTECLTDSAKDSANRLNLNKGQVYPMVNVIKITEIL

NFFAEICAEGTMRDWLGSYEGSVFWEPLLNLLCNSKIYSNKWGNSDLTLNSVITPQPYLKLEESVINFMSKVTSCHP

KNQETFTNNLIYVIRKAERKAKTGSNQSVSSGNGYKNSISGFTRRLVLQILLESEKILVSVRSELPLQKKEQNGQLI

SHHPSKRPNSHHLLFYLSTNVKCHEVLDQCGSVYSNLLPSLPTFDGNRAGNEASGSSSAGLSSVRESRKELFEIGLG

MGLGMEFLSVAAGVTAKDKRLKEAKNQAATLKKDLFSVFKMKIDDSKSMSQISDFGQLVHNACPDFILSNDTTISQI

LAMLKANNISLSTPCINLTLVQGRKTPPCSDEIMRADDDTPPMKAADFVPLPSPLQIFSSRGGLSLLAHYLPTVYPE

TPKSQIAPMDKDKSSHQNNDWVKVEPNEEIYEDLDDTLTESSSKLPVITSVPQHSLAAFGLFLKLPAYSEVLLRDKI

KAQCLLRLILGVTGDGEGNEIYSLALSTALPTLPFEVFRQLLDSSPLTTDDGVLLRRMVIEVGAIHLVLNCLGIFTH

HTSQSYQVPGTSELQPNVKTASSSTEEPITLSDDKGHMYWAKGTGFGTGSTQQSWNVEQALLRQKSEEEHVTVLLQV

LSSYINPGDKVPSSLTDETEINYRERDELLPELPPIFLDLLQQSCLIAALSSYLRNDSVLDITRHIPLYRAILQLLR

AISLSNQLVSLLMMRQNGENRTSIATLLSNMKCCVDTYASRLRIKTKAKSVSKSGVTTINVEDGEDEGLALLIPDIQ

ETFMLVQNATSTDMSMLEEQEQIQSIERPSMQSIEEKYLELMKKLQFDTFEMIAESDNGFRFTISHHFETNVRMAGD

RGHPARVKRLAQETVTLSTSLPLSYSSSVFVRCDTDRLDIMKVLITGPADTPYANGCFEFDVYFPPDYPNSPMMINL

ETTGRNSVRFNPNLYNDGKVCLSVLNTWHGRPEEKWNAQTSSFLQVLVSIQSLILVGEPYFNEPGFERSRGTPAATH

SSKEYNSNIYQATVRWAMLEQLKNPCPCFKEVIHTHFWLKRNEICTQIENWITELSKPQYSERNGRTISFNSMVLRR

NYRQLREELSKLPPPPGLEEMNNPFSVNATTPTTPS

>GAWM01008211_CsIAP2

MNIEENRLALLENWVDNSGISAQEIAAAGFYATRNGSEVQCYWCLIKVNSWQEGDNALEKHRQLSPNCPFIVNPRYC

GNIPIDSDIDFLDEATRLETYQNWPVSFIQPADLARAGFYYINRSDQVKCAWCQRVIGEWEVLDDPVTEHLKFSPAC

QKARSLTGANEVSDIGIGIQPVTPPKFPNYVSLASRIRSFANWKYDHVQDPTTLAEAGFYYFGNRDEVKCFHCGGGL

CFWLEQDQPWYEHAHWFPKCHFLLLAKGPLYVQQIQERHKNDPETKAHQIKTTPVQPIMTLDEAMDSEPVQICLQMG

LSIGRIKSLTKRHLEATGRPYSTPQALAEAILDDQREAECDDDDRETLQRPIRSMVANTLWSAIQATSSRTIENPTE

NSEFESRGRGERDLITPIPSGISTSRTNEITTVGEASGFQVSDSIAKDTEELTLEEENKRLKDARECKICMSNEIGV

VFIPCGHLVTCVQCAVAMTSCCMCRSDIKGRVRTFLP

>GAWM01009039_CsIAP1A*

MAPCYKVLKTKMATLTRIIKDTFQKHNDEIDNKDNKEKEKDPYDFMNPRNSTQTSPSPPASPRNVPTTITGLNKEKQ

RRLTFSNWNCPTTDKFLLAQIGFYFIGPTDLVKCYFCNVEIGMWQPEDNPVEEHLRWSPNCPLLHGRETSNEPIDAE

ALKRILPTISYDTCGIRAGNSIPPGSYPEISINHPNESNIRDLSPQPSSSSGSSQQIDITPTSMMAHRNEHPEFAIE

SHRLVSYEDWPKTMKQKPKELAEAGFYYTGKGDRVACFSCGGGLKDWEEMDVPWEQHAMWYSKCEYLKLMKGQEFID

EILARKSSPPSSYTEASNLGTSVAGSSKDEVKKPNEVAKCAGVAMEEPKTAAVSDSKMCKICYECEYNTAFFPCGHI

IACAKCASSVTKCPYCRQPFTKVMRVYFS

>GAWM01018859_CsIAP5

MENNENTSSPLNTKSAVKEQLKKFYFTEKDRLDSFKHWPFDDKSPCNIAKMAEAGFFWCGNEREIDSAACFLCNKHL

DGWEEEDDPWLEHSKHAPQCLFAKTGKPEGELTVEEILNIFETMLKNFVERKFTGEKMLVKKMVEQKRKELTKSMFR

>GAWM01009044_CsIAP1B

MEAQNISVPPSSLNLEKKRLLTFVNWNQPKINKRLMSQIGFYFTGPTNLVKCYFCKVEIGMWQSEDNPVEEHLRWSP

KCPLLNGHETNNVPIDAEAIKRLLFSLNPAGHKHSEYAIESRRLVSYKDWPKTMNQKPEDLAEAGFFFTGLQDKVKC

FSCGGDLYDWKETDVPWEQHAVFHSKCEYLKLMKGKGFIGAILASKRSEIWSDKCDKPDKDIPDKAMRTENLDKLIN

DAVRQSKMCKICFEREYNTAFFPCGHIFACDKCALNFKTCPVCRHPITQSLKIYFT

>CG12284_DmIAP1

MASVVADLPSYGPIAFDQVDNNTNATQLFKNNINKTRMNDLNREETRLKTFTDWPLDWLDKRQLAQTGMYFTHAGDK

VKCFFCGVEIGCWEQEDQPVPEHQRWSPNCPLLRRRTTNNVPINAEALDRILPPISYDICGANDSTLEMREHAYAEG

VIPMSQLIQSIGMNAVNAAGSVTGTAAPQPRVTVATHASTATQATGDVQPETCRPSAASGNYFPQYPEYAIETARLR

TFEAWPRNLKQKPHQLAEAGFFYTGVGDRVRCFSCGGGLMDWNDNDEPWEQHALWLSQCRFVKLMKGQLYIDTVAAK

PVLAEEKEESSSIGGVAVASTQASEEEQQTSLSSEEAVSGDVAPSVAPTAATRIFNKIVEATAVATPSTNSSGSTSI

PEEKLCKICYGAEYNTAFLPCGHVVACAKCASSVTKCPLCRKPFTDVMRVYFS

>CG8293_DmIAP2

MTELGMELESVRLATFGEWPLNAPVSAEDLVANGFFATGNWLEAECHFCHVRIDRWEYGDQVAERHRRSSPICSMVL

APNHCGNVPRSQESDNEGNSVVDSPESCSCPDLLLEANRLVTFKDWPNPNITPQALAKAGFYYLNRLDHVKCVWCNG

VIAKWEKNDNAFEEHKRFFPQCPRVQMGPLIEFATGKNLDELGIQPTTLPLRPKYACVDARLRTFTDWPISNIQPAS

ALAQAGLYYQKIGDQVRCFHCNIGLRSWQKEDEPWFEHAKWSPKCQFVLLAKGPAYVSEVLATTAANASSQPATAPA

PTLQADVLMDEAPAKEALALGIDGGVVRNAIQRKLLSSGCAFSTLDELLHDIFDDAGAGAALEVREPPEPSAPFIEP

CQATTSKAASVPIPVADSIPAKPQAAEAVANISKITDEIQKMSVATPNGNLSLEEENRQLKDARLCKVCLDEEVGVV

FLPCGHLATCNQCAPSVANCPMCRADIKGFVRTFLS

>CG6303_DmIAP6

MATEQHHQQRVLKQDGYLDLGDCNSAPSRPFEMRNVVYHPQLNVLLLFDNGSTVKVLDANSGVILQTYHLSSNGDSI

VHGRYMPLQDKILFWDGHNLGLRGDYNGVLLLDTILQAPIGQNDDYIKLEIILSEAIIFQNCITELESEGLECPCDI

SNELTQKINQAQLKAKKGIKAQRWNTICLEVPYSSLKLVSNNMVILLKRLERHIPVLAIASAINERLTDMMMGSRVP

DFGWNFSNFQRVLMHSEAVRRQTFEKWPHMDYKWALPDQMAQAGFYHQPSSSGEDRAMCFTCSVCLVCWEKTDEPWS

EHERHSPLCPFVKGEYTQNVPLSITYATNPALPAPGLGFDIISNSDYANVLCTSCSQTGELSVWSIERHLKLMHTFH

VPTLLNYIFEESFEWARVTAICVLPNARARTKVNYVYSAANYGGSGSSNGAGCNSGLNAVSGGKFGSVNAQHITSTS

TLRAGVVGSKIVLGVSVRQSSGELALRMVVLNIVEVDRNSESSTSVSNDSGSVSSGGGQLMKSSSPMVNVSAENNAT

VTQVNLESKDDDNKAMTPYEKFADGFDSNGFVSALMTYNKNNGVSQNTDDASALYDFDLCTLSQILDHNLEEPLSLM

VGSSNTVNVSNIGMGNEINKLVVDVEISHQNNNNNNNNNNEASSLGGNSSNNNNNIMINGGTNSSIDKMTAIEEIDC

VVESWTSVKRMNALDGASSGVNGVNHMDQEVIEIAEILPTTPKCNQLLVKLLRTKAPEAEGSKIIMATVAKEEEEED

EEQRTDESMETDNNAEGNVAAQLLVFDYDDTEISNDYTLAMTFSRAKFPKQLCILPHFNSSPEHKDAGSICVVCADG

TVEIYSLADFQGTMVIEEEGEHFESVVYCRNLDRLCCCSRQGGLLFYSLSDGENDSGDELLEMDDDCSTTLTQAADV

SVTDGGRQLARTDLLGKTLLANESICMDAGSEAAAIPNSSSAAQGAHVQTSPSASSAPSTNANLLAYKTADLTLEDL

KVFYALTQFDDKLTVYSAEVPSCWNDIGQVQNQRKQSQNMRHGGDERDFTRTWRLHNDATTWDEHIIELNLAQPVSL

GHIDLKFTVYQQCSNPAAIQVTLLKQNNNGFGYRMKGPHSSYKPNVIDDNIDLSYIANENPVLSEEYLLAHNAEVLA

GPIELSSCIDLCDQGGTATLTSPKLFKTRTRNFLLHIKTVSDPSKDGQNKTRGCDWLHEISISVRAVKSHSRISNGR

MQRIAMLESNVLLVQLLRIASDPASSSLAKNLSLDILNWICFIRLNRFRSPKSERLKDQINKQTAANIQDLLAQQFE

CISLAEKHIEQLLRNCVIYSERSTAHKCVKLLIMLTEGATNLPAEVQDHTTLDYSFKAAIANTFPELPRAQCGSVVR

WYMMLTCATSTAESHNSISEQAISLLKEIAAEIDKRWDPHCALLCTRFGLYGYPFEPEIFDFDFPNVSRQGPGSSVA

NVIRSSPTILPVTGLDIKRLSSIDGVDFRTFPYLIRGKSISNQLRGLLEVVQLHFNCVQTSEATRIDNIDSVGGNTG

ANVIIEDVMMMPKQVVAKEKGEEMLNDLVNDVECLVEEMKVDENEKQEKVDYDAFGLVNGFKDKTLSSLNSVKQTLK

EEVKKEKADIMDKLTIAKFLPKLSLLESYMQKKINEHISFDDFGKLDNWDGNTTPPFNLEVEAPIVCSEATSESNMS

QQATSAGGNILDDAADSEKITESLNANPCQPIAWHKLITPPPKQMIVIDRMHSGARRFVVLDFGQHILLTDLVIPSC

DELTSLNIDIWCFDEETDCTRLVQVNDIQTKTLVLSDIQPAPICRYLKLTIIGRIGMSATKCKVPLGRFFGHPVVLE

HDGYGDQLMKYIKHPTHSLQSQIKSLNALYEDVHCRYSLASSKLMDLLAPMRNSELSNVAHLQAFINKQREEELSGL

ENNNKVVSLYDECMLLQYQINVIRNVVLRLERALSPNSPTTTLLPGQSIPLTEDILRAASRDKLRVLSLSLVEVLLH

FSIEYGIKNILPVHQRFNAATAKALFNALVVYGDAQLQLATCSLLVRMCCFQPWWGDFLADTFCSLFSAQNCKAFPQ

DRIFFLLTYLGRRSIAMGACRSIVIDAVLKTLVKLLAPISPHYKFQSEQPSTSANAADRNAAMGTTSDLQLITWLLL

FLSVCLDDNERKDKSAARWDFMSCEGDFTKARPSATPNIKQLRCFKKRIIQQNKYLAQPYADWGKKIYMIQNEHPGI

FMELSTKSKGAGPTKSTSTGGKINMGSSGLCVGGPSSSSGNTSKSAASSSSPKNQAVPGTDGERDSNFDKGLKSLRM

DNIKVVIRGLFALLLEMDFDCNMDQFLLTCKVIARLVAACRPSVQLCKIVTIAQLQQLVRLSVWNDQQHPWAVHAIT

CLLQDLLDADKQFRDNDVTPTNDTPRTMEAAIQETRDLFSDYTSTASSCTEALFETLMPTAREFYQEAVKYNYLPSL

IECDDTEFDEMLNDIDMIERTKPVTKKESNALSKNTFNFFCKSISIALDSRLDVGLELHVETQLRRLTNRTSLDLYS

SLPQVLTNEFVSPPPEAAPWPEYLTQLWSGTEYNGDNTYVMFKRVFDSILAELHLEDTWVHLEQVLQMWLTLNCELS

DKPYTSGITHSDVPKIPFGANAVQGLLLALAWHSDIKLRTWCLGFQCLFLACNSLPIGDDADCTRINEAIVNDENFE

KVLLRFFSGYGMSSSIITNRCAGPTICKHLHELLLWLHSKSETSGIPCKRRLKDILLHVVLQLVQPGGSISNQQGPI

DAQNQLVRDLLMMPNDKGDLNIALKITESVSFLVYNNISNGERLQCQRGNENSPVGNNFSNLFANVLGSENPNKQNA

AICDNSLIINLLKLSSHMVLTEMPRQPSEVTIPEEEELSNQSQTDETKAEQLNTEGHRSKVPCIADWVLRHFPTMKR

LFGTLSQCSTNTFTMMSSGCFFSPKSNMILDDPQTIADAVFSLMITLNDKASHPRLVVVPICRYLEETTIPRNATLP

RLPHSEPFLWYISKVLEVPAAVQTFTQLGGIQIICHSLVRLNKTIINMQPGLISLIMQHLTRNTRFKRNNHVAASSA

CKKTTTGTGTTCPTSAQPPRSAAQYDGLINFAPFSHIVSENDATQSAEVLISNPNNSHRRPRSPAWTYMFYPNETHV

DLTITLPTAILLKEVQLVPHTTSLASCPSAVALELSRDYGLGSIPVGAPMATTGLTCIRLKLAKAEVATSIVLRLYK

PKDCGNVGLVQIAVLGQTIFGNRMHGLRSPSPFIDSLATCSSPVQTAVLAAMDADSMLEDDAFAKTSIGWVRILSRC

FHVAALQPDSKLADLIAAYPAAYPGFLEACCSLLNIMPMIPSLAQQHLETILLKLSAYNHEISLQLLRTLLWHTTPQ

VFKLSSDSVCDLIYEVVTGSTEHLLDKLRVLIDWVMQLHDNYSKQARCNNPQSGFVKVIASILWKVHTQQQLPELPL

LISSSLFETCFEWVSSLEHDEPLKSSFDSLLCALCFIKPELFNQLLVKLGVKLEPPARGQTDDSKVQSGSAWFRREG

SENLSVLLQRPTFLKTLALACQSPAAVYQMLDSGLPKLLAHAIYEYCMHLMPGSEPVASASTVPEDEPLANNQAAAA

ADDEDSSLTDFDKAEANVVYNTPLLSSSNVPKVLDFFAECCAEGPMRDWLGTMQGSVFWKPLLQLLCNTHAAQFSKT

LPKEQSFIRLERATINFFTRVSACHPGNQENLTSLLIGAIICKPLRFSHGVRPTISGFTRQMVLQLLLENEHITVSV

RSQQPLQRRDTLSAVLGGISSGASTSLPVAAVNNHPARRSSAHHMLFTVTTSTTCQEIMQNCVSVFSNLVYQQPTDQ

RAGETSASSSGVSSATAKSSESKMEKSSFLNFNNVEAGSMEFLTVGAAVAAKDKRIKDAKNQAAMNKDKETQTSSTN

LASNIFNVDEFLLQSANAVNGNQLVIPEYSDIVLAGDATISQVLASLQNAGHSLSTPCISFDLVLQQRSDDTSEAKK

TKAACTEPLPSPLQRFSSSGGLSLLAHYLPTVYPEHSGRKTTLVFSEKEKSPPLSDWVKLEPNDEIYEDLEDTLCEP

AAKLATVSSVPQHSLAAFGLFLRLPAYSDVLLRDKMRAQCLLRLVLGVTGDGDGNDIYSLSLAPSLPTLPFEVFRQL

LDSVPLSTDDGVLLRRVVIEVGAMHLVLNCLGIFSHQSHNNRIGAPISEPSPSGTSSGSGTIGNGSGNGSVSGTKTN

APEEATPSATSDDKSHMYWAKGTGFGTGSTTQSWNVEQALLRQKSEEEHVTVLLLVLASYINPGDCIPSEMCGEDIL

AYHDVRDVTGELPPIFQTLLQQSCLIPALSSYLRNDSVLDITRHIPLYRAILKLLRALSLSKMLVSLLQPSASGSGD

STPPIVELLTSMKTCVDTYAKRLKVNKKSNIKGQTHQLTFNIDDGDDEGLALLIPDIHETSVLVQKTTDADALINML

HTNEDGSAQLEPQSKSIEQRYLELMKKRQFDTFDMIVESDNNSFRFVVSHHFEKMVRLAGDRYHPSRVKRLAQEAVT

LSTSLPLSFSSSVFVRCDTDRLDIMKVLITGPADTPYANGCFEFDVFFPPDYPNQPMLINLETTGRHSVRFNPNLYN

DGKVCLSVLNTWHGRPEEKWNAQTSSFLQVLVSIQSLILVPEPYFNEPGFERSRGSPSGTNSSREYNSNIYQACVRW

AMLEQIRSPSQCFKDVIHKHFWLKREEICAQIEGWIEELGKPQYTERASRTISFNSMVLRRHYRHLREELSKLKPPR

GLEDLDAPFNPVATLPPMDVSAVAPSLAATNTVQAQPDDAIVTDITLLGENADECEADGDAEGDGEVDDGFKGFPQE

EGLLTGEEEVVEILSDTENESSMWQ

>CG12265_DmIAP5

MESPVVNEVAASLGGEKLEVFRKLNLLEQHRVESYKSWPFPETASCSISKMAEAGFYWTGTKRENDTATCFVCGKTL

DGWEPEDDPWKEHVKHAPQCEFAKLSCPERNLTVSQFLEILGTVVKGSIEKTCKAFKSSFVRENEKRLDEFTRNQK

>AGAP007294_AgIAP1

MAHALSLPAPPIDLPDNKHKDDDLACMSPEYFHIEENRLRSFTSRWPVTFISPNVLARYGFYYVGTDDTVKCYFCRV

EIGLWEPQDDVIQEHLRWSPYCPLLKKRPTNNVPLNANYLDAVPEPSFDTCGISVRHNSYAENADDRVRIDLDRLSG

DSWSGASDISLSSAAGAAAASAGESEPMPSVGSGYPNYAIEADRLKSYEDWPTSLKQKPQQLSDAGFFYTGMSDRVK

CFSCGGGLKDWEQEDDPWQQHAIWYSNCHYLQLMKGREFIQKCNELKEAASASSAASTSSAMSSASSQPSTDEGEDD

AGGDRRVPSDGKICKICFVNEYNTAFMPCGHVVACAKCASSVSKCPLCQQPFINVLRLYLS

>AGAP008420_AgIAP5

MESTHNSAKIYLLQEDREKSFKHWPFSDDKQCSIQKMAEAGFYWHGTETEIDIAACFVCGKELDGWEESDDPWSEHR

KHAPQCPFVKFGRPETHLTVMDGKCYWLNDEEKIKLTDITFALNLQCDEFVTIMMAT

>AGAP002651_AgIAP6

MASSSSSDDQWLKEDGYLNVDAESRSITYHPYLNVILVVGSNGEVKLLDVNSGVILQSYRISGTDLNTVRCRYLPQQ

DKMLIWNGRNICMRGDYNGVLLLDTILQAPVTSTDDRVRLELLLSEALLFLQCLQNLEEHGLENMSDVTNELTQKIG

EAQAHSKRGIKAQKWETVCLELPHSSLRMVASGVVMQLRRLDQHIPAMAIASAINERLTDLLRGARVTESAKSVQRF

QMYSEAARRQTFEAWPHMDYKWVLPDQMAQAGFYHQPGENGNKDRAMCFTCTVCLVCWEKTDEPWSEHERHSPECPF

VKGEFTQNVPLSVTYATSPAIATGGFSLISSGDRGVVFCTGNPSGDVTVWNIERQLTKVHEFQVKLHPDILTTTTIS

PTATVNSIELSALAAYFVRTPPGMILMPRRASLSLKPKMLGTKIVAGVRVNSTEPFDEDMDAYKHEPETTLLLIVYN

IEDPLLEDILHGVPMAVANGMPMAMANLPPGATVTLNAGVGANAKKTSLFTIMESTEDDAVKLLSERTNLLMDELKS

AKHKLITQKSNKAKKKQYADVSENDSSDVSALAPADTMPHTTLPSTSMNIKEAIYCIPLQYIELPPILIDSYDHYYI

SDTVPSSDNKYLLVVVKYDASTAAKDAPTAKESGVPTANAADEADEQQKQTTDGAESAGPRWYAILFLYFLNEDGLV

RLDDPLTTCLKQEQVPLEITMLPKCDGTGRHFGGPETEQGIFVMTCADGKLRIVSLKTLGIISEASVKDDRFVSVTY

CKSLERLCGCTAKGCLHFYSFYDLDADSSDERDEEIVVPSPAAIDATDVPCGGTARADGVQSMDDIDNVTAASTAGA

EEKQTNAGSTGTAQRTQTQQQQQQQQQQSQHHPDGDIGNVNNLKMLHTFTLFSELLTPYSAEVPACWNELEQAQKQR

RNPQHLRPGDDTHLTKTWRLHNDASTWDEHLIELNLPKCTSLGHIDFKFSLYQPCANSPAIQVTLLKQKSMGLCTRR

KTQSINRVDESINFNIGAGEGKHFVENPVLSEEYLQARNAEIVVGPIELASCMDLSEQGGCVTLTSPKLLKSKGRNY

LLHIKTMTDLSKDGQGKTRGKQTNGTGVGKSWLRRTTLGVFFPPIRSCLVFIKMLKARERKCFNEMELFLHSLFLRP

GCDWLNEISITVRATRQLYKVEQERAQRLAMLDSNMLLENLLGLLHQSTAETAELVDDGSGQENGTISPGENTIIMQ

QNLAIDILIWIVTIRMMRYRYPKNPFAKRAAPTELRKVASTDLNIQQTECVQIIEKHLEQTIRHCIVLANRSIAHKC

VKFISLALEGAQNMVDKNVCNAFEQTLNDAIIKCLPDVVNCNNAGALRWFALLISGTTLAENHLSIADHCLTLLKSV

AEELQKRNNPYTALLRTRFGLHGSPFDSEVFDAQLMDGRVAFGGGVAYPFGAGGTLGSSVLSGPSSIDLRLMCFADG

ADLKCLFDQLRNRSIGSHFVGLLEVEPLHYSCCATSDATRLENENLADGMMNNVKNVLVDKIFFSALQKHKLKSAGN

SSADTIGFPTYLQQTSTDSHAKPHAINIGSSDSEMAKELETFDDMYVDDLSCDMFNPTLIITDTAAAESAAAHGTAS

NSVADGPRSSKGVSFTANDANLDLQQGPLTSLLDNKIQEYFEDKSAEAEYAADQSGGLPWHKLLASPPKQTIVVERM

HSSAIRYVTLDFGAPIMLTDVIIPAHSDLASLSIDVWCFEEEADSVRLVVSQDIHSRTLVLSDLQPPPICRYLKITI

TGRYGMTATRCRIPMGSFYGHIVILDREAYADPVMKFLQKRKTNVQTQIKILKALYEDVHCRYCLASSKLMDLLVPY

FNSDASNIAHMQAFLNRMKDTSFGGALGSDGVPAECAKVTAAYEECIGFQHQLNVIRRVIDRIRPSVDLKHPTLAQL

MLPTQPTPLKPGDDLSSIYTDKLRIMSECLIEVVLQLVTTYGSMPVQHISQDMCNLLFDTMVIAGDAHTQLATCSML

VRMCCLESCRTTVIDAILRSLATLLAPLATSGASGMSIWCSTDLNLIGWILLFLSVCLDDGTEGRKDQNNMRWDFMS

GETDMVKARMNINNSGLRTLTRSFKKRLIQTKQYSSLTGGEIGNSIMVPSSLSKNETAGQDGSSAMSSSSGGGMHAT

SSTASNMTQLLSSGSKGVGKFVNIGGERTIRDTSSDTVMGHGMSASKGAGDTADGETPFDAGLKSMKIGKIIVVIRG

LIGLLLSMDFTCNMDLFLITCKIVARLVLACRPALQLSKIITTNQLLQLIRIAVWENQQQPWAVHAITCLLQDVLEA

DKSFKDDENDTSDSPNDDGAAVPYKQQHPMQSTAHHVSCDLSYADVAKSQLPSVVECDDPEMEEILIIDEIFSAREK

RFHRRDIGAFASFSSKYSITNKPVSVAMDARLEMGLDTNVEIVLRRLTTRSAFNLITSLPHVAMMPELLGIGASAGQ

PSDSLPPWPDTITDVWSGPEYLQGMETNVMLTEVFDNILSDLHQLDSWLNLEKILQLWLTLNGETLENIPGSCSTGL

NPYSFPRIPFGDRAVKGLLKALASHPNIKLRAWCLGFHCLILACKPHFEADCLDNMASSSDNHFRRMGTMIVQDENF

EKMLLRFFSGADQSLISMDGGSSRYAGPTVCKLVVELFIWLEIRCNVGEELKQTLLRVTLHLVQFGGAIANQQGPID

AQSQMIKELLNVPFNKSDLGIAMSIIECVSHLVYNNVVNVEKLYCQKTVESNNSGGMLGGGMRFSSLFATVFNAESN

RACKTATDSSLLVDLLKLASILVNTKNPHVSTGADGGSTAEDTASATSGSGETRPKVPCFADTVLQHSPTMNRLLST

LSHCSHSSLTMLVASTVSYGNGADSGSVKNLRNTYPELCTVADAVFQLLLYLSRTASQNELIVKPLFEYINNASNAR

HAMPKLHLSEPFLWFILKVLGTPSSVAIFTELGGIQVLCESLVRSNRALINTQPSLVSMIMQRLSKSSVGLHGTGGV

GGSGMAGGNGGGSSSKKSTPIVTTPRNEEGLINFAPYSTITSDNQSVQAADVLIQTPIASHRRARNPAWSYLFYPNE

SNVDLTITLPTAVLLKEVQLQPHLATLATCPSAVAIEVTRDSILGPIPITQPISTVGMTCIRLRFAQPEIATSVIIR

LYRPRDSMNIGLTQISILGTTTFGELTQPGPSGFGGSPMQNWPSCPMVAFNGASGSGARTSLGWLRVLTQCFGVTIY

YADQQLANRVIDAANEVTGFMEACCALLNIAPNSPNDTLQNLETVLLKLGLHSREMGLRLINTLLRQSIPQTFQLSN

DSISDLLYQLCTMQNEHTRDRLQAMLEWVLTLYERYRQSMAAGGTSTINQHRLALHATNPYSGFVRCLAAILWQAFA

TDLIPELLDMVSRELFDVLFSWVQELEQHEGGAGAGPLKKAIDALLCSVCCIRPEFFTMLLRRMGVLVPNLSTDLTA

SISDDRKDGERRTDDSKQEESDTTEWYSHLVIEDIASLDLSSSQLATIAMASQSPLAIQQLIDSGLPKLLNSVILEF

CRRATNYVERMRRGTVRAAASCTSQSGAAASSAGAGSTEGACLTDADKWSGSESTESAKLHPMVNIHKVTEILAFFT

EMCSEGHMRDWLGSHEGAIFWEPLLLLLCNSQLANVTRDITTQSCLELEECFIKFLSRATTCHPKNQEVLTINLISV

IRKSDPTEEAMHGGPTDGAAPPTTSAPPLLRSCISGFTRRLVLQILLESEKIMVAVRSDLPLLQSKEVSGTGAGGLY

NSIANHPSKRPNAHLMLFQLSTNAKCQDILDQCAAAVYQPILPSAVPAATSVATASQPAGSSSSAQGCRDSELWELG

IGLEFLSVAAGVTAKDKRLKEAKNQATTMRRKDLLSMFKMKMDDAKLSVPDGLFLTHSAVPEVIITSDTTISQLLTM

LKSAGISLSIPCINLNLVTTDAPSSGESSSMSSSSGPGSSAYMRATEFLPLPSPLQIFSSRGGLSLLAHYLPTVYPE

MPKTSAYYMDKDRSPSGAAGVGSAGAGNEWVKLEQMDEIYEDLDDIVAESSPKAQAITAIPQHSLAAFALFLKLPAY
SEVLLNDTVRAQCLLRLILGVTSDGEGNEIYSLPLSSTLPTLPFEVFRQLLESSPLTTDDGVLLRRMVIEVGAIHLV
LNCLSIFTHHNGSGCSVRTAGAASGQAGTSAATRISTGTGTNKSSSTMTGNATANNTEDQLNADDKGHMYWAKGTGF
GTGSTQQSWNVEQALMRQKSEEEHVTVLLQVLSSYINPGCNSYVISSGTEELHNFKDSFESVGELPPIFLDLIQQSC
LIPALSSYLRNDSVLDITRHIPLYRAILQLLRAISVSNQLAMLLVNKSASEGKLSIAGLLSNMKACVDTYASRLKVN
KKSNLKGQTQKIIVSLDDGDDEGLALMMHDIQLTSLLVQNATNIDITNAAEEEEKQLIPRPITKSVEDKYLEIMKAL
QFDTYEMIAESENGYRFTISHHFETNVRMAGDRGHPGRVKRLAQETVTLSTSLPLSYSSSVFVRCDTDRLDIMKVLI
TGPAETPYANGCFEFDVYFPPDYPNSPMMINLETTGRNTVRFNPNLYNDGKVCLSVLNTWHGRPEEKWNAHTSSFLQ
VLVSIQSLILVPEPYFNEPGFERSRGTPTGTHSSREYNSNIYQACVRYAMLEQLRHPCPCFQDVIHAHFWLKRNEIC
NQIEEWIAELSHPLQHERTGRTISFNAMVLRRQYRQLREELAKLTPPEGLEEADFPFNAGSNVTPTTPSTAATSTTT
A

>AGAP011326_AgIAP2

MSSASGSEVQPAEMPYMPEFAVLDARIRSFESWRFGHMQNPTRLAVAGFYYTGTDDEVRCFQCDAGLRDWLVTDDPW
QEHARCFAECTFLRLVFGADTVDEVLRNGIAGFKNGANTATTPSATVSGPIDETSSELAQRLREENKRMKQERECKI
CLTQEAEVVFMPCAHLLSCVQCSTGVDNCPVCRAVITHRFRAFIC

>AAEL009074_AaIAP1

MAGVMMAQVLSTPRDFTDNKVKEDNAYGHTATSVPISYHTEVARLESFRGWMVSFISKTELARYGFYYVGPNDMVKC
YFCRVEIGLWEPNDNVLSEHLRWSPYCPLLRKRQTNNVPIDASFLDQLPEPSYDTCGIRIRENSVAENAYSSSDRSS
SGSLTSPPSSLTSESSMASNGPVVQQLSAPVLPQQKLPEYPNYAIEAKRLESYEDWPKFMKQKPKELSDAGFFYTGK
SDRVKCFSCGGGLKDWEAEDEPWEQHAMWYSNCEYLKLMKGEAYIAHCLAKKESSSEENGSDSSQSSSLSVSAEEDN
TAMVGCSSDEDEPNRKLDTSRTCKICYVNEYNTAFSPCGHVVACAKCASSVTKCPLCRKPFTNVMRIYLM

>AAEL006633_AaIAP2

MNVEVNRVRTYRRWEATEWAMEDAFELLLAKAGFYATEQYLNVKCHFCGVTIFVGNSVSNIEAKHRELSPNCAFLLH
PDRTDNVRCFDADELKREEHRLATYVNWPISHISPSSLAKAGFYYTYNADQVKCAWCEGVIGQWELGDDPFVEHQKF
FPNCAKVISNGISSNPILDPTIGIQPVKTPYAPQFSSLDSRIRSFENWTTGHIQDPERLAQAGFYYLGRADEVHCFY
CDGGLRFWLADDDPWFEHARCFPKCQFVQLVKGQLFIENVQSQIKSTSSNQQQQMQASGPTMSLDEALATEPVQLAL
SMGLNAGRIRAVTKRQLDSTGHPYADSQALIEAVLDGQIQDEELEPSTSSRMDRRIESEVSRLLWTAISSTAGPNLS
SFSSTFSTPSPSFDSAPTSDGDVIVSSDPLSSPSTSSIANNASTSSAVKCNNVPESLAQMAAAARPTETAEVDKTLR
LEEENKRLKDARECKICMADEVGVVFCPCGHLVSCVQCAPAVTNCPVCRAVIKGRVRTFLS

>AAEL012446_AaIAP6

MANGADDQWLKEDGYLNVDTESVRIVYHPFLNVILVFTRAGEVKVLDVNSGVILQSYHVSENLPAQCRYLPDQDKIL

FWNGRNVSMRGDYNGVLLLDTILQAPVSQADDIIRIELLLSEAVLFVQCLQNLEQHGLENTADVINELTLKIGESQQ

HAKRGIKAQKWETICLELSHSSLRMVAGEMVMQLKRLDRHIPALAIASAINERLTDLLEGARVTEPSALNRFYMFSE

ATRWQTFEGWPHMDYKWVLPDQMAQAGFYHYPGDNGNDDRAMCFTCNVCLVCWEKTDEPWSEHERHSPECPFVKGEF

TQNVPLSVTYATSPAIATDGFSIISSGDRGNVFCTGNPSADVTVWNVERQLVKVHDFKVKLHPDILTTTSISRSAVV

NSIELTALSTYYMKHAGLVSKSKVASLSLKPKMLGSKIVCGIRVSSTETVDGKDETGTTLLLIVYNVEESTSCDEGG

NKQLNQASNVSVIPPTKKSSLSTIDEKYEEDIMKFFSGNTESQLLESIDKLIHLETLKKDDPSLCQQFGAKLDDTLR

KLIETSGSPSVGSVDKPASDDSPSSPTGHIEVVKGPTCISLPPPPPSAAGSNSGSSTQLSSVKSSQPDSVTSISTMG

SSSSPNTNVTSALSTATSSVSSGNCDINCIPLQYIEIPAEWHDNYRIAEVIPSSDNKYLLVVLRLIPKAAVDEKEST

KDDEKEVVEKKDEGEKEEHEEEIPEEIEEADWKTVLLLYFLTEDGLIKAGDPVVKQLSDEESPVEIVMLPKCDSSGR

SFGGPDTENGIFVMTCEDGKLRIFSLKTLNIVSEASVKDDHFVSATYCKSLERLCGCTAKGCLHFYSFYDLDADSSD

ERDDDVTCVIGNGSKAAAGADRSQYAEVDGAASSAAANLLKYDATPSTSSSPPQMPSAVATGASVTGENHLADALLA

YKPELSLPTLKVLYSLTLFNEMLTPYSAEVPGCWSELEQAQKQRRHPQHLRPGDDTHLTKTWRLHNDATTWDEHLIE

LNLPKCTSLGHIDFKFSLYQPCTNPPAIQVTLLKQKSIGLCSRRKTQSINRVDESINFNIGSSDGKNFIENPVLSEE

YLQARNAEILVGPIELAACMDLSEQAGSVTLTSPKLLKSKGRNYLLHIKTMTDLSKDGQAKTRGCDWLNEISITVRS

TRQVYKIENERAQRLAMLDSNLLLRNLLKLLYSADEAVHMHQSVIFDILIWIVSIRLVRYRYPKNPFAKKVVPATEI

KDVASSDINVQQSECIQIVERHLEEIIRHCVVRGNRSIAHKCVKFVSVALEGAQNMIDKDVCNSFEKSLKQAIITCL

PEIIHSNHAGALRWFTLLISGTSTCDSHGPISEKCISLLKDVASEMRKRSNPYTALLRTRFGLYGSPFESEIFDSQP

LTSKNTNVTYTCSITKTTGTGANNQSIDLRSVCIADGSELKFLPLQLRRRGIGNHFKGLLEVEPLHYVCSSTSDATR

LENVDANNMQATNIIDDFLMENTAQNNIEPVQNHIKLDEKENLDDDMMNNVKNILVDKIFYSALKKHKMKDDFINEA

KKSAEEIEIDPQNESFSEIGGWGPSNEPRMVFVGGNVTDASSIIEEKPQASITLNNKIQEFFEDSNADENANGLPWH

KLLSTPPKQMIVVERMHSGAMRYITLDFGAPIMLTDLIIPACSDLASLFIDIWCFEEEADSVRLVVSQDIGSRTLVL

SDLQPPPICRYLKITITGRYGMSATRCRIPMGSFYGHIVILDREGYADPVMKYLKNKKNNLPAQVKILKALYEDVHC

RYCLSSSKLMDLLQPLINSESSNIAHMQAFLNRIKENNGDQTGPGHSNTSAFQDNAKVYAVYEECMAFQHQLNVIKR

VIDRIKIPASLSDLPKQLKPGAADLSPIYTDKLRVLSECLIETLLHLITTYGVQNVANIYPYFDLETCNLLFDTLVI

NGDTHIQLATCSMLVRMCCFQSWWGEFLADKFLKLYSSQNSRIFPQDRVFFLLTYLGRKSISMGSCRSIVIDAILKS

LATLLAPLSQNSASGLNIWCNTDLNLLGWILLFLSVCLDDGMADGKKDQSNIRWDFMSGETDMVKARLNMGSGGLRT

LTRTFKKRFLQSKHYSSGLTGGNGNAVTEKMYMMNSDPLQTPASKLEMALKQHENQLKKLQNSVKQSFGDYFNEITK

AKSVRLPGGEGGSRSSQSGSSGSGSKDTSSDSSTNDNETAFDKGLKSLKIGNIIVVIRGLIGLILSMDFTCNMDLFL

ITCKIIARLVLACRPVVQLSKIITTNQLLQLVRIAVWENQQQPWAVHAITCLLQDVLEADKNYKDDENDSGNSSGDE

ATTSSEAGASARPPVPDTAFKPVQHTVQVSKDISYADAVKNQLPSLMECDDADMEDILILDDILEREKRVFKKDASA

TVGSGRNGMTFLYKTVSSAMDARLETGLDTNVEITLRRLAMKATFNLIASLPQVTAVDPLNPTQIELTAWPESIVEA

WSGEEYQQGLETNTMLTEVFDNILCDLHLVDSWLNLEKILQLWLTLNGETLEQVPGSNAPGLNAYSFPKIPFGDRAV

HGLLKALATHPNIKLRAWCLGFQCLILACKPHFEADYIDSTSTTSDNHFRKMGNLIVGDENFEKMLLRFFSGVDQSI

SSLDSNRYAGPTVCKLVLELFIWLELKCNVKEKLKEILLKVILHLVQFGGAISSQQGPIDAQSQLIKELLSFSYDKS

DLGVAMSIIECVSHLVYNNIVNVEKLYCYRASENSHSNSMYATRFGSLFATVLGPENARQCKTVTDSTVLIDLLKLA

SILVNTKNPRSGESDNAAAYESSTFNELNTSNESQTDEIKAEQQNIEPRPKTPCFADTVLQHSPTMTRLLSTLSHCS

TSSFAMLVASSMYCASINDSKSSSLTEPQTVADAVFQLLLYICRAATQTVLVVKPLFDYISNASSMRHAMPKLHLSE

PFLWFILKVLDNSASIAIFTDMGGIKVLCESLVRSNRVLINTQPSLVSMIMQRLSKSSNLQTTLSSSSKKSSMAATR

NEDGLINFAPYCTISSENQTAQPADVLIQAPIASHRRARNPAWSYLFYPNESHVDLTITLPTAVLLKEVQLQPHLST

LASCPSAVAIEITRDSNLGPIPITQPISTVGMTCIRLKFAQPEIATSVIIRLYRPRDATNIGLTQISVLGTTTFSDV

NGSSVAGPCWVTGTTPPQPAKPASDGTSEFFNDDDKAAKTSLGWLRILAQCSSVVMYNTDRQLANRVIMAATEVPGF

LEACCSLLNIAPLCPNIALNNLETVLLKIGLYSRECGLNLINILLKESIPQTFQLCNDSISDLLYHLCTTHNEYTGD

RVEAMLSWVQRLYERYHQNQVNRFVLHATNPYSGFIRCLSSILWQSYATDLIPDLPNMITKELFETLYDWNQELEHD

EPLKKAIDAMLCSVCCIRPELFTMLLKRMGVLVPNLSTDLTASISDDRKDGECITDDIKQEESDAAEWYSHLVIEDL

SRLNLSKAHLSTISMACQSPLAVQQLIDSGLPNLLTSVILEFCHRALNSINQHQKQSEVASGSVERDNREVFEEEQA

AAAAVAAATAGDGAEESSSCMTDADKEHHKYSGSGAKEVIYPMVNVQKVTEILGFFSEVCSEGHMRDWLGCFEGSIF

WEPLLLLLCNNKLANISPEVTPQACLDLEECLIKFLSKVTSCHPKNQEVFTVNLISVIRKSDSANVSSSGASAANGS

SSNQTGLNNRPNSGSKSCISGFTRRLVLQILLESEKIMVAVQSELPLQNKDPNPYNLSNHPSKRPNTHFRLFYLSTN

SKCQEIMDHCVTAYNRIIPNLPSDSRVSEVLIGSSNAGAAAGGSDNRKELWEMGLGMEFLSVAAGVTAKDKRLKEAK

NQATTMKQKDILSMFKMKIDDPKLTAPDGIILRHTAIPNGVITSDTTISQVLAMLKSSGISLSTPCINLNLSLAKNK

PDVELSCEASSSSSSSPILKAADFIPLSSPLQIFSSRGGLSLLAHYLPMVYPESPKSQQQLGDKDKSPPGGDWVKVE

QNEEIYEDLDDILADASPKAQAISAVPQHSLAAFALFLKLPAYSEVLLRDKVRAQCLLRLILGVTGDGEGNEIYSLA

LSSSLPTLPFEVFRQLLDSSPLTTDDGVLLRRMVIEVGAIHLVLNCLSIFTHHNNAGVSSNSNSSDNIQAAASNKGA

PGAAANGTDDQLNSDDKSHMYWAKGTGFGTGSTQQSWNVEQALLRQKSEEEHVTVLLQVLSSYINPGDKFPSNLDSE

VLSYRECSETLPELPPIFLDLLQQSCMIPALSSYLRNDSVLDITRHIPLYRAILQLLRAISLSNQLVSLLVNKNNEG

KISIAALLANMKACVDTYASRLKVNKKSNLKGQTQKITVSLDDGDDEGLALLIPDIQETSLLVQNATNVEALTVEEE

LKEVVPRPMAKSVEEKYMELMKALQFDTFEMIAETDNGYRFTISHHFETNVRMAGDRGHPGRVKRLAQETVTLSTSL

PLSYSSSVFVRCDTDRLDIMKVLITGPAETPYANGCFEFDVYFPPDYPNSPMMINLETTGRNTVRFNPNLYNDGKVC

LSVLNTWHGRPEEKWNAHTSSFLQVLVSIQSLILVPEPYFNEPGFERSRGTPTGSHSSREYNSNIYQACVRYAMLEQ

LKNPCPCFKEVIHTHFWLKRNEICAQIEDWIAELSKPLLNERTGRTISFNAMVLRRQYRQLREEFAKLKPPEGLDER

DYPFITGITPTTPSVPVCAGVEGSNNGAVDSSATTSPEKPLTSDDDESELLLQSSQGDIVMGEDEDDDDANVVDEVI

IKADVEDVAAGSSSSSNDKGTSIPDDGQDENPDLSPEEIVLSMVW

>CPIJ002102_CqIAP1

MTAQVLSIPRDYTDNKVKDENTSYGLTGTSVTYHIEVSRLESFLNWSIPFISKFELARFGFYYVGPGDMVKCFFCRV

EIGLWEPNDNVLSEHLRWSPYCPLLRKRPTNNQPLDASFLDQLPEPSYDTCGIQIRQHSVAENAYSSSDRSSSGSMS

SPPSSLTSESSMMSNTSGGVGATELQPPQQQHKLPEYPNYAIEAKRLESYEDWPKFMKQKPKELSDAGFFYTGKSDR

VKCFSCGGGLKDWEAGDEPWEQHAMWYSNCEYLKLMKGEEYIAQCLAKKENSSEMSEQPQDVGPSSSPQPSTSGVAS

AATTSLPSSQSSSLSTSVEESNPMTSMAAPMSGSSGLEEDEDEPNRKQDTSRTCKICYVNEYNTAFSPCGHVVACAK

CASSVTKCPLCRKPFTNVMRIYLM

>CPIJ019231_CqIAP2

MNVEFNRLRTFEQWEHASWTMETSFEEVAKAGFYATERFLEAKCHFCGATVYIGEQAVDIESKHRQLNPGCSFLLHP

DRTDNVRSFDAAELKREECRLATFVNWPVAHISPPALAKAGFYYTFNSDQVKCAWCEGVIGQWEVGDDPFTEHQKFF

PSCEKVIANGISSNPVLDSSIGIQPVKPPHAQHFSSLDSRIRTFENWTTGNIQDPERLAQAGFYYLGRADEVHCFHC

DGGLRFWLADDDPWFEHARCFPKCQFVQLVKGQLFIENVQTQIKNSSGQQPSGGAQSTATMTLDEALSTEPVQLALS

MGLNAGRIRAVTKRQLETTGQPFAQSQALIEAVLDGQIQDEELEPTTSSRMDRRIENEVSRLLWSAISSSTTPNLSS

FNSTFAPSASSPVSEVRSSAEATSTEIAEAAAAVPEPASVLRRRSSSEAVKPGDEKTHRLEEENKRLKDARECKICM

ADEVGVVFCPCGHLVSCVQCAPAVTNCPVCRAIIKGRVRTFLS

>CPIJ002689_CqIAP6

MATGDDQWLKEDGYLNVDTESVRIVYHPFLNVILVLARTGEVKVLDVNSGVILQSYRISDDSPPQCRYLPDQDKILF

WNGRAVSMRGDYNGVLLLDTILQPPISQADDNIRLELLLSEAVLFLQCLQNLEQHGLENTADVTNELTLKIGEAQQH

AKRGIKAQKWETVCLELPHSSLRMVAGGMVMQLKRLERHIPALAIASAINERLTDLIEGGRVTEPTAALNRFHMFSE

ATRRQTFEGWPHMDYKWVLPDQMAQAGFYHFPGDNGNDDRAMCFTCNVCLVCWEKTDEPWSEHERHSPECPFVKGEF

TQNVPLSVTYATSPAVDIGGEGFNIISAGVRGNVFCTGRPSADVTVWNIERQLSKVHDFQVKLHPDILTTTTISSSA

TVNDIELTALATYAVGSTTLSHGKPKVATLSLKPKMLGTKIVCGIRVNSTDPEADEPDDTLLLIVYNIEDAVPDEQQ

KNATSKQVPTSPSATNLPPAKKSSLSTIDEKYEDDFIKFLSDNTDSQLLESIDKLIHLDVLKKEEEQLNQKLGAKLD

EHLSKLIEASTGSTEKISVEDTNTSVDTLKGPFMANSLSPSGGESQLVSIKMTDSLNSLNVNNSNTNVSTALATATT

SSASCDISCIPLQYIELPLFTEAHEHYRIGEIIPSSDNKHLLVVLRLKEFKKEEEVKVVEPEKPQDNKADDEIPEEI

EHGTDGCRTVLFLFYLNEDGLVKADDPLIKRLADEESPLEIVMLPRFDGSGRSFGGPDTENGIFVMTCEDGKLRIVS

LKTLGIISEASVKDDDRFVSATYCKSLERLCGCTAKGCLHFYSFYDLDADSSDERDDDVTTINNKLTTDGGLATSNS

GVAPSNLLKYDATPSTSSSPAQVPGLGGATADSHPPGGEPLLAYKSELSMNTLRVLYSLTLFNEMLTPYSAEVPGCW

SELEQAQKQRRHPQQLRPGDDTHLTKTWRLHNDATTWDEHLIELNLPKCTSLGHIDFKFSLYQPCTNPPAIQVTLLK

QKSIGLCSRRKTQSINRVDESINFNIGSGDGKNMIENPVLSEEYLQARNAEILVGPIELASCMDLSEQAGSVTLTSP

KLLKSKGRNYLLHIKTMTDLTKDGQAKTRGCDWLNEISITVRSTRQVYKIENERAQRLAMLDSNLLLESLLKLLYSD

EESLQMQQNLVFDILIWIVSIRMVRYRYPKNPFAKKVIPTAEIKDAATADINGQQSECIQIIERHLEQAIRHCIVLG

NRSIAHKCVKFVSVALEGAQNMTDKDVCNSFEKSLKQAIITCLPEIINSNHAGALRWFTLLISGASTCDSHGPISER

CISLLKDVASEMRKRVNPYAALLRTRFGLYGSPFEAEIFDSQPLMSKNANVTYTCSITKTTGTGTNNQSIDLRSVCI

ADGSELKFLPLQLRRRGIGNHFKGLLEVEPLHYVCSSTSDATRLENVDANNIQATNIIDDFLMENTAQNNIETVQNH

IKLDEKENLDDDMMNNVKNILVDKIFYSALKKHKMKDDFNEAKKSSAEEIDAQNDNFNEIESWGPSSNEPRIVFVGG

NTNESGGSIIDDKSQASIALNNKIQEFFEDSNADENANGLPWHKLLSTPPKQMIVVERMHSGAMRYITLDFGAPIML

TDLIIPACSDLASLFIDIWCFEEEADSVRLVVSQDIGSRTLVLSDLQPPPICRYLKITITGRYGMSATRCRIPMGSF

YGHIVILDREGYADPVMKYLKNKKTNLPAQVKILKALYEDVHCRYCLSSSKLMDLLQPLINSESSNIAHMQAFLNRI

KENSGDPAAASGHANASSFQDNHKVYAVYEECMAFQHQLNVIRRVIDRIKGPGPSPDLPPLLKPGADLGPIYTDKLR

VLSECLIETLLHLITTYGVHNVTNIYSYFDLDTCNLLFDTLVINGDTHIQLATCSMLVRMCCFQPWWGEFLADKFLK

LYSSQNSRIFPQDRVFFLLTYLGRKSISMGSCRSIVIDAILKSLATLLAPLSQNSASGLNIWCNTDLNLLGWILLFL

SVCLDDGMTDGKKDQSNLRWDFMSGETDMVKARLNMGNGGLRTLTRTFKKRFLQSKHYSAGLTGGNSNAVTEKMYMM

NSDALQGTASKLEMALKQHENQLKKLQNSVKQSFGDYFNEITKVKSIRVPSGESRSSQAGGSGSGNGSKDGSSDGSA

NDNETAFDKGLKALKIGNIIVVIRGLIGLILSMDFTCNMDLFLITCKIIARLVLACRPVVQLSKIITTNQLLQLVRI

AVWENQQQPWAVHAITCLLQDVLEADKNYKDDENDSGNSSGDEATASSEATAAPRPPAPEATSSFKPVPLPVTKDIS

YADAVKNQLPSLMECDDADMEDILILDDMLEREKRVFKKDSNTSLSSSRNGLTFLYKTVSSAMDARLETGLDTNVEM

TLRRLAMKATFNLIASLPQVTVADALNPNNNVELPAWPETIIEAWSGVEYQQGMETNTMLTEVFDNILCDLHLVDSW

LNLEKILQLWLTLNGETLEQMPGSSAQGLNAYSFPKIPFGDRAVHGLLKALATHPNIKLRAWCLGFQCLILACKPHF

EADYMDANSSTSDNHFRKMGNLIVSDDNFEKMLLRFFSGVDQSISSLDSNRYAGPTVCKLVLELFIWLELKCNVKEK

LKEILLKVILHLVQFGGAISNQQGPIDAQSQLIKELLSFSYDKSDLGVAMSIIECVSHLVYNNIVNVEKLYCFRASE

SSNSNNMFGTRFGSLFATVLGSENARQCKTVTDNTLLIDLLKLASILVNTKNPRTGEDNAATYESASFSELNTSSES

QTDEIKAEQQNIEPRPRTPCFADTVLQHTPTMTRLLSSLSHCSNSSFAMLVASSMYSTSGISDSKNNTLSEPQTVAD
AVFQLLLYLSRTATQNLLVVKPLFDYINNASSMRHAMPKLQLSEPFLWFILKVLETASSVAIFTEMGGIKVLCESLV
RSNRALINTQPSLVSMIMQRLSKSSNLQTNLSSSSKKSSIATPRNEDGLINFAPYCTISSENQTAQPADVLIQAPIA
SHRRARNPAWSYLFYPNESHVDLTITLPTAVLLKEVQLQPHLSTLASCPSAVAIEITRDSNLGPIPITQPISTVGMT
CIRLKFAQPEIATSVIIRLYRPRDATNIGLTQISVLGTTTFSDINYGASSSSGSSNNTSNSAPSWTGGVSTSTSAMP
KPMGADEYHNDDDKVARTSLGWLRILAQCFSVVIYASDQQLSNRVIMAATEVPGFLEACCSLLNIAPYSPNFALQNL
ETVLLKLGLHSREFGLKLINILLKESIPQTFQLCNDSISDLLYHLCTTQNDFTRDRLEAMLTWVQRLYERYHQQQTN
RFVLHATNPYSGFIKCLASILWQACAIDLIPDLSNMITKELFETLYDWNQELDHDEPLKKAIDSVLCSICCIRPELF
TMLLKRMGVLVPNLSTDLTASISDDRKDGECITDDIKQEESDTAEWYSHLVIEDLSRLNLSRCQLSTISMACQSPLA
VQQLIDSGLPNLLTSVILEFCHRALNNVNAQSQKPKPSSQRSSVERDNREVFEEEQAAAAAAAAAAATESTDTMEAE
SGSSCMTDADKEHSKYPGSCPMVNIGKVTEILTFFTEVCSEGHMRDWLGCFEGSIFWEPLLLLLCNNKLAHLVPEVT
PQACLDLEECLIKFLSKVTACHPKNQEVLTVNLISVIRKSDPSAATVPPTGSAPNQATTTTNNRMPGNGKFCISGFT
RRLVLQILLESEKIIVAVRSDLPLQSKDQNLYNVSTHPSKRPNAHFLLFYMSTNSKCQDILDQCATVYNQIIPNLPS
DSRVGDAATASGSAPPGLGSDTRKELWEMGLGMEFLSVAAGVTAKDKRLKEAKNQATTMKQKDILSMFKMKIDDPKL
SSPEGVALTHTAVPNGIITSDTTISQLLAMLKSNGISLSTPCINLNLVEAKNKPDVDLTCESSGSSSSTPLVKAADF
IPLPSPLQIFSSRGGLSLLAHYLPMVYPETPKSQQHLGDKDKSPPGGEWVKVEQNEEIYEDLDDILADSSPKAQAIS
AVPQHSLAAFALFLKLPAYSEVLLRDKVRAQCLLRLILGVTGDGEGNEIYSLALSSSLPTLPFEVFRQLLDSSPLTT
DDGVLLRRMVIEVGAIHLVLNCLSIFTHHNGYGQSSGSNSSENSTVPTVANGTAVSVPTVGGTTTSSATTAAVATAE
DQLNSDDKSHMYWAKGTGFGTGSTQQSWNVEQALLRQKSEEEHVTVLLQVLSSYINPGDKIPSNLDTGEECSYRECS
ETLPELPSIFLDLLQHSCLIPALSSYLRNDSVLDITRHIPLYRAILQLLRAVSLSSQLVSLLVNRNNEGKISIAALL
SNMKACVDTYASRLKVNKKSNLKGQTQKITVSLDDGDDEGLALLIPDIQETSLLVQSATSVDSVAAGEDDQKENVPR
PVAKSVEEKYMELMKALQFDTFEMIAETDNGYRFTISHHFETNVRMAGDRGHPGRVKRLAQETVTLSTSLPLSYSSS
VFVRCDTDRLDIMKVLITGPADTPYANGCFEFDVYFPPDYPNSPMMINLETTGRNTVRFNPNLYNDGKVCLSVLNTW
HGRPEEKWNAHTSSFLQVLVSIQSLILVPEPYFNEPGFERSRGTPSGTHSSREYNSNIYQACVRYAMLEQLKNPCPC
FKDVIHTHFWLKRNEICAQIEDWIAELSKPLQNERTGRTISFNAMVLRRQYRQLREELTKLAPPEGGDLTEIDYPFN
TGITPTTPAVDPTSAVTAGSTPPEKDLPADKDIDDDENDEDPVQDFGEDEDNEVIVKPDEEIAAAAAAAAAELAAAQ
DENADLSPEEIVLSMVW

>CPIJ006694_CqIAP5

MVSTENIEKVFLLETDRVKSFKKWPYSGTSSCSIQKMAEAGFYWNGNDNEEDTAACFVCGKVLDGWEETDAPWEEHK

KHAPQCPFVKFGRAEAELTVEEMIDLLEAIMKARLQNGYNTMKDGLKACIEKKRKEMLKQLGKN

>AAEL014251_AaIAP5

MVQTENIEKVYLFEKDRVNSFKKWPYSGSSPCNIQKMAEAGFYWQGDDKEDEDTSVCFVCGKVLDGWEESDDPWEEH

KKHAPQCLFVKYGRPEAEMTCEEMLNLLEVILKGRIQSSYTALKDCLKAHIEKKRKEMTKQLSKNAa

Figure A.5.4 Protein sequences of Dipteran IAPs

Protein sequences used in ClustalW alignment and subsequent phylogenetic analysis from Figure 2A. IAPs are identified by their accession number, species abbreviation, and IAP subfamily. Aa, *Ae. aegypti*; Ag, *An. gambiae*; Cq, *C. quinquefasiatus*; Cs, *C. sonorensis*; Dm, *D. melanogaster.*

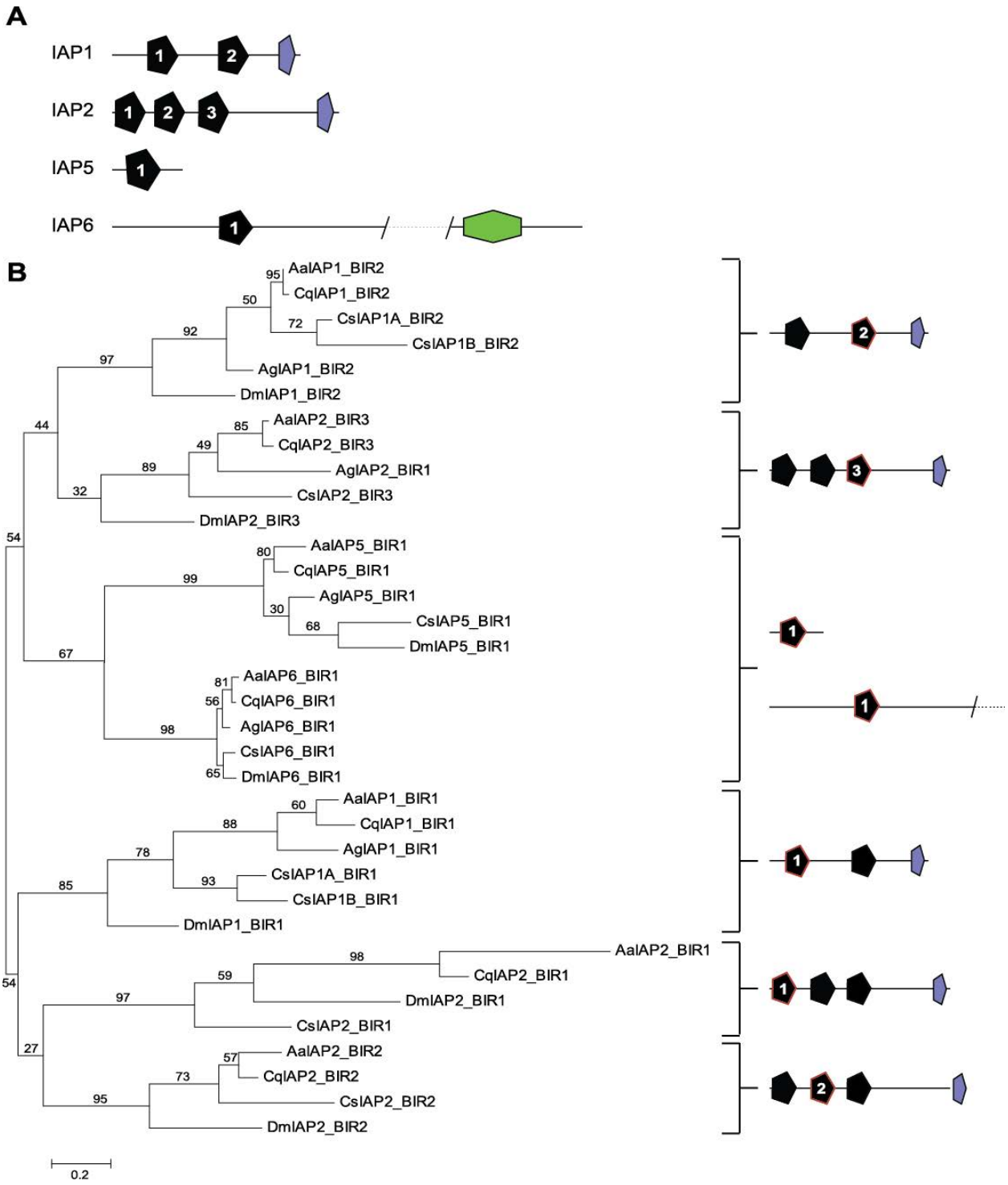

Figure A.5.5 Phylogenetic analysis of Dipteran IAP BIR domains

(**A**) Graphical representation of IAPs with numbered BIR domains (black pentagons). (**B**) Maximum Likelihood phylogenetic tree of Dipteran IAP BIR domains. BIR domains are

identified by their species abbreviation, IAP, and BIR number (as noted in A). IAP BIR domains (black) corresponding to different clusters are highlighted (numbered and outlined in red) as a visual aid. RING domains are shown in purple, and Ubiquitin Conjugating domains are represented in green.

Aa, *Ae. aegypti*; Ag, *An. gambiae*; Cq, *C. quinquefasiatus*; Cs, *C. sonorensis*; Dm, *D. melanogaster.*

>DmIAP1_BIR1

RLKTFTDWPLDWLDKRQLAQTGMYFTHAGDKVKCFFCGVEIGCWEQEDQPVPEHQRWSPNCPLLR

>DmIAP1_BIR2

RLRTFEAWPRNLKQKPHQLAEAGFFYTGVGDRVRCFSCGGGLMDWNDNDEPWEQHALWLSQCRFVKL

>AgIAP1_BIR1

RLRSFTSRWPVTFISPNVLARYGFYYVGTDDTVKCYFCRVEIGLWEPQDDVIQEHLRWSPYCPLLK

>AgIAP1_BIR2

RLKSYEDWPTSLKQKPQQLSDAGFFYTGMSDRVKCFSCGGGLKDWEQEDDPWQQHAIWYSNCHYLQ

>AaIAP1_BIR1

RLESFRGWMVSFISKTELARYGFYYVGPNDMVKCYFCRVEIGLWEPNDNVLSEHLRWSPYCPLLR

>AaIAP1_BIR2

RLESYEDWPKFMKQKPKELSDAGFFYTGKSDRVKCFSCGGGLKDWEAEDEPWEQHAMWYSNCEYLK

>CqIAP1_BIR1

RLESFLNWSIPFISKFELARFGFYYVGPGDMVKCFFCRVEIGLWEPNDNVLSEHLRWSPYCPLLR

>CqIAP1_BIR2

RLESYEDWPKFMKQKPKELSDAGFFYTGKSDRVKCFSCGGGLKDWEAGDEPWEQHAMWYSNCEYLKL

>DmIAP2_BIR1

RLATFGEWPLNAPVSAEDLVANGFFATGNWLEAECHFCHVRIDRWEYGDQVAERHRRSSPICSMVL

>DmIAP2_BIR2

RLVTFKDWPNPNITPQALAKAGFYYLNRLDHVKCVWCNGVIAKWEKNDNAFEEHKRFFPQCPRVQ

>DmIAP2_BIR3

RLRTFTDWPISNIQPASALAQAGLYYQKIGDQVRCFHCNIGLRSWQKEDEPWFEHAKWSPKCQFVLL

>AgIAP2_BIR1

RIRSFESWRFGHMQNPTRLAVAGFYYTGTDDEVRCFQCDAGLRDWLVTDDPWQEHARCFAECTFLR

>AaIAP2_BIR1

RVRTYRRWEATEWAMEDAFELLLAKAGFYATEQYLNVKCHFCGVTIFVGNSVSNIEAKHRELSPNCAFLL

>AaIAP2_BIR2

RLATYVNWPISHISPSSLAKAGFYYTYNADQVKCAWCEGVIGQWELGDDPFVEHQKFFPNCAKVI

>AaIAP2_BIR3

RIRSFENWTTGHIQDPERLAQAGFYYLGRADEVHCFYCDGGLRFWLADDDPWFEHARCFPKCQFVQ

>CqIAP2_BIR1

RLRTFEQWEHASWTMETSFEEVAKAGFYATERFLEAKCHFCGATVYIGEQAVDIESKHRQLNPGCSFLL

>CqIAP2_BIR2

RLATFVNWPVAHISPPALAKAGFYYTFNSDQVKCAWCEGVIGQWEVGDDPFTEHQKFFPSCEKVI

>CqIAP2_BIR3

RIRTFENWTTGNIQDPERLAQAGFYYLGRADEVHCFHCDGGLRFWLADDDPWFEHARCFPKCQFVQ

>CsIAP6_BIR1

RRQTFEQWPHMDYKWALPDQMAQAGFYHQPGESGGDRAMCFTCNVCLVCWEKTDEPWSEHERHSPDCAFVK

>DmIAP6_BIR1

RRQTFEKWPHMDYKWALPDQMAQAGFYHQPSSSGEDRAMCFTCSVCLVCWEKTDEPWSEHERHSPLCPFVK

>AgIAP6_BIR1

RRQTFEAWPHMDYKWVLPDQMAQAGFYHQPGENGNKDRAMCFTCTVCLVCWEKTDEPWSEHERHSPECPFVK

>AaIAP6_BIR1

RWQTFEGWPHMDYKWVLPDQMAQAGFYHYPGDNGNDDRAMCFTCNVCLVCWEKTDEPWSEHERHSPECPFVK

>CqIAP6_BIR1

RRQTFEGWPHMDYKWVLPDQMAQAGFYHFPGDNGNDDRAMCFTCNVCLVCWEKTDEPWSEHERHSPECPFVK

>CsIAP1A_BIR1

RRLTFSNWNCPTTDKFLLAQIGFYFIGPTDLVKCYFCNVEIGMWQPEDNPVEEHLRWSPNCPLLH

>CsIAP1A_BIR2

RLVSYEDWPKTMKQKPKELAEAGFYYTGKGDRVACFSCGGGLKDWEEMDVPWEQHAMWYSKCEYLK

>CsIAP2_BIR1

RLALLENWVDNSGISAQEIAAAGFYATRNGSEVQCYWCLIKVNSWQEGDNALEKHRQLSPNCPFIV

>CsIAP2_BIR2

RLETYQNWPVSFIQPADLARAGFYYINRSDQVKCAWCQRVIGEWEVLDDPVTEHLKFSPACQKAR

>CsIAP2_BIR3

RIRSFANWKYDHVQDPTTLAEAGFYYFGNRDEVKCFHCGGGLCFWLEQDQPWYEHAHWFPKCHFLL

>CsIAP1B_BIR1

RLLTFVNWNQPKINKRLMSQIGFYFTGPTNLVKCYFCKVEIGMWQSEDNPVEEHLRWSPKCPLLN

>CsIAP1B_BIR2

RLVSYKDWPKTMNQKPEDLAEAGFFFTGLQDKVKCFSCGGDLYDWKETDVPWEQHAVFHSKCEYLK

>CsIAP5_BIR1

RLDSFKHWPFDDKSPCNIAKMAEAGFFWCGNEREIDSAACFLCNKHLDGWEEEDDPWLEHSKHAPQCLFAK

>DmIAP5_BIR1

RVESYKSWPFPETASCSISKMAEAGFYWTGTKRENDTATCFVCGKTLDGWEPEDDPWKEHVKHAPQCEFA

>AgIAP5_BIR1

REKSFKHWPFSDDKQCSIQKMAEAGFYWHGTETEIDIAACFVCGKELDGWEESDDPWSEHRKHAPQCPFVK

>AaIAP5_BIR1

RVNSFKKWPYSGSSPCNIQKMAEAGFYWQGDDKEDEDTSVCFVCGKVLDGWEESDDPWEEHKKHAPQCLFVK

>CqIAP5_BIR1

RVKSFKKWPYSGTSSCSIQKMAEAGFYWNGNDNEEDTAACFVCGKVLDGWEETDAPWEEHKKHAPQCPFVK

Figure A.5.6 Protein sequences of the individual BIR domains of Dipteran IAPs

Protein sequences of BIR domains were identified using ScanProsite as detailed in Materials and Methods. Sequences were used in ClustalW alignment and subsequent phylogenetic analysis shown in Figure A.5. IAPs are identified by their species abbreviation, IAP, and BIR number (Figure A.5A).

Aa, *Ae. aegypti*; Ag, *An. gambiae*; Cq, *C. quinquefasiatus*; Cs, *C. sonorensis*; Dm, *D. melanogaster.*

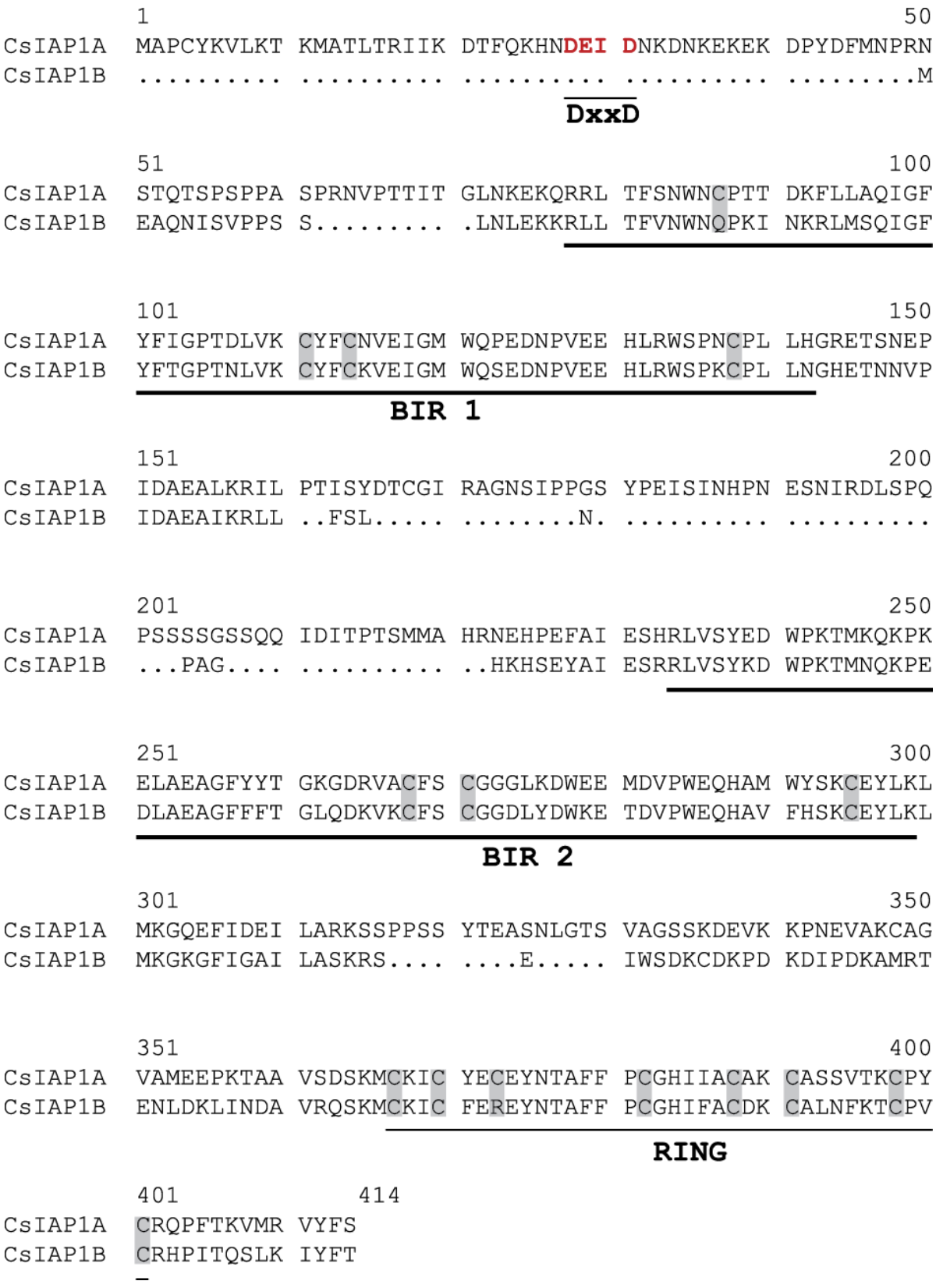

Figure A.5.7 Alignment of CsIAP1 putative orthologs

Figure A.7 Alignment of CsIAP1 putative orthologs

ClustalW alignment of putative IAP1 orthologs in *C. sonorensis*, CsIAP1A (GAWM01009039) and CsIAP1B (GAWM01009044). DXXD (red) motif and BIR and RING domains are underlined. Cysteine residues are highlighted (grey), and the linker region corresponds to the amino acids between BIR1 and BIR2.

>CsDRONC.A_GAWM01016707

KLYFNPGISVLGVNTNEVISAEKSELMTKREEPLKEVISIKDHVDIQNNDLQDGNNQMKLKSNQNHEQNEENLQLVP

YKGEINYHLNVERAGRFSYAKKFNIKTYEMMKKQRGVLFLINNINFKSNSHRNGAEVDKERLLALFSQLGFQLFYYE

DLGFQHFRILLKQFVVSEVLKNTDCLVFGLLTHGDDNGKHAYAEFCCGMYVNVQHIIDHFSNLNCTHLIGKPKIFLF

PFCRGTLSDCGVKQSSNFEGTQALPTLSDTVICHATSPGFMSIRDPVKGGRFLQSMVKIFAEHAHDTKFDDLMMLVE

MDVHKNNQSSEYKQVCSVTYNAFNKLFFNPGVQVVEEDHQLELIEEE*

>CsDRONC.B_GAWM01010674

MEQNDRLTILKNMQRLIDATDYELLADKCQQAKLLSNVMVKNIENDSNDTITRHKNLLKKITERGPTAFTVFKGICE

TDFKEAADILKFSPIDDNQKTFLSISESKRENERERREMYEGKSLSRVDAKSEPSTSNNSSSSSKSNGNKNENLLRL

EAYDGPIQKILEVK

>CsDRONC.C_GAWM01012987

MPKKVKKKSSKIIKKLIKLTNFDLLLEICIKMEKFADKVLENVLNTDLTMYERHKCLINLLVNVGYNEFLSICRMHF

PNAAILLEPDENRNTLNSENLKNNERSGAVKKSHTKVTLEPYVGVIQQKVKVKLRNRIHNSDHSEIITYDMNQEKRG

VLVFVNIIDFNDKSKYRIGAEADKASVLDLFNQFGFTLFYYENLTQMQFNGILKALSHDSNDYLKEANSLVFILSSH

GRVIQDTVYVDFSDGAYCSTDSILNNFNNVNCPSLHGKPKIFLFPFRRGDKYDCGIKTVINVSDDEQILGSVPTFSD

>CsDRONC.D_GAWM01010678

SSSSKSNGNKNENLLRLEAYDGPIQKILEVKRATRFGTVTRPGIETYSMKSKHRGVLFLVNIIDFKEKDKRRNGAES

DKEVLLDLFNQMGFKLFYYENINADQFSSLIKQLSSAGCLRMADCLVFGLLTHGSLTGQTTYVEFSDGLYYPTEQIV

QEFSNTNCKYLQGKPKIFLFPFCRGDRSDKGVIIYRQRSSRIETDNSAQFIEERIPTSSDIAICYATVPGFLTHRDP

KEGSWYIQGLTSVFEKHAHDAPFEDLMKLVELEVGSKNTDSGAIQTSSVEYRGFSKVLYFNPGYFGDTSETETNGNI

TNN*

>CsDRICE.A_GAWM01000206

MDTTGCCTTIPLKTKANPKLFSTATTNSQIARMPVERFGSEYNMNHKNRGYALIFNHEYFDVPSLKARSGTAADCEN

LVNTLQNLHFNVKVYKDLKYRDILKEVEGYANMDHSDNDCILVAILSHGELGYIYSREGQYKLDSIWSYFTANRCPT

LAGKPKLFFVQACQGDQLDGGITMLPDRTETDSGSTGLSYKIPIHADFLIAYSTIPGFYSWRNTTKGSWFMQSLCYE

LNQHGKKYDLLTLLTFVCRRVAIDFESNTPDNPSMHQQKQIPCITTMMTRLLRFTDK*

>CsDRICE.B_GAWM01002195

MSDYIDVYLLEKKLKVIIFNHTYFLNEPEKQRTLKIGEKVYECLRKLGNIEIEHVKSREEEILDENGAMHRRVIHDD

LMAANVLNLMKTVSENGDSYSGLIVFVSSHGGMGMIGGEFCEFIQAHDKSYRKSLLWECFLDKPGWKGKPLMFFFQA

CRGGDATPGVRMSIDASGISDVRIFPDLFIMNATLPGAVAFKSDQNSIFADTLCSEISKNAHHLDLNSIALNVCKEV

AQTFESCDMLEPKYYCSQQMPCIESTFTKYFFFSTKYQPHPKKEHYYESVQQPFILFLNYDNTFDDTVEDQTGEIER

IRQDTRFLVDTFEKIGYGSHVELNATFERYKELTAQYCNLKDKNTFMVIFNGFGKQDYVQMANEQIKLHKLWTELLP

DINSSELANEKPKVLLFLGKSVDVQINGLSGIVNRSCSQDEGAKNVKSCVRHFDGNKYTNIPITADMLLIFNYMEDN

QQLDGASPFVHHFCKVLDSQKTNDFLKAIVMTSKNLLEQNQTAPFFFTLRKPLPIKAN*

>CsDRICE.C_GAWM01002196

MSDYIDVYLLEKKLKVIIFNHTDFLNAPEKQRTPKIGEHFEECLRKILGHNIEIEHVKSREKEISDENGAMKMVNCH

DDLMATNVLKLIKTVSENGDSYSGLIVFVSSHGGMTIIHEEFCELIEAYDKKYRKSQLWECFRNKAGWKGKPLMFFF

QACRGSDSTQGVRSSIDASKISDLKEGMPQRIFPDLFIMNATQPGAVAFKSDKSSIFVEKLCSTLSESAHQLDLKSI

AVKVSNEVAQTFESCDMLEHEYFCSQQMPSFESTFTKKCYLFTQYQPHPKIDRYYESLEKPFILFLNYEEKDNQNGE

KHRIDKDTRLLRNYFEKIGYGTHEEPNATFKRYKELNNTLLDGACPFVRHFCNILINQKPKDFCEAI

Figure A.5.8 Putative *C. sonorensis* caspases

Protein sequences of *C. sonorensis* orthologs as identified by best reciprocal blast hit to DRONC and DRICE. Species abbreviation, caspase, and accession number identify the putative caspases. Cs, *C. sonorensis*.

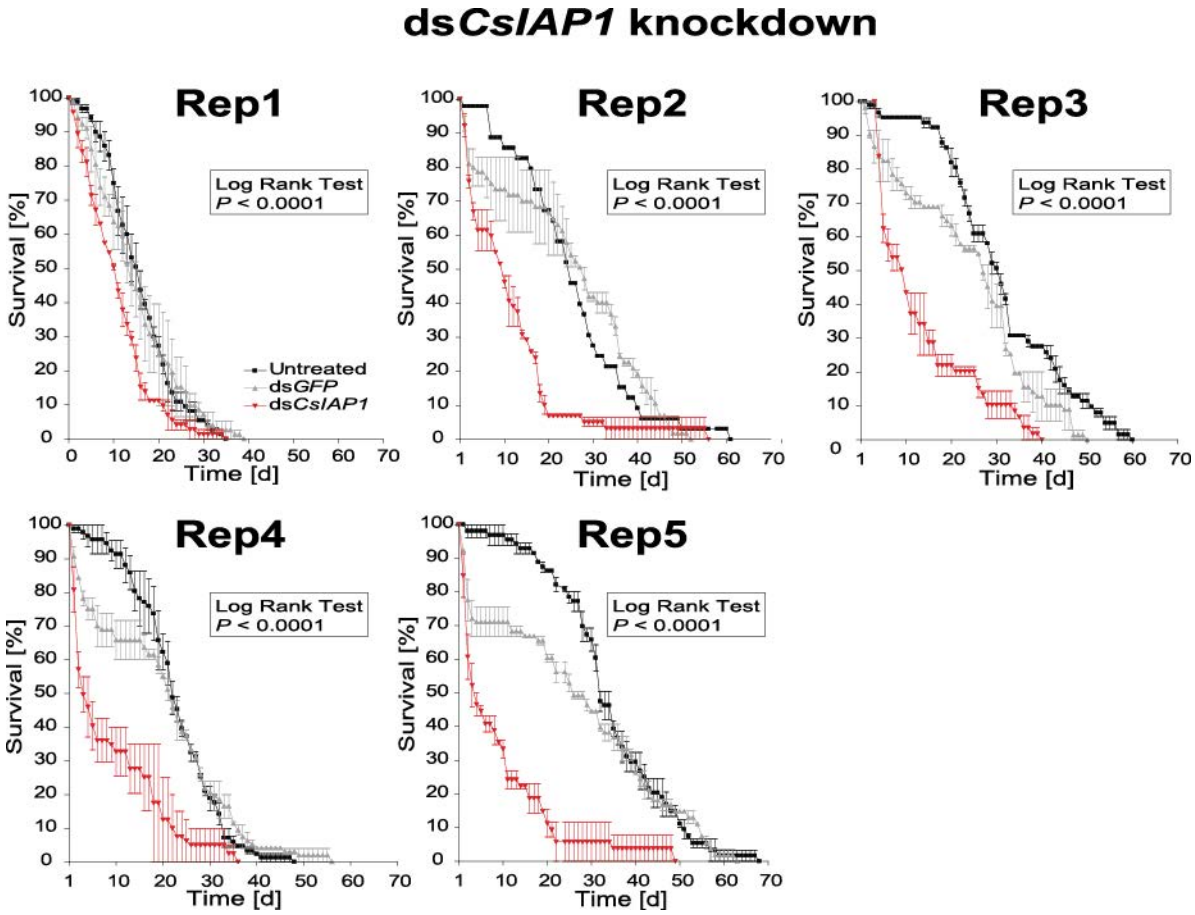

Figure A.5.9 Survival analysis of female midges after ds*CsIAP1* injection

(**Rep1-5**) Survival curves of individual biological replicates after ds*CsIAP1* injection shown in Figure 3B-C. Midges from Rep1-4 were analyzed for knockdown efficiency by qRT-PCR shown in Figure 4. Survival curves are presented as mean ± range of two technical replicates for each biological replicate (n=50 per technical replicate). Statistical significant differences between survival curves was assessed by Log Rank Test, resulting *P* values are indicated in figure.

Appendix B - Supplemental data for Chapter 3

Table 5.1 Quantification of midgut phenotypes after ds*CsIAP1* injection

Treatment	dpi	Total # of midguts examined*	# of midguts with normal morphology	# of midguts with altered morphology
Untreated	2	179	179	0
Untreated	5	197	197	0
ds*GFP*-injected	2	183	183	0
ds*GFP*-injected	5	187	187	0
*IAP1*kd	2	185	55	130
*IAP1*kd	5	188	44	144

*Table shows the raw data plotted in Figure 4F.

Table 5.2 Quantification of midgut phenotypes in midges injected with ds*DRONC*/ds*IAP1*

Treatment	dpi	Total # of midguts examined*	# of midguts with normal morphology	# of midguts with altered morphology
UT	2	179	179	0
ds*GFP*/ds*GFP*	2	184	197	0
ds*GFP*/ds*IAP1*	2	179	38	141
ds*GFP*/ds*DRONC*	2	183	183	0
ds*IAP1*/ds*DRONC*	2	164	60	104

*Table shows the raw data plotted in Figure 5.

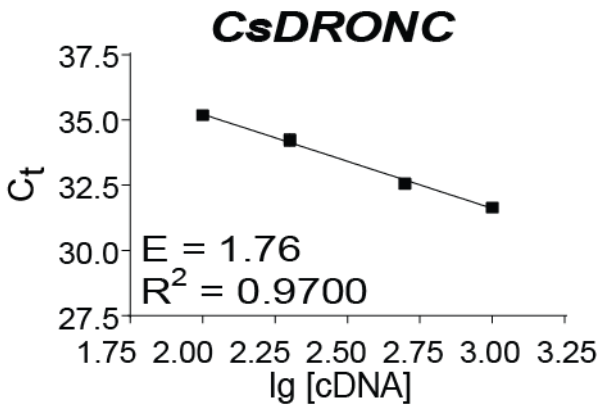

Figure B.1 Primer efficiency for RT-qPCR analysis

Primer efficiency was measured using a dilution series of cDNA stock from non-blood fed midges for RT-qPCR analysis. Graph shows lg values of cDNA dilution plotted against Ct values obtained with *CsDRONC* primers. R_2, goodness of fit; E, calculated primer efficiency.

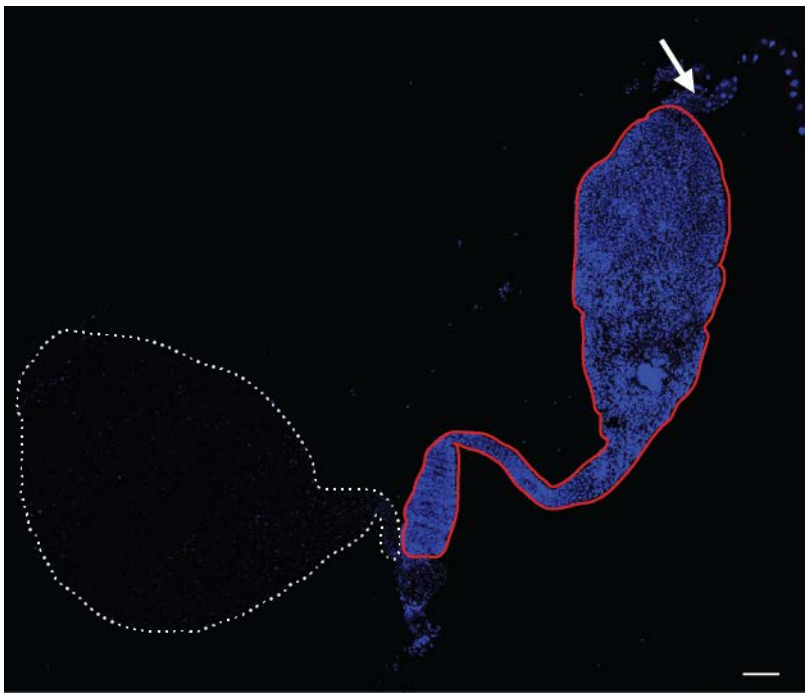

Figure B.2 Contour outline of midge midgut

Representative image depicts *C. sonorensis* alimentary canal stained with DAPI visualizing nuclei (blue). Midguts were outlined (red) using Zen Blue software (Zeiss, Jena, Germany) to determine area values shown in Figure 2. The crop (dotted line) and Malpighian tubules (start at arrow) were not part of the area measured, but were dissected with the midgut for qPCR analysis shown in Figure 1. Scale bar, 100 nm.

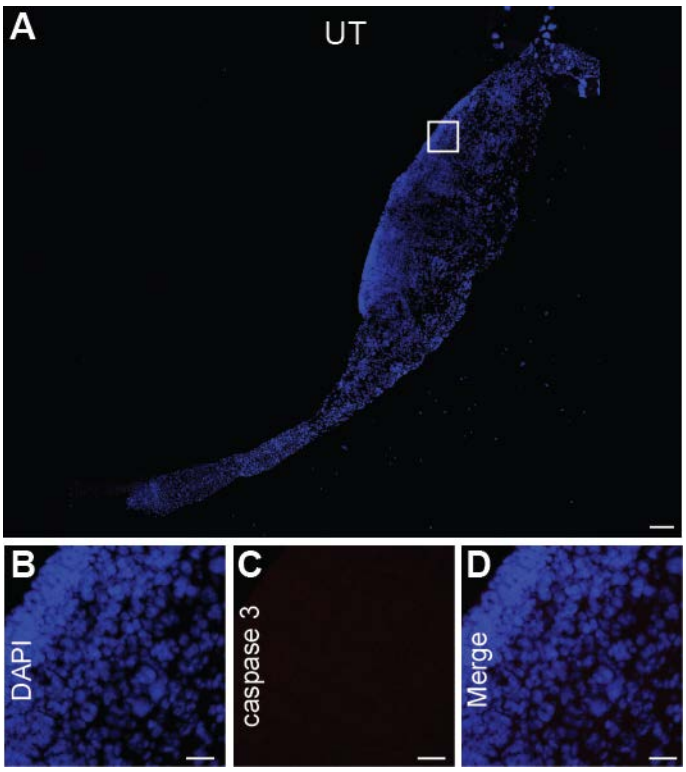

Figure B.3 Anti-active caspase 3 is not detected in midguts from untreated (UT) *C. sonorensis* staining of midgut tissues.

(**A**) Representative image of whole midge midgut at 2 dpi via DAPI stain (blue). Scale bar, 100 nm. (**B-D**) Midguts from UT midges showed no fluorescence in the red channel after staining with primary anti-active caspase 3 and secondary Alexa Fluor 594 goat anti-rabbit antibodies (red). Images were taken from midgut location denoted by white square. Scale bar, 20 nm.

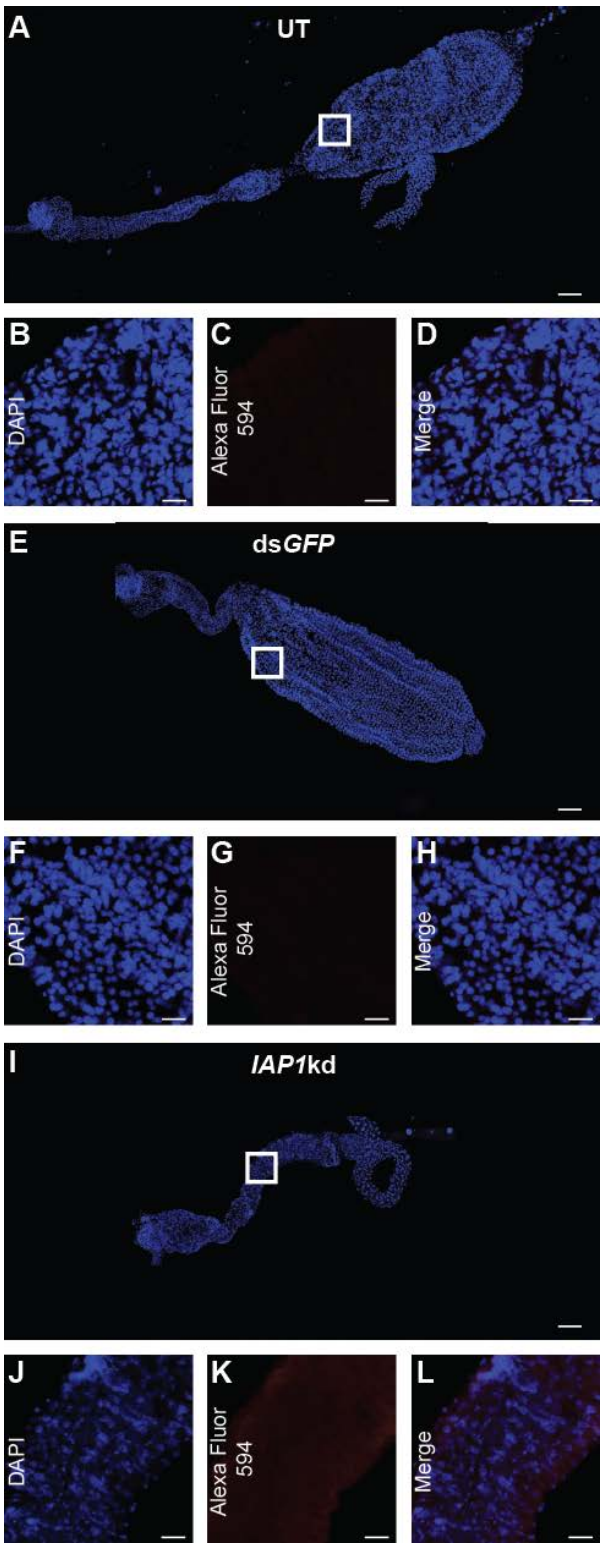

Figure B.4 Secondary antibody controls for active caspase 3 immunofluorescence analyses of midge midguts.

Figure B.4 Secondary antibody controls for active caspase 3 immunofluorescence analyses of midge midguts.

(**A, E, I**) Representative images depict DAPI-stained (blue) whole midge midgut at 2 dpi. Scale bar, 100 nm. Detailed views of midgut tissues from UT (**B-D**), ds*GFP*-injected (**F-H**), and *IAP1*kd (**J-L**) midges showed no fluorescence signal in the red channel after incubation with Alexa Fluor 594 goat anti-rabbit secondary antibodies alone. Detailed views were taken from midgut locations depicted by white squares. Scale bar, 20 nm.

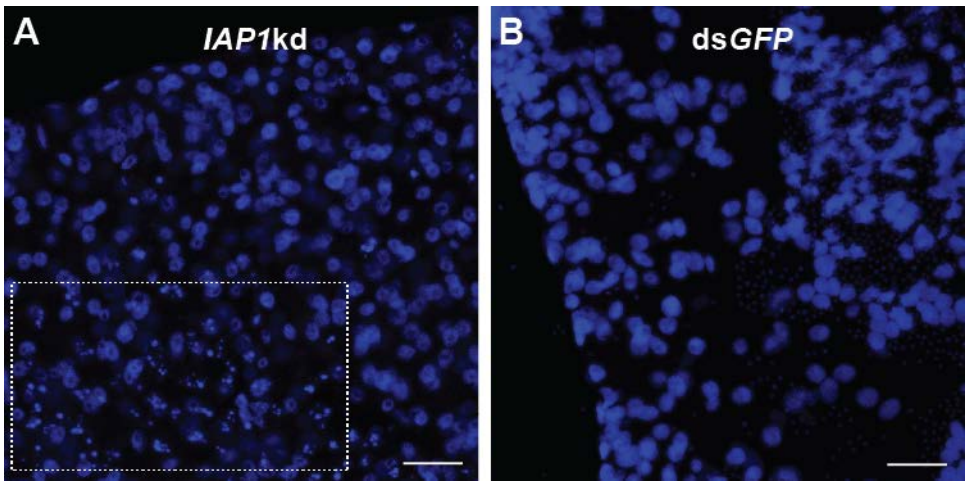

Figure B.5 Fragmented nuclei are commonly seen in midguts from *IAP1*kd midges

Images depict midgut nuclei stained with DAPI (blue). Images are enlarged from Figure 3B and F. Fragmented nuclei (dotted square) were only observed in *IAP1*kd midguts (**A**) when compared to controls (**B**). Scale bar, 20 nm.

>CG8091
RIGAEKDSKSLIHLFQELNFTIFPYGNVNQDQFFKLLTMVTSSSYVQNTECFVMVLMTHGNSVEGKEKVEFCDGSVVDMQKIKDHF
QTAKCPYLVNKPKVLMFPFCRGDEYDLGHPKNQGNLMEPVYTAQEEKWPDTQTEGIPSPSTNVPSLADTLVCYANTPGYVTHRDLD
TGSWYIQKF

>GAWM01016707
RNGAEVDKERLLALFSQLGFQLFYYEDLGFQHFRILLKQFVVSEVLKNTDCLVFGLLTHGDDNGKHAYAEFCCGMYVNVQHIIDHF
SNLNCTHLIGKPKIFLFPFCRGTLSDCGVKQSSNFEGTQALPTLSDTVICHATSPGFMSIRDPVKGGRFLQSM

>AGAP004754
RNGADIDGRNLISVFQQLGFVVFYYEDITMGDLKELLAQLKESEHLSCDCFAFYILSHGDHRKGSDYIFLHDNSLLRVEDLLTEFN
SVNCKRLVHKPKLFFISICRGVQSDLGAYRLSTNTERDGMIDPGKPLPSNIATYCDMLVCYATVPGFAAHRDTNTGSWFVESM

>AAEL011562
RNGAEADKYNLVSLFQQLGFTVFYYEDLTSDEFNNLIKELKQSSYLSTECFVFYILAHGNHTKGRDKIYLNDNSVLYVEDVLALFN
NANCPKLIRRPKLFFFSICRGDNPDYGTLRLAEHTERDGMINLKKDPPTNMPTYADMLICFSTVPGYAAHRDKQYGSWFVESM

>CG7846
RDGTDVDKERLIEVFSSMGYNVEAYDNVDHMGIIERIRSACDRSLVRDSLVVFILSHGFEEAVYASNSIAMKITDIEDLLCSYDTL
YYKPKLLIIQACQEKLVHKKKPNELFRIDVTTVSPDQHIDMLRAMSTVNGYAALRHTQTGSWFIGSL

>AGAP011693
RKGTEVDKSALERLFNDFGYDLLVEENITHHQILQAVQHAVQRTQPIHCSLVVCLLSHGQEGKVFGANSIPVEVRAIQQLMASERL
TGKPKLLIVQACQGADLQSAVPVPIYEHDGLEGSEKTASVFMDFLVAWSTVPGFASIRHIEKGSWFIQEL

>AAEL014148
RRGTEVDKMAILNLFTNLGYEPIVVENIPHLEIMNQVEQAVDRVEPHHCSLVICLLSHGQEGKVYGSNSIPVSVKAIERKMAARKL
TGKPKLLFVQACQGSGLQTAVDVAPRLEHDGPSSETTASVFVDFLVAWSTVPGFASIRHIEKGSWFIQEL

Figure B.6 Sequences of representative Dipteran DRONC and DREDD orthologs

Sequences are listed in fasta format. Accession numbers of DRONC orthologs are as follows: *D. melanogaster* (CG8091), *C. sonorensis* (GAWM01016707), *An. gambiae* (AGAP004754), *Ae. aegypti* (AAEL011562). Accession numbers of DREDD orthologs are as follows: *D. melanogaster* (CG7846), *An. gambiae* (AGAP011693), *Ae. aegypti* (AAEL014148). Sequences were used to produce protein alignments shown in Figure B.7 and the phylogenetic tree shown in Figure B.8.

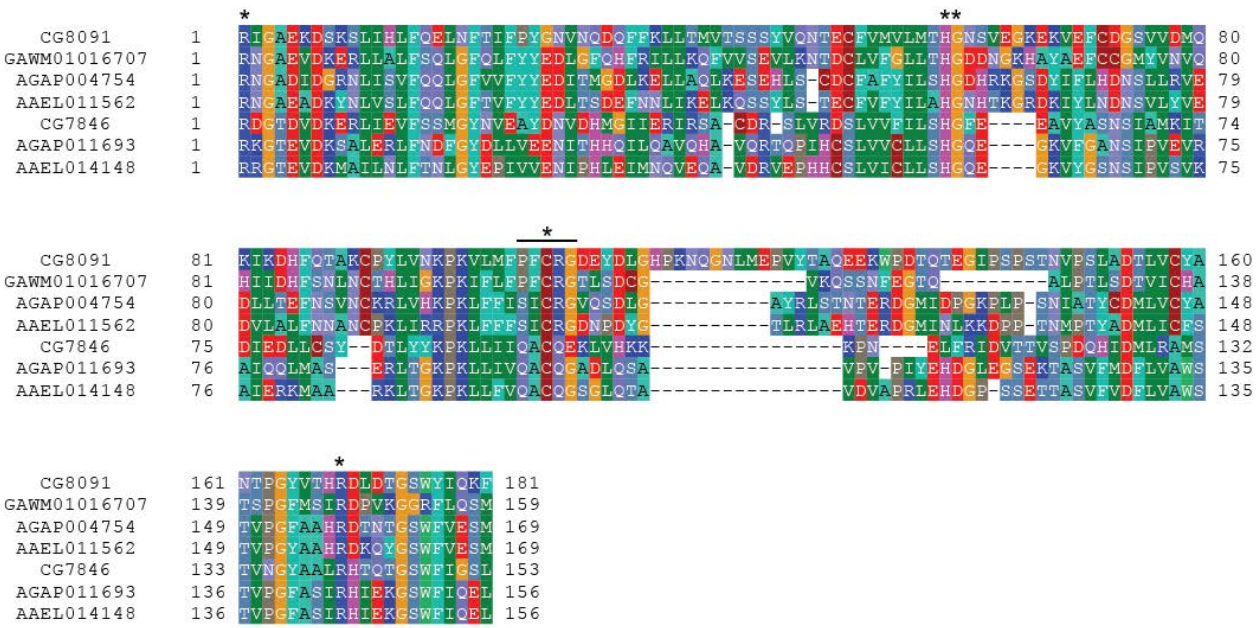

Figure B.7 Alignment of Dipteran DRONCs and DREDDs.

ClustalW alignment of the active caspase residues. *D. melanogaster* DRONC (CG8091) and its orthologs in *C. sonorensis* (GAWM01016707), *An. gambiae* (AGAP004754), and *Ae. aegypti* (AAEL011562) were aligned with *D. melanogaster* DREDD (CG7846) and its corresponding orthologs in *An. gambiae* (AGAP011693) and *Ae. aegypti* (AAEL014148). Residues considered critical for caspase function are denoted by asterisk (*) and the active site is denoted by (_*_).

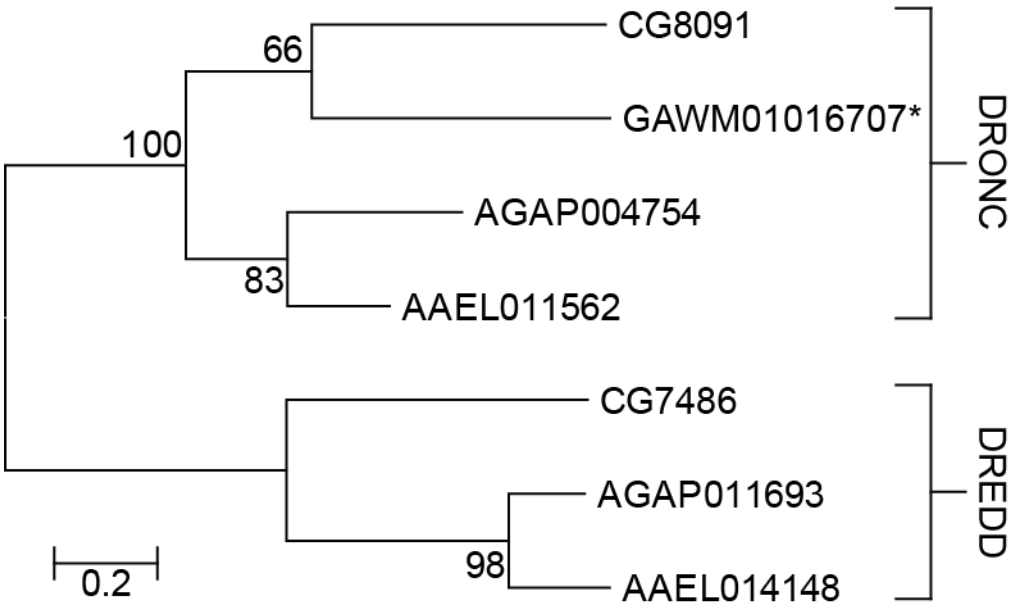

Figure B.8 Phylogenetic analysis of selected dipteran DRONC and DREDD caspases. Maximum likelihood phylogenetic tree of dipteran DRONCs and DREDDs identifies the *C. sonorensis* caspase with accession number GAWM1016707 as the ortholog of *D. melanogaster* DRONC. AGAP, *An. gambiae*, AAEL, *Ae. aegypti*, Mosquito and *D. melanogaster* gene accession numbers according to VectorBase and Flybase, respectively.

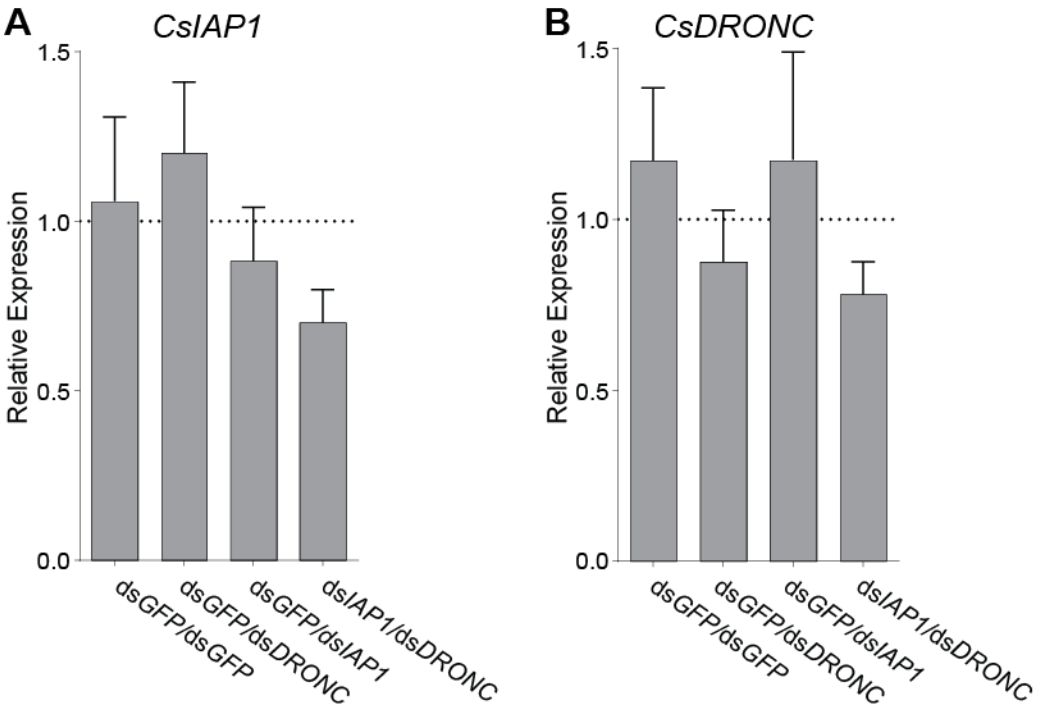

Figure B.9 Analysis of *CsIAP1* and *CsDRONC* transcript levels in co-injection experiments. Graphs show relative expression of *CsIAP1* (**A**) and *CsDRONC* (**B**) in whole midges at 5 dpi. All data was calibrated relative to UT controls (dotted line), and RT-qPCR results were calculated using elongation factor 1b as the reference gene. Data are presented as mean ± SEM from three biological replicates.

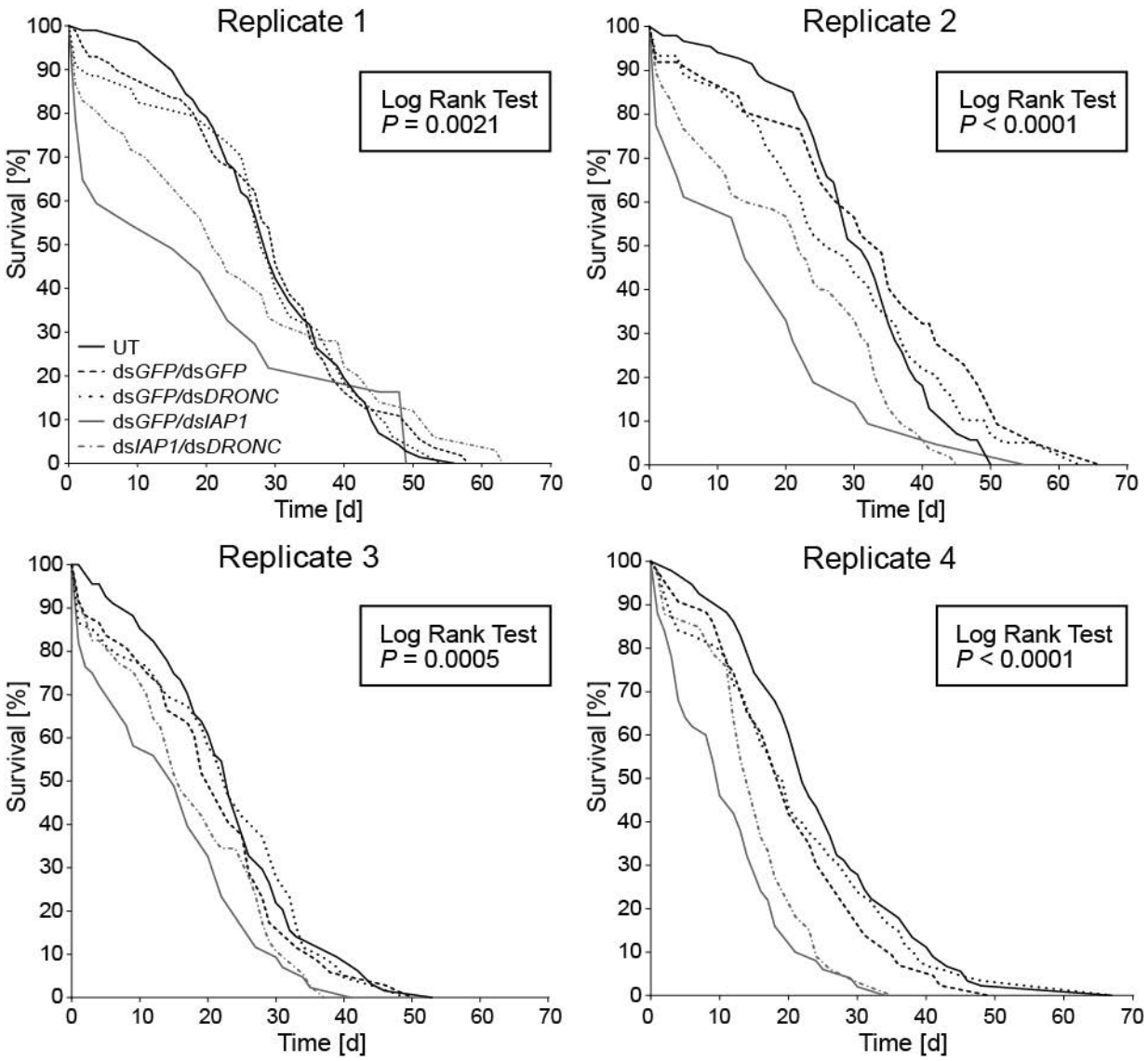

Figure B.10 Individual survival curves of ds*IAP1*/ds*DRONC*-injected midges.

(**Rep 1-4**) Individual biological replicates of survival curves of epistatic analysis shown in Figure 6A (n=100 female midges per treatment and biological replicate). Statistical significant differences between survival curves were evaluated by Log Rank Test, with resulting *P* values shown for each replicate.

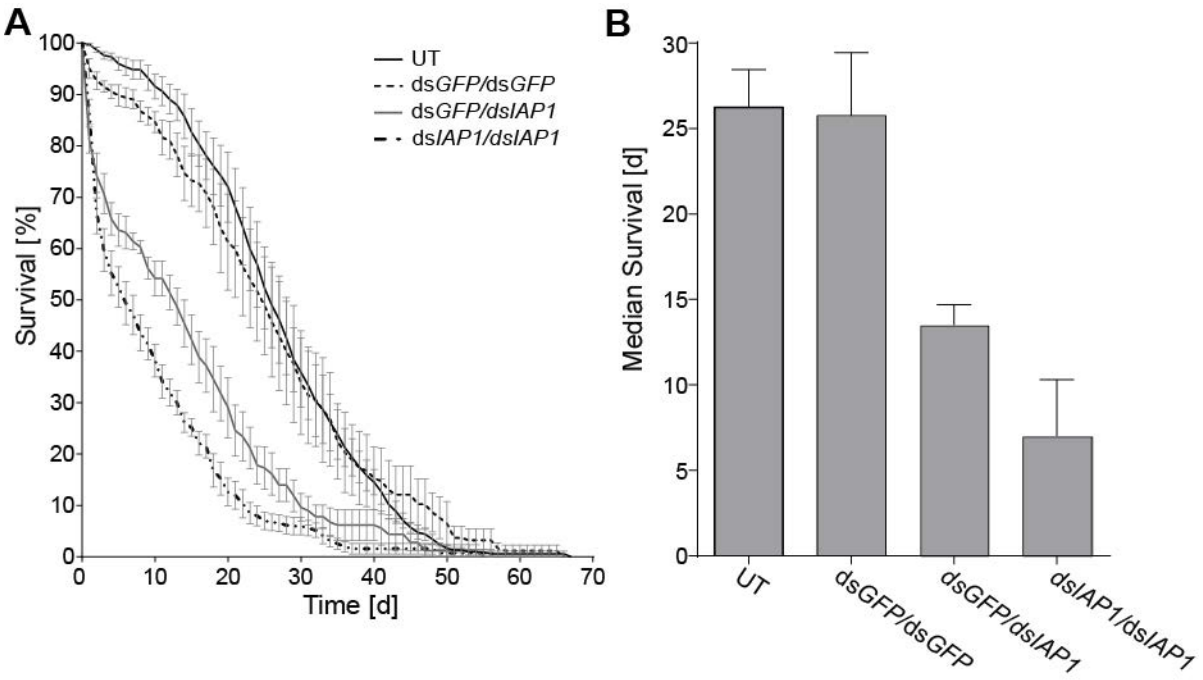

Figure B.11 Survival phenotype depends on dsRNA dose

(**A**) Graph shows survival curves comparing mortality rates of dsRNA-injected midges. All midges were injected with a total amount of 80 ng of dsRNA, resulting in a high dose of 80 ng of ds*IAP1* for ds*IAP1*/ds*IAP1*-treated midges, and a low dose of 40ng of ds*IAP1* for ds*GFP*/ds*IAP1*-treated midges. (**B**) Comparison of median survival between dsRNA doses. Data for the low dose experiment were combined from four biological replicates (Figure B.10), while high dose survival curves are from (Mills et al. 2015). All data are presented as mean ± SEM. UT; untreated control.

Appendix C - Supplemental data for Chapter 4

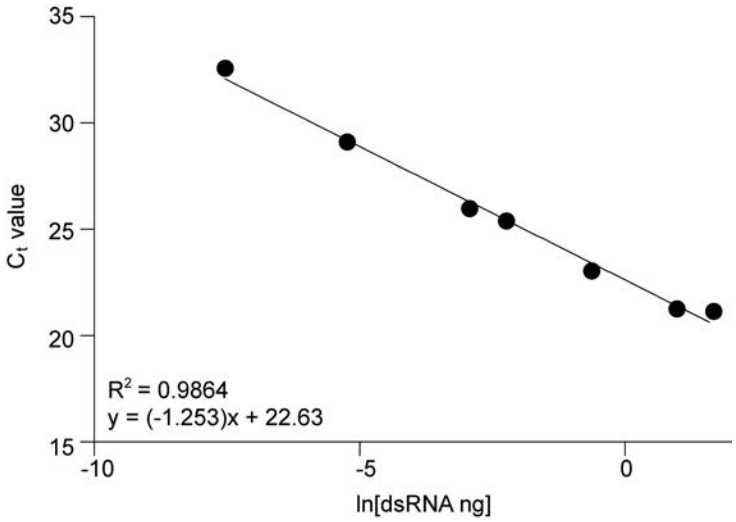

Figure C.1 Viral dsRNA qPCR standard curve of EHDV-2 genomic Ns3

Cycle thresholds (C_t) are plotted against the natural log of viral dsRNA concentration. The equation of the linear regression (solid line) was used to determine the amount of viral genomic dsRNA per midge and converted to viral genome equivalents as a measure for the number of total viral particles per midge according to Huismans et al (Huismans et al. 1979).

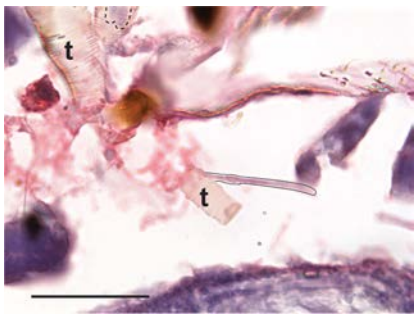

Figure C.2 IHC staining of EHDV-2 associated with tracheoles in *C. sonorensis*

IHC staining (red) indicating EHDV-2 infection is associated with the tracheoles (black line), while not found in the tracheal tinidea (t), lumen, or epithelia (dotted line). Scale bar = 25 μm.